



CRYOGENIC HELIUM GAS CONVECTION RESEARCH

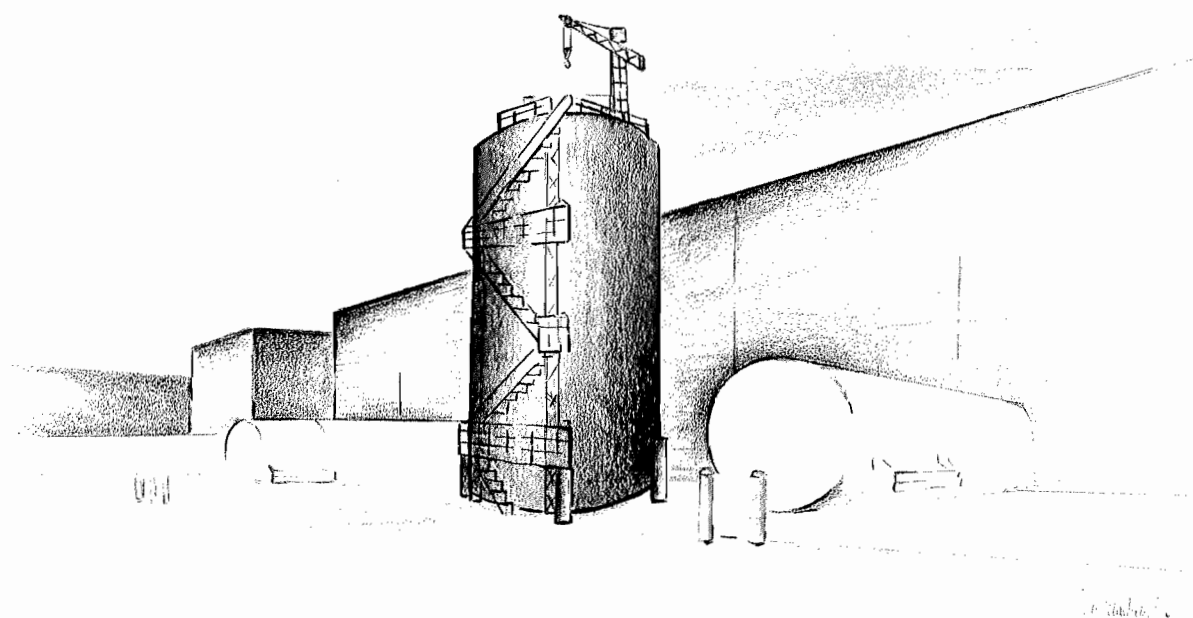
A Discussion of Opportunities for Using the Cryogenic Facilities
of the SSC Laboratories for High Rayleigh Number and High Reynolds
Number Turbulence Research

A Report to the Department of Energy under Grant No. DE-FG05-94ER40878
From the Department of Physics, University of Oregon
Eugene, Oregon 97403

Russell J. Donnelly, Editor
October 1994

CRYOGENIC HELIUM GAS CONVECTION RESEARCH

A Report from the Department of Physics
University of Oregon



Edited by
Russell J. Donnelly
October 1994

CRYOGENIC HELIUM GAS CONVECTION RESEARCH

A Discussion of Opportunities for Using the Cryogenic Facilities
of the SSC Laboratories for High Rayleigh Number and High Reynolds Number
Turbulence Research

A Report to the Department of Energy under Grant No. DE-FG05-94ER40878
From the Department of Physics, University of Oregon
Eugene, Oregon 97403

Preparation of this report was supported also by the Department of Energy
through a grant to Yale University, DE-FG05-94ER40876 and to Duke University
through grant DE-FG05-94ER40877.

Authors of This Report

Robert P. Behringer
Russell J. Donnelly
Michael McAshan
James Maddocks
Katepalli Sreenivasan
Chris Swanson
Xiao-Zhong Wu

Artwork

Jean Maddocks

Editor of Report

Russell J. Donnelly

October 1994

THE CRYOGENIC HELIUM GAS CONVECTION EXPERIMENT AT
THE SUPERCONDUCTING SUPERCOLLIDER LABORATORY

Participants

Principal Investigator:	Russell J. Donnelly, Professor of Physics University of Oregon
Co-Principal Investigators:	Robert P. Behringer Professor of Physics Duke University
	Dr. Michael McAshan, (Formerly of the SSC Laboratory)
	Katepalli R. Sreenivasan Professor of Mechanical Engineering and Physics Yale University
	Xiao-Zhong Wu Assistant Professor of Physics Northern Illinois University
Post Doctoral Associates:	Dr. Joseph J. Niemela University of Oregon
	Dr. Chris J. Swanson University of Oregon
	Dr. James R. Maddocks (Formerly of the SSC Laboratory)

Participant Contact Information (as of October 1994)

Name	Address	Telephone	Fax	e-mail
R. P. Behringer	Department of Physics Duke University Durham, NC 27708	919-660-2550	919-660-2525	bob@physics.phy.duke.edu
R. J. Donnelly J. J. Niemela Chris Swanson	Department of Physics University of Oregon Eugene, OR 97403-1274	503-346-4226	503-346-4708	russ@vortex.uoregon.edu
J. Maddocks	414 Ridgewood Dr. DeSoto, TX 75115	214-223-5086		
M. S. McAshan	Route 5, Box 21 Maypearl TX 76064-9805	214-435-2419	214-435-2283	
K. R. Sreenivasan	Mason Laboratory Yale University New Haven CT 06520-8286	203-432-4345	203-432-1054	krs@kolmogorov.eng.yale.edu
Xiao-Zhong Wu	Department of Physics Northern Illinois University Dekalb IL 60115	815-753-6467	815-753-8565	xwu@crsgi.erenj.com

PREFACE

The cancellation of the Superconducting Supercollider project by Congress required, among other things, an investigation into the best use of the remaining assets. The Department of Energy called for "Expressions of Interest" in March 1994 and our group responded to that opportunity, filing a document entitled *The Cryogenic Gas Convection Experiment at the Superconducting Supercollider Laboratory*. Subsequently, having been selected as one of a few successful Expressions of Interest, we applied for funds in June 1994 to make possible the material assembled here. The authors have greatly enjoyed the preparation of this report, because it has revealed to us the marvelous things which can be done in physics and engineering with the sizable cryogenic facilities available at the SSC Laboratories.

While this report comes from the Department of Physics at the University of Oregon, it represents the thinking of a substantial number of people and institutions. I am especially grateful to Professors Katepalli Sreenivasan of Yale University, Professor Robert Behringer of Duke University, Professor Xiao-Zhong Wu of Northern Illinois University and Dr. McAshan of the SSC Laboratories, all of whom participated in the writing of this report. We in turn have been helped in innumerable ways by Dr. James Maddocks of the SSCL. The design work at SSCL was aided by the efforts of Shaul Abramovich, Ted Niehaus, Ken Hess and Adnan Yucel. We engaged the services of Dr. Glen McIntosh of Cryogenic Technical Services in Boulder, Colorado, to prepare estimates of the costs of the new facilities, and to prepare a document and drawings which are contained in Appendix A of this report. Here at Oregon our whole group worked on the preparation: Greg Bauer, Dr. Joseph Niemela, Dr. Chris Swanson, and Janice Niemela.

An additional dimension was occasioned by the realization that the refrigeration available at site N-15 at the SSCL is large enough to support facilities for the testing of ship and submarine models. In an effort to understand some of the issues involved, we contacted Admiral M. Firebaugh of the Naval Sea Systems Command, who in turn put us in touch with staff of the Carderock Division of the Naval Surface Warfare Center. I was able to visit the Large Cavitation Channel at Memphis, Tennessee and to meet Dr. David Coder, Mr. Robert Etter and Mr. James Blanton at the LCC. I have also had the good fortune of being able to consult Dr. Richard Nadolink of the Naval Undersea Warfare Center in Newport RI, and Dr. Dennis Bushnell of NASA Langley Research Center. I am grateful to all these people for a rapid (and ongoing) education in the complexities of testing.

We have also been fortunate in assistance and encouragement from the Department of Energy. In particular Dr. Robert Diebold has been helpful to us on a number of occasions. We also benefited from personnel at the Texas National Research Laboratory Commission.

Perhaps the greatest single fact that has emerged from this study is the enormous utility a large helium cryostat can have in fluid dynamics research at low temperatures. We have identified several decades of research which could be done with such a facility, and hope very much that it will be possible to carry through to completion the exciting ideas which have emerged in the study reported here.

Russell J. Donnelly
Eugene, October, 1994

TABLE OF CONTENTS

1. Executive Summary

2 Scientific Program

2.1 Background on Liquid and Gaseous Helium

2.2 Scientific Opportunities in Turbulence Research

2.2.1. The Scaling Regimes in Turbulence

2.2.2. Examples of Scaling in Global Properties

2.2.2.1 The Nusselt number-Rayleigh number correlation

2.2.2.2 The scaling of the energy dissipation

2.2.2.3 The decay rate in grid turbulence

2.2.3. Inertial-Range Scaling

2.2.4. Local Isotropy

2.2.5. The Dissipation Range Scaling

2.2.6. Intermittency Models

2.2.7. The Relation Between the Dissipative and the Inertial Range Scales

2.2.8. Sweeping Time Correlations and Other Quantities

2.2.9. Large Scale and its Influence on the Inertial Range Scaling

2.2.10. Scalars

2.2.11 The Importance of Precise Measurements

2.3 Uses of the Cryostat

2.4 Other Possible Facilities at the SSC

2.5 Other Potential Users

2.6 Competing Facilities

3. The Proposed Facility

3.1 Background on Bénard Convection

3.2 Previous Work on Rayleigh-Bénard Convection

3.3 Helium-4 Near the Liquid Vapor Critical Point

3.4 Choice of Experimental Scales

3.4.1 Scaling Assumptions

- 3.4.2 Boundary Layer Thickness
- 3.4.3 Fluid Velocities and Circulation Frequencies in Thermal Convection
- 3.5 Measurement requirements
 - 3.5.1 Global Measurements
 - 3.5.2 Local Measurements

3.6 Other Uses for the Large Cryostat

4. Supporting Activities

4.1 Collaborating Laboratories and Personnel

- 4.1.1 Postdoctoral Fellows

4.2 Development activities at the University of Oregon

- 4.2.1 Program and Goals
- 4.2.2 Other Experiments

4.3 Summary of Instrumentation Development for Helium Turbulence

- 4.3.1 Average Flow Velocity
- 4.3.2 Use of Laser Doppler Anemometry in Critical Helium Gas.
- 4.3.3 RMS Vorticity
- 4.3.4 Temperature Gradient
- 4.3.5 Pressure Gradient
- 4.3.6 Lift and Drag
- 4.3.7 Flow Visualization
- 4.3.8 Bolometers
- 4.3.9 Wall Stress Gages
- 4.3.10 Ion Measurements

4.4 Verification of Fluid Properties at Duke University

4.5 Grid Turbulence Experiments at Yale University

- 4.5.1. Sweeping Grid in the Helium Cell
- 4.5.2 Temperature Fluctuations in Grid Turbulence
- 4.5.3. A Small-Scale Sweeping Grid Experiment with Water
- 4.5.4 Oscillating Grid Experiment

4.6 Participation by Professor Wu at Northern Illinois University

4.7 Conferences

5. Technical Program

5.1 Conceptual Design of Experimental Apparatus

- 5.1.1 Convection Cell Cryostat
- 5.1.2 Plate System
- 5.1.3 Towed Grid System

5.1.4 Cryogenic System	
5.2 System Operation	
5.2.1 Purification and Cooldown	
5.2.2 Calibration	
5.2.3 Inventory Management	
5.2.4 Inventory at High Densities	
5.2.5 Operation for Data taking	
5.2.6 Time-out Periods, and Warm up	
5.3 Work Breakdown Structure and Assumptions of Infrastructure Support	
5.4 Schedule	
5.5 Cost Estimate	
5.5.1 Capital Equipment Costs	
5.5.2 Labor Costs by Year	
5.5.3 Operating Costs	
5.6 Permits	
5.7 Funding Sources and Alternatives	

6. Cost Summary

7. Bibliography

Appendices

(Note: Appendices are internally numbered)

Appendix A	Report of Consultant
Appendix B	Flow Tunnels and Tow Tanks
Appendix C	Data Sheets
Appendix D	Plate Thermal Issues
Appendix E	Convection Cell Operating Regimes
Appendix F	Dictionary of Work Breakdown Structure
Appendix G	SSC Equipment Assumed to be Available
Appendix H	Detailed Schedule
Appendix I	Detailed Cost Estimates
Appendix J	Capabilities Fact Sheet
Appendix K	Conformance Matrix
Appendix L	Other Possible Sites for the Program

1 Executive Summary

This is a report prepared by a group interested in doing research in thermal convection using the large scale refrigeration facilities available at the SSC Laboratories (SSCL). We report on the research and development opportunities in such a project, the technical requirements and feasibility of its construction and operation, and the costs associated with the needed facilities and support activities.

The facility will be a unique national resource for studies of high-Reynolds-number and high-Rayleigh-number turbulence phenomena, and is one of the items determined as suitable for potential funding through a screening of Expressions of Interest. The proposed facility is possible only because of the advanced cryogenic technology available at the SSCL. Typical scientific issues to be addressed in the facility will be discussed. It devolved during our study, that while the main experiment is still considered to be the thermal convection experiment discussed in our original Expression of Interest, there are now a very substantial set of other, important and fundamental experiments which can be done with the large cryostat proposed for the convection experiment. We believe the facility could provide several decades of front-line research in turbulence, and shall describe why this is so.

Briefly, the goal of the convection experiment is to study thermal convection in critical helium gas up to conditions which begin to match those in the atmosphere and in sunspots. In order to accomplish such a goal, we need to design and build a cryostat which is 10 m high and 5 m in diameter. Nothing approaching this size has ever been built. But once one has such a cryostat, there is a very substantial number of experiments which can be mounted in the same cryostat. These experiments are, of themselves, fundamental to progress in understanding turbulence. Indeed, one can argue that it would make good sense to do one of these experiments, namely the towed grid experiment, before doing the thermal convection experiment. The towed grid is simpler in that it does not need a heated plate; and gaining experience with a simpler experiment would give us good experience with the cryostat, and more time to construct the heated plate, before beginning the main experiment.

A further benefit arises when one considers that there are other devices, such as wind tunnels and tow tanks which can also be operated with refrigeration on the scale available at site N15. These devices are of considerable importance to the testing of submarines and surface ships. We have added an Appendix B to this report containing considerable detail about these possibilities. They are placed in an Appendix because they require construction of facilities beyond the cryostat discussed in this report.

Unique features

1. The device proposed here will allow performance of the highest Rayleigh number convection experiment ever built, or likely to be built. The Rayleigh number approaches within a few orders of magnitude the magnitudes occurring in the atmosphere and the sun.
2. The highest Reynolds number towed grid experiments can also be performed in the facility as well. Other experiments can be inserted directly in the large cryostat. These include towed spheres and cylinders, Taylor-Couette apparatus, and fully instrumented wind tunnels for a variety of experiments. As the facility continues to be used, new ideas are bound to be generated. There is

little experience in the scientific and engineering communities doing high Reynolds number research on this scale.

3. The properties of critical gas and liquid helium I can be varied over a tremendous range. All existing turbulence facilities work with either air or water and the properties of these materials cannot be varied without enormous difficulty.

4. Our experiments will utilize the now idle cryogenic facilities at the N15 site of SSCL in a scientifically productive way at relatively modest cost.

5. The cryostat will open up a number of opportunities for a broad scientific community to become users of the facility.

Potential impact

1. The proposed research will produce lasting results of importance in turbulence - a grand problem of great practical importance and diverse applications.

2. The turbulence problem is a paradigm for problems with spatio-temporal structure and complexity, and advances made there are likely to have broad impact on neighboring fields of nonlinear science.

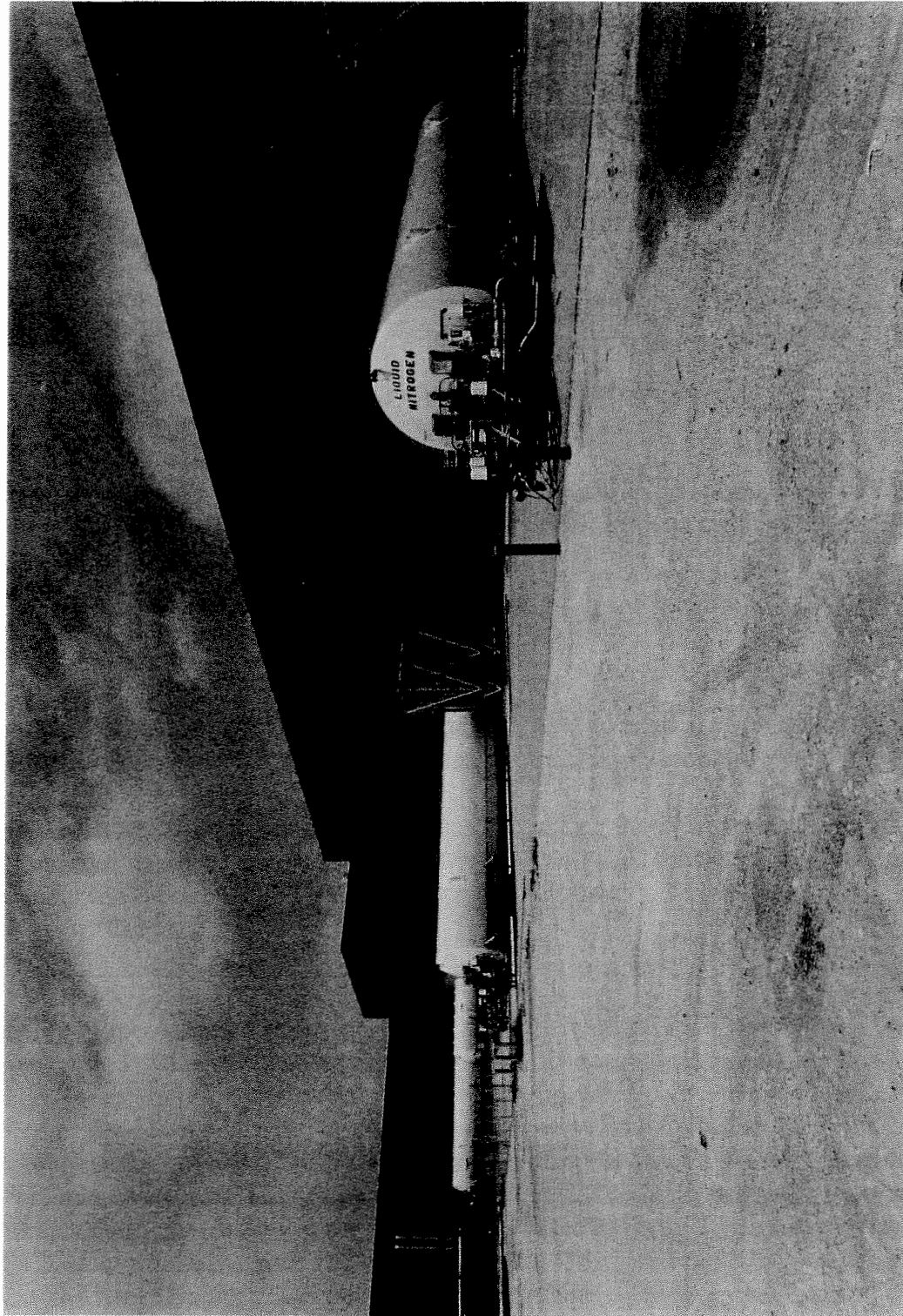
3. Experience gained there will be valuable for constructing helium test facilities in the future at Navy, NASA, Air Force, and other laboratories.

4. Implementation of our proposed facility will produce a new generation of scientists trained broadly in measurement, analysis, and understanding of complex systems.

5. The proposed facility gives an immediate impetus for pushing measurement technology. The increase in Reynolds numbers available will produce an urgent need for the development of technology in the sub-micron range for turbulence measurements.

Low Risk

It should be recognized from the beginning that the technical risk inherent in the proposed facilities construction and in the research program is low. The cryogenic technology that is employed in the program is the product of a long period of development in the national high energy physics laboratories of the country. Also, the scale of the experimental facilities are within the range of existing equipment of similar kinds, and within, also, the capabilities of commercial-sector industry to produce in a straightforward and economical way. The basic instrumentation employed in the experimental program is for the most part also available from commercial suppliers. The thermometry is of a kind widely used and well understood. The instrumentation for velocity measurement, the laser Doppler velocimeter, is a state of the art technology that is considered in the field to be very reliable. Its use in cryogenic situations has, however, been limited up to now to a smaller scale than that contemplated here.



Exterior view of the N - 15 Service building showing cryogenic tankage. The long tanks are for liquid nitrogen and three 44 cu-m liquid helium tanks are installed at this location, only one of which is visible here. The Convection Cell Cryostat is to be installed just in front of the vaporizer that can be seen in the center of this picture. The building height is 14 m and the Cell is 16.5 m high to the top platform.

2 Scientific Program

2.1 Background on Liquid and Gaseous Helium

- What matters in scaling of fluid flows are dimensionless parameters such as the Reynolds number, Re , and the Rayleigh number, Ra , defined respectively as:

$$Re = \frac{UL}{\nu},$$

with

U = characteristic velocity

L = characteristic length

ν = kinematic viscosity

and

$$Ra = \alpha g \Delta T L^3 / \kappa \nu$$

with

α Isobaric thermal expansion coefficient

κ Thermal diffusivity

L Height of convecting layer

ΔT adverse temperature drop across the layer

g acceleration of gravity

The Reynolds number is used as a measure of flow strength in isothermal fluid flows, and the Rayleigh number in scaling thermal convection. Very roughly, $Ra \sim Re^2$

- Most natural phenomena occur on large scales L and hence large Reynolds numbers
- To model such situations in the laboratory with a finite L requires the smallest possible ν
- The smallest kinematic viscosity of any substance which exists belongs to liquid and gaseous helium.
- Therefore the highest Reynolds and Rayleigh number flows which can be created on earth must eventually use helium.

Helium offers three fluids of dynamical interest

- **Critical Helium Gas**

A heavy gas of helium near the critical point at 5.2 K. It is dynamically a classical fluid, but has properties dependent upon temperature T and even more importantly upon pressure P . It is the principal working fluid for the apparatus discussed in this report.

- **Liquid Helium**

- **Helium I:** Liquid helium at temperatures above the lambda transition, 2.2 K. Helium I is known to be a Navier-Stokes fluid.
- **Helium II:** Liquid helium below the lambda transition. Helium II obeys two fluid equations for very slow flows but is a vortex-coupled superfluid at high Reynolds numbers and appears to obey classical scaling laws.

Possibilities for Use of the SSCL Helium Refrigeration Facilities

- Liquid flow tunnels using helium I and helium II
 - for model testing such as for nuclear submarines
 - for turbulence research (could be conceived as a National High Reynolds Number Facility)
- Free surface troughs for tow-testing ship models and for wave research
- Convection experiments using critical helium gas

The helium gas convection experiment is therefore only one of a wide class of experiments which can be undertaken with the proposed facility in such a way as to take advantage of the unique properties of helium at low temperatures. At the 7th Oregon Conference on Low Temperature Physics held in Eugene Oregon in 1989 numerous applications of liquid and near-critical helium gas to research and engineering investigations requiring high Reynolds numbers were discussed. These ideas are presented in a book edited by Russell Donnelly (*High Reynolds Number Flows Using Liquid and Gaseous Helium*, Springer-Verlag 1991). A central point addressed in the articles contained in this book is that Reynolds numbers several orders of magnitude larger are available with helium at low temperature than with room temperature fluids at any particular scale, owing mainly to its extremely low kinematic viscosity. In addition to being a research tool for turbulence, superfluid helium provides its own rich set of properties to study.

It seems inevitable that the applications of helium cryogenics in the area of high Reynolds number phenomena will grow in coming years, driven by the same kind of forces that drove, for example, the application of hard superconductors. In the one case it is the Reynolds number regime

that becomes available, in the other case, the high current densities and low dissipation. There is the same uniqueness of what can be achieved. Further, it seems clear that the large-scale helium cryogenic technology developed in the high energy physics laboratories of the world can be efficiently applied in this developing area. The scale of what is already available in the labs is appropriate, the systems and instrumentation problems are similar, and the expertise that the labs have developed can be applied immediately. Thus there is an opportunity for high energy laboratory technology to be a catalyst in a new field of endeavor.

Of the many possible experiments which can utilize the unique properties of low temperature helium, the large scale helium convection experiment was proposed first and foremost because it is a physics experiment with important theoretical consequences and important application in other branches of science and in engineering. In addition, it is well suited to the capabilities of the SSCL. In particular the refrigeration required and the general scale of the technical activity is consistent with that of the laboratory; the technology involved and the engineering and technical disciplines required are those found at the laboratory in the ordinary run of its business. The major piece of capital equipment needed by the experiment is a large helium tank in the form of a cylinder 5 m in diameter and 10 m in height. If filled with liquid helium, this tank would hold about 200,000 liters. If built, the tank would be the world's largest helium cryostat. The helium tank would be surrounded by vacuum and liquid nitrogen jackets in the usual way. This device can be integrated into the cryogenic facilities of the laboratory after completion of the work. (At SSCL this tank would have become a part of the Collider equipment at N-15.) These considerations also apply in varying degree to locating the experiment at Fermilab, Brookhaven, or CEBAF, but in general the argument is the same.

Although the team that will be involved directly in the construction and commissioning of the facility will be small (to maintain flexibility and to avoid escalated cost and other complications), a significant part of the interested community will be kept involved in advisory capacity as well as by means of two conferences scheduled during the five years of this proposed project. The group of scientists that will form the eventual users of this facility will be much larger than the initial team. Not only is this facility seen as an instrument for fostering several collaborations, but also as a source of education for a number of graduate students who will do their Ph.D. work, as well as a training ground for postdoctoral researchers.

It is our vision that during the scientific life of this facility, several types of high-Reynolds-number and high-Rayleigh-number measurements of lasting value will have been made. These measurements will act as an anchor for all theoretical development to follow. Further, they will be definitive enough that they will be able to distinguish among competing theories, and weed out the incorrect ones. Thus, lasting progress will have been made on one of the grand problems that has challenged many astute minds of this century and the last. The effort will have trained many young scientists on the traditions of solving facets of a complex problem so they may apply that training and knowledge to a variety of others. The potential economic impact and importance for US defense efforts are enormous.

In order to make these latter possibilities more concrete, we will discuss flow facilities and tow tanks in Appendix B.

2.2 Scientific Opportunities in Turbulence Research

Fluid turbulence is undoubtedly the most outstanding problem of classical physics that has remained unsolved to this day. It is a paradigm for spatio-temporal systems with many degrees of freedom interacting strongly nonlinearly. The intellectual stimulus that the turbulence problem has provided for the advancement in nonlinear science and chaos, field theoretical methods, advanced instrumentation, numerical and computational schemes, and so forth, has been extraordinary. On the practical side, turbulence is the "limiting factor" in the design and operation of various energy systems in aeronautical, chemical and mechanical engineering, as well as geophysics, meteorology, and other areas which strongly impact human life. For these reasons, an enhanced ability to understand and predict turbulent flows will have a large payoff. The most eloquent remarks in this regard were made by von Neumann in 1949 (von Neumann, 1949a, 1949b):

"The great importance of turbulence requires no further emphasis. Turbulence undoubtedly represents a central principle for many parts of physics, and a thorough understanding of its properties must be expected to lead to advances in many fields. ... turbulence represents *per se* an important principle in physical theory and in pure mathematics.

... These considerations justify the view that a considerable effort towards a detailed understanding of the mechanisms of turbulence is called for."

These remarks are just as true today.

Turbulence is intrinsically a high-Reynolds-number phenomenon, and it has always been clear that its quantitative understanding requires, most of all, precise data at high Reynolds numbers. (Note that, in the proposed facility, the key parameter is the Rayleigh number, which is roughly proportional to the square of the Reynolds number. Thus, very large Rayleigh number implies large Reynolds number as well.) To quote von Neumann again:

"... our intuitive relationship to the subject is still too loose... (and) we are still disoriented as to the relevant factors..."

At present, there are few opportunities for making detailed and extensive measurements at high Reynolds numbers with the required degree of control and precision. Even those aspects of turbulence which are understood qualitatively still rest on uncertain ground - at least because the theory seeks to understand infinitely large Reynolds numbers. While experiments and numerical simulations have, by and large, been carried out at low or moderate Reynolds numbers, such measurements cannot often make the needed distinction between the predictions of conflicting theories. While the high-Reynolds-number experiments in the atmosphere and oceans have contributed much to our understanding of turbulence, they suffer from the fact that one can only exercise poor control on experimental conditions; these flows are thus not ideal for asking fine questions that can settle crucial issues. It is our contention that well-planned experiments which combine careful experimental control and truly high Reynolds and Rayleigh numbers will provide fundamental new insights into the correct theories of turbulence.

We have examined the availability of various high-Reynolds-number facilities in the world with the following result. First, we know of no facility that will approach the Reynolds number range anticipated in the proposed facility; certainly, there are no facilities in the world today that can

achieve the Rayleigh numbers anticipated in the proposed facility. Second, most available facilities are wind and water tunnels and cannot be used for the convection and heat transfer measurements of the type that are invaluable for astrophysics (for example). Third, some of the existing high-Reynolds-number facilities are housed in mission-oriented government laboratories such as NASA, and are not available for basic research. Fourth, the flow quality of many of the industrial large scale facilities is poor and cannot be used for precision measurements. Finally, the feasibility of this type of apparatus and its usefulness for basic research has been established by the previous experiments carried out at the University of Chicago (see Wu, 1991). It is therefore our contention that the proposed convection facility will be unique in both the parameter range and its accessibility to the research community.

We note here some of the fundamental issues in turbulence which could be addressed in the proposed facility. For more than fifty years, Kolmogorov's ideas have ruled the horizons of research in turbulence physics (see Hunt, Phillips and Williams, 1991), and yet we are unclear about their status as a true theory. To this day we do not know whether Kolmogorov's ideas are exact for turbulence energetics in the inertial range of very large-Reynolds-number flows, or require non-trivial corrections. Experiments have consistently revealed some deviations from Kolmogorov's theory - and these deviations have been attributed to intermittency. But, the finiteness of the Reynolds numbers in the presence of shear, anisotropy and inhomogeneities render these observed corrections susceptible to varied interpretations. The kinematic and dynamic effects of the sweep of small scales by large scales are not understood in the theory of turbulence. In shear flows, for example, one does not know the scale of eddies that accomplish most of the turbulent transport. What is the asymptotic value of the drag coefficient of a sphere? What is the asymptotic Rayleigh number/Nusselt number relation in convection experiments? What is the role of aspect ratio on this relation? How much of the observed structure is due to the presence of the shear and how much is special to flow configuration? How much of the coherent structure observed at low and moderate Reynolds numbers survives at high Reynolds numbers? In particular, do plumes survive at very high Rayleigh number? How does their size scale with Rayleigh number? If they do survive, what shape should an asymptotic theory of their dynamics take? If they do not, what alternative form should the theory take? What role does dissipation-scale intermittency play in turbulence? Do small scales in passive scalars attain an asymptotic state independent of the shear? Do isotherms in the high Rayleigh and Reynolds number limit have a fractal character? What is the asymptotic shape of the probability density functions of velocity and temperature as well as their increments over inertial-range separation distance? Indeed, this is only a partial list of the issues to be settled.

These and other questions cannot be answered with any certainty from available measurements (or measurements possible in available facilities) because many properties of turbulence depend on the Reynolds number rather weakly (probably like power laws with small exponents of the order of 0.15, say). In many instances, the exponents (if such were to exist), cannot be determined with great accuracy unless there is a scaling of the order of three or so decades (never found in any controlled experiment so far). Imagine if one were to discover that there is no strict scaling at high Reynolds numbers (not an implausible scenario according to some investigators). That could set turbulence research on a different course altogether! This brief discussion, we hope, shows the wealth of problems that need to be addressed in a high Reynolds and Rayleigh number facility. We amplify our discussion of a few selected topics below.

2.2.1. The Scaling Regimes in Turbulence

A fundamental assumption in turbulence is that the phenomenon scales - that is, various power laws obtain in certain ranges of scales. The most celebrated among these scaling regions is the inertial range, which alone we shall consider as an illustration here. Empirical evidence from existing spectral measurements roughly suggests that the scaling range in isothermal turbulence is of the order of $Re^{3/4}/30$, where Re is the large scale Reynolds based on the root-mean-square velocity fluctuation and the integral scale of turbulence, or of the order $R_\lambda^{3/2}/300$, where R_λ is the microscale Reynolds number based on the root-mean-square velocity fluctuation and the Taylor microscale. To observe two decades of the spectral scaling, an R_λ of the order 1,100 will be required; to observe three decades of scaling, an R_λ of the order 5,000 will be required. Such high Reynolds numbers have so far been attained only in geophysical flows. Turbulence measurements in geophysical flows have given an enormous boost to the understanding of the scaling behavior, yet these flows are not well-controlled and the effects of spatial inhomogeneities, finite shear and the resultant anisotropy, and so forth, are not well understood. In fact, most available measurements on the high-Reynolds-number end come from shear flows in which the influence on some of the subtle measurements of flow inhomogeneity and anisotropy has not been understood satisfactorily. This situation makes it difficult to answer with complete confidence questions often raised by skeptics that there may be no strict scaling in turbulence, or that the various corrections to scaling vanish extremely slowly in Reynolds number. Since the measurements on which this scaling has been inferred often suffer from uncertainties associated with dubiously small scaling regimes, unexplained or ill-understood effects of shear, high turbulence level, and so forth, in order to establish the existence of scaling unambiguously and determine its precise nature, measurements at high Reynolds numbers and high Rayleigh numbers under controlled conditions are much needed. Below, we shall consider some examples of the type of questions to be explored in the proposed measurements. The list is illustrative, not exhaustive by any means. Two general articles of interest in this context are Frisch and Orszag (1990) and Nelkin (1994).

2.2.2. Examples of Scaling in Global Properties

2.2.2.1 The Nusselt number-Rayleigh number correlation in convection

The classical scaling expected from the marginal stability theory of Malkus (1954, 1963), Kraichnan (1962) and Howard (1966) is of the form

$$Nu = \left(\frac{Ra}{16Ra_c} \right)^{1/3},$$

where Ra is the Rayleigh number and Ra_c is a critical Rayleigh number of the order 1000. Some previous measurements had in fact reported observing the $1/3$ scaling, but the Rayleigh number range covered was rather small. The issue was examined thoroughly in the more recent measurements of Libchaber and colleagues at the University of Chicago (see, e.g., Wu 1991). They found that the exponent is about 0.285 ± 0.005 , even at Rayleigh number as high as 10^{11} . This result was quite surprising. Is this the scaling appropriate to infinite Rayleigh number, or is there a $1/3$ power-scaling at even higher Rayleigh numbers (because relatively robust arguments suggest that this might be so)? Equally simple arguments (Ed Spiegel, private communication) suggest an asymptotic half-power law. Although the experiments of Libchaber and Wu made at aspect ratios of

0.5, 1.0 and 6.7 yielded the same exponent, the question of the appropriate power-law for large aspect ratios is still unresolved. One strong motivation for the present measurements is to resolve the question of this scaling in the high-Rayleigh-number and high-aspect-ratio limit.

2.2.2.2 The scaling of the energy dissipation:

One of the premises on which the entire phenomenology of turbulence rests is that the average energy dissipation rate, $\langle \epsilon \rangle$, is independent of the fluid viscosity, and that it is determined entirely by the large-scale motion. Thus, we have the expectation that

$$\langle \epsilon \rangle = A u^3 / L$$

where A is a constant of the order unity, u is the root-mean-square velocity, and L is an integral scale of turbulence. All available measurements in grid turbulence as well as shear flows has been examined by Sreenivasan (1984, 1994). One must confess that, while the available data are suggestive of this relation, they do not support this result unambiguously. If the only unambiguous result to emerge from the proposed grid-turbulence measurements is the verification of this relation, it is our opinion that the measurements would be worthwhile.

2.2.2.3 The decay rate in grid turbulence

This is an old problem on which theory and measurements abound. Similarity considerations originally suggested a power law for the energy decay to be of the type

$$u^2 \sim t^{-1}.$$

Indeed, early measurements at Cambridge University seemed to suggest this to be true. It was later found (e.g., Comte Bellot and Corrsin 1966) that the power law has an exponent of about 1.27, not very different from the value $10/7$ expected from Kolmogorov's (1941) inertial-range scaling arguments at high Reynolds numbers (see below). In recent years, it has been recognized that initial conditions can have lasting influence on the decay rate (e.g., Reynolds 1990, George 1992). A decisive experiment has not yet been performed; the difficulty is not just one of Reynolds number, but also that the decay rate in conventional wind tunnel experiments can be observed only for a decade or a decade and a half in distance behind the grid (note the presumed equivalence between time and space in this instance). In decay experiments using a swept-grid experiment as proposed here, the power law can be expected to proceed uninterrupted for much longer times (e.g., Walker 1986), and this would provide the proper decay exponent, at least for a certain type of initial conditions. Further, changing initial conditions suitably would not be a problem.

2.2.3. Inertial-Range Scaling

The phenomenological arguments of Kolmogorov (1941) that allow us to deduce the scaling relation for the so-called structure functions, namely moments of velocity increments over a separation distance r , are too well known to need recalling here. The final result is that

$$\langle (\Delta u)^n \rangle = C_n \langle \epsilon \rangle r^{n/3}$$

where Δu is $u(x+r) - u(x)$, where the separation distance r is in the direction of the velocity component u and C_n , for all even n , are universal constants. (For odd n , one might take absolute values of velocity increments.) A special case of this equation is obtained via the Fourier transform of the second-order structure function which yields the result that the power spectral density is given by

$$\phi(k) = C_k \langle \epsilon \rangle^{2/3} k^{-5/3}$$

where k is the wave number, the spectral density $\phi(k)$ is defined such that its integral over all k yields the mean-square of the velocity component u , and C_k is a constant. This power law with an exactly known exponent has justifiably lured many people to attempt its verification, use, and formal understanding.

Alas, the situation is uncertain even today. Experiments show an approximately 5/3 region (in power spectrum as a function of the frequency, which is converted to wavenumber via the so-called Taylor's hypothesis), but the uncertainties mentioned early in this section do not preclude the possibility of an anomalous correction to the 5/3 slope. Some people (e.g., Kraichnan 1974, Chorin 1994, Yakhov 1994) have argued in different ways that the 5/3 exponent could well be exact; whereas there is a whole "industry" based on intermittency, starting with Kolmogorov (1962) and Obukhov (1962), which argues that there is a definite correction. Experiments (again based on Taylor's hypothesis) conclusively show that the exponents for high-order structure functions are not $n/3$ but substantially smaller (e.g., Anselmet et al. 1984 and some later papers which are in essential conformity with these previous measurements), but there are new theories (see later) which suggest that these are artifacts of finite shear and finite Reynolds numbers. There is probably no other single issue that has occupied the attention of researchers in turbulence than the scaling of inertial range structure functions. We believe that the only way to resolve this issue is to make definitive measurements at high enough Reynolds numbers where there is unambiguous scaling.

The same comment applies to all fractal scaling purported to apply to inertial range properties of turbulence (e.g., Sreenivasan, 1991a). Finally, it should be pointed out that the meaning of "high enough Reynolds number" is quite different for different quantities.

2.2.4. Local Isotropy

As has been emphasized by Nelkin (1994), the question of whether small scale and inertial range scales are isotropic at high Reynolds numbers is not a black and white issue. For example, when there is a strong mean wind as in the convection experiments with aspect ratio of the order unity, it is clear that its effect will be felt by various neighboring scales and become increasingly smaller as the scale size decreases. A good characterization of these effects is important for a good understanding of the way shear influences various aspects of scaling.

2.2.5. The Dissipation Range Scaling

Kolmogorov's arguments also suggest a certain form of the spectral density in the dissipation range of scales, but the evidence for its applicability (see, for example, Monin and Yaglom 1975) leaves a lot to be desired. There are alternative suggestions based on the multiscaling idea (Castaing et al. 1993), but the evidence for their applicability is not completely satisfactory either. The biggest pitfall has been the lack of reliable high wavenumber measurements. Of particular interest is the question of whether the high wavenumber spectral density is exponential (Foiás et al, 1990).

2.2.6. Intermittency Models

The fact that the small scales (both dissipative and inertial) in turbulence are intermittent in three-dimensional space (and perhaps time as well) has been appreciated for a long time. Many models, most of them based on the multifractal picture of turbulence (Mandelbrot 1974, Frisch &

Parisi 1985), purport to describe the observed intermittency in the energy dissipation rate and inertial range quantities (for a summary of these models, see Meneveau and Sreenivasan 1991; for some later developments, see, She and Levesque 1993, She and Waymire 1994). Of interest is the influence of intermittency on the spectral form discussed earlier, or the scaling of high-order structure functions. The verification of some details (see Meneveau and Sreenivasan 1991) need experiments at high Reynolds number, again because of the definitive scaling expected.

In addition to this generic need for high-Reynolds-number measurements, there is some urgency newly injected from some recent developments. There is some recent thinking that the inertial range is not intermittent (e.g. Grossmann and Lohse 1994), and that all the corrections that experimentalists have painfully deduced to be true are artifacts of the finite Reynolds numbers (L'vov et. al. 1994). This remains to be examined.

2.2.7. The Relation Between the Dissipative and the Inertial Range Scales

The best known work purporting to express the relation between the two ranges of scales is the so-called refined similarity hypothesis of Kolmogorov. In the simplest form, for separation scales r in the inertial range, the refined similarity hypothesis says that

$$\Delta u_r = V(r \epsilon_r)^{1/3}$$

where Δu_r is the velocity increment over a separation distance r , ϵ_r is the average of the energy dissipation rate ϵ and V is a universal stochastic variable independent of r and ϵ_r . Its verification has been attempted by several authors (for example, see, Stolovitzky et al, 1993), but there are many open questions: the precise nature of the relation for different components of ϵ_r are used, the precise shape of V itself, the deterministic relation between the inertial range scales and the dissipation scales in the presence of coherent structures (see figures 2(b) and 2(c) of Stolovitzky et al.), recent theoretical papers based on shell model calculations questioning the validity of the above relation (e.g. Grossmann and Lohse 1994), and so forth.

2.2.8. Sweeping Time Correlations and Other Quantities

In spite of the various corrections and remedies for the shortcomings of the original ideas of Kolmogorov, it is clear that they do work "reasonable well" (whatever that means exactly) for equal-time correlations of low order. When applied to other quantities such as Eulerian frequency spectra in flows with no mean motion, time correlations in a Lagrangian frame of reference, spectra of accelerations, kinetic energy, as well as high powers of velocity, etc., the performance of Kolmogorov-type arguments is not clear. The primary theoretical issue is related to the sweep of the small scales by the large scale motion. Those of us who have tried to characterize such features have been frustrated by the lack of high Reynolds number data under controlled conditions. We expect significant progress with the experiments proposed here.

2.2.9 Large Scale and its Influence on the Inertial Range Scaling

It now appears that we are evolving to a view of turbulence where "universality", even of small scale structures, has to incorporate the large scale explicitly. For this, as well as for reasons of intrinsic interest, the large scale is a key element in the turbulence theory. A proper theoretical

formulation which incorporates the large scale explicitly is still lacking, but rapid progress appears possible.

A similarly important question concerns the proper correlation between the energetic motion and the dissipative scales.

2.2.10. Scalars

Turbulence is an efficient mixer of scalars such as a dye, heat or species. Passive scalars are those that do not affect turbulence dynamics. For example, small amounts of heating introduced into a turbulent flow does not affect its dynamics, and the temperature is then considered a passive scalar. Large amounts of heating will cause density differences and result in buoyant forces, making the heat not longer passive. The mixing problem for passive scalars is seductive because of its simplicity (the governing equation is linear albeit with stochastic coefficients that are solutions of Navier-Stokes equations). There are serious questions of universality of the motion of passive scalars (e.g., Sreenivasan 1991b), and many distinctly ill-understood aspects of temperature fluctuations in convection experiments of Libchaber and colleagues (e.g., see the Ph.D. thesis of Wu).

2.2.11. The Importance of Precise Measurements

In the discussion above the accuracy of data needs to be explicitly emphasized. The data with which turbulence experts work has been collected over a period of many decades, often with less control of experimental conditions than is desirable. The project we are describing here will open the entire arsenal of condensed matter physics techniques to turbulent flows. This by itself should result in a revolution in the field.

We are aware of the fact that the large cryostat we are designing is on an unprecedented scale in low temperature physics. We are being careful to attempt simultaneous modern measurements in ordinary scale laboratories to guide us with the experiments in the large facility.

2.3 Uses of the Cryostat

The authors of this report have been surprised and pleased at the number of different experiments which could be done with the proposed facility. It is no exaggeration to say that we have identified enough experimental work to stretch over several decades. The very size of the facility encourages one to think in radically different terms than one is used to in either low temperature physics or fluid mechanics. Let us list some of the possibilities we have thought of: more details will be given in the technical sections to follow.

- The small aspect ratio, high Rayleigh number convection experiment. This is the chief aim of this report.
- Adjustable aspect ratio convection experiment. Here we plan to move the cooled upper plate downwards to make the aspect ratio larger (but of course at the expense of the highest Rayleigh numbers).
- Operation of the experiment in helium I.

- The towed grid experiment. Here a grid is towed upwards through the gas and the decay of the turbulence left behind is observed. We present some arguments that this should likely be done before the thermal convection experiment as it is the simplest experiment one can do in the tank, yet of fundamental importance in its own right.
- The oscillating grid experiment. Here the grid is drawn to the top of the apparatus and oscillated with some amplitude and frequency while observing the turbulence so created propagate down the tank.
- The turbulent burst experiment. Here again the grid is set near the top of the cryostat and impulsively drawn upward. This is known from work at Oregon to create a turbulent burst which will travel down the tank.
- The towed sphere experiment. Here a wire and pulley system is installed to tow a sphere at various speeds up the tank while measuring the drag. The same general idea can be carried out with other objects such as ellipses and cylinders.
- Taylor-Couette flow. Here a pair of independently driven concentric rotating cylinders is placed in the tank.
- Wind tunnel. Here a fan, test section and diffuser are lowered into the tank. Almost endless variations and elaborations of this arrangement can be conceived.

2.4 Other Possible Facilities at the SSC

Flow tunnels and tow tanks are possible uses of the same cryogenics as for the convection tank. We have not had sufficient time to study these in detail, but what we have learned is assembled in Appendix B.

2.5 Other Potential Users

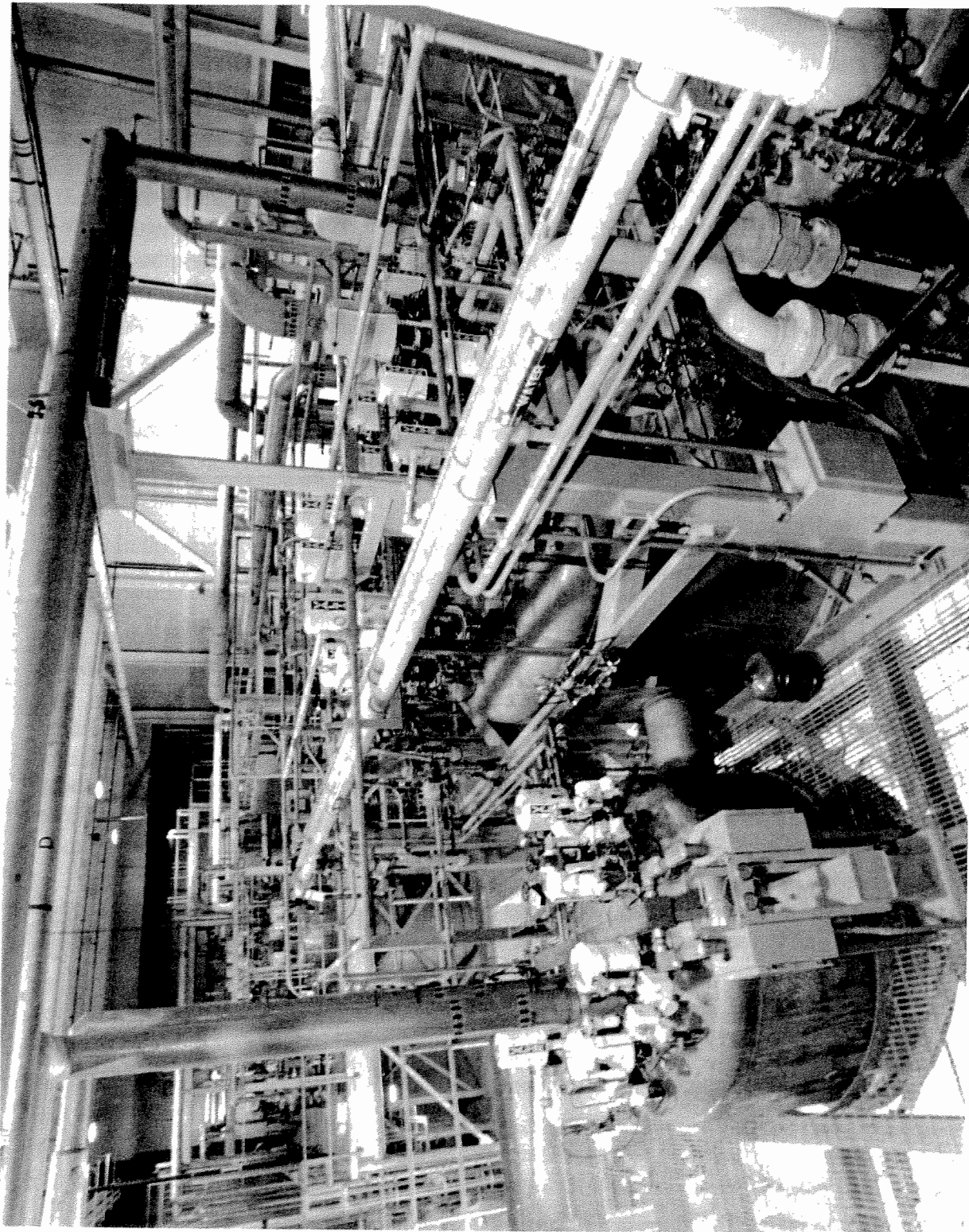
It should be clear from the discussion above that there is far more work to be done with the convection tank than could be accomplished in the careers of some of the authors of this report. We expect other groups will wish to use these facilities for the various experiments outlined above, and undoubtedly, for uses we have not thought of.

We propose to have two conference/workshops during the five year period of this work, one in the second year and one in the fourth year. This is the most direct way we can think of to get the advice, and hopefully involvement of other investigators.

Some means will need to be thought of to allow other groups to propose experiments, seek funding, and get time on this facility. An advisory committee with fairly broad representation from interested communities could be set up. There are many models of such use of central facilities in the United States and other countries.

2.6 Competing Facilities

It is important to realize that there are absolutely no competing facilities of the type discussed here anywhere in the world.



The interior of the N - 15 Service Building showing the cold boxes of two 4.5 kW helium temperature refrigerators. The top of one cold box with its attached turbine pod is seen in the foreground and the equipment of the second plant, N-15B, is seen in the background.

3 The Proposed Facility

3.1 Background on Rayleigh-Bénard Convection

Before proceeding to a technical discussion of the proposed facility, a description of Rayleigh-Bénard convection is appropriate. Intuitively, this is a very simple system. A layer of fluid of height L is heated from below and cooled from above. The result is a temperature difference ΔT and an associated gradient in the density ρ . For typical fluids with a positive thermal expansion coefficient, the denser fluid lies above the less dense fluid, creating a gravitationally unstable configuration. For small ΔT , the layer remains at rest. But if ΔT is large enough, convection will occur. Just above the onset of convection, the flow takes the form of closed circular stream lines. If the flow is visualized from above, the flow pattern consists of bands of up-and-down flows called convection rolls. With further increases in ΔT , the rolls become unstable. This typically results in unsteady or time dependent flow. With yet further increase in ΔT , the time-dependence passes through a chaotic regime where the rolls are still identifiable, but where the motion is difficult to predict. For even larger ΔT , the roll structure is lost, and turbulent flow sets in. Most of the temperature difference across the layer is now restricted to narrow boundary layers of thickness λ near the upper and lower horizontal boundaries.

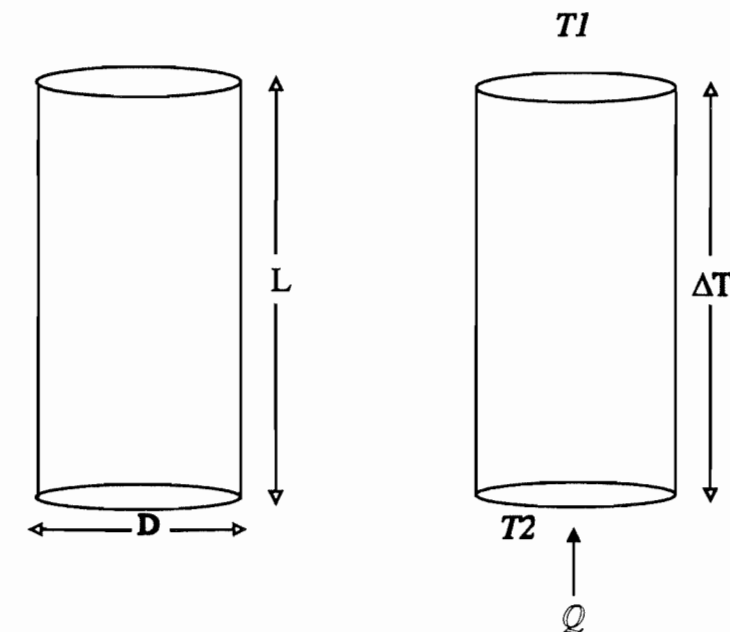


Figure 3.1 Basic quantities used in discussion of thermal convection.

There are several parameters which determine the character of the flow. These quantities are listed above. The key control parameter is the Rayleigh number, Ra , which is a dimensionless measure of ΔT . The dynamical equations for Rayleigh-Bénard convection contain only Ra and the Prandtl number $Pr = \nu / \kappa$.

In addition, the flow depends on the geometry of the container, as expressed by the aspect ratio $\Gamma = H/L$, where H is a characteristic horizontal size for the container, in our case the diameter

In addition, the flow depends on the geometry of the container, as expressed by the aspect ratio $\Gamma = H/L$, where H is a characteristic horizontal size for the container, in our case the diameter D . Thus, the scaled flow properties should be the same for two systems having the same set of parameters Ra , Pr and Γ (assuming that the geometry remains unaltered). For instance, the Prandtl number of low temperature helium is comparable to that for room temperature air.

The structure of flows as a function of Ra is important for understanding the reasons for a large scale convective turbulence experiment. The larger the Ra , the larger is the range of scales excited in the turbulent flow. Ra can be made large by choosing the fluid such that the combination $\alpha/\kappa\nu$ is large, by making ΔT large, or by making L large. To our knowledge, low temperature helium is the optimum fluid by a substantial margin for making $\alpha/\kappa\nu$ large. Although, in principle, ΔT could be made large, this is undesirable because the fluid will then no longer obey the Boussinesq approximation, rendering the theory considerably more difficult. For instance, for large ΔT , the density could no longer be assumed to depend linearly on temperature. Because Ra depends on the third power of L , extremely large Rayleigh numbers can be attained by making L large. Thus, by scaling L by a factor s , and otherwise leaving the system unchanged, Ra changes by s^3 . We will consider this point below when we discuss some of the technical design issues.

The heat flux, q , plays an obviously important role in Rayleigh-Bénard convection, since it generates the temperature difference, ΔT . Note that $q = Q/A$ where A is the cross-sectional area of the apparatus, and Q is the heat current. It is convenient to define a dimensionless measure of the heat transport, the Nusselt number, Nu : $Nu = Q/Q_c$ where Q_c is the portion of the heat current carried by conduction alone. Note that Nu depends only on the dimensionless parameters of the problem, i.e. Ra , Pr and Γ .

3.2 Previous Work On Rayleigh-Bénard Convection

Rayleigh-Bénard Convection is a huge field of research which we can scarcely do justice to in a report such as this. However the interested reader can consult the monograph by Chandrasekhar (1961), a review by one of us (Behringer, 1985) and a recent book by Koschmieder (1992). However the most significant of this past work for our purposes is contained in the articles by Threlfall (1975), Wu (1991) and Wu and Libchaber (1991).

Table 3.1

Summary of Definitions of Quantities Used in This Section

Geometrical parameters

- L Height of cell
- R Radius of cell
- D Diameter of cell
- Γ Aspect Ratio= D/L
- A Area of cell $A = \pi R^2$

Fluid properties

- ρ Density (g/cm^3)
- α Isobaric thermal expansion coefficient (K^{-1})
- μ Dynamic viscosity (*poise*)
- ν Kinematic viscosity (cm^2/s)
- k Thermal conductivity ($Wcm^{-1}K^{-1}$)
- C_p Specific heat at constant pressure ($Jg^{-1}K^{-1}$)
- κ Thermal diffusivity (cm^2/s)
- κ_T Isothermal compressibility ($cm^2/s^2/g$)

Flow properties

- $\Delta T = T_2 - T_1$ = temperature difference across the cell (K)
- Q Heat current (W)
- q Heat flux = Q/A (W/cm^2)
- Q_c Heat current from conduction only (W)
- Nu Nusselt number = Q/Q_c
- Ra Rayleigh number $Ra = \alpha g \Delta T L^3 / \kappa \nu$
- Re Reynolds number = $\nu L / \nu$, where ν is a characteristic velocity

Other properties

- g Acceleration of gravity

3.3 ^4He near the liquid-vapor critical point

The special properties of ^4He near its critical point make it an exceptional fluid for studies of high Reynolds turbulence. In this section, we review these properties, and indicate why they are so useful for studying convectively driven turbulence.

Figure 3.2 shows various aspects of the phase diagram of ^4He . In particular, part *a* of that figure shows the P - T phase diagram. The coexistence curve (CXC) separates the liquid from the vapor states (typified by sample isochores); this curve terminates in the critical point, P_c, T_c . At this point, $T_c=5.19\text{ K}$, $P_c=1706\text{ Torr}$; the corresponding density is $\rho=0.069\text{ g/cm}^3$ (Kierstead, 1973).

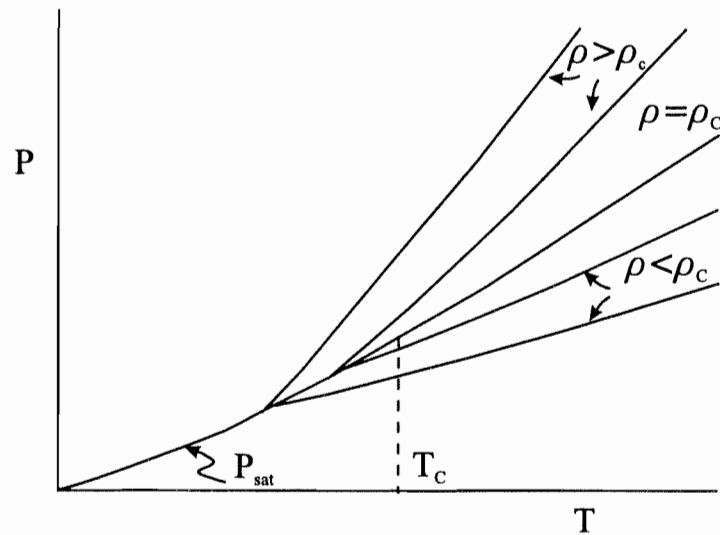


Fig 3.2a Phase diagram for helium near the critical point showing a sketch of the P - T diagram. The coexistence curve (CXC) terminates at the critical isochore. Other isochores lie below ($\rho < \rho_c$) or above ($\rho > \rho_c$) the CXC.

Part *b* shows typical isobars. This part of the figure also indicates why fluids near a critical point are useful for generating large Rayleigh numbers. In the two-phase region, isotherms and isobars are horizontal. As the critical point is approached, these curves remain flat. As a consequence, the compressibility $\kappa_T \equiv \rho^{-1}(\partial\rho/\partial P)_T$ and the expansion coefficient, $\alpha \equiv -\rho^{-1}(\partial\rho/\partial T)_P$ both diverge strongly at the critical point. Indeed, simple thermodynamics indicates that these two are simply related as $\alpha = \kappa_T(\partial P/\partial T)_P$; the slope $(\partial P/\partial T)_P$ is a non-zero constant at the critical point.

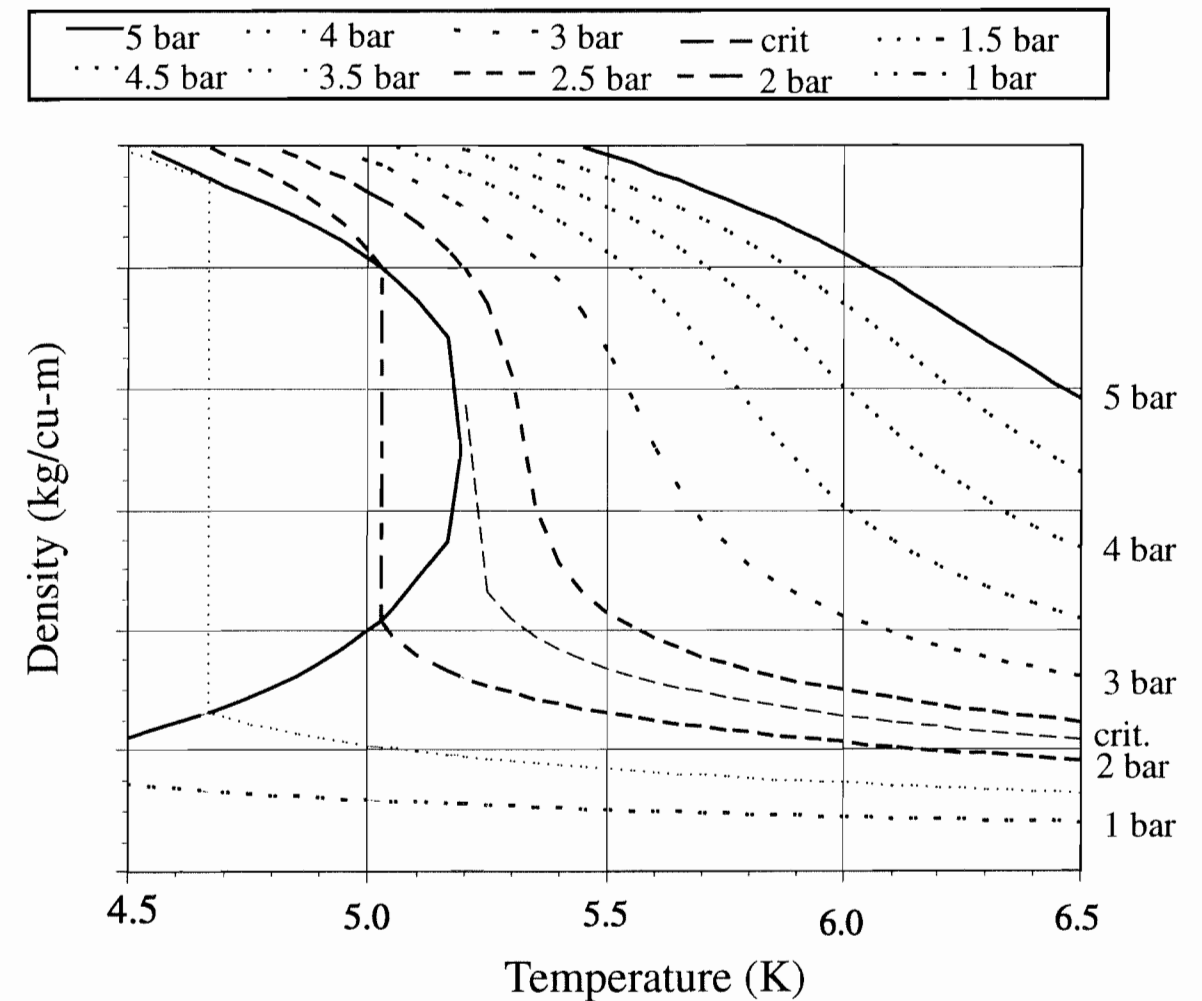


Figure 3.2b Phase diagram for helium showing P vs ρ for isobars near the critical point.

The behavior of thermo-hydrodynamic quantities near the critical point are typically characterized by power laws. The strong divergence of the compressibility and expansion coefficient is characterized along the critical isochore by the power law:

$$\alpha = \Gamma |\epsilon|^{-\gamma}$$

where $\gamma \approx 1.24$, and

$$\epsilon \equiv (T - T_c) / T_c$$

Singularities also occur in the specific heats. In particular, the specific heat at constant molar volume has a weak divergence along the critical isochore or the CXC:

$$C_v \equiv A |\epsilon|^{-a}$$

where $a \approx 0.11$, and A is a constant which depends on the sign of ϵ . Simple thermodynamics relates the specific heat at constant P to that at constant molar volume, v :

$$C_p = C_v + T v \alpha^2 / \kappa_T$$

The dominant terms in this expression come from the ratio α^2 / κ_T , so that C_p also has a strong divergence characterized by the exponent γ .

Various transport coefficients also come into play, and their properties near the critical point are important. The shear viscosity μ has a very weak singularity (the critical exponent is ~ 0.05); for practical purposes, it is nearly constant. On the other hand, the thermal conductivity k has a moderately strong divergence:

$$k \sim |\epsilon|^{-\gamma/2}$$

On combining all this information, we obtain the fact that the combination of fluid parameters which appears in Ra , $\alpha/\nu\kappa$, should diverge (along the critical isochore) as

$$\alpha/\nu\kappa = B|\epsilon|^{-x}$$

where $x = 3\gamma/2 \cong 2$. This is a very rapid divergence indeed, and allows an experimenter to obtain large values of Ra for moderate values of ΔT . It is also important to emphasize that the constant B is particularly large for helium, making it an excellent fluid for turbulent convection experiments.

An important issue is the actual size of the Rayleigh numbers which can be achieved. Ra depends on both the height of the convection layer, L , and on the fluid parameters. Indeed the L^3 dependence of Ra on L is crucial to the functioning of this experiment. With all other quantities held fixed, the Rayleigh number will increase by a factor of eight, nearly an order of magnitude for each doubling of L . Consequently, the largest feasible height is needed to attain very large Ra , and hence, very large Reynolds number, Re .

In designing a very large Ra experiment, the object is to maximize Ra by making L large and by choosing the operating point in an optimum manner. We consider this design feature for liquid helium in Table 3.1 and in Figure 3.3. Table 3.1 presents data for a number of different values of P and T for 4He . In all of these cases, the height of the convection layer is assumed to be $L = 10$ m, the height of the proposed experiment. This table contains information on a large variety of measures, and for the present, we focus on just the value of Ra which can be obtained. The first six cases correspond to P 's and T 's in the low temperature regime, whereas the seventh case pertains to room temperatures. This last case is included to indicate the enormous advantage accruing to low temperatures. All of the low temperature cases yield Rayleigh numbers of 10^{17} to 10^{19} , with typical $\Delta T \sim 0.5K$. By contrast, the high temperature case, case 7, yields a Rayleigh number of only $Ra \sim 10^{11}$ with $\Delta T = 50K$.

Table 3.2
Possible Convection Cell Operating Points

Case	1	2	3	4	5	6	7
Ave Density kg/m ³	20.00	37.50	10.00	16.00	70.00	70.00	0.16
Ave Temp. K	5.172	5.504	5.000	6.275	6.065	5.550	300.00
Pressure, bar	1.54	2.39	0.88	1.71	3.85	2.90	1.02
ΔT , K	0.56	0.56	0.50	0.50	0.50	0.10	50.00
Pr (at ave T)	1.14	1.99	0.88	0.91	2.44	4.56	0.66
Ra	4.87×10^{17}	4.57×10^{18}	6.86×10^{16}	1.00×10^{17}	1.01×10^{19}	1.05×10^{19}	7.34×10^{10}
Q-Factor	-5.26	-20.01	-2.22	-1.92	-1.69	-1.32	-1.85
X-Factor	0.638	0.165	0.842	0.848	0.645	0.774	0.879
$\gamma_0 = \Delta\rho/\rho$	0.265	1.600	0.152	0.131	0.473	0.238	0.168
$\gamma_1 = (\Delta\alpha/\alpha + \Delta\rho/\rho)/2$	0.436	1.829	0.190	0.169	0.294	0.170	0.168
$\gamma_2 = \Delta v/v$	-0.308	-0.621	-0.226	-0.179	-0.276	-0.125	-0.283
$\gamma_3 = \Delta\lambda/\lambda$	-0.045	0.453	-0.080	-0.047	0.164	0.085	-0.115
$\gamma_4 = \Delta C_p/C_p$	0.318	1.827	0.073	0.073	0.100	0.115	0.000

Additional information on the Rayleigh numbers which can be reached if $\Delta T = 0.5\text{K}$, and $L = 10\text{ m}$ is given in figure 3.3. Each curve corresponds to a different density of the helium. It is immediately obvious that the largest Ra 's can be reached by using relatively large densities, and that the largest Ra 's typically occur for $\rho \sim 70\text{ kg/m}^3$ at all cryogenic temperatures. Indeed these Rayleigh numbers can be made as large as $Ra \sim 5 \times 10^{19}$, a value which is otherwise impossible to obtain except in the very uncontrolled geophysical environment.

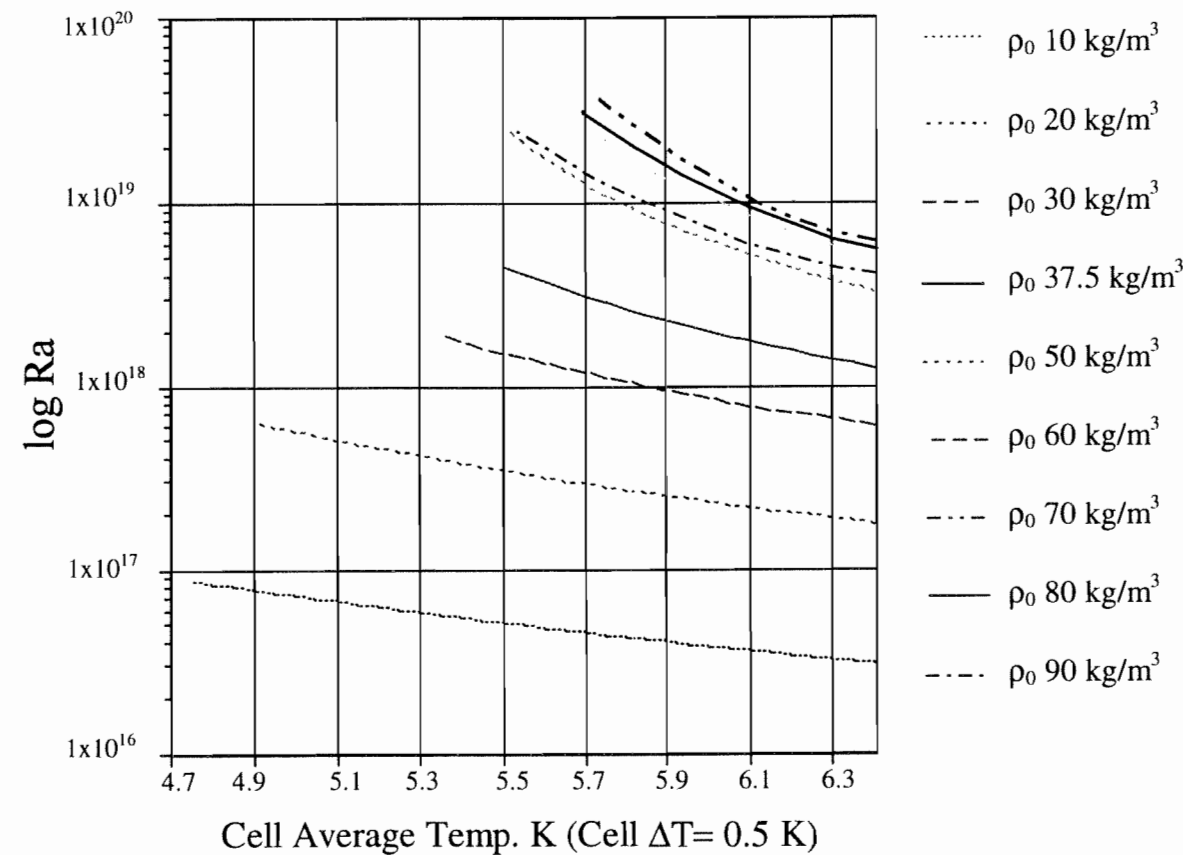


Figure 3.3. Critical Rayleigh numbers obtainable for various densities.

The Prandtl number is also of interest. Data for this quantity are given in figure 3.4. Prandtl numbers ranging from a bit less than 1 to ~ 4 are possible. For the largest Ra 's, the Prandtl number is about 4.

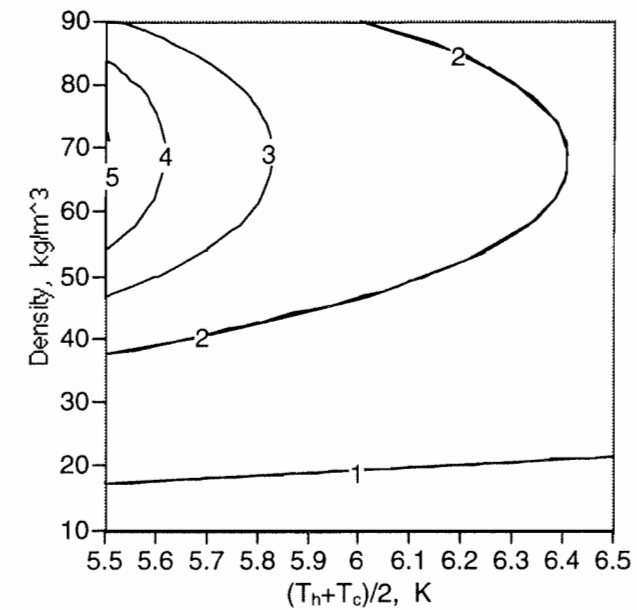


Figure 3.4 Data for the Prandtl number for low-temperature helium.

Large Ra can clearly be reached under the circumstances assumed above, but large Ra alone is not sufficient. If the material properties change too much throughout the fluid layer, then the Oberbeck-Boussinesq (OB) approximation (Oberbeck, 1879) ceases to be valid. In that event, it becomes difficult to make valid comparisons between existing theory, which is based on the OB approximation, and experiment. For convection at moderate Ra , i.e. for Ra near $Ra_c \approx 2000$, there is a well developed theory (Busse, 1967) to determine the effects of departures from the OB approximation. For the large Ra 's relevant to turbulent convection, the theory for non-OB effects is not as well developed. In this case, the temperature difference across the layer occurs almost entirely in two very thin boundary layers, one near the top bounding surface, and the other near the bottom bounding surface. Outside the boundary layers, in the vast bulk of the fluid, there is minimal temperature variation: the rapid flow maintains the fluid at nearly isothermal conditions. Hence, the fluid within the flowing region likely satisfies the OB approximation well. However, the dynamics at large Ra may depend on the boundary layers at the top and bottom of the convection layer, and it is important that the material properties at these two ends of the experiment be as nearly equal as possible. Necessarily, there will be differences in these properties, most importantly the thermal conductivity, because the two extremes of the cell differ by ΔT . The issue of how any differences in the properties at the boundary layers affect an experiment has been considered empirically by Wu and Libchaber (1991) in the context of some of their experimental results. In the paragraphs below, we discuss each aspect of departures from the usual assumptions of the OB approximation.

Near onset of convection for horizontally infinite (or experimentally a large aspect ratio) layer, the degree to which the Boussinesq approximation is satisfied can be characterized by the parameter P of Busse (1967):

$$P \equiv \sum \gamma_i P_i$$

where the summation extends over the five weakly Pr -dependent quantities P_i calculated by Busse, and the five quantities γ_i . Each of the latter is a factor of ΔT times, respectively, the logarithmic derivatives of ρ, α , (with an additional factor of $1/2$), ν, k , and C_p . The pattern which

is selected, either rolls or hexagons, depends on P and Ra (and also weakly on Pr). Very near onset, there is a hysteretic transition to hexagons. With increasing Ra , both hexagons and rolls are possible stable patterns, and finally, with a further increase of Ra to $Ra > Ra_b$, only rolls are stable. The region between the creation of hexagons and the transition to rolls at Ra_b is usually very small. For a typical case relevant to hard turbulence with $Ra \approx 10^{17}$ to 10^{18} , the parameter P can be kept as low as $P \approx 1$ to 2 , depending on the operating temperature and density. This is seen clearly in Figure 3.5, which presents data for P in the vicinity of the critical point.

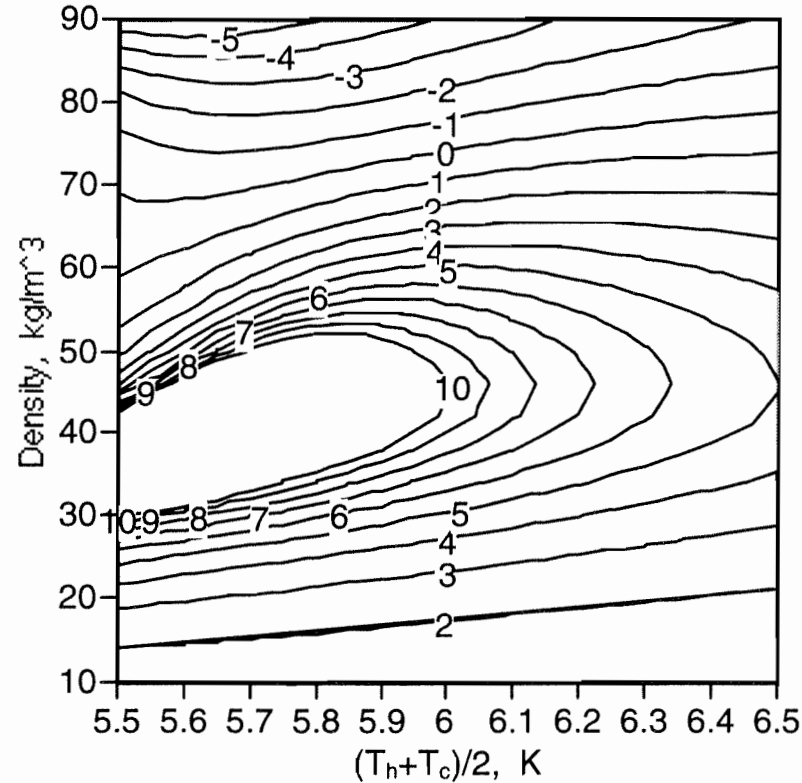


Figure 3.5 Data for Busse's parameter, P for helium near its critical point.

In that event, $(Ra_b - Ra_c) / Ra_c < 5 \times 10^{-2}$, and for any practical purposes, the effect of hexagons is irrelevant for large Rayleigh number flows. For the proposed experiments at small aspect ratio, the pattern near $Ra \approx Ra_c$ is strongly influenced by the vertical boundaries. However, the analysis of Busse strongly suggests that the issue of rolls versus hexagons is not a significant issue for the proposed experiments.

Of some concern is another effect discussed by Wu and Libchaber (1991). At the largest temperature differences and Rayleigh numbers which these experimenters considered, the fluid properties (in particular the thermal conductivity k) near the upper boundary can differ measurably from those at the lower boundary. Hence the two boundary layers may differ. Wu and Libchaber observed kinks in the data for $Nu(Ra)$ and for the RMS temperature fluctuations vs Ra which they attributed to these differences at the two boundary layers. These kinks occurred when the temperature difference across the upper boundary layer fell significantly relative to that across the lower boundary layer. The ratio of these two temperature differences is quantified by their ratio x . Thus, $x \approx 1$ implies that the two boundary layers are similar. On the other hand, Wu and Libchaber observed that the distribution of temperature fluctuations was not

strongly affected. Indeed, as noted the majority of the temperature difference across the fluid occurs in the two boundary layers near the top and bottom boundaries, while the central region is nearly isothermal. These investigators argued that the two boundary layers have a common value of a characteristic temperature scale set by

$$\Theta = \nu \kappa / g \alpha \lambda^3,$$

where the boundary layer thickness can be determined by integrating

$$q = -k \nabla T$$

across the boundary layer. This leads to the result that either boundary layer is given by

$$\lambda_i q = k_i \Delta T_i$$

where "i" is either t for top or b for bottom, and where ΔT_i refers to the measured temperature difference across the boundary layer. Also, k_i is the thermal conductivity at each boundary layer, or more properly, the average conductivity of each boundary layer,

In terms of the proposed experiments, several points are noteworthy. First, in the proposed experiments, x can be kept close to unity, as seen in the data of figure 3.6.

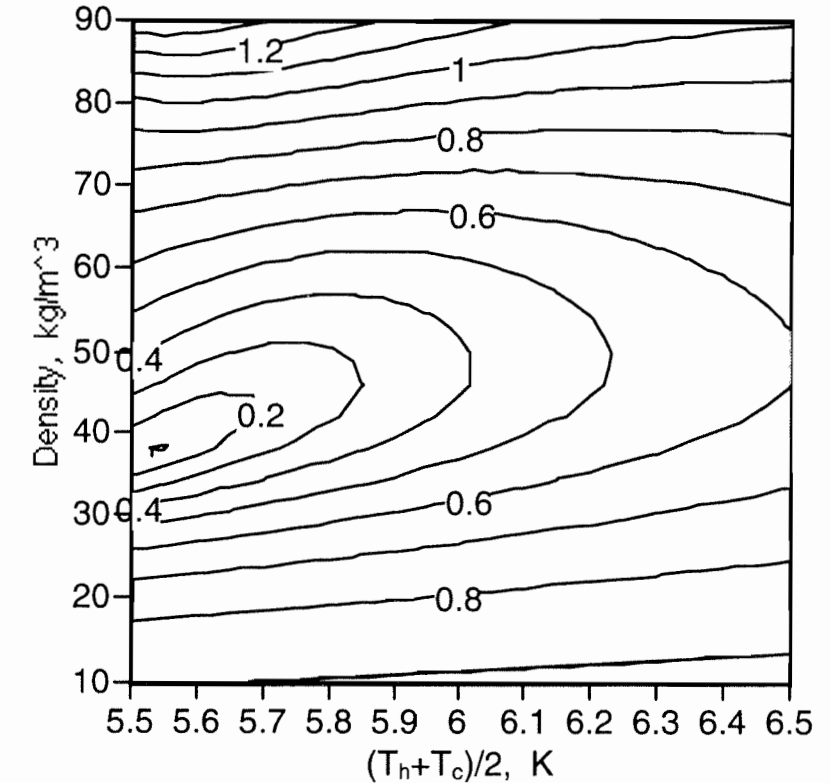


Figure 3.6 Data for the quantity of Wu and Libchaber which characterizes the difference of the two boundary layers. The ideal case is $x = 1$.

Second, in the part of the layer where the velocity is non-zero, the fluid is nearly isothermal, and hence there is no concern in this region, by itself, about non-Boussinesq effects. Third, there appears to be a well defined way to understand the differences in the two boundary layers. It will be interesting to see if the analysis of Wu and Libchaber applies to large experiments as well. Finally, the differences in the boundary layers are simply related primarily

to the difference in the thermal conductivity at the boundary (as well as, perhaps the parameter Θ). Consequently, the present experiments should be able to achieve a much higher range of Ra for which the boundary layers are effectively more identical to each other than those of any previous experiment. In the extreme range of Ra , we still expect that the effect of departures from the Boussinesq approximation will be confined to the boundary layers.

We conclude this section with the following observations:

- 1) Rayleigh numbers of as high as $Ra \cong 5 \times 10^{19}$ can be reached in a 10 m experiment. The highest Ra can be reached with densities of about $\rho = 70 \text{ kg/m}^3$.
- 2) The issue of departures from the OB approximation, as analyzed by Busse, is not of concern in these experiments. The parameter P can be small enough to confine all such effects to a negligible range in Ra near Ra_c .
- 3) The differences in the thermal conductivity near the upper and lower boundaries can also be maintained at a reasonable level, even for very large Ra . This also means that the Prandtl number will be well defined for the system.

3.4 Choice of Experimental Scales

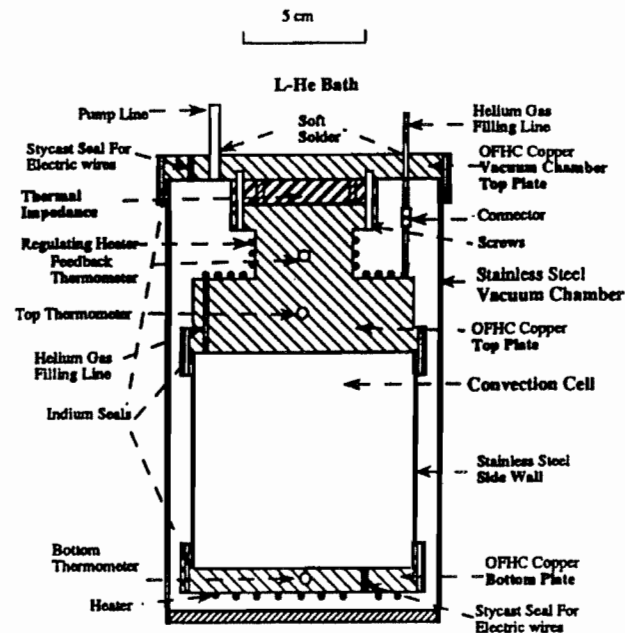


Figure 3.7 Diagram of one of the cells used by Wu in his PhD thesis research. The cell was mounted in a commercial helium dewar.

We confine our considerations to $L/D=2$ in order to extrapolate from measurements done at Cambridge University by Threlfall (1974) and at the University of Chicago by Albert Libchaber and his (then) graduate student Xiao Zhong Wu (1991).

For $Ra < 2000$ heat is transferred by conduction alone. For higher Ra there are successive regions of steady convection, oscillatory convection chaos, transition, soft and hard turbulence (identified by the signature of temperature fluctuations). The hard and soft turbulence regions are also identified by scaling relations where $Nu \sim Ra^m$. For many years it was assumed $m = 1/3$ for hard turbulence (Malkus, 1954, 1963; Howard 1966). The Chicago results suggest hard turbulence scales as $m = 2/7$, and the difference is experimentally significant. The results are shown in Figure 3.8. It appears that the $1/3$ region must lie at still higher Rayleigh numbers. While there exists some disagreement about details of the experiment, it is clearly important to increase Ra . The Chicago experiments got to Ra about 3×10^{14} . But geophysically and astrophysically significant Rayleigh numbers range to 10^{20} and more (see Normand, Pomeau and Velarde, 1977). Academic facilities cannot push much further than did Chicago ($L=40 \text{ cm}$): one might extend the cell to a meter or so but size and refrigeration requirements would soon intrude.

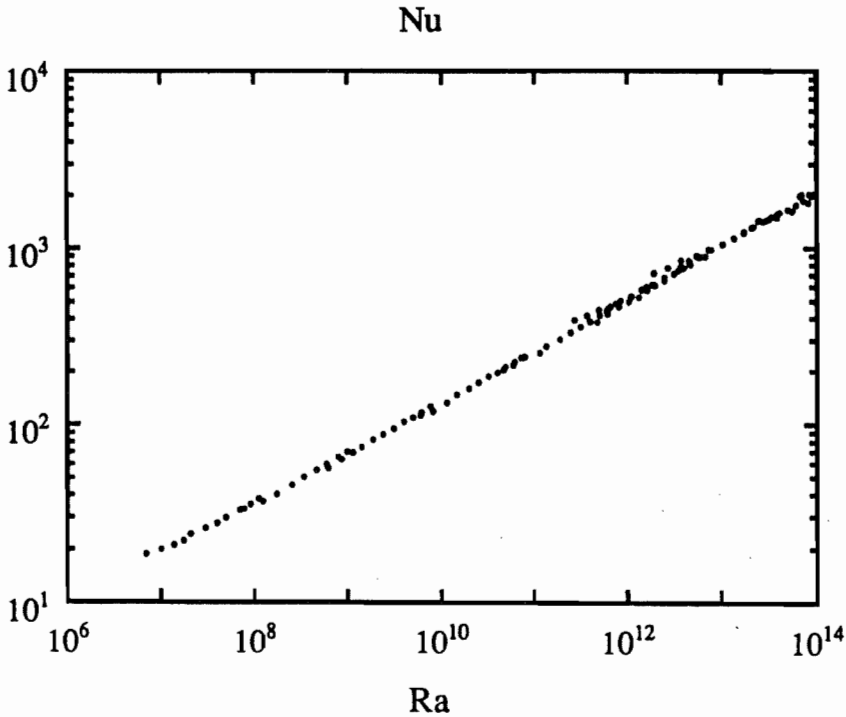


Figure 3.8. Results from a container of aspect ratio 0.5 from Wu's PhD thesis.

3.4.1 Scaling assumptions

In order to decide the size needed for the large experiment, we need to make some estimates. It would seem prudent to take data from Wu's successful experiment and use that data as a basis for estimates.

- Suppose we hold L/D constant, retain T and ΔT (we cannot change T without changing the fluid properties and we cannot increase ΔT without violating the Boussinesq approximation where fluid properties are considered constant over the height of the cell). Under these conditions we can multiply the present value of $L = 40 \text{ cm}$ by a scaling factor of s .

- $Ra \sim s^3, q \sim s^{-1}, A \sim s^2, Q_c \sim s$
 - $Q \sim NuQ_c, Nu \sim Ra^{0.285} \sim (s^3)^{0.285} \sim s^{0.855}, Q \sim s^{1.855}$
 - So scaling suggests that if the size of the cell is increased by a factor of s , the Rayleigh number increases as s^3 and the heat load increases by a factor $s^{1.855}$
 - Table 5 of Wu's thesis gives the following data (see also Figure 3.8)
 - $T = 5.504 \text{ K}, \nu = 4.81 \times 10^{-4} \text{ cm}^2/\text{s}, \rho = 3.75 \times 10^{-2} \text{ g/cm}^3, Ra = 2.67 \times 10^{14}, Q = 1.84 \text{ W}$
 - A cell 10 m high and 5 m in diameter operating near 5 K with a gas pressure of ~ 1500 torr would have $s=10/0.4=25$ and produce a Rayleigh number of 4.17×10^{18} . The heat load would be $Q=s^{1.855} \times 1.84 \text{ W} = 0.721 \text{ kW}$.
 - The refrigeration available from one unit at the SSC is 4000 W @ 4 K.
 - The volume of the proposed cell is $V = \pi R^2 L = 1.96 \times 10^8 \text{ cm}^3$, and the mass of helium gas is $M = \rho V = 7.36 \times 10^6 \text{ g}$. The volume of equivalent liquid at 4.2 K is $M / \rho_l = \frac{7.36 \times 10^6}{1.253 \times 10^{-1}} = 5.88 \times 10^7 \text{ cm}^3$. So the cell would take about 60,000 liters to fill.
- This experiment would be an enormous extrapolation from the Chicago experiment and we plan on building an intermediate sized model at Oregon and get it working before finalizing the SSCL apparatus. Let us suppose we choose an s of 2.5. So that we are dealing with a cell of $L=1 \text{ m}$. We might indeed choose a larger value of s , but we believe that a more modest scale will make it easier and more economical to use in an academic environment. Dr. Wu has pointed out that there are many improvements which can be made to his apparatus without making the scale too large.
- If we build a model at the University of Oregon which is 1m high. This would produce a Rayleigh number of 4.17×10^{15} , and the heat load would be $Q=10.1 \text{ W}$.
 - The volume of this cell would be $1.96 \times 10^5 \text{ cm}^3$ the mass of gas would be $7.36 \times 10^3 \text{ g}$. The volume of equivalent 4.2K liquid would be 58.8 liters.

3.4.2 Boundary Layer Thickness

The motion of the fluid in the cell can be considered to be a large inviscid circulation filling most the cell and constituting a thermal short circuit. The temperature difference takes place in boundary layers at the top and bottom of the cell. (Note that the sense in which the phrase "boundary layer" is used here is not the classical sense based on velocity considerations. Such a thickness, estimated by treating the flow as a wall jet is substantially higher).

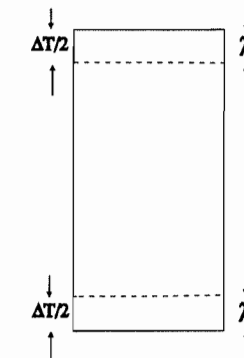


Figure 3.9 Boundary layers on the horizontal walls of the convection cell.

If the boundary layer thickness at the top and bottom of the can is λ , then the boundary layer thickness and Nusselt number are connected by $\lambda = L / 2Nu$. Since $L \sim s$ and $Nu \sim s^{0.855}$, $\lambda \sim s^{1-0.855} \sim s^{0.145}$. For Wu, $\lambda = 40 / (2 \times 2629) = 7.61 \times 10^{-3} \text{ cm}$. For the SSC $\lambda \sim s^{0.145}$ and since $s=25$, $\lambda = 1.21 \times 10^{-2} \text{ cm}$ and so probing at this scale is no more difficult than in Wu's experiment.

3.4.3 Fluid Velocities and Circulation Frequencies in Thermal Convection

The Rayleigh number can be considered to be the ratio of buoyancy to dissipation. This suggests the buoyancy force per unit volume on a packet of fluid warmer than its surroundings by an amount δT is

$$\rho g \alpha \delta T$$

To see that this is reasonable, consider a volume V of fluid surrounded by an adiabatic envelope, with the temperature and density inside given by T' and ρ' surrounded by ambient liquid at T and ρ . Suppose $T' > T$ and $T' = T + \delta T$. Then $\rho' = \rho + \delta \rho$ where $\delta \rho = -\alpha \rho \delta T$. The net force is

$$\delta \rho V g = -\alpha \rho \delta T V g$$

The mass is $\rho' V \approx \rho V$. So the acceleration is

$$-\frac{\alpha \rho \delta T V g}{\rho V} = -\alpha \delta T g$$

Wu finds that $\delta T \approx 0.01 \Delta T$ where ΔT is the temperature drop across the whole cell. In fact Wu reports $\delta T \approx Ra^{-1/7}$. All this suggests that if the fluid element falls (or rises) a distance L , the final velocity will be

$$v \approx \sqrt{2 \alpha \delta T g L} \approx \sqrt{2 \alpha 0.01 \Delta T g L}$$

For Wu's cell, $L = 40 \text{ cm}$, $\alpha = 0.967 \text{ K}^{-1}$ and $v = 20.6 \text{ cm}$ which is the right order of magnitude of observed velocities. The velocities scale as $s^{1/2}$ so for the 10m cell $v = 103 \text{ cm/sec}$.

The circulation frequency $f = v/P$ where P is the perimeter of the cell. For Wu this is 0.17 Hz (about as observed) and for the large cell $f = 3.4 \times 10^{-2} \text{ Hz}$, and the circulation frequency varies as $s^{1/2}$. Wu's velocity measurements relied on bolometry. Very likely this can be improved by the use of wall shear stress gages which were invented for room temperature Taylor-Couette work, but have been successfully used in helium I here at Oregon. Another important possibility is LDV which we report on briefly elsewhere.

3.5 Measurement requirements

3.5.1 Global Measurements

A variety of scientifically relevant quantities will be measured. These include the Nusselt number (a dimensionless measure of the overall heat transport), local thermal fluctuation measurements, velocity anemometry measurements, and velocity measurements using suspended particles. The technology for all of these measurements exists. The ease of implementation of the measurement techniques will vary depending on type.

The Nusselt number is particularly easy to obtain, and requires only a measure of the temperature difference between the plates, and the heat flux to the bottom plate. (Corrections are necessary for heat which is radiated and for parallel conduction paths, but these are typically relatively small and exactly determinable.) Temperatures can be measured to better than 0.5 mK, and the temperature difference across the fluid layer will be about 0.5K. The actual electrical heating power supplied to the bottom plate is easily determined to a very small fraction of a percent. The corrections to determine the fraction of the heat actually traversing the fluid are the ultimate limiting factor in determining the Nusselt number, and will likely lead to uncertainties which will need careful evaluation and consideration.

3.5.2 Local Measurements

Local thermal measurement can be made by suspending small superconducting bolometers or other temperature sensors in the fluid. The experiments of Wu and Libchaber have already shown that this technology works, and a determination of the correlation of fluctuations between bolometers gives a measure of the mean velocity of convection at the location of the sensors.

Recent work (Murakami, Yamazaki, Nakano and Nakai, 1991; Ichikawa and Murakami, 1991) has shown that small particles can be suspended in helium, allowing for local (and perhaps global) measurements of the velocity. This area is one which may require the greatest development, but the payoff would be significant. We defer a discussion of Laser Doppler Velocimetry to the following section on supporting activities, because there needs to be considerable development work done. Section 4 also contains a more detailed discussion of devices suitable for observing flows of both gaseous and liquid helium, and the need to improve them. Visualization of the flow: again using neutral particles, one can probably visualize the flow (especially plumes, if they survive at such high Rayleigh numbers) using optical techniques.

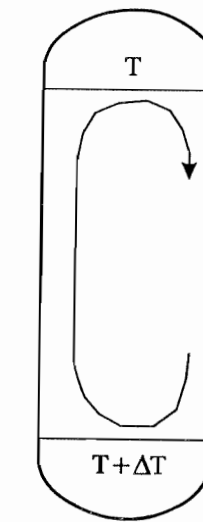
3.6 Other uses for the large cryostat

As we remarked in Section 2 above, once planning began on the large cryostat we realized that a cryostat of such unprecedented size allows one to think of experiments in a completely different way than one is used to in an academic low temperature laboratory environment. To illustrate our present thinking, refer to the conceptual sketches in Figure 5. We follow the lettering identifying the sketches. When we give numerical examples of what can be achieved, note that they are merely order-of-magnitude calculations to estimate extreme operating conditions accessible because of the N-15 refrigerator. We use the operating conditions quoted from Wu's thesis:

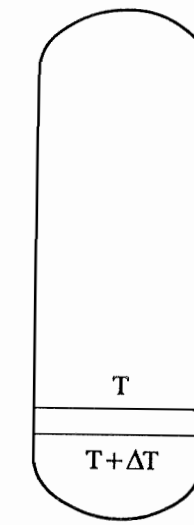
$$v = 4.81 \times 10^{-4} \text{ cm}^2 / \text{s}, \rho = 3.75 \times 10^{-2} \text{ g} / \text{cm}^3.$$

- a) *The small aspect ratio, high Rayleigh number convection experiment.* This is the chief aim of this report.
- b) *Adjustable aspect ratio convection experiment.* Here we plan to move the cooled upper plate downwards to make the aspect ratio $\Gamma = D / L$ larger (but of course at the expense of the highest Rayleigh numbers). When the required liquid level is not too high, we could in principle operate in helium I.
- c) *The towed grid experiment.* Here a grid, initially at the bottom of the tank, is towed upwards through the gas and the decay of the turbulence left behind is observed. We present some arguments that this should likely be done before the thermal convection experiment as it is the simplest experiment one can do in the tank, yet of fundamental importance in its own right. Doing towed grid first would allow more time to work on the more complex heated bottom plate, and gain operating experience with the large cryostat. Numerical estimates for this experiment are contained in section 4.5 below.
- d) *The oscillating grid experiment.* Here the grid is drawn to the top of the apparatus and oscillated with some amplitude and frequency while observing the turbulence so created propagate down the tank.
The turbulent burst experiment. Here the grid is brought near the top of the vessel and impulsively pulled upwards a certain distance. It is known that a sharply defined burst of turbulence will propagate downward through the gas (this was a PhD thesis topic of Michael Smith at the University of Oregon).
- e) *The towed sphere experiment.* Here a wire and pulley system is installed to tow a sphere at various speeds up the tank while measuring the drag, probably by means of a strain gage mounted to measure the force required to pull the sphere. To give an idea of what can be achieved, consider a sphere of radius 1m pulled impulsively down the tank, reaching a steady velocity over most of the path of 20 m/s. Assuming the drag coefficient is $C_d \cong 0.4$
$$D = \frac{1}{2} \rho U^2 \pi R^2 C_d = 9.4 \times 10^8 \text{ dynes.}$$
 The power dissipated is about 200 kW, but the experiment lasts less than a second. The Reynolds number reachable is 4.2×10^8 compared to less than about 10^7 ever achieved.
- f) *More general towed objects.* It is possible to tow other shapes of body such as ellipsoids, and even bodies of a shape which will produce lift as well as drag. Again a second strain gage could be mounted so as to measure the lift force.
- g) *Wind tunnels.* Here a contraction, test section, diffuser and fan are lowered into the tank. Many variations and elaborations of this arrangement can be conceived. Suppose we pick a pipe of diameter $d=2R=1$ m and $L=10$ m for the test section. Let us pick a mean flow rate of $U=20$ m/s, then the Reynolds number obtainable is 4.2×10^8 . This is huge compared with anything available today.

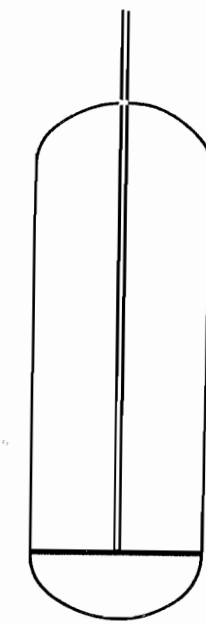
h) *Taylor-Couette flow*. Here a pair of independently driven concentric rotating cylinders is placed in the tank. Strain gages can be used to measure the torque and fluctuations to very high Reynolds number. To give an idea of what is achievable, let $R_2=200$ cm, $R_1=145$ cm, $d=55$ cm $L=630$ cm (to use the same radius and aspect ratios as Lathrop, Fineberg and Swinney, 1992). Then the Reynolds number depends on the rate of rotation: let us choose 100 radians per second. Then we can reach a Reynolds number of 1.66×10^9 . The power dissipated is about 2.6 kW, well within refrigeration capabilities, and increasing the achievable Reynolds number by three orders of magnitude over that reached by Lathrop et al.!



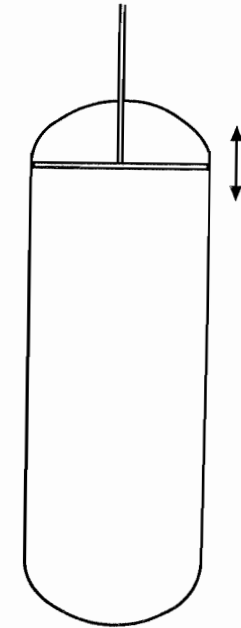
a



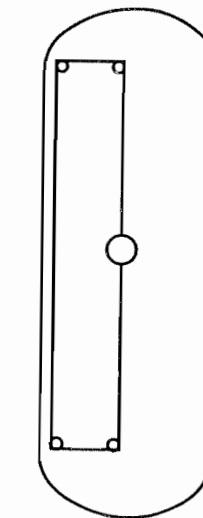
b



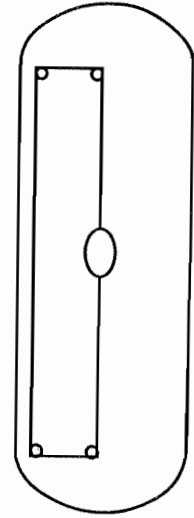
c



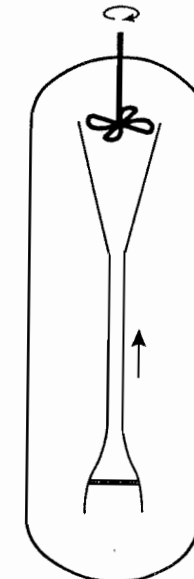
d



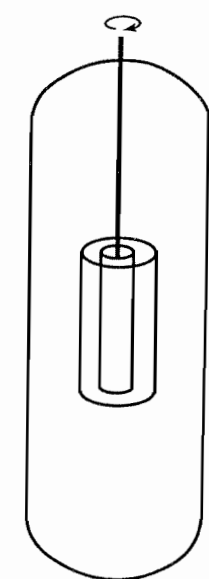
e



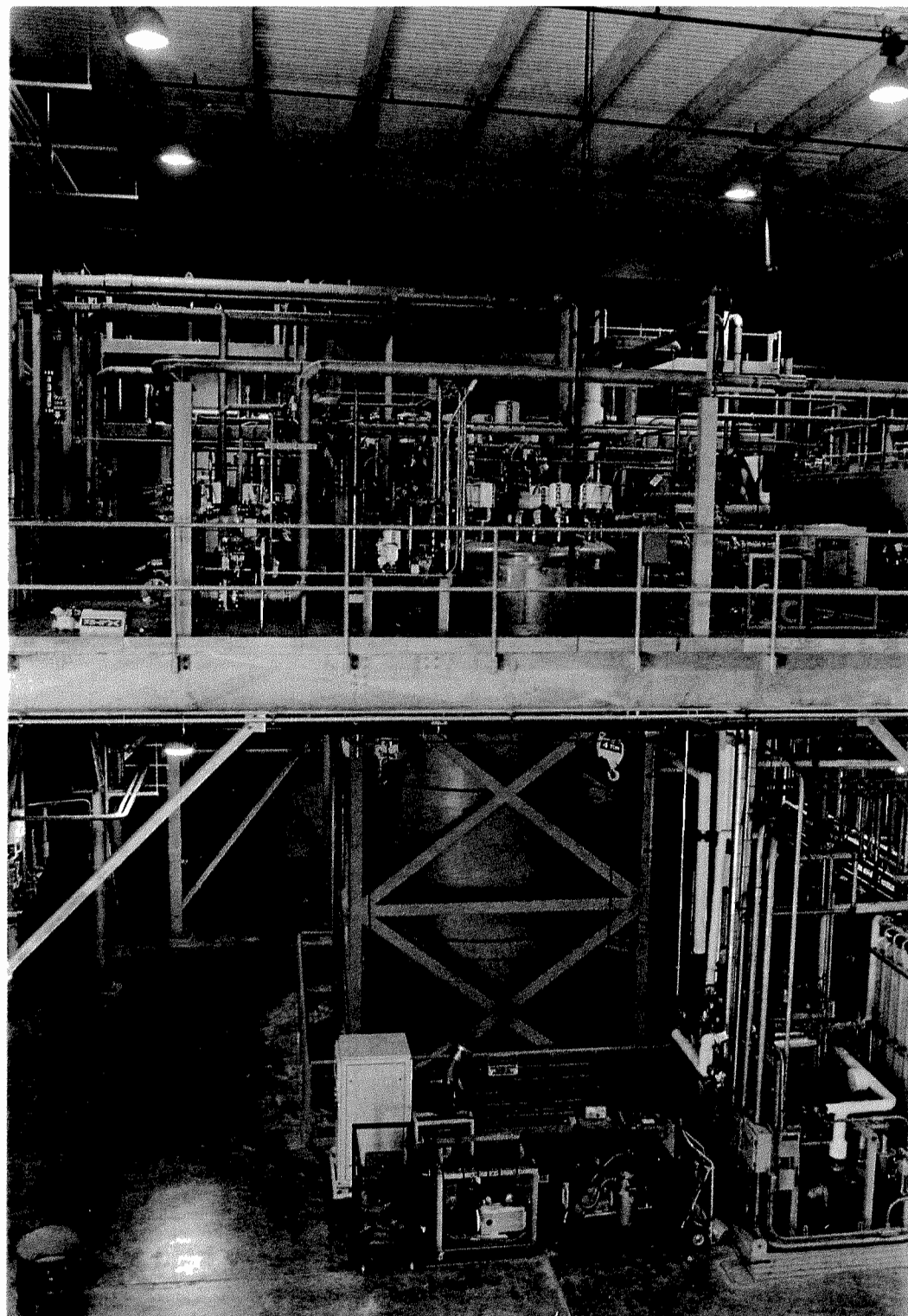
f



g



h



Refrigeration cold box of the N - 15B refrigeration plant at SSCL. This equipment will operate the Convection Cell. The rated capacity of this refrigeration plant is 4.5 kW at 4.4 K or 36 g/s liquefaction (1000 llhr). It has good turn-down capability and flexibility of operation, and is capable of meeting the complete range of operating requirements of the Cell.

4. Supporting Activities

4.1 Collaborating Laboratories and Personnel

The project we are discussing here is unprecedented in size and complexity in low temperature physics and fluid mechanics. We have given considerable thought on how to minimize the risks, and enhance the probability of overall success by drawing on the experience our team has in various aspects of this research. Let us summarize briefly how we see using our collective expertise in support of this work

- *Xiao-Zhong Wu*, Northern Illinois University. It was Dr. Wu's PhD thesis (Wu, 1991) which led to the idea of this large cryostat, and his success at the University of Chicago in making the experiment work and producing results which attracted widespread interest in several fields of research. The design for the Texas cryostat is based on an extrapolation of Dr. Wu's experimental results, and this project should benefit from his experience.
- *Katepalli Sreenivasan*, Yale University. Professor Sreenivasan is a recognized expert in turbulence research and has many years of experience at Yale and elsewhere. He is advising on the quantities which need to be measured, instrumentation development, and intends to build a model of the towed grid experiment using water as the working substance at Yale University. The data from the Yale experiment will be a useful benchmark to compare data from the large cell
- *Robert Behringer* Duke University is an expert on Bénard convection and has written the standard review article on the subject (Behringer, 1985). He is paying special attention to the state of the fluid and adherence to such matters as the Boussinesq approximation. His group will undertake an accurate redetermination of the thermodynamic and transport properties of helium near the critical point (in conjunction with work at the University of Oregon) and also will work on instrumentation, in collaboration with the Yale group.
- *Michael McAshan* was in charge of the cryogenics department of the SSC and has intimate knowledge of the facilities available and how best to use them.
- *Russell Donnelly*, University of Oregon, has worked for many years in both classical and helium hydrodynamics. He intends to undertake two major tasks at Oregon. One is instrumentation development, and the second is construction and operation of a 1 m high convection cell as a test bed for ideas and techniques to be used with the large cryostat. He will, in addition, collaborate with the Duke group on measuring properties of helium.

4.1.1 Postdoctoral Fellows

As a matter of general policy, we believe we will be able to attract the most talented post docs if they perceive they are to be part of the major experiment in Texas. Therefore we intend to attach the post docs to be assigned to experiments in the universities to the SSC Laboratories. During the first two to three years some of these post docs will be assigned to experimental work at Yale, Duke and Oregon and will likely be needed full time in Texas after that point.

4.2 Development activities at the University of Oregon

4.2.1 Program and Goals

Fundamentally, activities at the University of Oregon are to be in support of the large facility at the SSCL. There are two aspects to this support program. The first is to construct a considerably smaller convection apparatus to serve as a test bed for developments in Texas. Our present judgment is to build an apparatus on a scale of 50 cm in diameter and 100 cm in height. This would constitute a scaling factor of $s=2.5$ from the Chicago experiment and one tenth the scale of the proposed facility at SSCL. We have chosen a relatively modest increase in height from the Chicago experiment after considerable deliberation. The chosen $s=2.5$ allows a considerable increase in maximum Rayleigh number over the Chicago experiment, yet remains a small enough academic experiment that relatively rapid changes can be made for development of techniques to be transferred to SSCL. In particular the cell will be capable of operating up to 4 bar where there appears to be an advantageous region for operating within the Boussinesq limits.

We are also advised by Dr. Wu that there are a number of significant ways in which the Chicago experiment might be improved upon with no change in scale whatever. Most of these are in the area of instrumentation.

The second goal is to use the Oregon experiment as a test bed for detector development. Indeed one of the main lessons learned by the Oregon group over the past several years is how lengthy the process is when one seeks to make an advance in detector sensitivity or capability. It is rather unglamorous, tedious development work. It is also absolutely essential for progress in turbulence research.

We expect to need two post docs for the entire five years in Oregon, one to work on the convection experiment and one to do detector development.

4.2.2 Description of Oregon Cryostat

The development activities at the University of Oregon require the use of a flexible cryostat system. The primary capability of this system is that it must be able to carry out at a reduced physical scale the convection experiments and the towed grid experiments that form the program of the 10 meter cryostat, and it must provide the capability to investigate the performance of the instrumentation systems that are to be used there. In addition, this laboratory system must be able to carry out design verification measurements associated with construction and operation of the 10 meter facilities. Examples of the investigation of instrumentation might include the requirements for the successful application of Laser Doppler Velocimetry (LDV) to the measurement of velocities in the towed grid cell, and comparison in the convection cell of LDV and bolometer arrays for velocity measurement. Examples of verification experiments include evaluation of the plate thermometry and thermal control system and comparison of the operation of the convection cell in Region 1 and Region 2 of helium density. In addition, measurements in a laboratory-scale cell are necessary to provide continuity with previous work on helium convection and thus to define the program for the large-scale system. It is in the course of operation of the Oregon system that the experience is acquired that is necessary to plan the operating program of the 10 m cell and to interpret its results.

A preliminary design for the Oregon cryostat is illustrated in the figure on page A-9, labeled the Oregon Free Convection Cryostat, and in the paragraphs below, the functionalities required are described. This system is composed of four major components: the outermost wall of the cryostat is a vacuum jacket, 40 inches in diameter and about 7 feet tall; inside this is a liquid nitrogen shield with an attached LN reservoir insulated with multi-layer insulation; within the LN shield is a 20 K shield cooled by an attached G-M cryocooler; inside this shield is the cell assembly. The cell assembly includes the cell itself, a stainless steel cylinder with integral copper bottom and removable copper top plates. Attached to the top of the cell is a helium reservoir coupled to the top plate thermally by a gas space. Around the cell is a helium-cooled shield attached to the liquid helium reservoir. The cell and reservoir and each of the shield assemblies are supported by a neck tube passing up to the top plate.

This general layout is a compromise between flexibility and ease of operation. The use of a common vacuum jacket makes it easier to incorporate things like optical windows and mechanical feed-throughs into the design, but it makes disassembly a more difficult task, since all of the shields have to be removed. In order to mitigate this problem, the nitrogen and helium shields have attached thermosyphon cooling loops. This improves the shield performance and makes it unnecessary to achieve good thermal contact where the shield is attached. The figure on page A-9 does not show features like the optical windows. The design and integration of these is part of the final design.

Another important feature of the design helping to contribute to flexibility and the rapid turn-around of this cryostat is the removable cell top plate. Although it is difficult to see this illustrated in the figure, the top plate has a hole in its center connected by means of a stainless steel tube passing up the neck tube. In the figure a copper-tipped stainless tube is shown inserted in this top-plate access tube. The top plate together with this tube can be removed from the cryostat after disassembly of the cell. In the convection cell, this tube provides for helium transfer into the cell, for pressure relief, and as a place to install instrumentation wiring. In the towed grid cell, it provides for the operation of the grid. Because the top plate can be removed from the cryostat together with this tube and replaced with another plate differently equipped, the time required to change from one mode of operation to another is kept to a minimum. As an example of how this feature is used, a top plate with the appropriate wiring and fixtures for thermometer calibration can be prepared and when ready, quickly be installed in the cryostat for operation.

The cryo-cooler is included in the design in order to reduce heat leak and helium consumption during operation, but more important it is included in order to cool the system down to 20 K before helium transfer thus saving many liters of liquid helium in each operating cycle. The cryo-cooler is connected to the helium reservoir by a neon-filled heat pipe. After helium transfer, this neon is frozen out, turning off the thermal contact.

Another helium-saving feature in the design is the use of a helium-filled gas space between the cell and the helium reservoir. This space acts as an adjustable thermal resistance for the control of top plate temperature during operation of the convection cell. The gas pressure in this cell is adjusted from very low values to values near one atmosphere, and the thermal conductance that can be achieved goes from very low values to the maximum required for operation of the convection cell at high Rayleigh number in region 2 of the helium density. This pressure adjustment as well as safety relief is accomplished through a concentric space in the neck tubing. There is a gauge line shown in the diagram as well. By using this method of

temperature adjustment rather than a solid thermal resistance and a heater as is done in the 10 m cell system, helium consumption is considerably reduced.

Operation of the Oregon cryostat begins, after pump and purge, with cooldown by liquid nitrogen. The nitrogen tank is filled, and the whole interior contents of the cryostat is cooled through a soft insulating vacuum. The multi-layer package outside the nitrogen shield controls heat leak from the surroundings during this operation. The G-M machine is then started and the vacuum space pumped out. The cell assembly is cooled by means of the neon heat pipe together with the 20 K shield to the neighborhood of 20 K. Helium can then be transferred into the cell assembly. The cell is kept filled with helium gas during the 20 K, and depending on what cell inventory is needed, it can be closed off during helium transfer or maintained at 1 bar pressure. In the latter case, after the transfer is completed the cell is filled with saturated gas, and if still higher density is needed, an amount of liquid helium can be transferred into the cell itself through the top plate access tube. The cell is then brought to the required operating conditions by adding heat with the bottom plate heater. The top plate temperature is adjusted through the pressure of the gas in the same thermal resistance space as described above.

4.2.3 Other experiments

We have listed in Section 3 above a number of experiments which might be done in the large facility. Clearly these same variations can be done in the 1m cell at Oregon. Our projection is that the Oregon apparatus will be fully occupied trying to keep up with the construction activities in Texas. The only variant which is likely to be tested at Oregon is the towed grid, which should likely be done first at both locations, since it offers a way to get good data without building the complicated bottom heated plate. The most demanding and time consuming activity is probably the work on detector development.

4.3 Summary of instrumentation development for helium turbulence

A number of instruments have been mentioned in the sections above. It seems worthwhile to try to summarize the present state of instrumentation so that one can appreciate the tasks which lie ahead. We summarize below the instrumentation which has been used, or is shortly to be tested in various helium flows.

The reader should be aware that this list of detectors is comprehensive: that is they are detectors for use in critical helium gas helium I and helium II. Some of these detectors would be of use in the apparatus described in Appendix B for flow tunnels and tow tanks.

4.3.1 Average flow velocity

If one wants to measure the average flow velocity in a channel there are a number of methods available. These have been reviewed for cryogenic engineering use in helium II by Van Sciver, Holmes, Huang and Weisend (1991). Methods include turbine flowmeters, venturis, fluidic flowmeters (measuring vortex shedding) and flowmeters based on propagation of temperature or pressure pulses.

4.3.2 Use of Laser Doppler Anemometry in critical helium gas.

Murakami and his students have been successful in seeding helium II with neutral buoyant HD particles and with quartz microspheres and have been successful in both doing Laser Doppler Velocimeter (LDV) measurements of a counterflow produced jet and of flow visualization (Ichikawa and Murakami, 1991; Murakami, Yamazaki, Nakano and Nakai, 1991).

Laser Doppler anemometry has been shown to be extremely useful in studies of turbulent flows. Mean flow velocities, RMS velocity fluctuations, velocity time series, and temporal and spatial velocity correlations can in principle be determined. Thus LDA is particularly well suited for this project.

LDA has been successfully used in liquid helium by seeding the flow with neutrally buoyant hydrogen-deuterium particles (Murakami, Yamazaki, Nakano and Nakai, 1991). However, since we are working in a gas and in a cryogenic environment, some technical concerns in the use of LDA must be addressed. The two primary concerns are *optical access* to the fluid and *seeding*.

Optical access can be achieved by the insertion of quartz glass windows in the walls of the tank. This allows all of the optics and traversing equipment to be located at room temperature. Because of the pressurized working environment the size of the windows is limited. Thus probing the flow in the center of the tank through a single set of windows will necessitate a very small beam crossing angle and a consequently large control volume. For instance, consider two parallel beams separated by 10 cm which were focused down onto a measurement volume 2.5 meters from the outside wall. The angle between the intersecting beams would be 2.2° and the length of the control volume would be 15 cm! On the other hand using a beam separation of 20 cm and making measurements 1 meter from the focusing lens reduces the measuring volume length by a factor of 12. Clearly, care will need to be exercised in probing the center of the tank but the problem is not insurmountable.

Seeding must also be carefully considered since it is impossible to obtain neutrally buoyant seeding particles in critical helium gas and typical methods of aerosol production could not be easily adapted to cryogenic conditions. However, helium gas has some submicron impurities which are very difficult to filter out and scatter laser light. This was brought to our attention by Professor W.F. Vinen, who found, while doing very high resolution Brillouin scattering experiments in liquid helium, that unless prefiltering at helium temperatures was successful, the liquid helium was full of microscopic particles (probably dissolved solid air) which remained suspended for hours. Fortunately, what was his bane may be our boon.

The sizes and concentrations of the impurities are not well characterized but they can be easily and abundantly produced (by introducing air into the helium at specific points in the cooling process for instance). Filtering could again be used to remove particles of too great a size to improve the signal to noise ratio. On the other hand, it would be interesting to investigate LDV methods in flowing liquid and gaseous helium without deliberate seeding.

These impurities have densities much greater than that of helium gas and settling of the particles may be an issue. However, particles with one micron diameter have extremely slow terminal velocities and very long settling times. For example, for a particle with diameter of $1\text{ }\mu\text{m}$ in helium gas of density 0.001 g/cm^3 , the terminal velocity is 0.03 cm/sec . Thus considering the vigor of the turbulence settling will not be a concern.

Of more concern is whether these particles can follow the turbulent fluctuations at high frequency. In air at standard pressure and temperature the largest size particle which will follow the flow is around 5 microns. Because the viscosity of helium is less than that of air, the particle size needs to be correspondingly less. On the other hand, the helium gas will be pressurized increasing the density of the helium compared to air and increasing the allowed particle size. Accounting for both of these factors, particles of about 0.5 to 1.5 μm will be optimal in critical helium gas.

We conclude that velocity measurement using LDA is feasible in critical helium

Bielert and Stamm (1994) have succeeded in visualizing Taylor-Couette cells in helium II at relatively high Reynolds numbers using glass spheres.

Hot wire methods should work well at low temperatures, provided the flow has a substantial mean velocity (wind) to carry away the joule heating of the probe. While the heating can be made quite small due to the available high resolution in measurement techniques, hot wires are not necessarily suitable for investigation of thermal convection in critical gas. Wu used 200 μm bolometers in his experiments mounted closely together and measured a mean flow velocity in his cell of the order of 10 cm/sec by means of delayed correlation of fluctuations.

If LDV measurements can be successfully used, so too, in principle, the multiple -particle Particle Image Velocimetry (PIV) can be used to give a two dimensional sheet of velocity information in a flow. However, the degree of difficulty in seeding critical helium gas sufficiently well for use of LDV methods is not known. Hence the development of some new velocity measuring device suitable for critical helium gas should be a high priority.

4.3.3 RMS vorticity

For the experiments involving vortex-coupled superfluid flows, it is possible to use the technique second sound attenuation for determination of RMS vorticity. Experiments at Oregon have used a 1x1 cm channel with nuclepore transducers. These transducers are 9 mm in diameter and recessed slightly behind the main channel. We have used this arrangement to study the decay of towed grid turbulence and the propagation of turbulent bursts from impulsive starting of a towed grid (Smith, 1992). It appears from data obtained by Smith in his thesis, that the relatively large nuclepore transducer pair seems to behave as if it were much smaller than 9 mm. Perhaps the region of substantial amplitude of resonance in the channel is large enough that the characteristics of the detector do not matter much. We have fabricated superconducting bolometers as small as 60 microns as receivers and not observed much change in performance. It appears therefore that to obtain a spatially confined second sound attenuation measurement, some way must be devised to excite a locally confined second sound resonance.

4.3.4 Temperature gradient

Temperature gradient and absolute temperature measurements have been developed to a fine art for liquid helium studies. High resolution thermometers developed by Lipa, *et. al.* (1981), Steinberg and Ahlers (1983), and Duncan (1988) now reach nanokelvin or subnanokelvin

resolution. Standard germanium thermometers have somewhat reduced resolution but very fast response times.

4.3.5 Pressure gradient

Pressure gradient and absolute pressure measurements have also been developed to a high degree of sensitivity, principally by using a capacitance manometer consisting of a light diaphragm near a fixed electrode as a capacitance transducer. The sensitivity has been made extremely high by means of bridges or resonance circuits, and can easily detect sub Angstrom movements of the diaphragm. Typical resolution is better than 1 part in 10^8 of the capacitance under study.

4.3.6 Lift and drag

NASA has promoted the development of magnetic suspension and balance systems. These devices are discussed in depth in several articles in the book by Donnelly (1991a). When operating at helium temperatures superconducting devices are possible and the conventional magnets used for many existing systems can be replaced by superconducting magnets. These systems measure not only lift and drag on a suspended body, but also they can be used to execute sophisticated maneuvers at the same time. This reflects their early use for aerodynamical purposes.

Superconducting suspension systems are in an advanced state of development. NASA Langley has ordered a superconducting suspension system from a commercial firm, and the control systems have been worked out by MIT's Draper Laboratory.

4.3.7 Flow Visualization

Flow visualization in cryogenic helium has been used successfully by Murakami and his students at Tsukuba University in Japan (Ichikawa and Murakami, 1991; Muakami, Yamazaki, Nakano and Nakai, 1991).. They have been able to use both neutrally buoyant HD particles and quartz microspheres. Photographic resolution of the flow structure looks promising.

4.3.8 Bolometers

Bolometers have reached a high degree of development at low temperatures, and are used in applications such as long wavelength infrared detection (Nolt, Radostitz, Kittel and Donnelly, 1977). A common use in liquid helium is for second sound detection. Deposited carbon becomes a semiconductor at low temperatures and exhibits a rapid rise of resistance with lowered temperature.

4.3.9 Wall Stress Gages

Wall stress gages were first developed for fluid mechanics by Lambert, Snyder and Karlsson (1965). They consist of a very sensitive bolometer which is heated above the environmental temperature and give information about the shear at the location of the bolometer. In Taylor-Couette flow a wall stress gauge gives the equivalent information as torque measurements.

Wall stress measurements in Taylor-Couette flow of helium I have been reported by Wolf, Perrin, Hulin and Elleaume (1981). They used an aquadag painted layer $\sim 1 \times 5$ mm carrying a DC power of typically 10^{-5} Watt. Similar measurements (unpublished) have been carried out at Oregon using a similar detector which was simply a second sound receiver used in helium II in the same apparatus.

4.3.10 Ion measurements

Ion measurements have been carried out for many years in liquid helium (see Donnelly, 1991b). Originally the aim was to study the mobility of the ions and hence to deduce their structure and their interactions with the fluid. When the quantized vortex rings were discovered, ions were the means of deducing their dynamics. Ions have also been used in various ways in hydrodynamics, including turbulent flows. An example of this application is described by Awshalom, Milliken and Schwarz (1984).

Since ions are trapped on the cores of quantized vortices in helium II, they could, in principle, be used to measure RMS vorticity. However various complications arise when the ions are trapped, as they can move along the cores of the vortices. At the present state of development, ions can locate vorticity spatially in a turbulent flow, but cannot easily determine the magnitude.

4.4 Verification of Fluid Properties at Duke University and Oregon

The fluid properties which play a role in determining the state of the system through the Rayleigh number Prandtl number or other parameters are listed under fluid properties in Section 3.1. One part of the project will involve a check on the existing literature to ensure that the calculated Ra and Pr are indeed correct for a given situation. Of the fluid parameters listed in Section 3.1, all but the compressibility play a role. In the following paragraphs, we discuss briefly the measurement strategy for determining these quantities.

Overall, one or more cryostats will be needed to carry out the measurements. The cryostat must be designed to operate at pressures up to at least 5 atm, and to carry out high resolution experiments, typically with temperature resolution of $1 \mu K$.

The density and expansion coefficient will be determined in one set of experiments. The density will be measured along isobars as a function of temperature, using capacitive techniques. In particular, the helium sample will occupy the gap of a parallel plate capacitor. Variations in the density result in changes in the dielectric constant, as given by the Clausius-Mosotti relation, and hence the capacitance. Capacitances can be resolved to 1 part in 10^9 at the

temperatures of interest. Consequently, the density can be precisely determined. The expansion coefficient can then be extracted by numerical differentiation.

The dynamic viscosity will be determined by torsional oscillator measurement. A cylindrical cavity connected to a torsion rod will show damping which is a function of the viscosity (and density). Because very high intrinsic Q's can be produced at low temperatures with such oscillators, the viscosity can be very precisely determined. A combination of these experiments with the density measurements will lead to a determination of the kinematic viscosity.

Of the thermal properties, the most important is the thermal diffusivity, since that appears in both Ra and Pr. This quantity will be determined by one of two methods. In the first method, the response of a thin layer of fluid to an AC heat flux will be determined. Recent measurements at Duke have shown that this is a very successful and easy way to determine κ . Alternatively, we will use a thin layer of fluid and DC heat flux measurements to determine the thermal conductivity k . This combined with standard heat capacity measurements will be used to provide an alternative determination of the thermal diffusivity.

Professor Behringer will also work in collaboration with Professors Sreenivasan and Donnelly in the development of visualization techniques and high precision local probes.

4.5 Grid Turbulence Experiments at Yale University

4.5.1. Sweeping grid in the helium cell

In recent measurements it is becoming increasingly clear that the mean shear as well as the large scale anisotropy could have perceptible influence on the scaling exponents of turbulent energy spectra, multifractal spectra of energy dissipation, structure functions in inertial range, the non-dimensional energy dissipation rate, and so forth. Similarly, the spectra of acceleration and pressure fluctuations could be influenced by these same factors, and are additional to possible finite Reynolds number effects. As of now, one does not have a sound theoretical knowledge for deducing finite shear and finite Reynolds number effects. Reliable data in shear-free turbulence at high Reynolds numbers appears critical to have as a standard, without which further progress seems elusive. It is believed that the proposed grid experiment will provide those data.

Until now, the highest Reynolds number experiment in grid turbulence is that by Kistler and Vrebolovich (1966). The highest Reynolds number, R_M , based on the mesh size of the grid and the velocity upstream of the grid, U_0 in that experiment, was 2.4×10^6 . More relevant is the so-called large-scale Reynolds number, R_L , based on the longitudinal integral scale L and the root-mean-square velocity u' ; this was as high as 1.33×10^4 in the Kistler-Vrebolovich experiments. The so-called microscale Reynolds number, R_λ based on the Taylor microscale λ and u' is often used a standard reference Reynolds number in various flows; this Reynolds number went as high as 670. These experiments were carried out in the huge high pressure wind tunnel in Southern California before it was dismantled. Even though these measurements are very valuable, they show several inconsistencies from the previous ones. Some of these inconsistencies are the larger anisotropy of turbulence energy, substantially larger Kolmogorov constant, a decay rate that is characterized by a unity power-law rather than 1.25 now believed to be the more appropriate, and so forth.

All other grid experiments have been done at far lower Reynolds numbers. The best-documented experiments are those due to Comte-Bellot and Corrsin (1971) whose highest R_M , R_L , and R_λ were, respectively, 3.4×10^4 , 250 and 65. These experiments are the best of their kind, but it can be said on hind sight that many of the measurements of interest today were not made at the time.

In the existing generation of university-based experimental facilities, the wind tunnel at Illinois Institute of Technology has been built especially for good quality turbulence research. This facility is just being put to use, and there are plans for grid turbulence measurements in that facility. For some plausible configuration of the grid and a typical (incompressible) velocity that the tunnel is capable of producing, the R_M , R_L and R_λ are likely to be on the order of 5×10^5 , 1.2×10^4 and 500. These lie between the Kistler-Vrebolovich values and the Comte Bellot-Corrsin values.

In the proposed apparatus, the expected mesh Reynolds number R_M , the large-scale Reynolds number R_L and the microscale Reynolds numbers R_λ are on the order 1.3×10^7 , 1.3×10^5 and 1800. Besides being much larger than any attained before or likely to be attained ever, the experiment has the advantage that the turbulence decay can be observed for a much larger time (in terms of a suitable characteristic scale). This is made possible because the grid will be swept in stationary fluid (unlike the experiments mentioned above where the grid was stationary and fluid at constant speed was streaming past the grid producing turbulence behind it). Such experiments also exist (e.g., Dickey and Mellor (1980), Falco (1972), Walker (1986)). We first discuss some design parameters of the proposed experiment and point out its advantages as well as disadvantages.

The proposal is to sweep a grid of bars in stagnant helium. We propose to use a square grid of square rods, as is the usual practice. Square rods are chosen instead of round rods primarily because the separation points for the former is fixed unlike that for round rods (and this may have some effect on the decay characteristics). The criss-crossing rods will be in two different planes, bolted and probably welded together, consistent with standard practice. One can make a grid by arranging all these rods to lie in one single plane, but the additional expense involved may not be justified, and we plan to proceed with traditional biplane grids.

Towed or swept grids are somewhat rare in occurrence compared to stationary grids in wind tunnels, and so their virtues and problems ought to be briefly mentioned. In the latter, observations are restricted typically to twenty or so characteristic time scales without side-wall contamination. In towed grids, observations can extend to much longer duration (in fact as long as one can measure the constantly reducing signals with decent accuracy). This allows for more definitive statements to be made about scaling laws and final period of decay. Extreme efforts at preconditioning the upstream flow (such as large contractions, honeycombs and screens) are not needed. No effort needs to be made to account for tunnel-wall divergence. On the other hand, the usual measurement procedures do not obtain: one cannot use time averaging but has to resort to ensemble averaging; one cannot use Taylor's hypothesis (a great convenience in traditional measurements, but also a source of many uncertainties); one cannot use hot-wire because there is no large bias velocity as in wind tunnel measurements. Of all the disadvantages, the last one is the most undesirable and needs some hard thinking in terms of alternatives.

It is proposed to generate turbulence by sweeping the grid vertically upward at a constant speed through the quiescent cell containing helium I at constant temperature. (No heating of the bottom and top plates in the cell will be necessary in principle, but maintaining the two plates at

the same temperature may be necessary to avoid large-scale stratification. For a study of temperature fluctuations in grid turbulence, some heating of the turbulence generating grid, or another secondary grid, will be needed; this will be discussed below.) Measurements of the resulting turbulence will be made. After a certain time, the grid will be returned to its original position to the bottom of the tank, and sufficient time will be allowed for the helium gas to return to rest. The process will be repeated. Ensemble averaging has to be used, and so several repetitions will be required. The grid is chosen to have a solidity of 0.44, mainly because previous experiments with this solidity have been conducted successfully in water at low Reynolds numbers (e.g., Walker, 1986). The end parts will be terminated free without any ring-like structure. They will be held to within a few millimeters of the wall of the cell, and covered with Teflon protections. The apparatus for sweeping the grid will be automated to be able to repeat many cycles, and the needed safety features will be included to eliminate effects such as position miscount and power failure. (In such events, the motor will be turned off automatically and brakes will be applied to halt the motion of the grid.)

Our first thought is to use a laser Doppler anemometry with some seeding particles. (This is a nontrivial issue in helium and will be discussed elsewhere in the report. At the least, one can imagine sweeping a hot-wire probe attached to the grid at a certain known distance behind it. This too will be nontrivial because of the strong demands it places on the constancy of the grid speed and on its vibrations, but these issues can be solved with some care and effort.) Each data collection cycle will begin when the grid has passed through the probe volume. Both single-point and two-point measurements will be attempted. A pulse to the computer port enables data acquisition when the grid passes a preassigned position. The grid speed itself will be measured optically. Efforts will be made to minimize stratification effects.

The following dimensions appear suitable for the grid:

- Mesh size, M (center-to-center) = 15.6 cm. This allows, in a 5 meter diameter tank, about 32 meshes, which should be adequate.
- Width of the square bars making up the grid, $d = 3.75$ cm (this gives a solidity of 0.44. Solidity is the fractional solid area in projection and is given, for a square grid, by the formula $(d/M) [2 - (d/M)]$. Significantly larger solidity could produce large-scale instability of the type discussed by Corrsin (1963).

The following parameters are expected to be typical of the operating conditions:

- upward speed, $U_0 = 240$ cm/sec (If necessary, twice this speed can be attained without much problem.
- downward speed = 100 cm/sec
- top cut-off position = 50 cm below the top plate
- bottom cut-off position = 50 cm above the bottom plate
- waiting time at the top = 250 sec ($U_0 t/M = 4000$)
- waiting time at the bottom = 500 sec (or as large as needed for the velocity fluctuations to die down to very low levels)

Considering these as typical numbers, we may estimate the following turbulence parameters:

Turbulence levels are estimated to be 6 cm/sec at $U_0 t/M = 50$ and 0.4 cm/sec at $U_0 t/M = 4000$. Both are eminently measurable.

Between these two conditions:

- (a) the longitudinal integral length scale is estimated to vary between 10 cm and 60 cm, respectively
- (b) the Reynolds number R_L is estimated to vary between 1.3×10^5 and 5×10^4 respectively
- (c) the Taylor microscale λ is estimated to vary between a 1.5 and 12 mm respectively
- (d) the microscale Reynolds number R_λ is estimated to vary between 1800 and 1000 respectively
- (e) the Kolmogorov microscale varies between about 15 μm and 180 μm

The microscale on the lower end would be difficult to resolve, while that towards the upper end is not orders of magnitude different from what occurs in geophysical situations. For reference, it is possible to make hot-wires using superconducting material with sizes on the order of 10 μm (Castaing et al. 1994).

The Reynolds numbers are significant improvements over the highest values ever created or likely to be created in grid turbulence. Note that, while even higher Reynolds numbers can be obtained in geophysical turbulence, these flows are far from being isotropic and homogeneous, and experimental conditions are not sufficiently controlled.

4.5.2 Temperature fluctuations in grid turbulence

The problem of turbulent mixing of passive scalars is a subject of intense research. On the one hand, the problem is linear (with turbulent velocity serving as the stochastic coefficient for the advection term), which should make it easier to understand. On the other hand, arguments in favor of universality and asymptotic independence of initial conditions typically characteristic of nonlinear phenomena are less likely to be applicable to passives scalars, making it difficult to draw broadly valid conclusions. The literature on this subject is abundant and some unresolved problems have been pointed out over and over again (e.g., Sreenivasan 1992). Some non-universal aspects concern power spectral exponents, the structure-function scaling exponents, the derivative skewness, fractal dimensions, and so forth. It again seems equally important for a standard experiment at very high Reynolds number where these issues are explored thoroughly. It is expected that measurements of temperature fluctuations in the grid turbulence discussed above will provide the needed answers.

Much is known about the best manner of introducing temperature fluctuations into grid turbulence without affecting the dynamics of the velocity field. The best way seems to be to add another auxiliary screen behind the grid which can be heated independent of the turbulence-generating grid. One can imagine adopting this scheme. Alternatively, one can heat the grid itself, although this is less desirable because of the strong initial coupling it introduces between the velocity and temperature fields.

4.5.3. A small-scale sweeping grid experiment with water

The novel features of this experiment could benefit immensely from related laboratory experience on a smaller scale: The control needed on the motion of the grid and its accurate

balance, the precise cycle of its motion, the possibility of using scanning laser Doppler anemometry for multipoint measurements, data acquisition routines, the effect on the flow of incomplete meshes (because of square meshes housed in a circular section), and so forth, need some direct prior experience. Scientifically, it would be important to have a low-to-moderate Reynolds number complement for the high Reynolds number experiment proposed so that a wide Reynolds number can be examined: One generally obtains much firmer grasp of scaling laws by spanning wide Reynolds number range. For purposes of interpretation of, and confidence in, the helium data (with which most turbulence people are unfamiliar), it also seems useful to have some data in water (with which everyone is familiar). Finally, it seems helpful to have the capability to visualize the flow in some detail (for example, near the incomplete meshes).

For these reasons, it appears appropriate to build a small-scale apparatus using water as the working fluid where all the needed experience can be gained. We propose to build just such an apparatus at Yale using a circular tank about 50 cm in diameter and 100 cm high. An identical grid to the one proposed for the helium cell will be constructed and its performance will be assessed. The solidity will be identical. Data similar to those expected in the helium cell will be obtained and analyzed.

We shall also seriously consider repeating the experiment with the nested screen configuration mentioned in the previous section.

The relevant Reynolds numbers for the water experiments are expected to go as high as the following numbers.

- Mesh Reynolds number: 7×10^4
- The large-scale Reynolds number: 2800
- The microscale Reynolds number: 260

From previous experience, these are at the low end of where one expects a measurable inertial range, and could provide a nice complement to the high Reynolds number data in the helium cell.

Incidentally, we know of no such experiment currently running or being planned at present.

4.5.4 Oscillating grid experiment

In geophysical applications such as wind-mixing in the upper oceans, it is often useful to know how a shear-free mixed layer grows with time, especially in stratified regions. A common experimental technique used to study these effects is to oscillate a grid in a tank of fluid and examine how the mixed region grows into the ambient. Such studies can be done in the present set up by oscillating the grid.

4.6 Participation by Professor Wu at Northern Illinois University

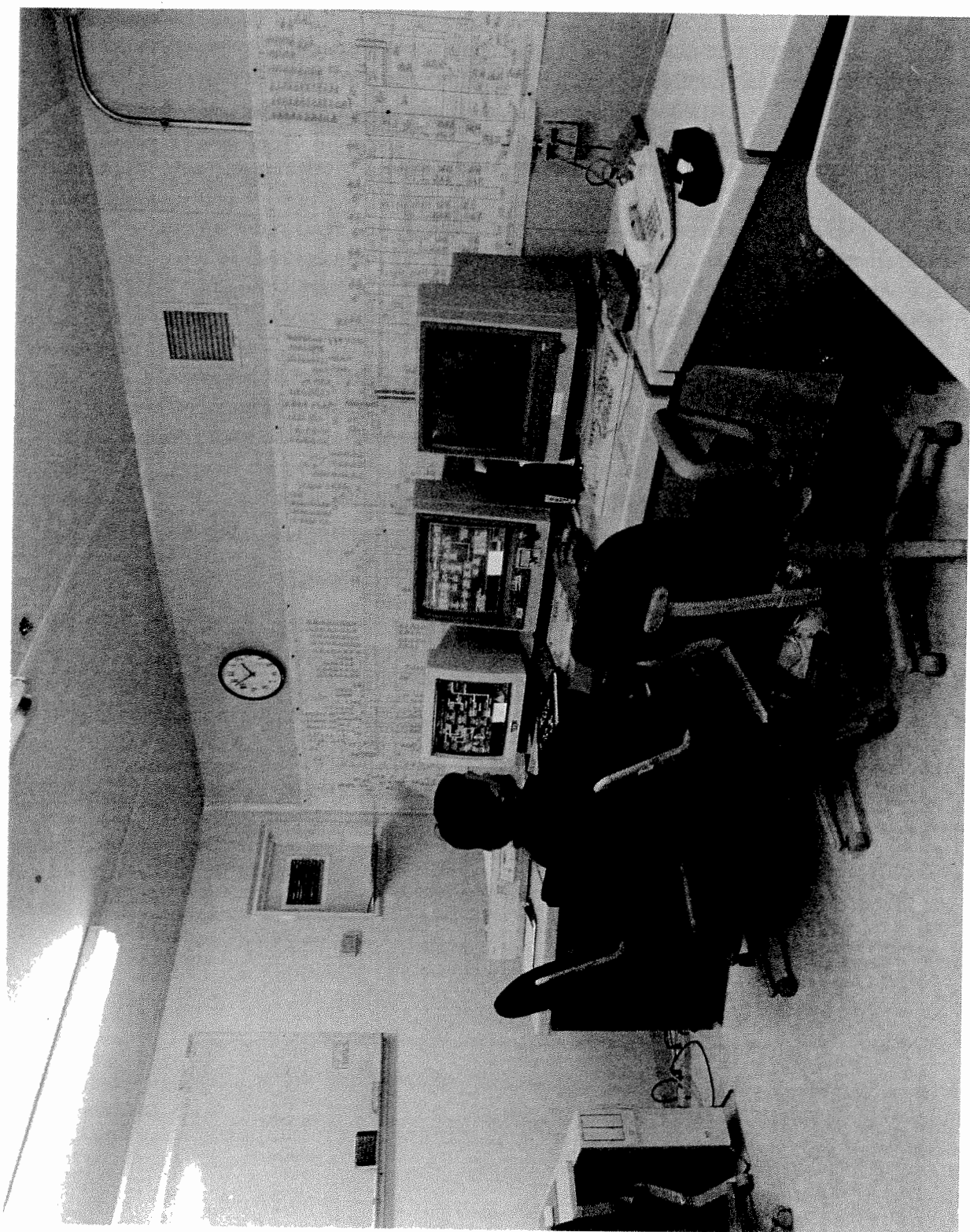
Xiao-Zhong Wu did his PhD thesis at the University of Chicago and is now teaching at Northern Illinois University at Dekalb. We have conferred often with Dr. Wu throughout this planning exercise, and realize how important it will be to have his continuing advice. Therefore we have included in the budget in Section 6 funds for his time and travel. At first, he would be involved heavily in the Oregon experiment, for that program must stay ahead of the construction of the large cell in Texas.

4.7 Conferences

The authors of this report are well aware that there will be a need for much input from the rest of the fluid mechanics and low temperature physics communities when this project is underway. While invited papers, electronic mail and newsletters may have some place, it seems to us that what is called for is a more formal way to sample the thinking of our colleagues, and to try to involve a significantly larger number of researchers in the area of high Reynolds number turbulence.

Over the years there have been a series of relatively small conferences and workshops at the University of Oregon in low temperature physics and fluid mechanics. The largest of these (not in the "Oregon" series) was LT20, held in 1993 and involving some 1200 physicists from all over the world. The book on which this report is, in part, based, was the product of the 7th Oregon Conference.

We suggest that in the second and fourth years of this project that conferences be organized welcoming input from all concerned. By the second year we will be well into the construction phase of the large cryostat and should be in a good position to predict schedules. By the fourth year of the project we should be in production, and again it would be worthwhile providing a second opportunity for the community to make its input, and hopefully to join in the use of the facility.



The refrigeration plants at the SSCL N - 15 site are completely computer controlled and all operations including startup, cooldown, liquefaction and refrigeration are semi-automated. The controls of the Convection Cell cryogenic system will be integrated with the refrigeration plant control system so that its operation will be straightforward and low-risk.

5. Technical Program

In the following section, a conceptual design is presented for the proposed convection cell. Design studies have been carried to a level of detail which allow identification of the primary tasks involved in constructing and operating such a cell. Following the conceptual design, the required work is outlined, and defined in the form of a Work Breakdown Structure (WBS) Dictionary. Based on the WBS, a preliminary schedule is provided. Costs are estimated using the WBS, and a budget is developed that is compatible with the schedule. Special permits required to build and operate the cell are addressed, especially with regard to their impact on cost and schedule. Finally, possible sources of funding are discussed.

In considering the content of the technical program, it should be recognized from the beginning that the technical risk inherent in the proposed facilities construction and in the research program is low. The cryogenic technology that is employed in the program is the product of a long period of development in the national high energy physics laboratories of the country. Also, the scale of the experimental facilities are within the range of existing equipment of similar kinds, and within, also, the capabilities of commercial-sector industry to produce in a straightforward and economical way. The basic instrumentation employed in the experimental program is for the most part also available from commercial suppliers. The thermometry is of a kind widely used and well understood. The instrumentation for velocity measurement, the laser Doppler velocimeter, is a state of the art technology that is considered in the field to be very reliable. Its use in cryogenic situations has, however, been limited up to now to a smaller scale than that contemplated here.

Thus the pieces are in place here to provide a great research and development opportunity. The facilities and the basic experimental techniques provide for important science output with a high probability of success. Furthermore, the prospect of advancing the state of the art in techniques applicable in a broad way to high Reynolds number research is excellent.

5.1 Conceptual Design of Experimental Equipment

The major system required by the proposed experimental program consists of a principal subsystem, the convection cell cryostat, together with auxiliary subsystems for its operation both with the towed-grid for turbulence studies, and with heated and cooled plate boundaries for the study of convection. This cell is operated at helium temperature by means of one of the 4.5 kW refrigeration plants located at the N-15 SSC Site. Further discussion of the cryogenic facilities at SSCL appear in Appendix J. Table 5.1 lists basic requirements for the experimental system and gives some explanatory discussion. The conceptual design of the experimental systems is based on the requirements in this list. In the following paragraphs the subsystems are described and illustrations are introduced.

5.1.1 Convection Cell Cryostat

This is a vacuum-insulated and shielded cylindrical vessel with the axis vertical. The inside dimensions are 5 m in diameter and 13.2 m high, with a total volume of 250 cu-m. This vessel is illustrated in section in Figure 5.1.1, and design details and dimensional information are given in Appendices A and C. Also shown in this figure is the location of the top and bottom copper plates that form, together with the cylindrical wall of the inner tank, the boundaries of the convection cell. A view of the vessel in elevation is shown in Figure 5.1.2. The cell is 5 m in diameter with 10 m of height between the plates and the overall dimensions of the outside of the vacuum jacket is 6.5 m diameter by 16.5 m high to the upper platform.

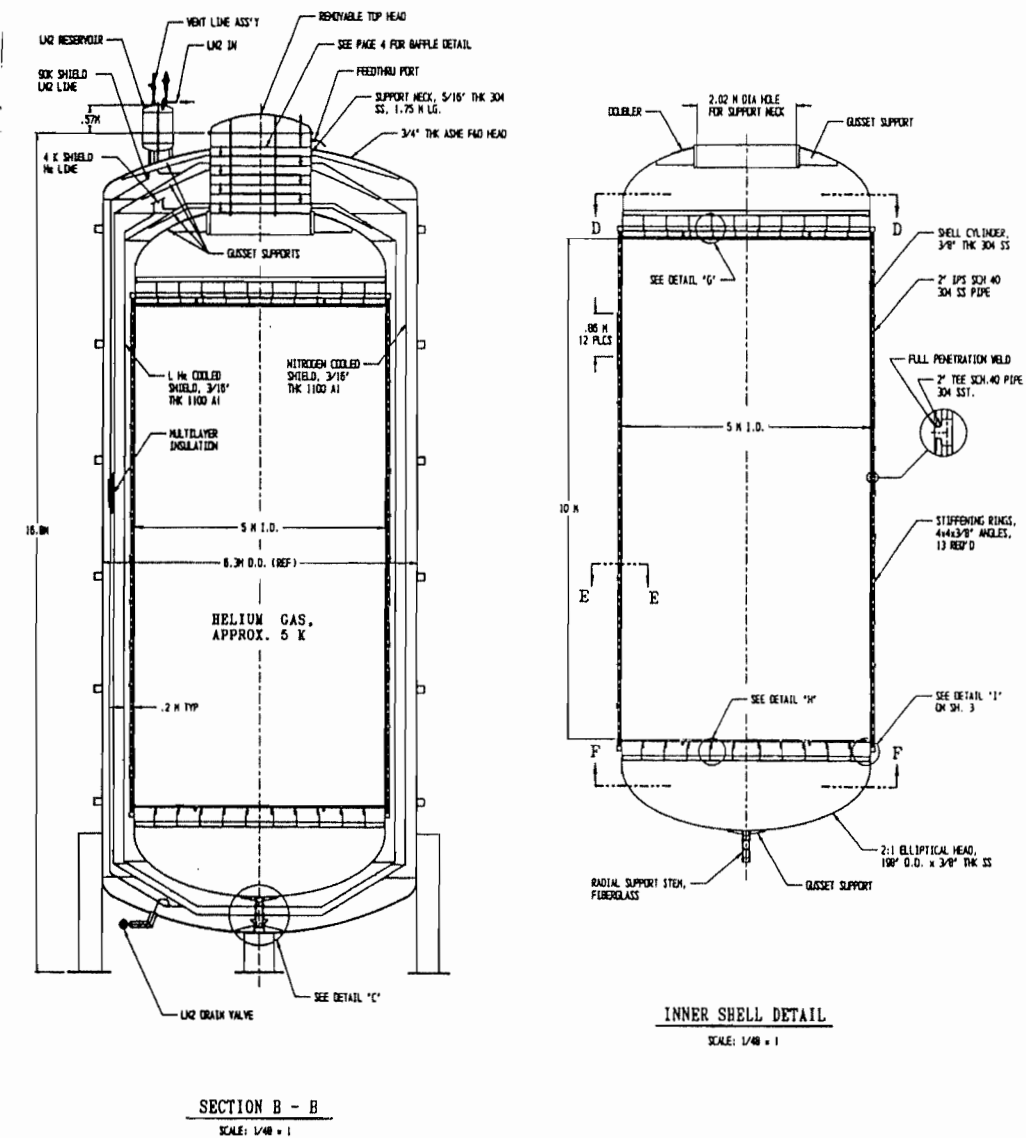


Figure 5.1.1 Convection Cell Cryostat Cross Section

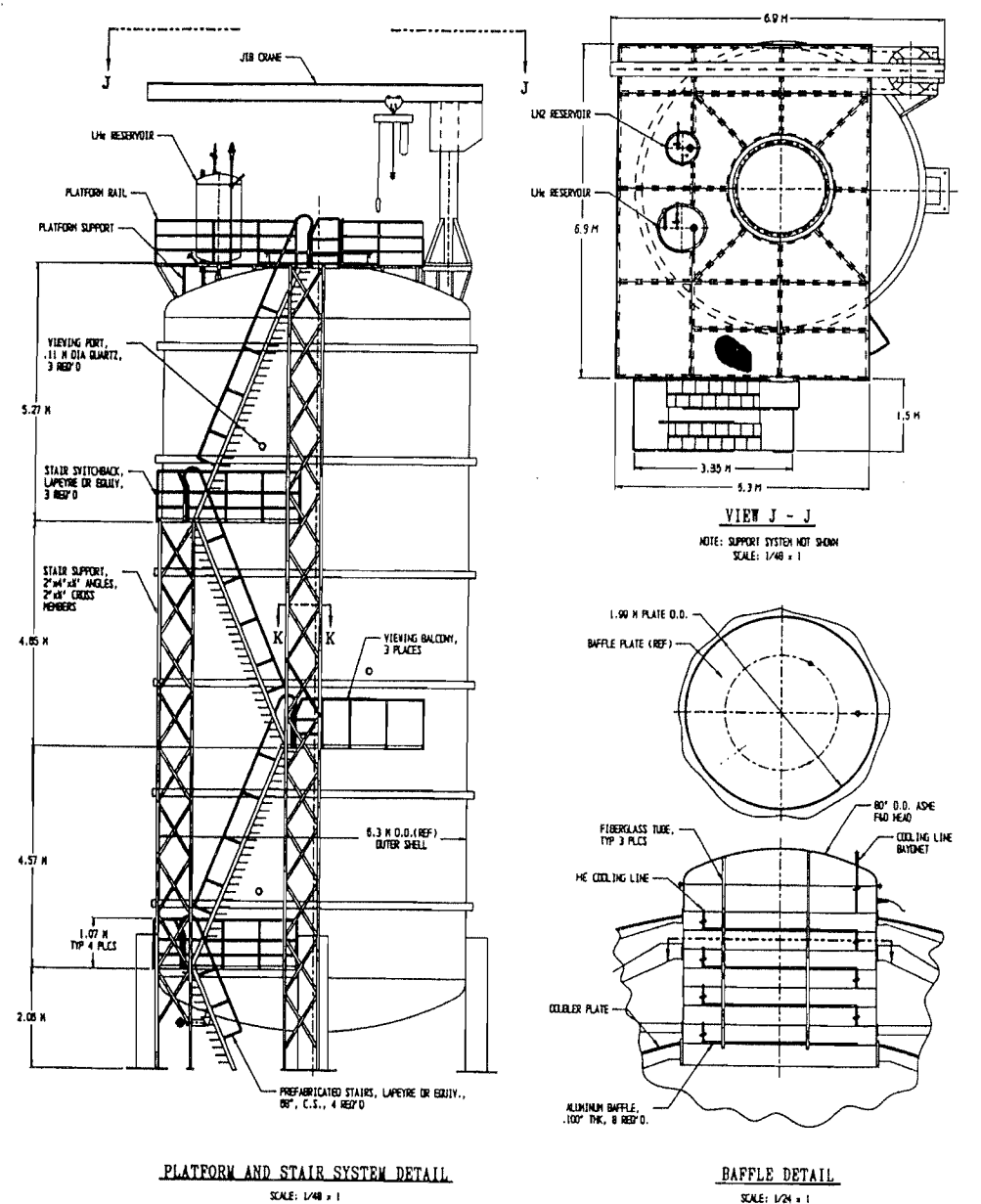


Figure 5.1.2 Convection Cell Cryostat Elevation

The cell cryostat is located adjacent to the Service Building at the N-15 site of the SSC Laboratory. This building contains two helium refrigeration plants, the N-15A plant which operates for the String Test Facility next door, and the N-15B plant which is dedicated to the convection experiment. Figure 5.1.3 shows a plan view of the service building with the location of the N-15B plant and the cell cryostat indicated. An artist's conception of this installation appears as the frontispiece of this report. To give a feeling of scale: the parapet of the Service Building is 14 meters high, about 2.5 meters lower than the top platform of the cell cryostat.

The vessel is conceived of as a piece of cryogenic tankage of conventional specification and construction. It is to be designed and built by a commercial vendor to ASME standards and code stamped. The vendor will deliver the vessel to the site, erect and assemble it, and participate in the acceptance testing. All of the other systems, the plate system and its instrumentation and the grid system and its instrumentation, will be installed in the vessel after it is delivered. This way of proceeding not only reduces the cost and risk associated with this major piece of equipment, but it also provides the flexibility appropriate to the range of research opportunity that is presented here. Additional important features of the design concept for the cell cryostat are discussed below.

Inner vessel: This is a cylindrical stainless steel vessel with ellipsoidal heads. It is designed for 5 bar internal and 1 bar external pressure and for a density of contents of 130 kg/cu-m. The external pressure rating comes about not because there is to be external pressure under normal operation but because external stiffening is needed to achieve the roundness that is required. The inner vessel does operate at internal pressures less than 1 bar, and if there is loss of insulating vacuum during commissioning or operation in this pressure regime, the inner vessel must not collapse.

In addition to the stiffening rings, in the vacuum space immediately outside the tank wall, six 2 inch IPS conduits are installed. These connect the spaces in the tank above and below the plates and tee into the tank in several location as well. The conduits provide a path for the installation of instrumentation and control wiring and other devices that must be kept outside of the cell itself.

At the top of the inner vessel is a neck tube providing access to the working volume. This neck is 2 m diameter with 1.3 m of length for thermal gradient. The thermal gradient (from 300 K to 5 K) is stabilized and controlled by means of a stack of removable baffles that are cooled by means of an attached tube carrying a flow of helium from the refrigeration plant. The refrigeration provided by this upward-flowing stream together with a heater on the lowest baffle allows the heat flow down the neck to be controlled and the temperature of the bottom baffle to be adjusted.

The access provided by the neck tube allows personnel to work within the experimental space. In this way the plate system, the towed grid system, and instrumentation systems can be installed or removed and maintained. The jib crane shown in Figure 5.1.2 is cost effective in providing easy materials handling through the neck tube. The warm-up and cool-down cycle of the Cell Cryostat with the N-15 refrigeration plant is short enough (one week) to allow good flexibility and low schedule risk in the experimental program.

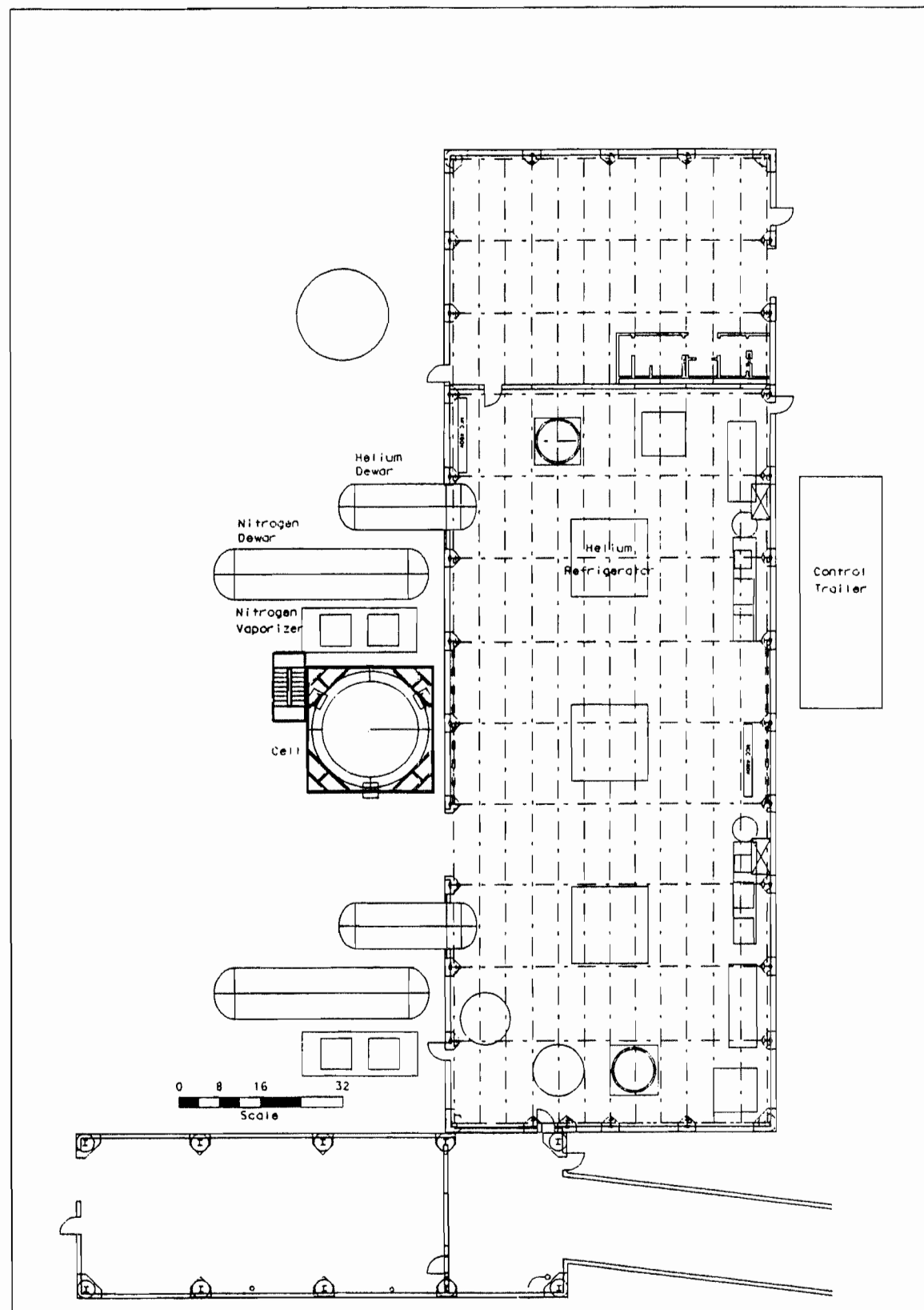


Figure 5.1.3 Plan View of Convection Cell Location

The neck tube also provides access for all of the wiring and mechanical connections to the experimental space. Wiring will be routed from feed-throughs in the room-temperature wall of the neck tube down the inside of the tube to connectors inside the head of the inner vessel. From there, cabling will be run to the top and bottom plate systems and instrumentation systems using the conduits mentioned above where necessary. The wiring harnesses will have their own helium refrigeration bleed in parallel with that of the neck tube baffles and will not have to be disturbed when these baffles are removed for access to the inner vessel.

The exception to the plan to provide all access through the neck tube is in the provision of optical access in the cylindrical wall of the cell for the use of laser Doppler velocimetry (LDV). The limitations of this technique together with its importance to the research program require that windows be provided. The windows in the inner vessel will be installed from within the vessel on flanges welded in pockets in the wall. Thus the inner surfaces of the windows can be made flush with the inside wall of the cell. Windows in the vacuum jacket of the cryostat together with thermal radiation control tubes through the shielding and the Multi-Layer Insulation (MLI) in the vacuum space will be installed through and attached to larger flanged openings in the jacket wall. For the purposes of costing, six such windows in pairs near the top, the middle and the bottom of the experimental space are included in the estimate for the tank. Access to the outside of these windows via balconies on the outside of the tank is also included. Systems needed for housing the LDV systems and provision for their environmental requirements are included as a part of the LDV system estimate.

The weight of the inner vessel and its contents are supported by the neck tube. This places the major part of the support heat load at the top of the tank where it is isolated from the working volume of the cell by thermal stratification. The verticality of the inner vessel is maintained by a center post at the center of the bottom of the tank that slides vertically to accommodate thermal expansion. Thus the attitude of the inner vessel will not change warm-to-cold, and the plates can be adjusted to meet the requirements for plane and level at room temperature from within the tank.

Thermal Control: The inner vessel of the Cell Cryostat is vacuum insulated, and within that vacuum space are a liquid nitrogen shield with multi-layer insulation and within that, a 4 K helium-cooled shield. Both shields are constructed of aluminum plate with tubes welded on for cooling. The LN shield is operated by means of a small phase separator and thermosyphon providing circulating saturated fluid in the tubes. The helium temperature shield is cooled by a Joule-Thomson loop from the refrigeration plant and controlled on outlet temperature. In this way, the shield can be adjusted to the same thermal gradient as the cell if this capability is needed.

As has been explained in previous paragraphs, the top and bottom thermal boundaries of the convection cell are formed from copper plates erected within the inner vessel of the Cryostat. Thus the thermal and the pressure boundaries of the cell are not the same, and there is a space filled with helium gas both below the bottom plate and above the top plate. In order to reduce the effect that these volumes of gas have on the measurements made in the cell, the gas in these regions is stratified and made stable by establishing a suitable thermal gradient. Below the bottom plate this involves placing a refrigerated shield in the bottom of the tank to make certain that no heat leaks result in rising thermal plumes. Since the bottom plate is a heated surface, the region below it tends to be stable even without additional shielding. It is essential, however, that the temperatures in this region be under positive control. The top plate is a cooled surface, and

so the region above it also tends to attain a stable gradient. This is particularly the case since the heat leak associated with the neck tube stratifies the upper parts of this volume. Temperature control of the region above the top plate is accomplished by the system mentioned above that adjusts the temperature of the bottom baffle of the neck tube stack.

5.1.2 Plate System

The upper and lower boundaries of the convection cell are formed by 5 m diameter copper plates, the upper one cooled and the lower one heated. Basic requirements for the plate system are presented in Table 5.1. The system consists of the plates together with their support and adjustment systems and the heating, cooling and thermometry subsystems. The program for the plates includes one major procurement of the copper parts and supports, a trial assembly at the site during which the heating, cooling, and other parts are assembled on the plates, and finally disassembly and reassembly in the Cell Cryostat. After installation, the plates are adjusted for flatness and level.

Plate System Mechanical: The copper plates of the cell are constructed of material of OFHC specification, rolled and quarter hard, 1.5 inches thick 36 inches wide and 96 inches long. For the material, thermal conductivity and resistivity ratio are the important quantities to control as well as yield strength which should not be too low. The OFHC specification is used for the purposes of costing recognizing that it may not be the cost optimum. The thickness is chosen with both thermal and mechanical considerations in mind. Appendix D contains an analysis of the thermal issues in the design of the plates. The thickness must be great enough so that the plate will have the right stiffness to be supported by a reasonable number of hangars, and great enough also that the back of the plate does not need to be completely covered with heaters or cooling tubes in order to attain the required temperature uniformity.

The layout of the plate assembly together with some of the details of its construction are illustrated in Appendix A, Sheet 3. Each 5 m diameter plate is assembled from 13 variously-shaped pieces. All of the joints between plate sections are formed by machining each piece to half thickness in an overlap one inch wide. These overlap joints are bolted from the back side into a blind hole with thread insert. In this way the plate can be accurately joined mechanically with well-controlled step and gap dimensions. Each copper assembly is supported at multiple points from a stainless steel framework resting in a rolled angle welded inside the top and the bottom of the inner vessel of the cell cryostat. The supports are attached to the plate also by bolting into blind holes with thread inserts. The supports will be adjusted with the aid of a laser alignment system to achieve the required plate flatness and level. These requirements are not particularly stringent. The support structures that are shown in the figure are worked out in sufficient detail for the purposes of costing, but they are not optimized for the rapid convergence of a plate alignment procedure or ease of assembly inside the tank. Such optimization is a task for the detailed design activity.

The heaviest piece of a plate divided in the way described above is 750 kg. The installation of one of these pieces begins with lifting by the crane by means of a rotating fixture bolted to the surface near the center of mass. The piece is lowered in a vertical attitude through the neck tube and then rotated into the horizontal inside the tank. For the bottom plate, the piece can be placed directly in the location in which it is to be installed. For the top plate, the piece once it is inside the tank can be transferred, if this is required, to a hoist suspended from the

support framework above the final location and lifted into position. The square section in the center of each plate is a manhole, easily removed by the crane to permit access to the cell or the bottom of the vessel. This manhole is not bolted down and can lift for pressure relief if this is needed. It may be surprising to recognize that only 0.5 psi differential is needed to lift the weight of the thick copper plate.

Constructed in the way described above, the copper plates for the convection cell present no particular difficulties and present low risk in the project. All of the materials required are readily available, and the fabrication steps can easily be performed to the tolerances needed. The installation sequence, although requiring close attention to safety and carefully designed procedures, can be carried out in a straightforward way.

Plate System Thermal: The top plate requires a temperature control system that consists of cooling tubes containing saturated helium circulated by a thermosyphon, a thermal resistance, and a heater. These elements must be distributed over the back of the plate, and thermal modeling indicates that for the most uniform temperature distribution, the heaters should be located with the cooler-thermal resistance combination and that the combination should be spaced approximately 3 inches apart on the plates. Because a uniform distribution of tubes is desired together with symmetrical spacing with respect to the joints between plate sections, ten or eleven assemblies will be attached to the back of each section running parallel with the joints. The tubes will be run across the transverse joints in the plates, and the manhole section will have its own independently connected set of tubes. The thermal analysis is described in Appendix D together with a discussion of appropriate materials and attachment methods for the assemblies. Appendix A, Sheet 5 shows the general arrangement of the plate components.

A variety of materials can meet the requirements of the cooling assembly. Either 6063 extruded aluminum tubes or square copper hollow conductor can be used for the high thermal conductivity parts and brass, stainless steel or kapton can be used for the thermal resistances. Suitable heater units are available commercially. A particularly convenient form of heater is insulated with kapton and self-adhesive. These heaters have specifications that meet the uniformity requirements of this application. The heaters will be applied in 34 inch lengths and connected so that all of the heaters in a 34 inch square of the plate operate on a single circuit. There will be about 27 such modules on the top plate.

An issue in the thermal design of the plates is the uniformity of contact resistances. These vary with force and joint thickness in ways that could be difficult to control. This problem will be managed by making joint areas large enough so that contact resistances can be made a small part of the total, and then bolting down the cooler-thermal resistance tube assemblies to the plate at 3 inch intervals. In this way the variations in contact resistance can be kept to a small enough scale so that the plate can average out any variation without temperature variations greater than what is required. Even with this plan, it will be necessary to make some verification measurements in the Oregon cryostat to be sure that the thermal resistance system design performs properly.

The bottom plate requires heaters only, and these will be the same heaters in the same arrangement as those used on the top plate. These will be held down to the back of the plate by means of strips bolted also at 3 inch intervals. The top and bottom plates are therefore mechanically very nearly the same, and the thermal systems differ only in the omission of the cooling tube-thermal resistance units on the bottom plate. Both the heaters on the two plates and the cooling tubes on the top plate are designed for a total load of up to 2 kW operating with the

helium thermosyphon. The plate cooling system has a refrigeration capacity of 4 kW under forced-flow conditions. A further discussion of the operation of the cryogenic system of the cell cryostat is presented in Section 5.1.4.

Adjustment of Cell Aspect Ratio: The aspect ratio (cell diameter/cell height) is adjusted by lowering the top plate. The smallest ratio that can be achieved is 0.5, limited by the 10 m height of the cell cryostat, but operation at larger ratios is provided as required. The support structure of the top plate is designed such there are tie bolts at four points around the periphery where the cross beams hang from the support angle welded to the inside of the tank. This is not clearly shown in Appendix A, Sheet 3. The procedure for lowering the plate assembly begins with picking up the plate by means of a fixture attached to the two main cross beams. The bolts mentioned above can then be removed and the plate lowered down the vessel. The four bolts are replaced by rods of the correct length, and the plate assembly is secured at the required position. The weight of the plate is such that rigging services for this operation will have to be provided by contract. The cryogenic piping and the electrical connections are extended to operate in the new position.

A crucial issue in carrying out the adjustment outlined here is roundness of the tank. If the tank does not meet the roundness specification, the adjustment of plate position will have to be made by disassembly and reassembly of the plate system in the new position.

Plate Thermometry System: Thermometers are needed on both the top and bottom plates. On the top plate, an array of thermometers is needed to provide information on which to control the temperature uniformly over the plate. Thus a pair of thermometers is mounted on each of the 34 inch squares. These are attached at convenient locations near the diagonal of the square and between cooling tube strips. These thermometers are best mounted in holes in the copper so that the point of measurement is close to the front side of the plate. One of the pair of thermometers on a square is used to regulate the temperature through feedback to the heater power supply serving the heaters on that square. The temperature can be set to the desired value above the saturated temperature in the tube array through adjustment of the heat flux in the thermal resistances between the tubes and the plate. This is a familiar technique in low temperature physics here adapted to distributed operation. The second thermometer on each square serves for redundancy in the control function and for an independent, open-loop monitor of the plate temperature.

As described above, the bottom plate operates at constant heat flux rather than at constant temperature. The thermometer array on this plate serves to monitor the average temperature of the cell boundary and to provide information on the fluctuations and spatial correlations of the heat flux. For the purposes of costing, it is assumed that the thermometer array on the bottom plate is the same as that installed on the top plate.

Thus there are 54 thermometers total installed on each plate. A total of 120 thermometer channels are included in the cost estimate, allotting 12 to other purposes within the cell. Each channel includes a calibrated germanium resistance thermometer, mounting hardware, cabling, connectors and feed-through, an electronic resistance bridge, a computer interface, and operating software. In addition there are in the system programmable power supplies for the plate heaters together with their cabling and interfaces.

A general requirement on the thermometry system is the attainment of stability and resolution of 0.5 mK over the somewhat difficult range of 4.2 - 6.5 K. The large thermometry system of the SSCL ASST string test has germanium thermometry which achieves a resolution

on the order of mK in the same temperature range with rather generalized DC electronics. It seems certain on the basis of this recent experience that the requirement of 0.5 mK resolution and stability with conventional, but probably AC, electronics specialized to the germanium device can be achieved for the costs estimated.

The problem with this thermometry system at the level of 0.5 mK lies with the primary device calibration. Germanium sensors are commercially available with a 5 mK calibration accuracy, and it is the cost of these in quantities of one that appear in the cost estimate. Approximately half of the device cost represents the cost of calibration, and the quantity needed here is very attractive to the suppliers. However, 5 mK accuracy meets the requirements of the experiment only at the upper end of the range of expected values of cell ΔT . On the other hand, experience with individual germanium thermometers in the laboratory absolutely confirm their ability to retain a calibration at a level orders of magnitude more accurate than that required here. It is very desirable, therefore to be able to extend the calibration accuracy of the sensors for the convection experiment downward by a factor of 5 - 10 beyond what is offered commercially. Several alternatives are available to get this calibration work done. The commercial supplier can do it under special contract, it can be done in a national laboratory or in a university laboratory as a special project, or it can be done by the convection experiment team. The Oregon cryostat would serve very well for calibration if this could be fit into its program. However this calibration is accomplished, it is necessary for verification testing of the thermometry system to be done at Oregon. In addition, it is necessary to provide time and an operating process for the cell that will allow the performance of the thermometry system to be verified at the temperatures of saturated helium at the beginning of each period of experimentation. This is described further below.

It is clear that the thermometry system discussed here represents a somewhat higher program cost risk than the cell cryostat or the mechanical components of the plates. The calibration task is not on the critical path of the program schedule, and time is allotted here for the uncertainties, minimizing the schedule risk. We believe, however, that this risk is not as great as that represented by the development required for some of the instrumentation needed by the research program. The technical issues are clear, and the problems can be managed successfully.

Multiplexing of Electronics

Ideally, the convection cell should have uniform temperature on the top and bottom copper plates. This can only be approached in practice by careful design, together with temperature measurement and control, particularly with its large scale and high heat flux. As is described above, the plate thermometry system performs the dual function of control of the temperature of the upper plate, and the monitoring and measurement of temperature of both plates. In the monitoring and the measurement functions, in cases where high bandwidth is not needed and where high resolution and high stability is at a premium, the possibility exists of using the techniques that have been well worked out and successfully employed in many low temperature laboratories. This problem was addressed at Duke University in the summer of 1994.

The need to measure the temperature at so many points immediately raises a problem—typical high precision measurements of this type are carried out with sophisticated AC bridge circuits with expensive electronics. For instance, in Figure 5.1.4a, we show a typical high-precision bridge circuit. An audio frequency AC generator provides a low-voltage signal through a transformer to the bridge which consists of a ratio transformer (a highly precise inductor with

variable center tap) a resistive germanium thermometer, R_g , a standard resistor, R_s and a lock-in amplifier. The ratio transformer should be a programmable version so that data acquisition can be carried out under computer control. We propose to significantly reduce the asset of instrumentation needed by multiplexing

This entails an arrangement such as that sketched in Figure 5.1.4b, the thermometry circuit which shows *only* one thermometer out of many in the scheme. Using relays, different thermometers are switched into or out of a bridge; this substantially reduces the number of expensive components needed. The switching is easily managed by a microcomputer and some simple electronics consisting of discriminators. They have built a test version of the switching electronics in which we can successfully switch between any of five thermometers. One final point about the multiplexing scheme is that when the thermometers are switched out of the bridge, they must still be kept at their normal operating state, or else there is a long transient following the application of the bridge current. In the Duke University working model and the proposed actual version, they provide a second voltage source which is used to keep the thermometers under bridge power while they are out of the bridge circuit.

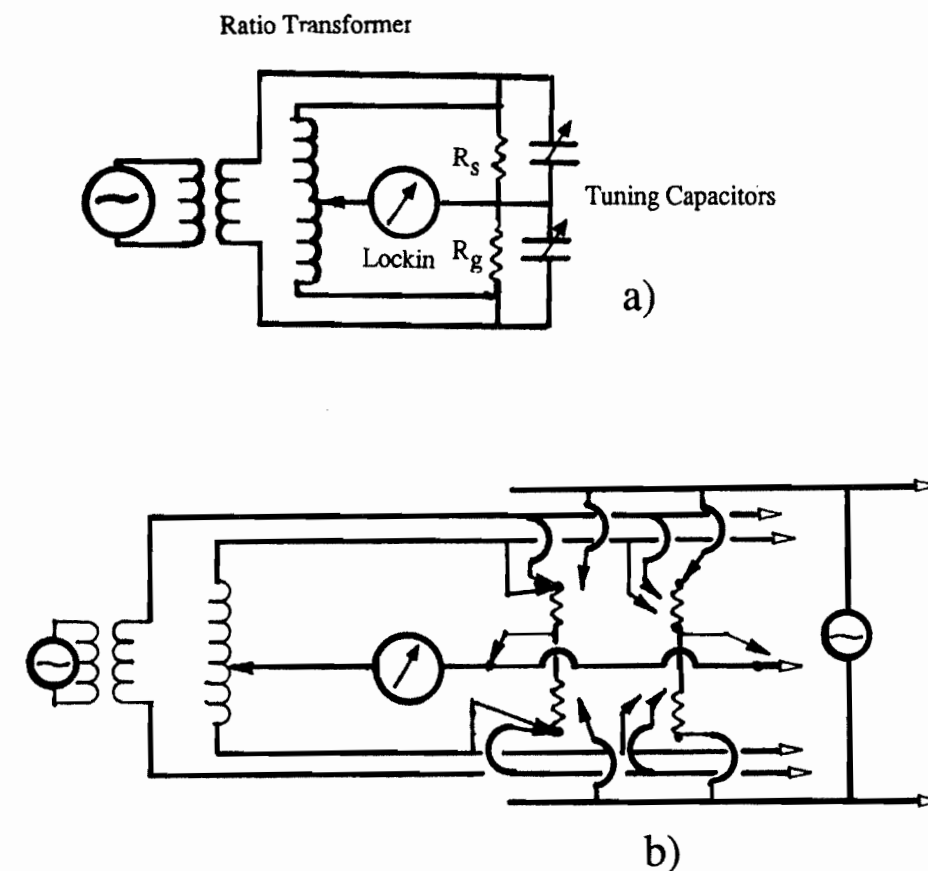


Figure 5.1.4 Schematics for (a) a single high precision thermometry bridge, and (b) part of a multi-plexed version. In (a) the four arms of the bridge consist of a ratio transformer, a fixed standard resistor, R_s , and a germanium thermometer, R_g . The balance state of the bridge is detected with a lock-in amplifier. An extra pair of leads is used to carry the drive voltage down into the cryostat in order to reduce spurious drift due to changes in the lead resistance induced by changes in the lead temperatures. Part (b) shows an additional feature for the multiplexed version which is a second AC source which keeps the thermometers in their normal state when they are switched out of the bridge. This will significantly reduce the unwanted transients when thermometers are switched. The switching is achieved by discriminators and relays (not shown). Voltage to the discriminators is provided by an inexpensive laboratory microcomputer, which can control and carry out measurements for many thermometers at once. This figure shows only two out of many thermometers which can be sampled by a single bridge circuit. The left thermometer is shown as active. The right thermometer is kept warm by the extra AC source, shown on the right.

5.1.3 Towed Grid System

The towed grid experiment is placed in the program before the first operation of the convection experiment. The first operation is carried out before the plate system is installed, but it can be re-assembled at any time and operated with the plates present.

Some details of the towed grid system are illustrated in Appendix A, Sheet 7 and 8.

Grid Construction: The grid is constructed from 1.5 inch square by .065 wall 6063 extruded aluminum tubing spaced on 6 inch centers in two planes at right angles. the tubing is assembled by fillet welding in the corners formed where the tubes cross. In order to get the grid through the neck tube and the manhole and into the tank, it must be made in four racks. These are assembled by means of joints in the tubing supported by pairs of 1.375 by 0.25 inch flat bars secured with flat-head screws. The weight of the assembled grid is about 200 kg. It is desirable to allow space inside the tubing for the installation of electric heaters so that heated grid experiments can be conducted. Requirements for this heater system have not yet been developed.

Towing System: In order to minimize stress and the deflection the grid is picked up at points on the corners of an 8 - 9 foot square. The four lines are spooled onto a horizontal drum located under the cover of the neck tube and driven by a bevel gear. The grid is accelerated to 2.4 m/s in 0.5 m, towed at constant speed for 9 m and then decelerated in 0.5m. If the plates are not installed, there will be room to tow for 10 m rather than the 9. If this schedule is followed, the accelerations are about 0.6 g and the peak power required about 7.5 kW. For the purposes of costing it has been assumed that hydraulic control is used.

5.1.4 Cryogenic System

The cryogenic system of the cell cryostat falls into two parts which are treated as separate tasks in the WBS. The first part includes the components of the system, valves and so forth, that are integral to the cryostat itself. The costs associated with this part of the system are included with the cell cryostat itself (WBS 2.1). The second includes the piping needed to connect the cell to the N-15B refrigerator (WBS 2.3) and the control system needed for operation (WBS 3.2).

Cell Cryogenic System: A process diagram of the cell cryogenic circuits are shown in Figure 5.1.5. This diagram indicates all of the control and relief devices needed for operation of the system, but it does not show all of the temperature instrumentation needed for loop control. The costs of this instrumentation, 8 channels of diode thermometers, are, however, included in the estimate.

Two systems are shown in the figure, one for operating the liquid nitrogen shield and the other for operating the helium shield, the neck tube, and the cell components. The liquid nitrogen system consists of a thermosyphon phase separator, supply valve with level controller, fill, and drain valves. A preliminary layout of these LN system components are shown in Appendix A, Sheet 5.

The helium cryogenic system has six circuits and a number of components. These are listed with comments below:

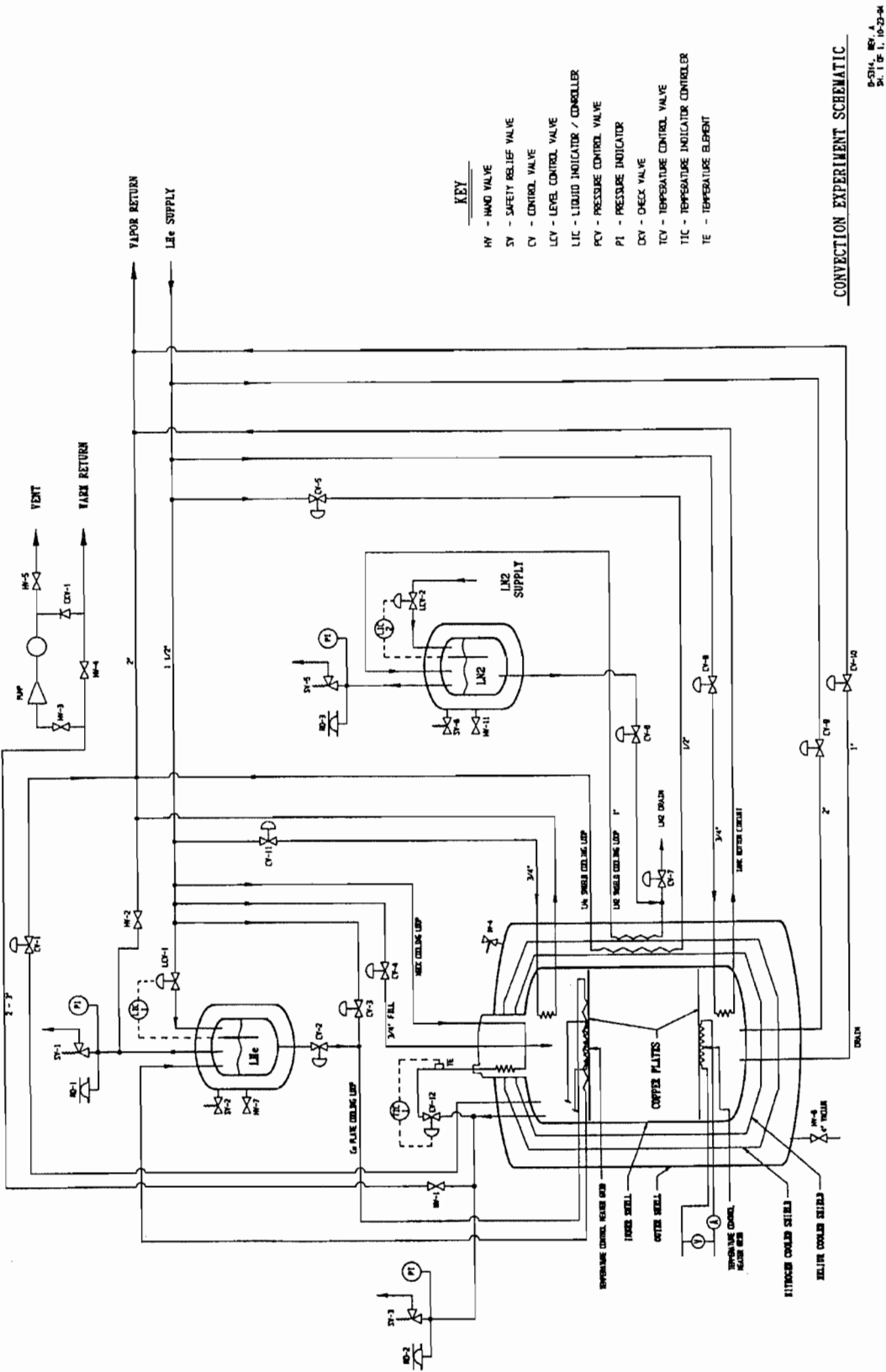


Figure 5.1.5 Process Diagram of Cell Cryogenic System

- 1) Cell cooldown and inventory control: This system consists of a fill line controlled by valve CV-4, and a vent line controlled by valve CV-1 both entering the top of the cryostat inner vessel, and a similar pair of fill and vent lines, controlled by valves CV-9 and CV-10, entering the bottom of the vessel. This system allows for the establishment of cooldown and warmup circulations through the vessel either from top to bottom or vice-versa. It also permits the adjustment of inventory by filling into the top of the vessel or draining either gas from the top or liquid from the bottom.
- 2) Top Plate Thermosyphon Loop: The approximately 70 tubes attached to the top plate are all connected in parallel between two headers, one supplying liquid helium from the bottom of a phase separator tank and the other returning a mixture of liquid and gas to the top of the same tank. A preliminary layout of the phase separator dewar and its associated components is shown in Appendix A, Sheet 6. This circulation is maintained by the heat input which causes boiling in the tubes. The rising two-phase mixture has a lower average density than the down coming liquid, and this pressure difference maintains the flow. This arrangement is referred to as a thermosyphon, and it is commonly used in cryogenic systems in situations where two-phase cooling must be delivered to a distributed load. The liquid level in the phase separator dewar is maintained through control valve LCV-1. The liquid helium passes through valve CV-2 into the inner vessel of the cell cryostat and is distributed through the header system into the tubes attached to the back of the top plate. The two -phase mixture returns to the separator by a second line. Valve CV-2 may be closed and CV-3 opened to force flow delivered from the refrigeration plant directly through the tubes. This circuit is used in cooling down before the temperature conditions make it possible to use the thermosyphon.
- 3) Tank Top Circuit; This is a Joule-Thomson loop providing cooling to the fin tube recondenser in the top of the tank. The conditions of the helium supply to the cell cryostat are a pressure of 3 - 4 bar and a temperature of 4.4 K. This fluid is expanded through valve CV-11 into the cooler where a mixture of liquid and gas is produced. Heat input into the cooler evaporates the liquid, and the gas is returned to the refrigeration plant at 1.2 bar and a temperature just above saturation. The J-T valve is controlled on cooler outlet temperature.
- 4) Tank Bottom Circuit: This has the same arrangement as the tank top circuit, the J-T valve being CV-8. In this case, the refrigeration is delivered to the region below the bottom plate for the purpose of thermal control.
- 5) Helium Shield Cooling Loop: This is a third J-T loop providing refrigeration to the helium cooled shield of the cell cryostat.
- 6) Neck Tube Cooling Loop: This is a line supplying helium at the supply conditions to the bottom of the neck tube. This stream passes up through a heat exchanger in the neck tube and exits near room temperature to be returned to the refrigeration plant in

the warm return line. This stream is controlled by a warm valve and temperature controller in the neck tube outlet.

- 7) Cryostat Warm Return Line: This is a pipe line that returns gas from the top of the neck tube to the refrigerator compressor plant suction. This line is used to return warm gas when cooling down the inner vessel of the cryostat, for supplying warm gas when letting up the vessel, and for other utility functions. In addition, this line has a roughing pump that can be switched in for evacuation of the inner vessel or for reducing inventory when operating at very low densities.

Cryogenic Piping and Controls: In addition to the cryogenic system of the cell cryostat, additional components are needed to complete the system. These include vacuum insulated piping to connect the cell cryostat to the N-15B refrigeration plant, and a computer control system for operation of the cryogenics. The piping run from the cryostat to the refrigeration plant cold box is about 75 feet. Two runs of vacuum insulated helium piping is needed for connection. All of the valves and controls are either within the cell cryostat or are included in the units of the refrigeration plants. A third vacuum insulated line for liquid nitrogen is needed to connect the cell cryostat with the LN tank located next to it. The forth line of piping that is needed is the warm return line. This more or less follows the route of the helium lines.

Computer control is provided for the cell cryostat by extending the control system of the N-15B refrigeration plant to include its valves and instruments. This plan includes only the process controls of the cryostat and not the instrumentation of the plates or other experimental apparatus. These are provided with their own dedicated data system discussed in the paragraph below. The refrigeration plant process control system is many times larger than that required to control the cell, and it is be extended by the addition of a PLC unit and input-output cards. Thus the cell cryogenic system appears to the operator of the equipment as a part of the refrigeration plant system, and operations can be fully integrated for reliability and safety. Costs for both the hardware and the software needed for this plan are included in the estimates and in the program schedule.

5.1.5 Data Acquisition

In addition to the 120 channels of thermometry and the power supply control that is discussed in the paragraphs above, additional instrumentation is required for the measurement of velocity and other quantities in the course of the towed grid and the convection experiments. To include the costs of acquiring and recording data in the experimental program, an additional 64 channels 16 bit A/D together with the crates and communications cards, a computer, file server, and software development are assumed. Also for the purposes of estimation, the data acquisition is assumed to be located in a small portable building located on the upper deck of the cell cryostat. Communications runs in a tray across the roof of the Service Building and into a Controls Trailer which is located in the alleyway between the Service and the Compressor buildings. The layout of these facilities appears in Figure 5.1.3. Costs for this Controls Trailer have not been included in the budget, but all other parts of the data acquisition system and its installation are estimated.

5.2 System Operation

5.2.1 Purification and Cooldown

Operation of the cell cryostat begins with checkout and inspection. During this activity, inspection of the condition of the cell, installation of the neck tube baffle, installation of the neck tube head, inspection of the safety equipment, continuity checks of the cell electrical systems, and computer and control system diagnostic routines are run. The cell insulating vacuum is roughed out and the high-vacuum pumping started. The inner vessel is also roughed out and re-filled with helium gas. Permission to operate is received from the Laboratory Safety Officer. Development of procedures for the startup of the cell systems and their approval by an appropriate review board is a task listed in the WBS and included in the cost estimate.

When the system is ready for cooldown to begin, a circulation of purified room temperature helium gas through the cell from bottom to top is begun. This together with the cooldown to liquid nitrogen temperatures is accomplished using the CCWP (Cleanup, Cooldown, Warmup, Purification) unit of the N-15B refrigeration plant system. This unit can provide a flow of 50 g/s of dried and purified helium gas at 4 bar at any temperature between 300 and 80 K.

The room temperature gas is circulated until the impurity content of the returning gas falls to a satisfactory level. This circulation dries the inside of the cell and removes the last traces of air. The CCWP then programs down in temperature and the cell is cooled to 80 K. With a flow of 50 g/s this takes less than 24 hours, but a slower rate can be chosen.

As the temperature of the gas returning from the cell begins to fall, the cold box of the refrigeration plant is started and cooled down. When the cell reaches 80 K, the CCWP is turned off and a flow of cold gas from the refrigerator is turned on, again flowing upward through the cell. The gas returns to the cold box and is recirculated. Using the refrigeration plant in this way, the cell can be cooled to helium temperature and filled with cold gas. At this point, the cooldown process is completed.

5.2.2 Calibration

At the beginning of an operating period it may be necessary to bring all parts of the cell to well defined conditions of uniform temperature in order to check the performance of thermometry and bolometry systems. This is done by filling the bottom the inner cryogenic vessel with a few hundred kilograms of liquid helium and boiling this with the 2 kW heater installed in the bottom of the tank. A metal mesh layer above the heater is needed in order to assure the production of saturated gas. The gas thus produced is refluxed by a fintube cooler in the top of the tank. Operation of this cooler is described above in the paragraphs on the cryogenic system of the cell. The liquefied helium falls on top of the top plate and rains down through the cracks onto the bottom plate. From there it returns to the bottom of the tank. By this process the entire volume of the cell is brought as close as possible to the saturation temperature of the refluxing helium. This temperature will, of course, be higher at the bottom of the cell than at the top, but it will be predictable at all levels in the tank and adjustable over the saturation range from 4.4 K to something like 4.9 K. The pressure and temperature in the cell is controlled by a feedback loop on cell pressure controlling the flow of refrigerant through the fintube cooler.

5.2.3 Inventory Management

The first operation in bringing the cryostat into operation either with the towed grid or with the convection cell is the establishment of the required density and temperature of helium within the tank. How this is done depends on what density is required. Operating regimes for the convection experiment are discussed in Section 2 of this report and in Appendix D. Two interesting regions of density are identified: Region 1 with helium densities about 20 kg/cu-m and below; and Region II, at densities of 60 - 80 kg/cu-m.

At the end of calibration or of a complete cooldown, the tank is filled with cold gas near saturated conditions at density of about 16 kg/cu-m. If the density that is required for operation is less than this value, the tank is warmed up by a stream of gas from the refrigeration plant. The flow enters the tank at the top and the cold, dense gas is returned to the refrigeration plant and liquefied into helium storage. This operation can raise the temperature and stop at any level all the way to 300 K, but as subsequent cooldown of the cell must be accomplished by indirect cooling via the top plate, the practical limit for density adjustment is in the neighborhood of 50 K. At this temperature, the density is 1 kg/cu-m. If the density required is still less than this, it is necessary to rough pump the tank down to the needed level. Otherwise, when the needed density is reached, flow through the cell is stopped, and the top plate cooling system or the tank top fintube cooler is used to return the vessel and its contents to the operating temperature. This is in most cases between 5 and 6 K.

If the density required for operation is greater than 16 kg/cu-m, liquid helium is added to the cold tank in the correct amount. The cell is then valved off, and heat is added to the cell until the operating temperature is reached. This is done initially with the 2 kW heater in the tank bottom. If the convection cell is being operated, the bottom plate heater and the top plate cooler are brought into operation, and the final conditions adjusted with them. If the towed grid is being operated, the heat content of the helium can be adjusted by means of the 2 kW heater and the fintube tank-top cooler. Motion of the grid will stir the contents sufficiently to even out the temperature. It is straight forward to install a "ceiling fan" in the neck tube of the cryostat if this is found in the final design analysis to be necessary.

In thinking about the operations just described, it is important to recognize that this cryogenic system has a very large heat capacity: if the tank is charged to the level of 20 kg/cu-m, the capacity rate of the volume is 16 MJ/K. Thus a 2 kW heater or cooler requires 2 hours to change the tank temperature by 1 K.

5.2.4 Inventory at High Densities

As described in Appendix J, the capacity of each the three liquid helium storage tanks at the N-15 site of the SSC is 44 cu-m. This can be filled with 40 cu-m of liquid helium for a total contents of 4,860 kg. This will fill the cell cryostat to a density of about 20 kg/cu-m. One of these tanks is attached to the N-15B refrigeration plant, and so is available for use by the convection experiment full-time. A second tank is located in the same building, and it is probable that it, too can be used by the convection experiment at least on a part-time basis. These two tanks provide all of the storage that is needed for a flexible program of operation with the Region 1 density range. Operation in Region 2, at 70 kg/cu-m requires more helium inventory than can be stored at the N-15 site. In order to operate in this region, liquid helium has to be delivered in bulk and transferred directly into the cell cryostat. The N-15B refrigeration

plant has the equipment both to unload and to reload helium tanker trucks. Two deliveries are required. At the end of such an operating period, the helium inventory has to be loaded back on the tanker trucks, and shipped back to the supplier. The helium would thus in effect be rented for use in the cell. This is a troublesome and time-consuming series of operations, and only one such operating period has been included in the program proposed here.

Region 2 operation of the cell at higher aspect ratios requires a lower total helium inventory since the tank volume above the top plate can be stratified to lower density. Likewise, a towed grid experiment can be performed with 5 m tow in tank half-full of saturated liquid helium.

5.2.5 Operation for Data Taking

In the preceding paragraphs, the process of cooling down and of establishing operating conditions in the cell cryostat has been described. Steady operation at the selected conditions is a straightforward matter: in the case of convection cell operation, the refrigeration plant operates to provide cooling to the helium temperature shield in the cryostat, the neck tube bleed, the cryostat bottom shield, and the upper plate. Under most circumstances this last load dominates.

Operation of an unheated towed grid requires much less refrigeration power than the convection experiment, and the N-15B refrigeration plant can not be turned down effectively below about 1 kW. The most economical way of proceeding is to shut down the refrigeration plant once the operating point is reached, and either maintain the helium-cooled shield and the neck tube cooling on streams drawn from the cryostat contents or simply not use them. As an example of this last procedure, begin the operating period at 20.7 kg/cu-m and 4.8 K. The pressure at this point is 1.4 bar. Valve the tank off and add 137 watts of heat for a week: the heat leak is an order of magnitude lower than this, but there is heat input by the motion of the grid. The final state is a pressure of 2.8 bar and a temperature of 7.77 K. The viscosity increase during this week is a factor of 1.45. A final choice of process with which to operate the towed grid experiment will be made during the process of detailed operations planning, but it is clear at this point that there are satisfactory possibilities.

5.2.6 Time-Out Periods and Warmup

During the course of operation of the cell in the experimental program it will be desirable to be able to allot periods for equipment maintenance or preliminary data analysis during which the refrigeration plant and other machinery is not operating. The means by which this is accomplished depends on the operating conditions. When the cell is operating at densities below 10 kg/cu-m, the quickest way to shut down is to warm up to 20 K and liquefy the inventory into storage. The refrigeration plant can then be shut down and the cell left to slowly warm up. If the cell is operating at higher densities in Region 1 or in Region 2, the most efficient way of proceeding is to lower the temperature in the cell to saturation and liquefy the contents into the bottom of the tank. The refrigeration plant can then be shut down and the cell left as described in the preceding paragraph, either valved off or with a shielding bleed. In either of these two conditions the cell can be left for the order of two weeks and then brought back into operation with minimum refrigeration plant operating time overhead.

When it is necessary to warm the cell up for access to the inner vessel, the processes discussed in the preceding paragraphs are performed in reverse. First the helium inventory is

stored in the liquid helium storage tanks or shipped out. The cell is then warmed up by means of a flow of helium gas from the refrigeration plant and the CCWP unit. This flow passes through the cell from top to bottom, and it is programmed in temperature as required to prevent thermal shock. The minimum time required for warmup is twice the minimum time required for cooldown, about two days.

Table 5.1
Helium Convection Experiment
Design Requirements

Convection Cell

Pressure Rating
5 bar

Maximum distance between top and bottom plates (L)
Maximum L = 10 m

Minimum aspect ratio
Minimum D/L = 0.5 (diameter of 5 m)

Desired variability of aspect ratio.
Continuous variability is not necessary. Desired aspect ratios are 0.5, 1, 2, 4, 8, 100

Roundness of convection cell wall
 $\pm 0.5\%$ is acceptable. Less than $\pm 1\%$ may be achieved if stiffening rings are added. These will also provide insurance against collapse of inner vessel due to loss of guard vacuum during operation at subatmospheric pressures.

Surface smoothness of convection cell wall
Industry standard for steel plate

Verticality of convection cell wall
 $\pm 0.1\%$ of L applied to every point on the wall relative to plumb line. This quantifies allowable waviness as well as deviation from vertical

Largest acceptable flow obstruction, such as pressure or temperature sensor, that can be tolerated near the convection cell wall.

All devices permanently installed within the convection cell must be flush with the surface. Note: wiring cables or conduits for instrumentation may not be run up the inside of the wall. Penetrations in the wall for conduit in the vacuum space or other ports are acceptable

Rayleigh number range
(10^{11} - 10^{19})

Heat leak through the side wall
Total heat leak must be kept to that required to allow accurate calorimetry. This is not a very severe requirement as long as heat leak is spread uniformly over the wall. Localized heat inputs producing "hot spots" on the wall are not acceptable.

Heat conduction up the side wall

This is not a free parameter - wall thickness is given by ASME code for pressure rating of 5 bar. The conductivity introduced by this wall thickness, however, is not significant in the experiment.

Plate System

Required flatness
Surface roughness: ± 10 mm, or best achievable
Waviness: ± 0.2 mm, or best achievable
Deviation from level: a small fraction of a degree, roughly ± 2 mm

Step height where plate sections meet
 ± 0.1 mm, or less

Allowable gap, if any, where plate sections meet
less than 1 mm

Circumferential gap
This gap must be caulked with plastic foam, metal wool or a skirt, but complete leak tightness is not required. Some gas flow around and through the plate must be allowed for operational reasons.

Vibration concerns
Vibration wave lengths will much longer than measurement scales will be of little consequence. Sources of high frequency vibration must be evaluated in the final design process and after the instrumentation plan is complete.

Maximum operating temperature or temperatures.
Cooled Plate: 6K
Heated Plate: 6.5 K

Maximum allowable plate temperature deviation from operating point, assuming that large scale fluctuations in the flow near the surface of the bottom plate cause local fluctuations in the power flow from this plate:

Expected amplitude, as a function of frequency, of the power flow at a point on the plate.

Expected spatial extent of point-to-point correlation of the power flow from the plate.
Little is known about exactly what to expect in the way of temperature fluctuations, power amplitude fluctuations, and the spatial extent of these fluctuations. These quantities instead are among the objects of the research. In view of this, it is appropriate to operate the heated plate at constant heat flux. The heater system must be designed to produce a uniformity of $\pm 1\%$, and a thermometers must be distributed over the plate to monitor the temperature and its fluctuations. The cooled plate is to be operated at

constant temperature controlled by distributed thermometers. Temperatures in the plate system are to be measured and controlled to within ± 0.5 mK or $\pm 1\%$ of T whichever is larger. Bandwidth requirement of these measurements has not been determined in detail, but there is no expectation that this will be an issue.

Towed Grid System

Grid Dimensions

A grid made of square bars 1.5 inches on a side arranged on 6 inch centers in each of the two orthogonal directions provides the properties required.

Grid Towing Schedule

The grid is towed at the constant speed of 2.4 m/s over a length of 9 m within the tank. After a measurement period, it is lowered in 100 s. After a pause for the decay of motions of the helium, the cycle is repeated.

Operating Conditions for the Towed Grid Experiment

The towed grid experiment is to be designed to operate at any thermodynamic conditions that the cell cryostat can support.

Compatibility with the convection cell equipment

The towed grid is to be designed to be operated either before or after the plate system for the convection experiment is installed.

5.3 Work Breakdown Structure and Assumptions of Infrastructure Support

In order to develop an estimate of the cost to construct and operate the 10 meter cell, a Work Breakdown Structure (WBS) has been developed. This amounts to a compilation of tasks associated with (1) university support programs (2) construction of mechanical systems (3) construction of electrical systems and (4) operations. Since the university portion of the program is discussed in detail and costed elsewhere in this report, only a very brief outline of that portion of the program is included here.

The WBS outlined below serves as the basis for estimating costs and determining scheduling requirements. It is used to estimate manpower requirements for each year of the program. In addition, it contains a listing of capital equipment under the task heading of procure, or purchase. In this way it also serves as a basis for estimating capital equipment costs. Both the cost estimate and schedule are discussed in following sections.

In putting together the WBS, it is assumed that a number of management activities will be provided by the host facility, including those duties normally carried out by Personnel, Accounting, Procurement, Safety, and Quality Assurance departments. The indirect costs associated with these activities are included in the budget as overhead, but are not included in the WBS.

Each of the primary elements in the WBS, then, is broken down into subelements, as indicated in the following outline. The listing of capital equipment is broken down into system, subsystem, and component. This breakdown is not necessarily carried out to the lowest level possible, but rather to that level at which a reasonably accurate cost estimate can be obtained. Thus, some items are costed at the system level while others are costed at the subsystem or component level. In addition, the following line items are included, for purposes of estimating manpower requirements:

- Design, review, and specification
- Procurement
- Inspection and/or acceptance testing
- Installation
- Systems testing and debugging.

A complete WBS dictionary is contained in Appendix F.

WBS Outline

1. University support programs
 - 1.1. Oregon experiment
 - 1.2. Duke university projects
 - 1.3. Yale university projects
2. Mechanical systems
 - 2.1. Vessel system
 - 2.1.1. Design, review, and specify
 - 2.1.2. Procure
 - 2.1.3. Develop commissioning procedures
 - 2.1.4. Develop safety procedures
 - 2.1.5. Commission
 - 2.2. Plate Systems
 - 2.2.1. Design, review, and specify
 - 2.2.2. Procure
 - 2.2.3. Perform trial assembly
 - 2.2.4. Install
 - 2.3. Cryogenic Supply System
 - 2.3.1. Design, review, and specify
 - 2.3.2. Purchase piping
 - 2.3.3. Install
 - 2.3.4. Test
 - 2.4. Vacuum System
 - 2.4.1. Design, review, and specify
 - 2.4.2. Purchase equipment
 - 2.4.3. Install
 - 2.4.4. Test
 - 2.5. Towed Grid System
 - 2.5.1. Design, review, and specify
 - 2.5.2. Purchase system

- 2.5.3. Install
- 2.5.4. Test
- 2.6. Utilities
 - 2.6.1. Design, review, and specify
 - 2.6.2. Procure
 - 2.6.3. Install ventilation system
- 2.7. Site Work (Foundation)
 - 2.7.1. Design, review, and specify
 - 2.7.2. Procure
- 3 Electrical systems
 - 3.1 AC power
 - 3.1.1 Design, review, and specify
 - 3.1.2 Procure and take delivery
 - 3.1.3 Checkout
 - 3.2 Cryogenic supply controls
 - 3.2.1 Design, review, and specify
 - 3.2.2 Purchase
 - 3.2.3 Install
 - 3.2.4 Program
 - 3.2.5 Checkout and debug
 - 3.3 Data Acquisition System
 - 3.3.1 Design, review, and specify
 - 3.3.2 Purchase
 - 3.3.3 Install
 - 3.3.4 Program
 - 3.3.5 Checkout and debug
 - 3.4 Plate controls and heaters
 - 3.4.1 Design, review, and specify
 - 3.4.2 Purchase
 - 3.4.3 Install
 - 3.4.4 Program
 - 3.4.5 Checkout and debug
- 4. Operations
 - 4.1 Operate towed grid
 - 4.1.1. Prepare operating procedure
 - 4.1.2. Perform experiments
 - 4.2 Operate convection cell
 - 4.2.1. Prepare operating procedure
 - 4.2.2. Commission plates
 - 4.2.3. Perform experiments

5.4 Schedule

The proposed Cryogenic Helium Gas Convection Research fits well into a five year program, with the university support programs continuing throughout the five years. Design, construction and operation of the 120 meter cell will take place in parallel. Specifically, design and construction of the 10 meter cell will take place in the first two years of the project. The first year is devoted to design, specification and procurement, the second to fabrication and delivery. The cryogenic supply system with controls, the vacuum system, towed grid system, and all utilities will be installed in the first quarter of the third year. The second and third quarters of the third year are dedicated to commissioning the cell cryostat. Immediately after commissioning, a set of towed grid experiments will be conducted, with completion scheduled for the end of the first quarter in the fourth year. The remainder of the fourth year is given over to installing the plates in the vessel, instrumenting, and commissioning them. The entire fifth year is reserved for convection cell experiments.

A representative schedule, showing the timing required to complete the Program in five years, is contained in Appendix H. It is based on the WBS and is consistent with the manpower estimates contained in the budget, as well as, those contained in the detailed cost sheets presented in Appendix I. The university support programs are included with milestones indicating the timing for completion of sensor development, property measurement, and preliminary experimental work. The Oregon cryostat is to be completed by the end of the first year, allowing a full year for development of velocity measuring techniques before the start of towed grid experiments in the 10 meter cell. Continuing development of sensors for convection experiments in the 10 meter cell are to be completed by the end of the third year, for installation with the plate system. Likewise, preliminary towed grid results will be finished by the end of the second year, and property measurements by the end of the third year.

In putting together the schedule, it is especially important to estimate the times involved in completing all tasks on the critical path with a fair degree of accuracy. It is reasonably straightforward to estimate the time required for completion of minor tasks, and even if the estimates turn out to be off by a factor of two, the impact on schedule and budget will be minor. However, if a major task, such as vessel design, is off by a factor of two, very significant schedule and budget effects will result. Unfortunately, it is much more difficult to estimate the time required to complete such large tasks. For instance it is difficult to imagine exactly how many man-weeks will be required to complete a conceptual design for the main vessel. It is much easier to imagine that a scientist, CAD designer, and team of engineers would be able to accomplish this task in some fixed amount of time. Therefore, a procedure for developing the schedule has been adopted that assumes the existence of a team for each of the five years.

The process, then, is an iterative one. Assuming the existence of teams, a preliminary schedule for completion of all WBS tasks is worked out. Based on the schedule, labor requirements for each WBS item are determined, and a detailed set of manpower requirements is developed. A few iterations provide a realistic manpower estimate that is consistent with both the WBS and the schedule, as well as, a schedule that can be met with the assumed manpower.

5.5 Cost Estimate

Each item in the WBS is included as a line item in the Detailed Cost Estimate contained in Appendix I. Labor requirements as reported above, and, where appropriate, quantity and unit price are provided for each item from WBS elements (2) and (3). Operating costs and labor requirements associated with WBS (4) are also included.. Materials and supplies, travel expenses, contingency, and overhead are estimated at a higher level. University costs are reported elsewhere.

5.5.1 Capital Equipment Costs

Cost estimates for capital equipment are based on one of:

- Vendor quote
- Catalog price
- Engineering judgment
- Professional consultant

By far the greatest capital equipment expenses are associated with the 10 meter cell and the copper plates. The cost of these items, together with the towed grid system, have been estimated by Cryogenic Technical Services Inc., a cryogenic consulting firm with many years of experience building cryogenic vessels similar to the 10 meter cell. The details of those estimates are contained in Appendix A, and only the rolled-up costs appear in the cost sheets of Appendix I. A summary of the capital equipment expenses is shown in Table 5.2.

Table 5.2 Summary of Capital equipment cost estimates.

WBS number	Description	Cost (k\$)
2.1	Vessel system	1250
2.2	Plate system	414
2.3	Cryo. supply system	111
2.4	Vacuum system	40
2.5	Towed grid system	68
2.6	Utilities	45
2.7	Foundation	10
3.1	AC power	13
3.2	Cryo. control system	11
3.3	Data acquisition sys.	435
3.4	Plate control system	258
Total		2655

5.5.2 Labor Costs By Year

In estimating the labor costs for each year, the number of man-weeks estimated for each task are summed by labor category and used to fix the number of full-time employees required. This is an approximating procedure that results, for example, in 113 man-weeks being the equivalent of 2 full time employees. In another case 39 man-weeks results in 1 full-time employee. An annual rate of pay is then applied to the number of full-time employees in order to arrive at the labor costs for each year. Rates appropriate to the Applied Superconductivity and Cryogenics Technology Center proposed for establishment at the site of the former SSC Laboratory have been used where available. It is assumed that these rates include the cost of benefits, but not the cost of overhead, which is included as a separate category in the budget. It is also assumed that engineers, technicians, CAD designers, and administrative assistants are available from a central pool at the host facility, on a time-shared basis. The estimated labor costs for each of the five years are shown in Tables 5.3 through 5.7.

Table 5.3 Labor costs for first year.

Year 1			Labor cat	Eng	Sci	Post doc	Tec/ Drft	Admi n
Sched tasks	Sched time							
Design	Vessel system	26		64	8	16	8	8
	Cryo supply sys	6		6	2	2	0	1
	Vacuum sys	6		3	1	1	1	0
	Towed grid	6		6	2	2	1	1
	AC power	2		3	1	1	0	0
	Cryo controls	2		3	1	1	0	0
	DACQ sys	26		47	12	12	6	6
Procure	Vessel system	26		32	16	8	4	4
	Cryo supply sys	18		3	1	1	1	1
	Vacuum sys	18		2	1	1	1	0
	Towed grid	24		3	1	1	1	1
	AC power	24		2	0	0	0	0
	Cryo controls	24		3	0	0	0	0
	DACQ sys	26		24	6	6	3	3
Total (MW)				201	52	52	26	25
FTE				4.0	1.0	1.0	0.5	0.5
Base pay (k\$)				60	100	45	44	25
Labor/Yr (k\$)				240	100	45	22	13
3 Post docs						135		
Total labor (k\$)								555

Table 5.4 Labor costs for second year.

Year 2			Labor cat	Eng	Sci	Post doc	Tec/ Drft	Admi n
Sched tasks	Sched time							
Install	Coord. vessel inst.	52		2	12	0	0	7
	DACQ sys	13		12	1	3	6	0
	foundation	4		1	1	1	0	0
Write	Commission plan	14		5	2	3		3
	safety procedures	14		5	3	0		3
	DACQ program	26		12	2	12		3
Checkout	DACQ sys	13		12	1	12	24	
				24				
Design	Plate system	26		1	5	8	13	2
	utilities	6		1	1	0	2	0
	foundation	4		24	1	1	1	0
	Plate controls	26		1	5	8	4	1
Procure	utilities	18		1	1	0		1
	foundation	12		0	1	1		1
	plate sys	26		12	3	0		4
Total (MW)				113	39	49	50	25
FTE				2.0	1.0	1.0	1.0	0.5
Base pay (k\$)				60	100	45	44	25
Labor/Yr (k\$)				120	100	45	44	13
3 Post docs						135		
Total labor (k\$)								457

Table 5.5 Labor costs for third year.

Year 3		Labor cat	Eng	Sci	Post doc	Tec/ Drft	Admin
Sched tasks	Sched time						
Commission vessel	26		21	13	26	26	6
Procure Plate delivery	4		1	1	3	4	3
Plate controls	26		12	10			9
Install Plate trial assy.	13		4	2	8	39	
Cryo supply sys	9			3			
cryo sup. control	4		1	1	3	8	
Vacuum sys.	6			2	4	12	
towed grid	7			2	4	14	
utility (contract)	8		1	3	5		
plate controls	6		2	2	4	12	
Test Cryo supply sys	1				1	1	
cryo sup. control	1		1		1	2	
Vacuum sys.	1				2	2	
towed grid	1				2	2	
plate controls	4		4		4	4	1
Program plate controls	13		6		8		
cryo sup controls	2		2		2		
Write operating plan	12		2	4	10		4
Operate Towed grid	13		6	6	13	13	
Total (MW)			63	49	100	139	23
FTE			1.0	1.0	2.0	3.5	0.5
Base pay (k\$)			60	100	45	44	25
Labor/Yr (k\$)			60	100	90	154	13
2 Post docs					90		
Total labor (k\$)							507

Table 5.6 Labor costs for fourth year.

Year 4		Labor cat	Eng	Sci	Post doc	Tec/ Drft	Admin
Sched tasks	Sched time						
Install finish trial assy.	13		4	2		39	
Plates in vessel	26		13	7	26	78	
Operate finish towed grid	13		13	13	26	13	12
write op. proc.	12			4	26		6
comm. plates	12		13	7	26		6
Total (MW)			43	33	104	130	24
FTE			1.0	1.0	2.0	2.5	0.5
Base pay (k\$)			60	100	45	44	25
Labor/Yr (k\$)			60	100	90	110	13
2 Post docs					90		
Total labor (k\$)							463

Table 5.7 Labor costs for fifth year.

Year 5		Labor cat	Eng	Sci	Post doc	Tec/ Drft	Admin
Sched tasks	Sched time						
Operate convection cell	52		13	50	200	50	25
Total (MW)			13	50	200	50	25
FTE			0.25	1.0	4.0	1.0	0.5
Base pay (k\$)			60	100	45	44	25
Labor/Yr (k\$)			15	100	180	44	13
Total labor (k\$)							352

5.5.3 Operating Costs

Operating costs consist primarily of the expenses associated with operating the 4 kW refrigeration plant at the N-15 site, and the cost of additional helium for operation in the high density regime, near the end of the program. The costs for refrigeration include operators and range from \$2,000 to \$3,000 dollars per day depending on the load. These rates are appropriate to the Applied Superconductivity and Cryogenics Technology Center proposed for establishment at the site of the former SSC Laboratory and were supplied by members of the team working on that Project Definition Study.

For purposes of cost estimation, 78 five-day weeks of operation are allowed for, at an average of \$2,500 per day. This results in refrigeration expenses totaling \$975,000. Given the fact that this is an experimental program, the results of which are unknown, it seems likely that a number of weeks will be spent in the analysis of data and refinement of experimental procedures. During these weeks the refrigerator can be turned off. Since the heat leak into it will be very small, its temperature will rise only slightly. Thus, the method described above for estimating refrigeration costs is considered to be reasonable.

An additional \$100,000 of helium gas is included for operating in the high density gas regime described in Appendix E. These experiments are expected to take place near the end of the five-year program. Thus, the total operating costs are estimated to be \$1,075,000.

5.6 Permits

In determining the kind of permitting that is required for the facilities construction and operation of Helium Convection Experiment, two possible situations can exist. First, the N-15 site of the SSCL can remain U. S. Government property. In this case, the project is self-permitting with adherence to the applicable requirements of U. S. Department of Energy Order 6430.1A, *General Design Criteria*, and adherence to the requirements of the National Environmental Policy Act. The second situation that can obtain is that the N-15 site can have been transferred to some non-federal organization. In this case, a local building permit is required and is the key to all of the inspection and certification processes required for construction of the facility.

Since cryogenic equipment of the same kind as the cell cryostat is already installed at the N-15 Site, and since cryogenic operations are already underway there, a good basis exists on which to deal with permitting.

5.7 Funding Sources and Alternatives

It is not possible, at this stage, to identify firm sources of support. A project of this scale would require a formal proposal, peer review, site visits, and many other contractual considerations.

However the usual sources of funds for fluid mechanics experiments are the Office of Basic Energy Sciences of DOE, the Division of Materials Research, and Division of Engineering

of NSF, and various programs of ONR and AFOSR. It is possible the Division of Physics of NSF might take some interest in nonlinear physics, but we know of no actions at present.

We believe our research could lead to a National High Reynolds Number Test Facility which could possibly be integrated in some way with other proposed uses for the cryogenic facilities.

6. Cost Summary

The following is a summary of the estimated costs of the project. Further detail on the costs can be found in Appendix A, Appendix I and section 5.5.

The authors are pleased that the direct costs reported here for the project after a summer's detailed work are surprisingly close to the direct costs estimated in our Expression of Interest. The Expression of Interest estimated direct costs of \$7,700,000 (overhead figures were not known) The present report gives \$8,284,457, and of course overhead estimates are far from firm because the legal entity which will be in charge is still unknown.

The costs have been assembled in five parts reflecting the organization of the research program. The focus of the activities centers around the construction and operation of the 10-meter cell located at the N-15 site in Texas. The cryogenic facilities located at this site make possible the research program discussed in this report. The scientific resources and leadership needed to carry out the research are assembled from university groups active in the field of convection and turbulence research, and the engineering, technical and operating support are employed through the Texas organization.

The budget projections are constructed to make the costs associated with each part of the program clear. The budget projection for the principal program centered on the 10-m cell and budget projections for each of the four university support programs are presented separately. These are assembled and summarized on the sheet immediately below.

Implicit in the budget projections is a basic organization of the construction program and of the research activity: The scientific leadership of the program and its management is the responsibility of a collaboration including the university principal investigators together with the Chief Scientist who is based at the site of the 10-m cell, and who is responsible for the engineering, procurement and construction activities and for day to day operations. He is assisted by a staff associated with the host organization and university visitors. This is discussed further in Section 5.5.2. Among this staff, and essential in achieving a smoothly coordinated and technically complete project, are four research associates. In the early part of the program a portion of these together with the technical and engineering staff on the construction of the facilities and apparatus. After operations begin, the research associates work with the collaboration in carrying out the research program.

In the view of the authors of this report, this organization provides the features necessary for the success of the program. What must be achieved is first, contact with the relevant research communities and informed scientific judgment that leads to the cogent definition of the research program and a well-balanced design of the experiment. These must be complemented by good engineering and construction management personnel, well informed about the priorities of the research of the research program and the many technical issues and optimizations in the design of the equipment and of the operating procedures. And last, but equally important, is a professional operating staff, dedicated to safe and efficient performance of the operation of the experimental program.

Summary Budget

Site		Year 1	Year 2	Year 3	Year 4	Year 5	Total
Ten Meter Cell Site	Capital	\$790,000	\$1,375,000	\$809,000	\$60,000	\$60,000	\$3,094,000
	Other	\$685,000	\$537,000	\$750,000	\$706,000	\$1,182,000	\$3,860,000
Univ. of Oregon	Capital	\$150,200	140,000	\$0	\$0	\$0	\$290,200
	Other	\$96,446	\$104,080	\$88,048	\$91,295	\$95,052	\$474,921
Duke Univ.	Capital	\$20,500	\$5,000	\$5,000	\$0	\$0	\$30,500
	Other	\$36,211	\$35,806	\$37,464	\$26,143	\$26,988	\$162,612
Yale Univ	Capital	\$75,000	\$5,000	\$5,000	\$0	\$0	\$85,000
	Other	\$36,040	\$32,807	\$34,674	\$36,646	\$38,729	\$178,896
Northern Illinois Univ. Capital		\$0	\$0	\$0	\$0	\$0	\$ 0
	Other	\$19,414	\$20,481	\$21,603	\$22,791	\$24,039	\$108,328
Total Direct Costs		\$1,908,811	\$2,255,174	\$1,750,789	\$942,875	\$1,426,808	\$8,284,457
Indirect Costs		\$480,211	\$401,596	\$512,484	\$485,581	\$751,744	\$2,631,616
Total		\$2,389,022	\$2,656,770	\$2,263,273	\$1,428,456	\$2,178,552	\$10,916,073

Indirect Costs

These costs are unknown. This report has included indirect costs at 55% of all expenses except capital equipment. This is a typical level used by universities.

Ten Meter Cell Program Budget

Item	Year 1	Year 2	Year 3	Year 4	Year 5	Total
1. Salaries & Wages						
Chief Scientist	\$100,000	\$100,000	\$100,000	\$100,000	\$100,000	\$500,000
Engineer	\$240,000	\$120,000	\$60,000	\$60,000	\$15,000	\$495,000
Post-Doc	\$180,000	\$180,000	\$180,000	\$180,000	\$180,000	\$900,000
Technician/Draftsman	\$22,000	\$44,000	\$154,000	\$110,000	\$44,000	\$374,000
Administrative Assistant	\$13,000	\$13,000	\$13,000	\$13,000	\$13,000	\$65,000
Total salaries, wages, and fringe benefits	\$555,000	\$457,000	\$507,000	\$463,000	\$352,000	\$2,334,000
2. Perm. equip. (Incl. ~20% contingency)	\$790,000	\$1,375,000	\$809,000	\$60,000	\$60,000	\$3,094,000
3. Domestic travel and local support	\$30,000	\$30,000	\$30,000	\$30,000	\$30,000	\$150,000
4. Operating costs	\$0	\$0	\$163,000	\$163,000	\$750,000	\$1,076,000
5. Materials and expenses	\$100,000	\$50,000	\$50,000	\$50,000	\$50,000	\$300,000
Total direct costs	\$1,475,000	\$1,912,000	\$1,559,000	\$766,000	\$1,242,000	\$6,954,000

Equipment

10 meter cell complete	\$1,250,000
Copper plates	\$414,000
Cryogenic control system	\$11,000
Cryogenic supply system	\$110,000
Data acquisition system	\$134,000
Foundation	\$10,000
LDV apparatus	\$300,000
Plate control system	\$258,000
Power	\$14,000
Towed grid works	\$68,000
Utility	\$45,000
Vacuum system	\$40,000
Sub-Total	\$2,654,000
Contingency	440,000
Total Equipment	\$3,094,000

Personnel Costs

Title	Annual Salary
Chief Scientist	\$100,000
Engineer	\$60,000
Technician/Drafts.	44,000
Post-Doc	45,000
Admist. Assist	25,000

Fringe benefits are included in the above figures.

University of Oregon Budget

Item	Year 1	Year 2	Year 3	Year 4	Year 5	Total
1. Salaries & Wages						
(a) R.J. Donnelly, P.I., 1.0 FTE, 2 Mo.	\$18,000	\$18,900	\$19,800	\$20,800	\$21,900	\$99,400
(b) 1 Graduate Student	\$10,000	\$10,500	\$10,900	\$11,600	\$12,200	\$55,200
(c) Undergraduate lab assistant	\$3,000	\$3,000	\$3,300	\$3,300	\$3,600	\$16,200
2. Other Personnel Expenses	\$6,655	\$7,169	\$7,711	\$8,308	\$8,972	\$38,815
Total Salaries, Wages and Fringe Benefits	\$37,655	\$39,569	\$41,711	\$44,008	\$46,672	\$209,615
3. Permanent Equipment	\$150,200	\$140,000	\$0	\$0	\$0	\$290,200
4. Domestic Travel and local support	\$6,000	\$6,000	\$6,000	\$6,000	\$6,000	\$30,000
5. Materials and Expense	\$48,000	\$53,000	\$34,000	\$34,000	\$34,000	\$203,000
6. Tuition Remission (1 student)	\$4,791	\$5,511	\$6,337	\$7,287	\$8,380	\$32,306
Total Direct Costs	\$246,646	\$244,080	\$88,048	\$91,295	\$95,052	\$765,121

Fringe Benefits

33.36% to 37.36% of (a) and 5% of (b) and (c)

Equipment

Year 1

1 m convection cell	\$85,250
Edwards 300E helium leak detector	\$18,000
SRS 830 dual phase lockin	\$3,700
LR-700 resistance bridge/controller	\$12,500
HP35665A signal analyzer	\$15,250
ESI DT72A ratio transformer	\$4,500
MKS 390HA pressure transducer	\$2,500
Computer workstation upgrades	\$8,500

Year 2

LDV system	\$140,000
------------	-----------

Material and Supplies

Year 1 - 1000 hours of shop time @ \$38/hr and 10,000 in materials and supplies

Year 2 - 1000 hours of shop time and 15,000 in materials, supplies and helium (\$8.00/liter)

Years 3, 4 and 5 - 500 hours of shop time and 15,000 in materials and helium

Yale University Budget

Item	Year 1	Year 2	Year 3	Year 4	Year 5	Total
1. Salaries & Wages						
(a) K. Sreenivasan, 1.0 FTE, 2 Mo.	\$22,000	\$22,990	\$24,025	\$25,106	\$26,235	\$120,356
	\$0	\$0	\$0	\$0	\$0	\$ 0
	\$0	\$0	\$0	\$0	\$0	\$ 0
2. Other Personnel Expenses	\$7,040	\$7,817	\$8,649	\$9,540	\$10,494	\$43,540
Total Salaries, Wages and Fringe Benefits	\$29,040	\$30,807	\$32,674	\$34,646	\$36,729	\$163,896
3. Permanent Equipment	\$75,000	\$0	\$0	\$0	\$0	\$75,000
4. Domestic Travel and local support	\$2,000	\$2,000	\$2,000	\$2,000	\$2,000	\$10,000
5. Materials and Expense	\$5,000	\$5,000	\$5,000	\$0	\$0	\$15,000
Total Direct Costs	\$111,040	\$37,807	\$39,674	\$36,646	\$38,729	\$263,896

Fringe Benefits
32% to 40% of (a)

Equipment

Tank, grid, and auxiliaries \$15,000
Motor and Controls \$35,000
Data acquisition & analysis \$13,000

Duke University Budget

Item	Year 1	Year 2	Year 3	Year 4	Year 5	Total
1. Salaries & Wages						
(a) B. Behringer, 1.0 FTE, 2 Mo.	\$15,200	\$15,960	\$16,758	\$17,956	\$18,480	\$84,354
	\$0	\$0	\$0	\$0	\$0	\$ 0
	\$0	\$0	\$0	\$0	\$0	\$ 0
2. Other Personnel Expenses	\$3,511	\$3,846	\$4,206	\$4,687	\$5,008	\$21,258
Total Salaries, Wages and Fringe Benefits	\$18,711	\$19,806	\$20,964	\$22,643	\$23,488	\$105,612
3. Permanent Equipment	\$20,500	\$5,000	\$5,000	\$0	\$0	\$30,500
4. Domestic Travel and local support	\$2,500	\$3,000	\$3,000	\$3,500	\$3,500	\$15,500
5. Materials and Expense	\$15,000	\$13,000	\$13,500	\$0	\$0	\$41,500
Total Direct Costs	\$56,711	\$40,806	\$42,464	\$26,143	\$26,988	\$193,112

Fringe Benefits
23.1% to 27.1% of (a)

Equipment

Two Lockin amplifiers \$15,000
Two ratio transformers \$4,000
Chart recorder \$1,500

Materials and Supplies

Liquid helium and liquid nitrogen \$10,000 - 11,00
Machine shop \$2,500 - \$5,000

Northern Illinois University Budget

Item	Year 1	Year 2	Year 3	Year 4	Year 5	Total
1. Salaries & Wages						
(a) X. Z. Wu, 1.0 FTE, 2 Mo.	\$9,120	\$9,576	\$10,055	\$10,557	\$11,085	\$50,393
	\$0	\$0	\$0	\$0	\$0	\$0
	\$0	\$0	\$0	\$0	\$0	\$0
2. Other Personnel Expenses	\$1,094	\$1,245	\$1,408	\$1,584	\$1,774	\$7,105
Total Salaries, Wages and Fringe Benefits	\$10,214	\$10,821	\$11,463	\$12,141	\$12,859	\$57,498
3. Permanent Equipment	\$0	\$0	\$0	\$0	\$0	\$0
4. Domestic Travel and local support	\$4,200	\$4,410	\$4,630	\$4,860	\$5,100	\$23,200
5. Materials and Expense	\$5000	\$5,250	\$5,510	\$5,790	\$6,080	\$27,630
Total Direct Costs	\$19,414	\$20,481	\$21,603	\$22,791	\$24,039	\$108,328

Fringe Benefits
12% to 16% of (a)

7 Bibliography

Much of the pertinent bibliography for this report is contained in the papers published in the conference proceedings by Donnelly (1991a). Readers wishing a more complete set of references should consult that volume.

- Anselmme, F., Y. Gagne, E. J. Hopfinger and R. A. Antonia (1964) *J. Fluid Mech.* **140**, 63.
 Awschalom, D. D., F. P. Milliken and K. W. Schwarz (1984) *Phys. Rev. Lett.* **53**, 1372.
 Behringer, R.P. (1985) *Rev. of Mod. Phys.* **57**, 657.
 Bielert, F. and G. Stamm (1994) preprint submitted to *Physics of Fluids*.
 Busse, F.H. (1967) *J. Fluid. Mech.* **30**, 625.
 Castaing, B. Y. Gugne and M. Marchan (1993) *Physics D* **68**, 387.
 Castaing, B., B. Chabaud, and B. Herbal (1994) "A hot wire anemometer operating at cryogenic temperature," preprint.
 Chandrasekhar, S. (1961) *Hydrodynamic and hydromagnetic stability* (Oxford, Clarendon Press).
 Chorin, A. J. (1994) *Vorticity and Turbulence* Springer Verlag (Chapters 3 and 6).
 Comte-Bellot, G. and S. Corrsin (1966) *J. Fluid Mech.* **25**, 657-682.
 Corrsin, S., *Turbulence: Experimental methods*. In *Handbuch der Physik*, vol. VIII/2 (eds. S. Flugge and C.A. Truesdell), Berlin, Springer.
 Dickey, T.D. and G. L. Miller (1980) *J. Fluid Mech.* **99**, 13-31.
 Donnelly, R. J., (1991a) ed. *High Reynolds Number Flows Using Liquid and Gaseous Helium*, Springer-Verlag.
 Donnelly, R. J., (1991b) *Quantized Vortices in Helium II* (Cambridge University Press).
 Duncan, R.V. (1988) Ph.D. thesis, University of California at Santa Barbara.
 Falco, R.E. (1972) Ph.D. thesis, Princeton University.
 Foias, C. O. Manley and L. Sirovich, (1990) *Phys. Fluids A2*, 161.
 Frisch, U. and G. Parisi, (1985) In *Turbulence and Predictability in Geophysical Fluid Dynamics*, eds. Ghil, M. Benzi, R., and Parisi, G. North-Holland, p. 84.
 Frisch, U. and S. A. Orszag (1990) *Physics Today*, **43**.
 George, W. K. (1992) *Phys. Fluids A4*, 1492.
 Goldstein, R. J. (1983) *Fluid Mechanics Measurements* Hemisphere Publishing Company
 Grossmann, S. D. Lohse, (1994) *Phys. Fluids* **6**, 611.
 Heiserman, J. (1981) In *Fluid Dynamics* ed. R.J. Emrich New York, Academic Press, p. 413.
 Howard, L.N. (1966) In *Proc. of the 11th Int. Congr. of Appl. Mech.* Munich (Germany) ed. Gortler, H., Springer, Berlin.
 Hunt, J.C.R., O.M. Phillips and D. Williams, editors, (1991) "Turbulence and stochastic processes: Kolmogorov's ideas 50 years on," Royal Society of London.
 Ichikawa, N. and M. Murakami (1991) In *High Reynolds Number Flows Using Liquid and Gaseous Helium*, ed. R. J. Donnelly, Springer-Verlag.
 Kierstead, H.A. (1973) *Phys. Rev. A7*, 242.
 Kistler, A. L. and T. Vrebalovich, (1966) *J. Fluid Mech.* **26**, 37-43.
 Kochmieder, E L. (1992) *Bénard Cells and Taylor Vortices*, Cambridge University Press
 Kolmogorov, A.N., (1962), *J. Fluid Mech.* **13**, 82.
 Kolmogorov, C.R., (1941), *Acad. Sci. URSS* **30**, 301.
 Kraichnan, R.H., (1962), *Phys. Fluids* **5**, 1374.
 L'vov, V.S., Procaccia, I. and Fairhall, A.L., (1994), *Phys. Rev. Lett* (submitted).

- Lambert, R. B., H. A. Snyder and S. K. F. Karlsson (1965) *Rev. Sci. Instr.* **36**, 924.
- Lathrop, D. P., J. Fineberg and H. L. Swinney (1992) *Phys Rev* **A46**, 6390.
- Lipa, J., B.C. Leslie and T.C. Walstrom (1981) *Physica* (Amsterdam) **B107**, 331.
- Malkus, W.V.R. (1954) *Proc. Roy. Soc. (London)* **A225**, 196.
- Malkus, W.V.R. (1963) In *Theory and Fundamental Research in Heat Transfer*. Pergamon, Oxford.
- Mandelbrot, B.B., (1974), *J. Fluid Mech.* **62**, 331.
- Meneveau, C and Sreenivasan, K.R., (1991), *J. Fluid Mech.* **224**, 429.
- Monin, A.S. and Yaglom, A.M., (1975), *Statistical Fluid Mechanics, V. II.*, Cambridge, Mass.
- Murakami, M., T. Yamazaki, D.A. Nakano and H. Nakai (1991) In *High Reynolds Number Flows Using Liquid and Gaseous Helium*, ed. R. J. Donnelly, Springer-Verlag.
- Nelkin, M., (1994), *Adv. Phys.* (to appear).
- Nolt, I. G., J.V. Radostitz, P. Kittel and R.J. Donnelly (1977), *Rev. Sci. Instrum.* **48**, 700.
- Normand, C. Y. Pomeau and M.G. Velarde (1977) *Rev. Mod. Phys.* **49**, 581.
- Oberbeck, A. (1879) *Ann. Phys. Chem.* **7**, 271.
- Obukhov, A.M., (1962), *J. Fluid Mech.*, **13**, 79.
- Reynolds, W.C., (1990), In *Whither Turbulence*, ed. J.L. Lumley, Springer-Verlag.
- Rudnick, I. (1976) In *Proc. Int. School Phys., "Enrico Fermi" - Course LXIII - New Directions Phys. Acoust.* ed. D. Sette, North-Holland Publ., New York.
- She, Z.S. and Leveque, E., (1993), *Phys. Rev. Lett.*, **72**, 336.
- She, Z.S. and Waymire, E.C., *Phys. Rev Lett.*, (to appear).
- Smith, M. R.(1993) Ph.D. thesis, University of Oregon.
- Sreenivasan, K.R., (1984), *Phys. Fluids* **27**, 1048.
- Sreenivasan, K.R., (1991a), *Annu. Rev. Fluid Mech.*, **23**, 539.
- Sreenivasan, K.R., (1991b), *Proc. Roy. Soc. Lond.*, **A434**, 165.
- Sreenivasan, K.R., (1994), In *Developments in Fluid Mechanics and Aerospace Sciences*, (to appear).
- Steinberg, V. and G. Ahlers (1983) *J. Low Temp. Phys.* **53**, 255.
- Stolovitzky, G., Kailasnath, P., and Sreenivasan, K.R., (1992), *Phys. Rev. Lett.* **69**, 1178.
- Threlfall, D.C. (1974) Ph.D. thesis, University of Cambridge.
- Threlfall, D.C. (1975) *J. Fluid Mech.* **67**, 17.
- * Van Sciver, S.W., D. S. Holmes, X. Huang and J. G. Weisend, II, (1991) *Cryogenics*, **31**, 75.
- von Neumann, J. (1949) "Recent theories of turbulence," Report to ONR.
- von Neumann, J. (1949) In *Collected Works, Vol. VI* p. 437 (ed. A. H. Taub, Pergamon Press, 1963.
- Walker, M.D., (1986) Ph.D. thesis, Johns Hopkins University, Baltimore, MD.
- Wolf, P.E., B. Perrin, J.P. Hulin and P. Elleaume (1981) *J. Low Temp. Phys.* **44**, 569.
- Wu, X.Z. (1991) Ph.D. thesis, University of Chicago.
- Wu, X.Z. and A. Libchaber (1991) *Phys. Rev.* **A43**, 2833.
- Yakhot, V., (1994), "Spectra of Fluctuations of Velocity, Kinetic Energy and Dissipation Rate in Strong Turbulence", preprint.

Appendix A - Report of Consultant

Report of Consultant, Dr. Glen McIntosh
Cryogenic Technical Services, Inc.
3445 Penrose Place, Suite 230, Boulder Colorado 80301
Phone 303-444-6010

A.1 Vessel Systems

A.1.1 Design

The vessel system is designed to provide a large isothermal cryogenic volume for the Rayleigh Number, towed grid, and other related experiments. Volume available for the Rayleigh Number experiment is 5 m diameter by 10 m high and an additional meter of height can be used for the towed grid traverse. The vessel may be used for the temperature range from ambient to less than 4.2 K for pressures from high vacuum to 71.46 psia (4.927 Bar). The vessel features a 2 m diameter neck opening for insertion and removal of experimental equipment. A 3 ton jib crane is mounted on the upper vacuum jacket head to facilitate lifting components (**Not personnel**) from the ground and down into the experimental volume. Personnel access is provided by an external stairway and a 5.3 X 6.9 m grating above the upper vacuum jacket head.

Seven concept drawings are provided to aid in the description of the proposed vessel assembly and Dwg. D-5314 presents a concept of the cryogenic system for the Rayleigh Number experiment. Sheets 1, 2, and 4 of Dwg. C-5201 are particularly instructive. Sheet 1 shows an elevation of the tank assembly which includes the helium dewar used to support thermosiphon cooling of the upper Rayleigh Number heat transfer plates. Sheet 2 shows a section of the vessel assembly with a view of the liquid nitrogen thermosiphon dewar and it also includes a detail section of the inner shell. Sheet 4 shows an overall external view of the vessel assembly, a top view of the platform, and a detail section of the neck. These, and the remaining drawings are referenced in the detail sections to follow.

A 1.2 Tabulated Design Details

External Shell:

Material:	Carbon Steel	
Diameter - OD	6.30	m
Height, less the neck	16.80	m
Thickness	19.05	mm
Total area	314	m ²
Total weight	68,000	kg
Operating temperature	300	K
Operating pressures		
Internal	1.33x10 ⁻⁴	Pa
External	1.00x10 ⁵	Pa

Inner Vessel:

Material: 304 Stainless Steel		
Diameter - ID	5	m
Height	13.75	m
Thickness	10	mm
Total area	228	m ²
Total weight	12,500	kg
Inner volume	229	m ³
Operating pressures		
Internal	4.927	Bar
External	1.000	Bar

80 K Shield + MLI:

Material: 1100 Al		
Diameter	5.9	m
Height	15	m
Thickness	4.76	mm
Total area	330	m ²
Total weight (aluminum)	4,366	kg
Operating temperature	78	K
Number of layers MLI	50	
Total weight MLI	450	kg
Refrigeration		
Tube diameter	10	mm
Tube installation: 4 parallel loops		

4 K Shield:

Material: 1100 Al		
Diameter - OD	5.5	m
Height	14.5	m
Thickness	4.76	mm
Total area	281	m ²
Total weight	3,674	kg
Operating temperatures	4.5 - 8	K
Refrigeration		
Tube diameter	10	mm
Tube installation: 4 parallel loops		

4 K Reservoir Dewar:

Material: 304 Stainless Steel		
Inner pressure	0.15	MPa
Outer pressure	0.0003 - 0.4	MPa

Total volume	0.3	m ³
Helium inventory	37.5	kg

LN₂ Reservoir Dewar (80 K):

Material: 304 Stainless Steel		
Inner pressure	0.25	MPa
Total volume	0.1	m ³
LN ₂ inventory	80	kg

A.1.3 Vacuum Jacket

Details of the vacuum jacket are shown on Sheet 1 and on Section B - B of sheet 2. As shown, the vacuum jacket has an O.D. of 6.3 m (248 inches) and overall height to the neck flange is 16.8 m (55.12 ft). Material is A285, Grade C carbon steel with a 3/4 inch cylinder thickness. Six stiffening rings are used to bring the external operating pressure up to 1 atm. ASME torispherical heads are used top and bottom. These heads will be purchased with a 1 inch nominal thickness and extensive gusseting will be required on the upper head to support the mass of the inner assembly suspended from it.

The vessel assembly is supported by four rectangular legs welded to the lower portion of the cylinder. Support plates attached to the legs will be carefully grouted to assure that the vessel stands vertically. The legs themselves are designed for Seismic Zone 0 and a wind load of 30 lb/ft² in accordance with the Uniform Building Code for the Waxahachie area.

A 1.4 Liquid Nitrogen Cooled Shield

The liquid nitrogen shield is shown in Section B - B of Sheet 2. Both the cylinder and fabricated truncated cone heads are made of 3/16 inch thick, 1100 aluminum plate. Extruded 6063 aluminum tubes with welding tabs are used to carry the thermosiphon flow of liquid and gaseous nitrogen to and from the external reservoir located at the top of the assembly. (Details of the LN₂ vessel are shown on Sheet 5.) Liquid from the reservoir is piped to the bottom of the shield with minimal linkage to heat sources and then divided into four parallel streams attached to the shield which rise to a return manifold at the top. For the projected MLI heat load of 0.5 W/m², temperature variation on the shield will approximate 1 K. This will have negligible impact on thermal radiation to the 4.5 K shield.

The liquid nitrogen shield will also serve as a heat intercept to the 2 m neck opening. Plans are to make a mechanical connection between the upper shield head and a stainless steel ring on the neck. The heat intercept function is performed by multiple flat copper cables running from the shield to a copper band silver brazed to the neck. The cables will be bolted to the shield with Indium washers for thermal contact and soft soldered to the copper strip on the neck.

The nitrogen shield will be covered with approximately 50 layers of MLI consisting of 300 to 400 Angstrom double aluminized Mylar interleaved with No. 2250 Reemay spunbonded polyester. This combination is cost effective, low in moisture absorption, and it is strong and relatively easy to handle. Q/A for this combination is expected to be around 0.5 W/m². Preliminary plans are to make up 17 layer batts for ease of installation and to displace the

exposed joint areas. A combination of Velcro strips and Nylon straps with Velcro ends will be used to hold the batts next to the shield while it is horizontal during fabrication.

A.1.5 Helium Shield

The helium shield will be fabricated and attached to the tank neck as described above for the nitrogen shield. The material and thickness and cooling coil arrangement will be the same as for the liquid nitrogen shield. The helium shield differs from the LN₂ shield in that it is not covered with MLI and cooling is by forced flow of liquid helium from the refrigerator. As shown on Dwg. D-5314, the cooling loop is supplied via control valve CV-5 with the exhaust mixture of vapor and liquid flowing back into the vapor return line.

A.1.6 Helium Vessel

The helium vessel is shown on Sheet 2 of the enclosed drawings. It has an ID of 5 m and the cylindrical height is approximately 11.25 m. The tank has 2:1 ellipsoidal heads which match the 3/8 inch thickness of the cylinder. This shell will be fabricated and stamped as an ASME Code unfired pressure vessel. With 100 % X-ray, the allowable operating pressure is 71.46 psia. 13 stiffening rings are welded to the OD of the cylinder to raise its ASME external pressure rating to 1 atm. (This vessel can be evacuated for leak checking.)

As shown on Sheet 2, the inner vessel has a 2m ID opening for experimental access which also serves as the support neck. This 5/16 inch thick neck provides very rigid lateral support of the dewar ($I = 60,627 \text{ in}^4$) which virtually eliminates the need for the lower trunnion support except during fabrication. While convenient mechanically, the large neck opening does introduce a substantial thermal load on the system. This is overcome by heat intercepts on the exterior of the neck and by a forced cooling liquid helium bleed to the stack of 8 radiation baffles in the neck. Bleed flow is controlled by warm external valve CV-12 on the flow schematic. A detail of the baffle and cooling bleed line is shown on Sheet 4.

Six, 2 IPS, Sch. 40 pipes are arranged vertically around the tank. These pipes, which also penetrate the inner shell at the center, provide communication from top to bottom of the tank out of the experimental volume for instrumentation. They may also contribute to transient pressure equalization. As shown in Section E - E on Sheet 3, these pipes are located close to the tank in order to fit inside the stiffening ring flanges. This reduces the diameter of the two shields and vacuum jacket by approximately 5 inches.

Although not shown on any of the concept drawings, the inner shell is equipped with three pairs of viewing ports which communicate with external ports shown on Sheet 4. The internal ports consist of 6 inch diameter, 1 inch thick quartz windows having a 4 1/2 inch diameter aperture. The windows are set out radially from the tank ID to stay out of the experimental volume. The window sealing system called out utilizes the proven technique of Indium seals with stainless steel clamp rings. Cap screws holding the clamp rings have Invar washers which result in increased sealing force as temperatures are reduced. The windows are also mounted on the inside of the tank so that sealing force is augmented by tank pressure.

A 1.7 Plate Systems Integration

Primary support of copper plates for the Rayleigh Number experiment stems from two large stainless steel angles welded to the ID of the inner vessel. These rings are shown on Sheet 2 and detailed on Sheet 3. Plans are to augment these rings by two large beams passing on either side of the center plate openings. Then, each of the 1 1/2 inch thick OFHC copper plates, top and bottom, are to be supported from pairs of rails which bridge across from the peripheral ring and the two center beams. Each 34 X 94 inch plate will have four adjustable hangers/thrust pins (two per rail) for leveling. A concept of this adjustment is shown in Detail "H" on Sheet 3.

Plans are to machine the OFHC copper plates with matching bevels so that they can be bolted together to make smooth and accurate heat transfer surfaces. A concept machining drawing, B-5278, illustrates the planned approach.

A.1.8 Internal Cryogenic Piping System

Proposed internal cryogenic piping is depicted on the Convection Experiment Schematic, Dwg. D-5314. Features include thermosiphon loops for liquid helium cooling of the upper convection heat transfer surface and liquid nitrogen cooling of the 78 K shield. Forced flow helium loops are provided at the top and bottom of the Convection tank and to cool the neck and baffle system. The 4.5 K shield also has a controlled forced flow cooling loop.

Two helium lines enter the bottom of the tank. The 1 IPS pipe can be used for cooldown via valve CV-10 and the 2 IPS line, with valve CV-9, is available to dump the contents back to the vapor return line. Finally, valve CV-7 permits draining the 78 K shield for faster warm-up.

A.1.9 System Interfaces

The system will be piped so that three cold and one warm pipe will connect with the cryogenic facility. Cold pipes include the liquid helium and nitrogen supply lines plus the helium cold vapor return. Helium gas is returned in the one warm line.

Present plans are to provide a 4 inch vacuum pumping line equipped with an on-line turbo pump system. The vacuum jacket will also be equipped with a vacuum relief device to protect the system in case of internal leakage or other operating problems. The helium and nitrogen thermosiphon dewars will have separate static vacuums protected by pumpout/relief valves.

Electric power and instrumentation connections will be brought to a central point on the upper platform. Plans are to enclose this area to protect terminal blocks and switch gear from the elements.

A 1.10 Auxiliary Equipment

A stairway and platform installation and a jib crane are provided for the safety and convenience of installation and operating personnel. Both items are shown on Sheet 4. As

shown, the stairway is equipped with extended landings to facilitate access to the three sets of viewing ports. The 3 ton jib crane has power traverse and rotation in addition to its lift capability. With its enlarged chain basket, the crane can lift items off the ground and lower them to the bottom of inner shell. It should be noted that this crane **is not** rated for carrying personnel.

A 1.11 Delivery, Field Assembly, and Commissioning

Preliminary information received from Dallas fabricator, Prentex Alloy Fabricators, suggests that this tank can be shop fabricated nearby and moved a few miles to the former SSC site. The tank is too large for long distance transport but the cost of moving it a relatively short distance is more than compensated by the reduced cost of shop manufacture compared to field fabrication.

Therefore, the project concept is to have the basic tank shop fabricated at the closest viable facility and moved to the site after closure and final leak check. After erection at the site, the jib crane, stairs, and platform would be installed for use by experimental personnel. At this point, the cooled neck could be installed and thermal performance checked out prior to installation of either the towed grid or free convection experiments. This thermal test should be the basis for final acceptance of the system from the fabricator.

A.1.12 Towed Grid Experiment

The large neck opening and working volume in the free convection tank provides the flexibility for other experiments. A towed grid turbulence experiment is one possibility. As shown on Sheet 7, the free convection upper neck assembly could be replaced with a special cover housing an external hydraulic system and motor with an internal (warm) cable reel. As visualized, this could take the grid shown on Dwg. B-5312 and tow it upward nearly 11 meters. Calculations indicate that the proposed system could accelerate the grid to 2.4 m/s over a height of 1/2 m, tow it upward at 2.4 m/s for 9 to 10 m, and then decelerate to a stop in another 1/2 m. Greater speeds would be possible but care must be taken to limit acceleration so that the grid does not fly past its stopping point when the power is turned off.

The grid shown on Dwg. B-5312 can be lowered into the tank in three pieces. Once inside, the three pieces can be joined without welding and can be disassembled without cutting. This type of flexibility will add to the utility of the cryogenic system.

A 1.13 1/10 Scale Free Convection Cryostat

In order to check out design and operating details of the 5 m diameter free convection experiment and as a useful apparatus in its own right, the University of Oregon proposes to construct and operate a 1/10 scale unit. As shown on the drawing. D-5255, this cryostat has several features which will make it easy and economical to operate. These principal features include:

A two-stage Gifford-McMahon (G-M) refrigerator is provided to assist in cooldown and to maintain a shield at approximately 20 K to further reduce liquid helium consumption during operation.

The G-M cold head is thermally linked to a neon heat pipe which will be effective in cooldown of the inner assembly but will freeze out and contribute negligible heat leak when the cold section is below 20K.

The "soft vacuum" technique is used to link the boiling liquid helium reservoir with the top of the convection heat transfer plate. This makes it possible to closely match the rate of cooling. (A Minco heater is provided for this purpose.)

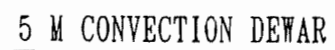
If required to speed the cooldown process, limited soft vacuum heat transfer will be used in the main vacuum space. This will shift the overall cooling load to less expensive liquid nitrogen at the price of some delay while a good insulating vacuum is recovered.

The 0.5 m diameter, 1 m high experimental volume is accessible without cutting or breaking joints. This will facilitate changes in instrumentation or experimental variables. Also, removing a center plug permits installation of a small towed grid experiment.

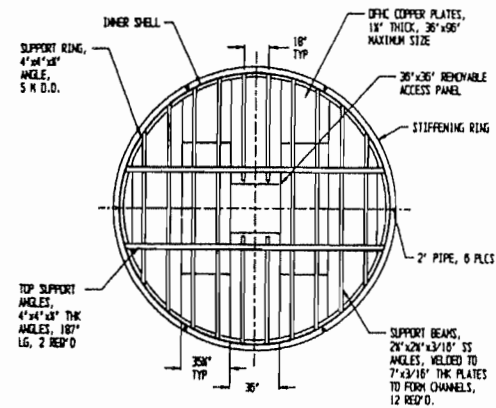
The experimental volume is designed for a pressure range from high vacuum to 5 Bar internal. It is rated for 1 atm external so that it may be evacuated for leak checking.

A 1.14 Pricing Estimate

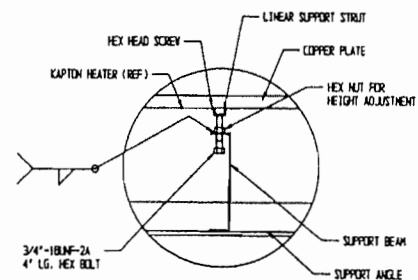
Texas Convection Tank	
Materials, purchased parts, and services	\$610,547
Labor 8776 hours @ \$50/hr.	\$438,800
Engineering design	<u>\$108,250</u>
Total	\$1,157,597
Convection Tank Copper Plates	
Raw material and purchased parts	\$200,007
Plate machining and drill and tap	\$120,000
Labor for fabrication and installation	\$165,200
Detail engineering	<u>\$18,570</u>
Total	\$503,777
Towed Grid Experiment	
Raw material and purchased parts	\$11,844
Labor for fabrication and installation	\$77,188
Detail engineering	<u>\$11,160</u>
Total	\$100,192
Oregon Convection tank	
Material and purchased parts (with 40% margin)	\$35,358
2-stage G-M refrigerator (direct purchase)	\$16,500
Labor 668 hours @ \$50/hr.	<u>\$33,400</u>
Total	\$85,258
Total for ten meter cell experiment	\$1,761,566
Total for all items above	\$1,846,824



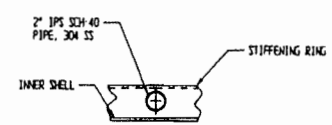
A-10



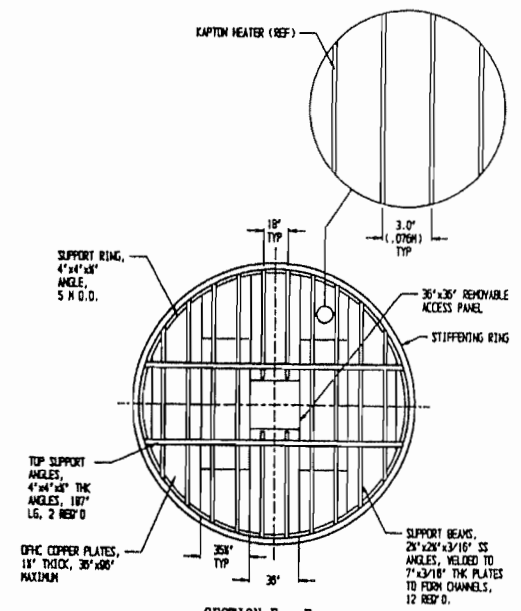
SECTION D - D
TOP PLATE SUPPORT SYSTEM
NOTE: HEATERS AND COOLING COILS OMITTED FOR CLARITY.



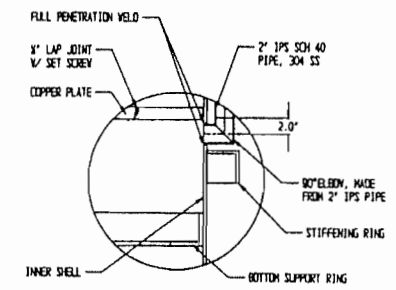
DETAIL "E"
BOTTOM SUPPORT SYSTEM LINKAGE



SECTION E - E

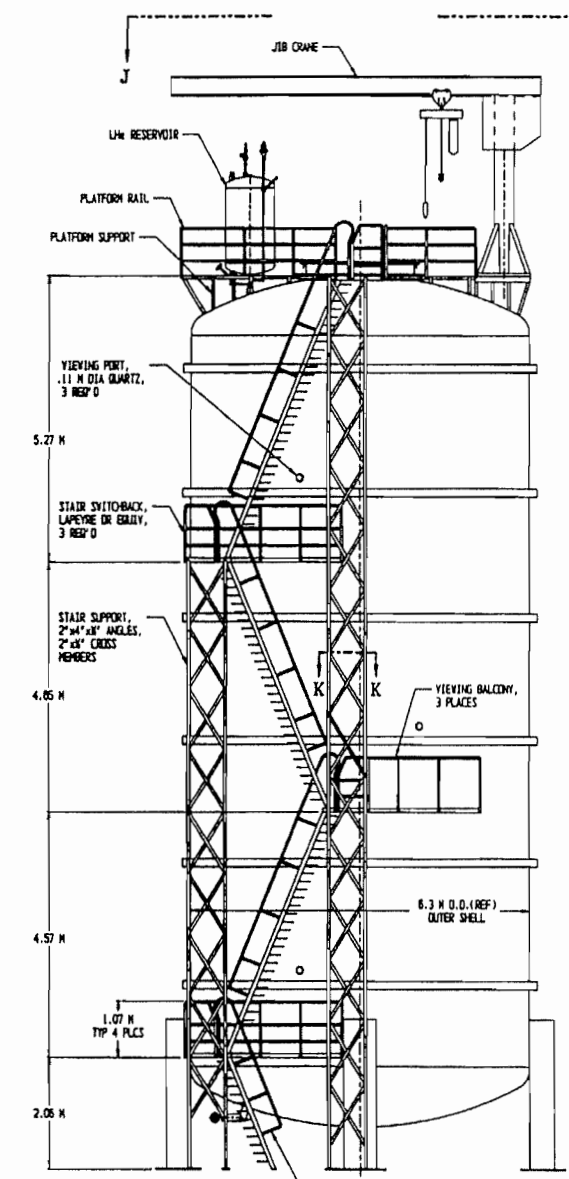


SECTION F - F
BOTTOM PLATE SUPPORT SYSTEM
NOTE: HEATERS OMITTED FOR CLARITY.

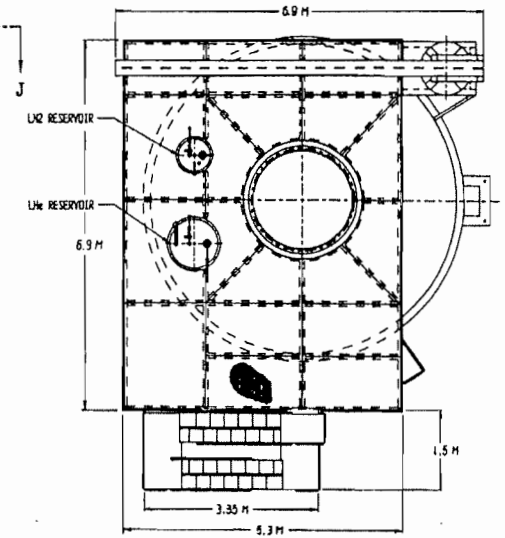


DETAIL "I"
PIPE PENETRATION DETAIL

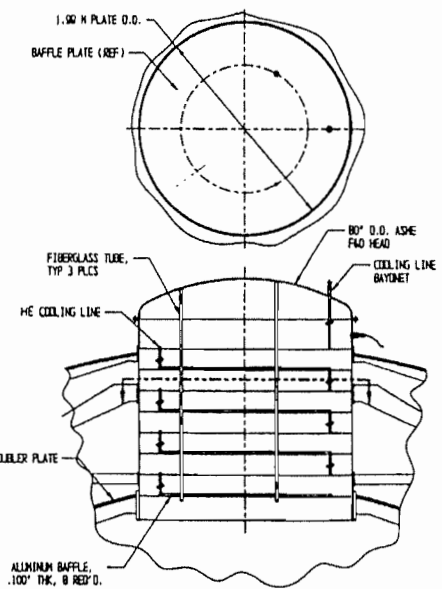
DWG C-5201, 10/14/94
SHEET 3 OF 7



PLATFORM AND STAIR SYSTEM DETAIL
SCALE: 1/4\"/>

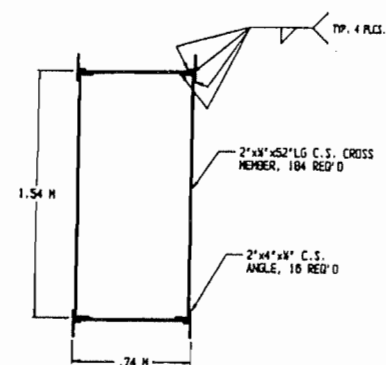


VIEW J - J
NOTE: SUPPORT SYSTEM NOT SHOWN
SCALE: 1/4\"/>

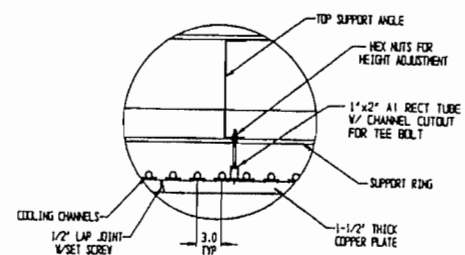


BAFFLE DETAIL
SCALE: 1/4\"/>

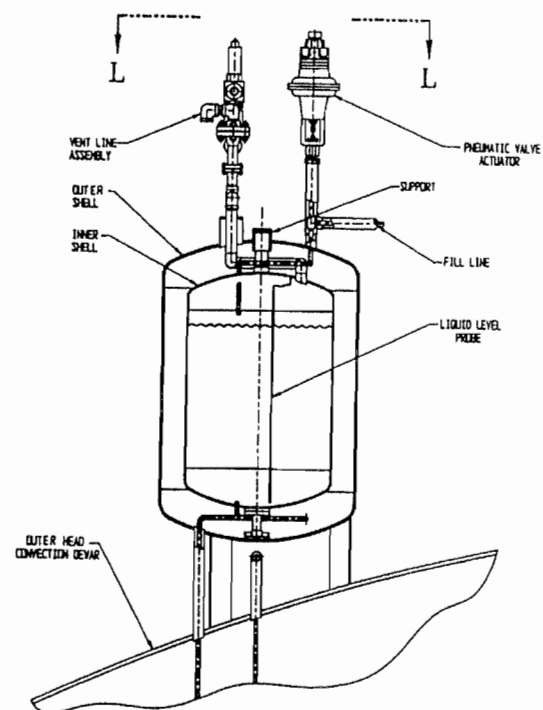
DWG C-5201, 10/14/94
SHEET 4 OF 7



SECTION K - K

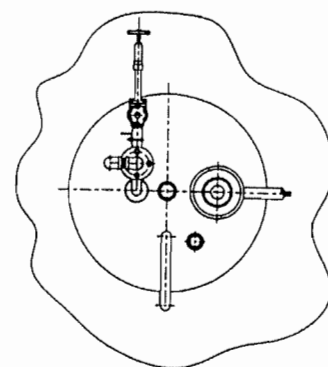


DETAIL "G"
TOP SUPPORT SYSTEM LINKAGE



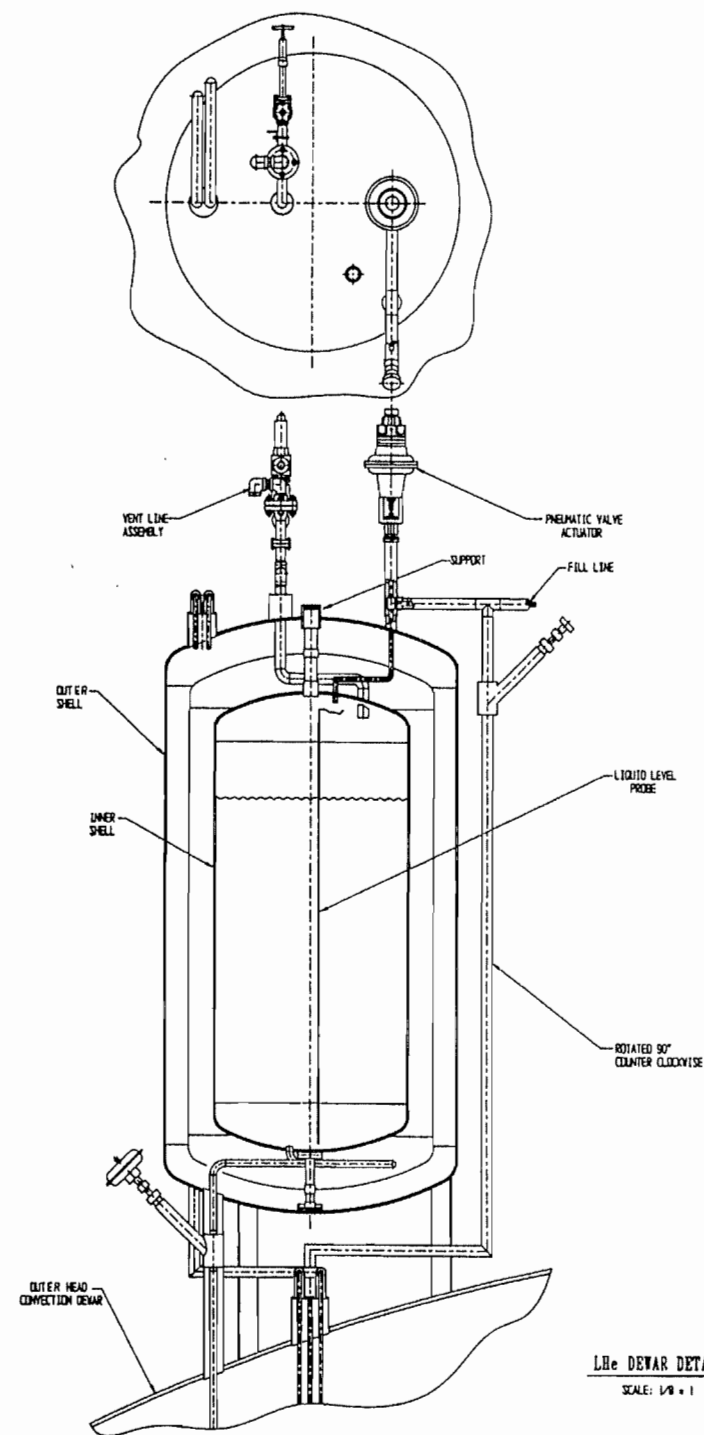
LN2 DEWAR DETAIL

SCALE: 1/8" = 1"



VIEW L - L
SCALE: 1/8" = 1"

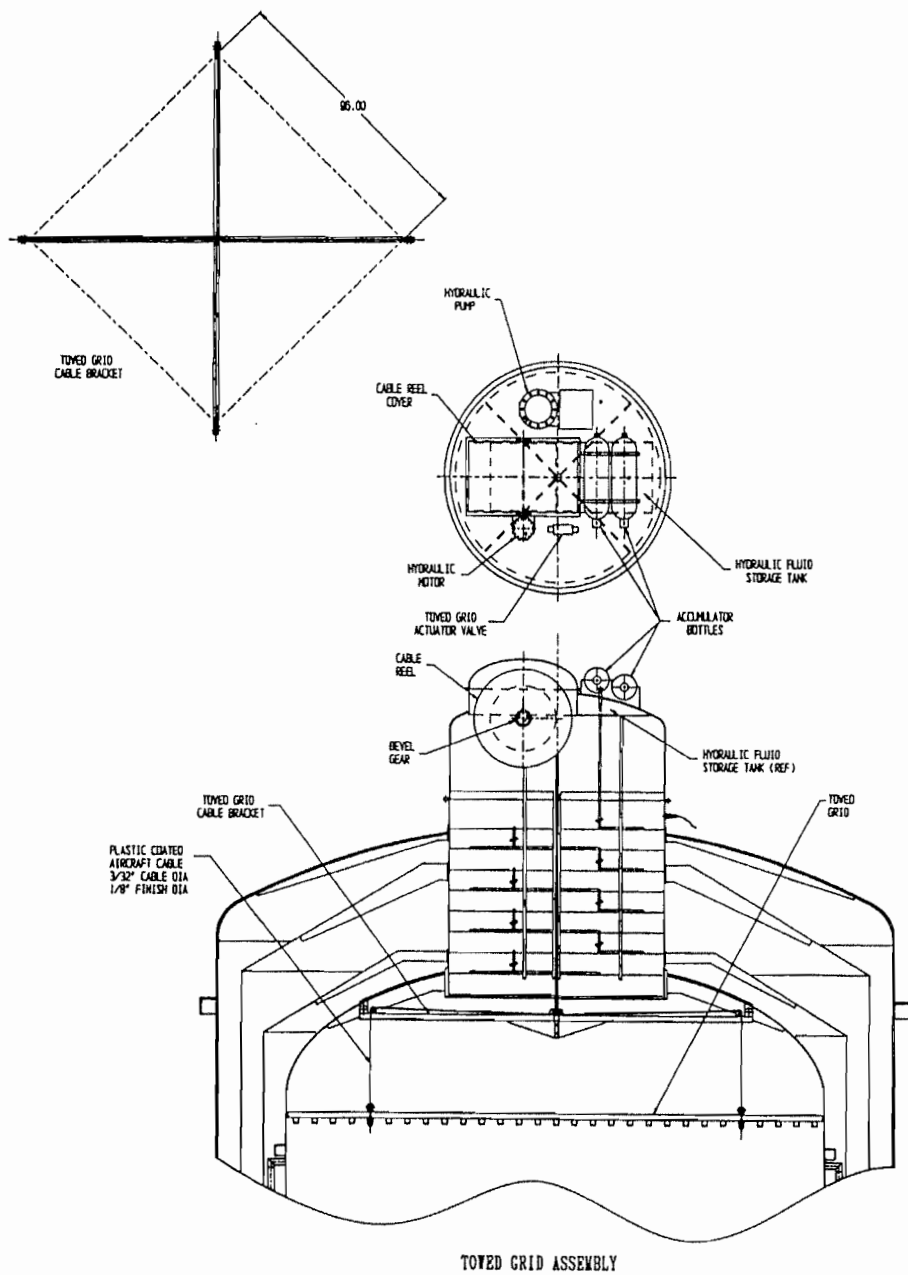
DWG C-5201, 10/14/94
SHEET 5 OF 7



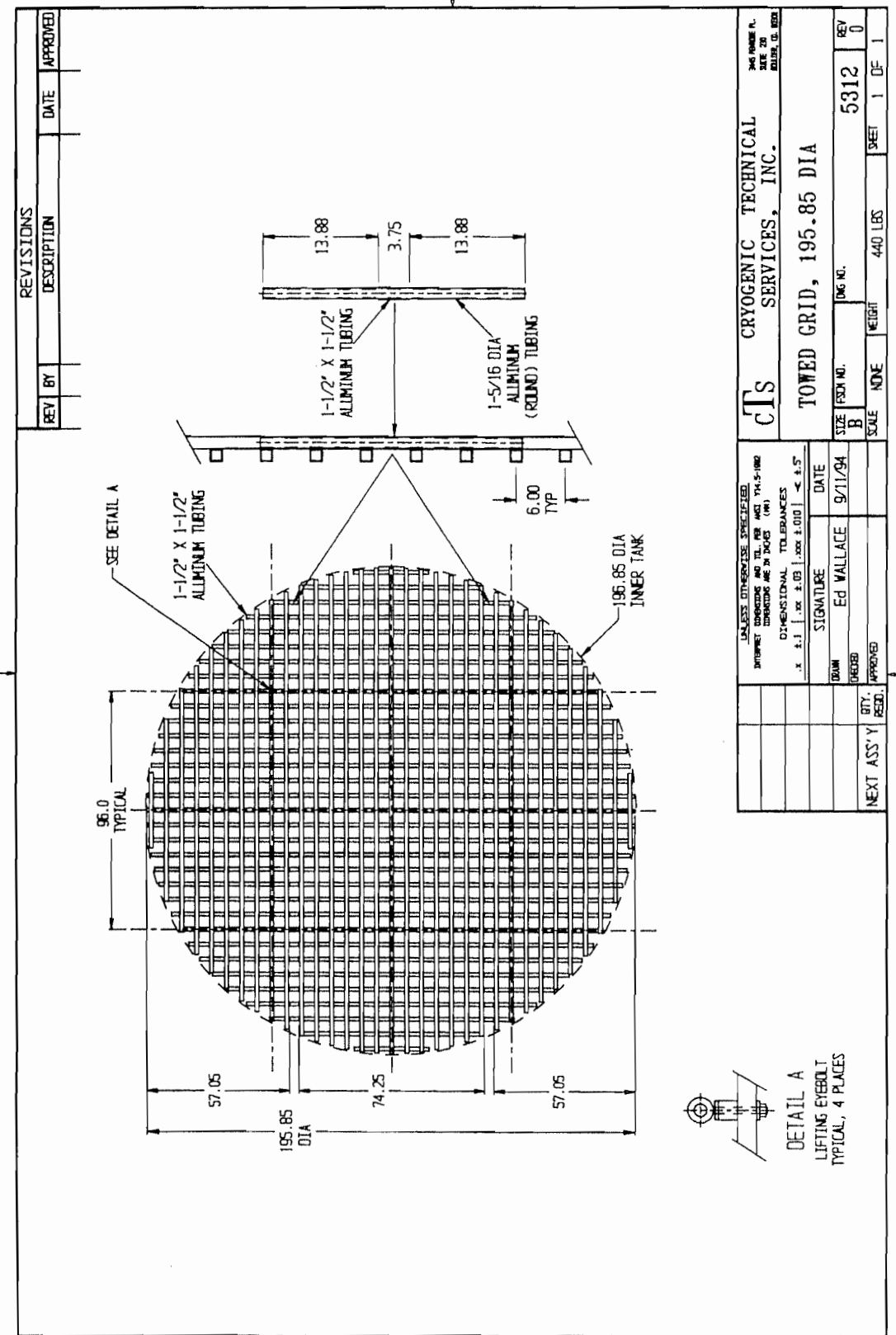
LHe DEWAR DETAIL

SCALE: 1/8" = 1"

DWG C-5201, 10/14/94
SHEET 6 OF 7



DWG C-5001
10/14/94
SHEET 1 OF 7



Appendix B - Flow Facilities and Tow Tanks

B1. Background

When the importance of the use of helium as a test fluid was fully appreciated, a conference was held at the University of Oregon the proceedings of which was subsequently published as a book entitled "*High Reynolds Number Flows Using Liquid and Gaseous Helium*" edited by Russell J. Donnelly. Prominent among the discussions was a consideration of using liquid helium I or helium II as the working fluid in a tunnel for observations on objects such as spheres or models of submarines. The use of liquid helium for the testing of submarines, in particular, offers enormous reductions in cost over the present practices of operating scale models or testing full scale submarines at sea. Therefore one can expect that the pressures of economies alone will eventually require the use of helium test facilities.

At the time, the largest obstacle was seen as the provision of refrigeration for such facilities, and an "academic tunnel" of 30 cm test section dissipating 100 watts was proposed. As a further illustration of the potential of helium liquid, a 125 cm tunnel was proposed dissipating about 1000 Watts. The latter proposal seemed ambitious because refrigerators of such capacity are essentially unknown in academic laboratories.

Similarly it was realized that tow tanks offer advantages for testing of surface ships. The wide variety of conditions accessible with liquid helium allows one to match simultaneously not only the Froude number but also the Reynolds number; something which is impossible when testing in water tow tanks.

Since that time, the cancellation of the SSC and the search for uses of its assets has revealed the enormous contribution that high energy physics has made to low temperature physics in the construction and successful commissioning of large scale refrigeration of the type featured in this report.

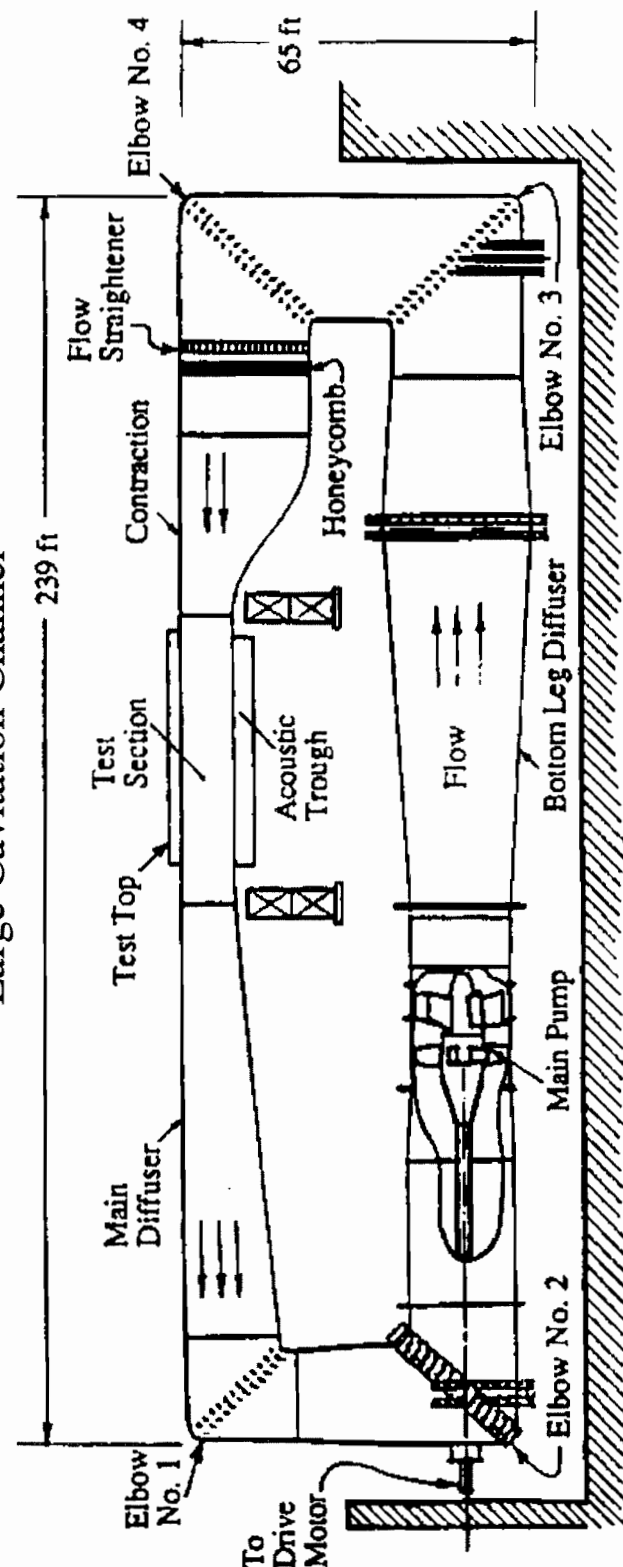
The new prospects made available by the refrigeration capabilities discussed here were brought to the attention of the Naval Sea Systems Command, and the discussion that follows is in part influenced by discussions with NAVSEA and the Naval Undersea Warfare Center in Newport RI.

While we did not have the resources to undertake serious design and cost estimates for tunnels and tow tanks, the freedom to think about the possibilities independent of the refrigeration requirements was significant, and we believe this brief appendix adds significantly to what is known about these problems.

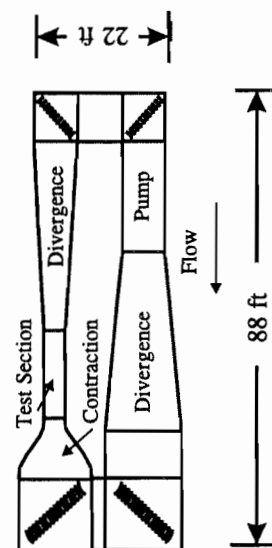
B2. Flow Facilities

The low kinematic viscosity of helium (on the order of $2 \times 10^{-4} \text{ cm}^2 \text{ s}^{-1}$ compared to 10^{-2} for water and 0.15 for air), makes it possible to create, for a fixed Reynolds number, a flow with an apparatus which is fifty times smaller than that using water and seven hundred and fifty times smaller than that using air. Consider the world's largest water tunnel, the Large Cavitation Channel (LCC), located in Memphis, Tennessee. We illustrate this impressive facility in the figure on page B-2. The total length of this apparatus is 239 ft, and at first sight

Large Cavitation Channel



Flow Circuit for 125 cm Helium Tunnel



LCC	
Test section width	3.05 m
Channel Reynolds #	5.5×10^7
Kinematic viscosity	$10^{-6} \text{ m}^2/\text{s}$
Maximum flow speed	18 m/s
Shaft Horsepower	14,000 Hp
Temperature	20 °C

Helium Tunnel	
Test Section width	1.25 m
Channel Reynolds #	3.0×10^8
Kinematic viscosity	$10^{-8} \text{ m}^2/\text{s}$
Maximum flow speed	2.2 m/s
Shaft Horsepower	1.2 Hp
Temperature	1.6 K

one might believe that a comparable helium facility might be constructed fifty times smaller. This is not, however, the optimum size.

First, real submarine Reynolds numbers (based on length) are an order of magnitude higher than can be reached by the LCC and so higher Reynolds numbers should be obtained if possible. Second, too great a reduction in size creates difficulties due to the complexity needed in model design. Lastly, a more subtle problem arises with regard to turbulent length scales. As the Reynolds number increases the Kolmogorov scale becomes smaller. So small in fact that the surface roughness of the model becomes a concern.

We illustrate in the figure on page B-2 a conceptual helium flow facility with a size selected with the above constraints in mind. It is discussed on pp. 36 and 37 of Donnelly's (1991a) book. In such a facility it would be possible to deploy a model of length 14.6 ft (comparable to the 20 ft model used by David Coder in the National Transonic Facility) which operates at the Reynolds number of a submarine at sea, 1.75×10^9 (based on the length). This facility uses a flow circuit of 88 ft. The use of liquid helium would allow the model to be suspended by a superconducting magnetic suspension and balance system. The system would measure lift and drag, and allow limited maneuvering of the model without physical contact (that is there would be no sting at all). The model could easily contain a propulsor so that it could literally fly into the tunnel. A smaller model could be used to execute spectacular maneuvers even at right angles to the flow.

There is a great deal of low temperature instrumentation developed and being developed for measurement of turbulent flows in liquid and gaseous helium. These are summarized in Section 4.3 of this report.

The acoustical uses of a helium tunnel are also of interest. An enormous amount is known about sound in liquid helium. Typical references are reviews by Heiserman and by Rudnick. Many forms of transducer have been developed and no doubt could equal the performance of anything operating in water. In fact, many measurements could be improved by employing some of the highly sophisticated devices used in condensed matter physics, such as SQUIDS, superconducting films and other quantum-based devices.

The properties of helium and the size of the above-mentioned facility raise some questions about the feasibility of using helium for acoustical testing. The first question regards velocity of sound. The velocity of sound in liquid helium is around 220 m/s compared to 1500 m/sec in water. Thus there will be a certain crowding of resonances for helium compared to water at the same scale. The acoustic impedance of liquid helium is $0.03 \times 10^6 \text{ kg/m}^2 \text{ sec}$ compared to water which is $1.48 \times 10^6 \text{ kg/m}^2 \text{ sec}$. This means that sound will tend to reflect off boundaries and be absorbed less than in water. If one wanted to construct an anechoic chamber for helium, there would need to be a research and development phase first.

Cavitation needs to be considered as well. The cavitation number is defined as

$$Ca = \frac{P - P_v}{1/2 \rho V^2}$$

The larger the cavitation number the less likely it is that the fluid will cavitate. In acoustical measurements one tries to avoid cavitation in the flow so large cavitation numbers are desirable.

In helium the difference between pressure and vapor pressure is easily controllable by changing the temperature. The closer one operates to 4.2 K the smaller will be the numerator. Thus a helium wind tunnel should be operated away from the boiling point to avoid cavitation. Consider next the denominator. In the conceptual facility discussed, for a specific Reynolds

number, the velocity of the helium will be considerably less than that of water since $v_{\text{helium}} < v_{\text{water}}$. Furthermore the density of helium liquid is almost an order of magnitude less than that of water. Thus the dynamic head of helium will be nearly two orders of magnitude less than in the water case. Consequently, unless one were to operate very near the boiling point of liquid helium the cavitation number will be considerably larger in helium than in water. As an example let the Reynolds number in the LCC be set at 10^7 at standard temperature and pressure. The cavitation number is 16. For the helium tank at atmospheric pressure, $T = 4.15 \text{ K}$, and an identical Reynolds number, the cavitation number is 870.

Despite the large cavitation numbers, cavitation is observed in liquid helium. The cause for this is local heating. Because helium has such a small heat capacity, a small local input of heat (from a fan blade for instance) can raise the temperature of a small region to the boiling point. Thus when cavitation is a concern the best operating point would be at the lowest temperature. This effect would be almost completely absent in helium II which has an almost infinite thermal conductivity owing to its superfluidity. Further study would be required to address this question more carefully.

B3. Tow tanks

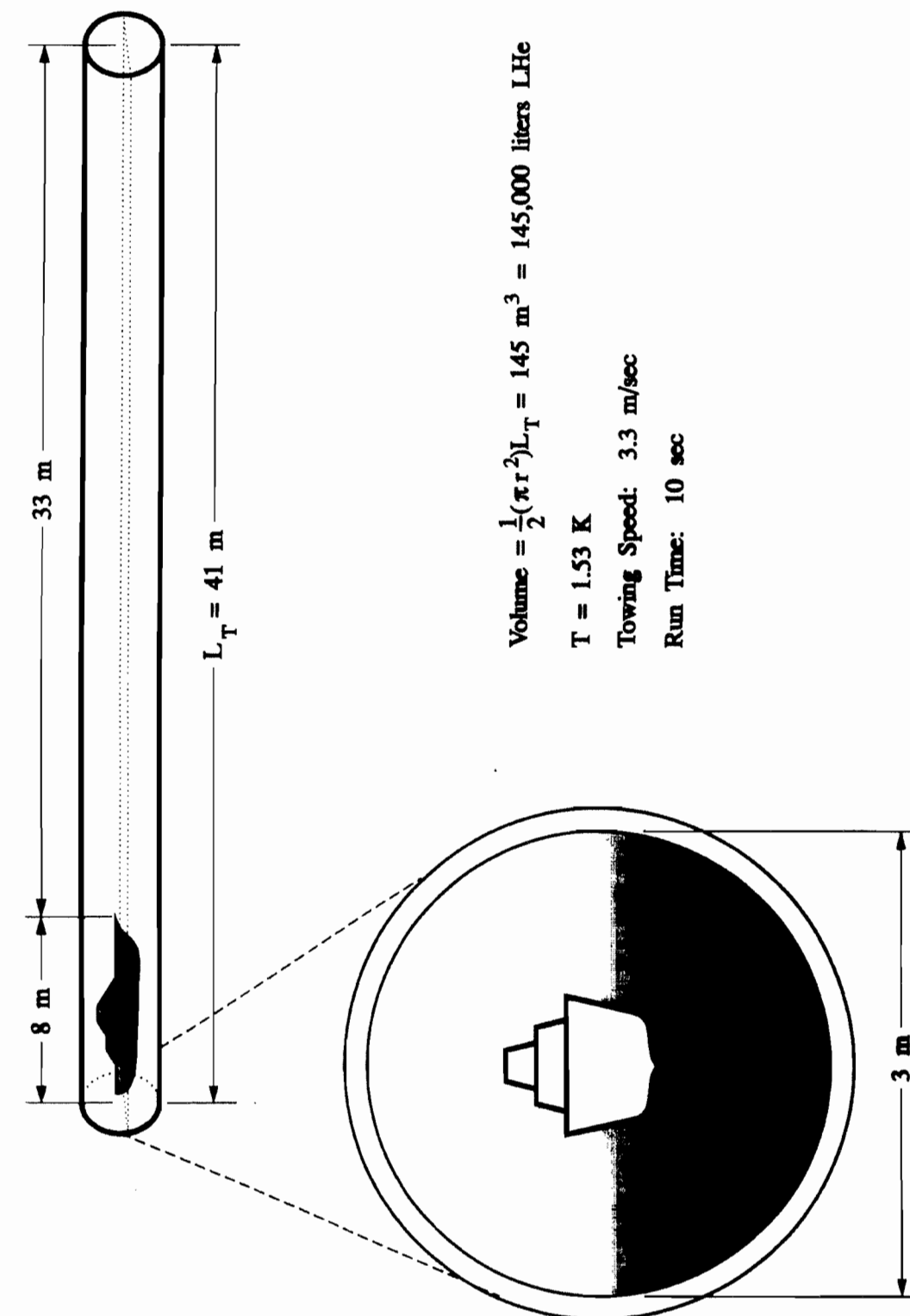
One of the principal advantages of helium over most substances for testing is the ability to change the properties over a wide range by means of adjusting the temperature. And almost no demonstration of this fact is more dramatic than the application of helium to tow tanks.

In testing surface vessels by towing through water troughs it is well known that the wave drag can be successfully modeled by matching the Froude numbers, but the Reynolds numbers turn out to be low by about two orders of magnitude. Since temperature is a variable, it is not difficult to match two, and sometimes more, quantities simultaneously. For example it is possible to match the Weber number governing surface tension at the same time as the Froude number. The underlying theory behind all this is simple and is explained in Donnelly's book (pp. 41-45) in some detail, together with design curves.

As an example, the figure on page B-5 shows a model located in a tow tank with an 8m model which can be towed at 3.3m/s to model a 200m surface ship moving at 16.5 m/s. The Froude and Reynolds numbers are both matched.

B4. Prospects for Using the SSC Assets for Tunnels and Tow Tanks

Several years ago when these ideas were first put forward at a conference in Eugene, the major roadblock to implementing the ideas was the lack of large scale refrigeration. Now that the SSC has been canceled, the problem of having a refrigerator amply sized for this work is solved, at least in principle. There has also been rapid progress in the laboratory owing to the usefulness of liquid helium for studies of high Reynolds number turbulence. This progress has included an increasing theoretical understanding of the rather mysterious circumstance that helium II appears to behave as a Navier Stokes fluid at Reynolds numbers in excess of the order of 1000. There has also been work at Oregon in a 1 cm channel using a towed grid to create turbulence. Running in helium II at grid mesh Reynolds number of the order of 100,000



produces an entirely classical decay of vorticity as determined by second sound absorption. There has also been substantial progress in detector development and a continuous flow facility of the order of 2.5 cm in diameter is out of the machine shop.

The greatest (and totally unexpected) advance has been the DOE support for the present report. Here we have been able to do serious engineering studies on the cryostat discussed here and for the first time obtain real cost estimates of various operations.

What has been learned through this study is just how much detail must be mastered in putting together large scale cryogenic systems. It would, in our opinion, be premature at this moment in time to try to construct a flow facility or tow tank at SSCL for actual production use by the Navy. At the time of writing we do not know what the prospects for funding of the convection project will be. But there is no doubt that if this convection project went forward, an enormous amount of important information would be gained, which would benefit the needs of the Navy over the long term. Russell Donnelly has been engaged in productive discussions with the Navy Sea Systems Command, and the Navy Undersea Warfare Center on the actual problems of testing submarines.

Appendix C Data Sheets and Enthalpy Tables

CONVECTION CELL DATA SHEETS		
	units	Data
External shell		
Diameter	m	6.3
Total height	m	16.8
Height, less the neck	m	15.8
Wall thickness	mm	19.05
Total area	m2	375
Material		Steel
Density	kg/m3	7900
Total weight	kg	56416
Total volume	m3	460
Operating temperatures	K	300
Operating pressures		
internal	Pa	1.33E-04
external	Pa	1.00E+05
Installation procedure		TBD
Inner vessel		
Diameter	m	5
Total height	m	13.82
Height-straight section	m	10
Material		SS
Thickness	mm	9.53
Density	kg/m3	7900
Total area	m2	256
Total weight		19280
Inner volume	m3	180
Operating pressures		
internal	Pa	300-4E05
external	Pa	1E05-1.3E-4
Helium density @4 E05 Pa, 6.2 K	kg/m3	70.00
Total helium inventory -70kg/m3	kg	12593
Operating temperature	K	(4.2)5.5 - 7
Metal enthalpy @5 K	J/kg	5.95
Metal enthalpy @90 K	J/kg	8.80E+03
Metal enthalpy @ 300 K	J/kg	9.20E+04
Heat to be removed during cooldown to 90K	J	1.60E+09
Heat to be removed during cooldown from 90K to 6K	J	1.70E+08
Heat load (no MLI) (total)	W	12.361

Convection Cell Data Sheet (contd.)		units	Data
IR		W/m2	1.40E-05
Total IR		W	0.004
Gas conduction		W/m2	9.20E-03
Total Gas conduction		W	2.36E+00
Support (total)		W	10
Thermal conductivity @ 6K		W/cm-K	0.004
Specific heat @6K		J/kg-K	3.5
Cell Height		m	10
Aspect ratio (diameter/cell height)			0.5, 1, 2, 4, 8, 100
Roundness (% of diameter)		%	±1%
Verticality		mrad	±1
Wall waviness		mm	±10
Upper plate			
Material			Cu
Diameter		m	5
Thickness		mm	40
Density		kg/m3	8930
Thermal conductivity		W/cm-K	3.7
Thermal expansion coefficient			
Mass		Kg	7010
Support material			SS
Support material mass + refrigeration pipes and heaters		kg	2103
Operating temperatures			(4.2)5.5 - 7
Temperature Homogeneity		mK	±0.5
Plate installation requirements			
Surface roughness		mm	±0.01
Waviness		mm	±0.2
Step height		mm	±0.1
Horizontality		mm	±2.0
Plate module width		mm	750
Plate module maximum length		m	2.5
Number of plate modules			15
Installation procedure (coarse)			TBD
Installation procedure (meas. and fine shimming)			TBD
Change of elevation procedure			TBD
Change of elevation - additional support mass			TBD

Convection Cell Data Sheet (contd.)		units	Data
Copper enthalpy	@ 300 K	J/kg	8.00E+04
Steel enthalpy	@ 300	J/kg	9.20E+04
Copper enthalpy	@ 90 K	J/kg	8.10E+03
Steel enthalpy	@90 K	J/kg	8.80E+03
Copper enthalpy	@ 6 K	J/kg	1.61
Steel enthalpy	@ 6 K	J/kg	5.95
Plate enthalpy	@ 300 K	J	5.61E+08
Support enthalpy	@ 300 K	J	1.93E+08
Plate enthalpy	@ 90 K	J	5.68E+07
Support enthalpy	@90K	J	1.85E+07
Plate enthalpy	@ 6 K	J	1.13E+04
Steel enthalpy	@ 6 K	J	1.25E+04
Heat to be removed during cooldown to 90 K			6.79E+08
Heat to be removed during cooldown from 90 K to 6K			7.53E+07
Refrigeration system			
Pipe Dia.		mm	
Distance between Pipes		mm	
Total heat load			3000
Total cooling system mass (installed on plates)		kg	TBD
Installation procedure			TBD
Heater System			
Total power		W	2500
Distance between elements (lateral)		mm	120
Element material			
Element model/power/type of installation			
Total heating system mass (installed on plates)			
Installation procedure			
Lower plate			
Material			Cu
Diameter		m	5
Thickness		mm	40
Density		kg/m3	8930
Thermal conductivity		W/cm-K	3.7
Thermal expansion coefficient			
Mass		kg	7010
Support material			SS
Support material mass		kg	1402

Convection Cell Data Sheet (contd.)		units	Data
Operating temperatures			(4.2)5.5 - 7
Temperature Homogeneity		mK	±0.5
Plate installation requirements			
Surface roughness		mm	±0.01
Waviness		mm	±0.2
Step height		mm	±0.1
Horizontality		mm	±2.0
Plate module width		mm	750
Plate module maximum length		m	2.5
Number of plate modules			15
Installation procedure (coarse)			
Installation procedure (meas. and fine shimming)			
Copper enthalpy	@ 300 K	J/kg	8.00E+04
Steel enthalpy	@ 300	J/kg	9.20E+04
Copper enthalpy	@ 90 K	J/kg	8.10E+03
Steel enthalpy	@90 K	J/kg	8.80E+03
Copper enthalpy	@ 6 K	J/kg	1.61
Steel enthalpy	@ 6 K	J/kg	5.95
Plate enthalpy	@ 300 K	J	5.61E+08
Support enthalpy	@ 300 K	J	1.29E+08
Plate enthalpy	@ 90 K	J	5.68E+07
Support enthalpy	@90K	J	1.23E+07
Plate enthalpy	@ 6 K	J	1.13E+04
Steel enthalpy	@ 6 K	J	8.34E+03
Refrigeration system			
Pipe Dia.			
Distance between Pipes		mm	
Total heat load			
Total cooling system mass (installed on plates)		kg	
Installation procedure			
Heater System			
Total power			2500
Distance between elements (lateral)		mm	120
Element material			
Element model/power/type of installation			
Total heating system mass (installed on plates)			
Installation procedure			

Convection Cell Data Sheet (contd.)	units	Data
4 K shield		
Diameter	m	5.4
Height	m	15
Thickness	mm	4.76
Material		Al
Total area	m ²	300
Total weight	kg	3859
Operating temperatures		4.5 - 8
Enthalpy of Aluminum @ 300 K	J/kg	1.70E+05
Enthalpy of Aluminum @ 90 K		1.30E+04
Enthalpy of Aluminum @ 6 K		1.21
Shield Enthalpy @ 300 K	J	6.56E+08
Shield Enthalpy @ 90 K		5.02E+07
Shield Enthalpy @ 6 K		4.67E+03
Refrigeration		
Tube Dia	mm	
Tube Density	mm	
Tube Installation		
Heat load		
IR	W/m ²	0.13
Gas conduction	W/m ²	0.01
IR Total	W	39.02
Gas conduction Total	W	3.00
Total load		42.02
He flow (nominal) in=4K.4bar;out = 8 K.1.5 bar	g/s	5
Thermal conductivity @ 6 K	W/cm-K	0.84
Density	kg/m ³	2700
Thermal expansion coefficient		
Supports		TBD
Installation procedure		TBD
80 K shield + MLI		
Diameter	m	6.1
Height	m	14
Thickness	mm	2
Material		Al
Total area	m ²	317

Convection Cell Data Sheet (contd.)	units	Data
Total weight (aluminum)	kg	1712
Operating temperatures		4.5 - 8
Number of layers of MLI		
Total weight MLI	kg	
Enthalpy of Aluminum @ 300 K	J/kg	1.70E+05
Enthalpy of Aluminum @ 90 K	J/kg	1.30E+04
Enthalpy of Aluminum @ 6 K	J/kg	1.21
Shield Enthalpy @ 300 K	J	2.91E+08
Shield Enthalpy @ 90 K	J	2.23E+07
Shield Enthalpy @ 6 K	J	2.07E+03
Refrigeration		
Tube Dia	mm	
Tube Density	mm	
Tube Installation		
Heat load		
IR	W/m ²	1.5
Gas conduction	W/m ²	0.01
IR Total	W	475.50
Gas conduction Total	W	3.17
Total load		478.67
He flow (nominal) in=4K.4bar;out = 8 K.1.5 bar	g/s	5
Thermal conductivity @ 6 K	W/cm-K	0.84
Density	kg/m ³	2700
Thermal expansion coefficient		
Supports		
Installation procedure		
Inner Vessel bottom Cooling (4 K Inner conic shield)		
Maximum Diameter	m	5
Height	m	0.3
Thickness	mm	2
Material		Al
Total area	m ²	19.63
Total weight (aluminum)	kg	106
Operating temperatures		4.5

Convection Cell Data Sheet (contd.)	units	Data
Enthalpy of Aluminum @ 300 K	J/kg	1.70E+05
Enthalpy of Aluminum @ 90 K	J/kg	1.30E+04
Enthalpy of Aluminum @ 6 K	J/kg	1.21
Shield Enthalpy @ 300 K	J	1.80E+07
Shield Enthalpy @ 90 K	J	1.38E+06
Shield Enthalpy @ 6 K	J	1.28E+02
Refrigeration		
Tube Dia	mm	
Tube Installation		
Heat load		
He flow (nominal) in = 4.5K, 4bar; out = 5 K.	g/s	0.05
Thermal conductivity @ 4 K	W/cm-K	0.84
Density	kg/m3	2700
Thermal expansion coefficient		
Supports		
Installation procedure		
	units	data
4 K Dewar		
Material		SS
Inner pressure	MPa	0.15
Outer Pressure	MPa	0.0003-0.4
Total volume	m3	0.15
Helium inventory	kg	21
LN2 Dewar (80K)		
Inner pressure		
Total volume		
LN2 inventory		
Total inner vessel mass including plates and supports	kg	37612
Inner vessel wall		19280
upper plate		7010
lower plate		7010
plates support		4206
conic shield		106
Refrigeration and heating system		0

Convection Cell Data Sheet (contd.)	units	Data
Total outer vessel mass including shields, neck pipes and support	kg	61987
external wall		56416
4 K shield		3859
90 K shield		1712
MLI		0
refrigeration system		0
Neck system		
Total He inventory in the inner vessel		
	max	kg
	min	kg
		12593
		5.496
TOTAL MASS (of the inner vessel+outer shell+shields)	kg	112192
Total He inventory in the refrigeration system excluding refrigerator		12693
Total nitrogen inventory		
Total He flow in the shields (normal operation)	g/s	2.101
Total He flow in the upper plate (3000W)	g/s	150
Total N2 consumption for normal operation	g/s	2.39
Total expected N2 consumption during shield cooldown	kg	1.34E+03
Time to cooldown to 90 K (15g/s)	hours	24.88
Total expected N2 consumption for system cooldown to 90 K	kg	14811
Time to cooldown to 90 K	hours	82
(assuming 50 g/s LN2 supply to the refrigerator)		
Time to cooldown to 4 K.		

Helium Convection Experiment
Cell Cooldown Enthalpy

Enthalpy in a system consisting of 20,000 kg of stainless steel, 15,000 kg of Copper, and with a volume of 250 cu-m filled with helium at 1 atm. pressure.

T - Equilibrium temperature of system (K)
H_s - Enthalpy of stainless steel component (enthalpy in Joules)
H_c - Enthalpy of copper component
H_{tot} - Total enthalpy of metals
H_h - Enthalpy of helium component
kgHe - Mass of helium component (kg)
ρ - Density of helium component (kg/cu-m)

T	H _s	H _c	H _{tot}	H _h	kgHe	ρ
300	1.84E+09	1.20E+09	3.04E+09	6.38E+07	40.6	0.16
200	9.46E+08	6.36E+08	1.58E+09	6.41E+07	60.9	0.24
100	2.28E+08	1.58E+08	3.86E+08	6.50E+07	121.8	0.49
90	1.76E+08	1.22E+08	2.99E+08	6.52E+07	135.3	0.54
80	1.30E+08	9.02E+07	2.21E+08	6.55E+07	152.2	0.61
70	9.07E+07	6.22E+07	1.53E+08	6.58E+07	174.0	0.70
60	5.78E+07	3.87E+07	9.65E+07	6.62E+07	203.0	0.81
55	4.41E+07	2.87E+07	7.29E+07	6.65E+07	221.4	0.89
50	3.24E+07	2.01E+07	5.25E+07	6.68E+07	243.6	0.97
45	2.28E+07	1.28E+07	3.56E+07	6.72E+07	270.7	1.08
40	1.52E+07	7.17E+06	2.24E+07	6.77E+07	304.6	1.22
35	9.86E+06	3.94E+06	1.38E+07	6.83E+07	348.2	1.39
30	6.18E+06	2.19E+06	8.37E+06	6.92E+07	406.3	1.63
25	3.73E+06	1.19E+06	4.92E+06	7.03E+07	488.0	1.95
20	2.14E+06	5.75E+05	2.72E+06	7.21E+07	611.1	2.44
15	1.13E+06	2.17E+05	1.34E+06	7.50E+07	818.7	3.27
10	4.88E+05	5.69E+04	5.45E+05	8.13E+07	1252.7	5.01
5	1.19E+05	2.42E+04	1.43E+05	1.08E+08	2995.5	11.98

Helium Convection Experiment
Oregon Cell Cooldown Enthalpy

Enthalpy in a system consisting of 20 kg of stainless steel, 100 kg of Copper, and with a volume of 0.2 cu-m filled with helium at 1 atm. pressure.

T - Equilibrium temperature of system (K)
H_s - Enthalpy of stainless steel component (enthalpy in Joules)
H_c - Enthalpy of copper component
H_{tot} - Total enthalpy of metals
H_h - Enthalpy of helium component
kgHe - Mass of helium component (kg)
ρ - Density of helium component (kg/cu-m)

T	H _s	H _c	H _{tot}	H _h	kgHe	ρ
300	1.84E+06	7.99E+06	9.83E+06	5.11E+04	0.0	0.16
200	9.46E+05	4.24E+06	5.19E+06	5.13E+04	0.0	0.24
100	2.28E+05	1.05E+06	1.28E+06	5.20E+04	0.1	0.49
90	1.76E+05	8.15E+05	9.91E+05	5.22E+04	0.1	0.54
80	1.30E+05	6.01E+05	7.32E+05	5.24E+04	0.1	0.61
70	9.07E+04	4.15E+05	5.05E+05	5.26E+04	0.1	0.70
60	5.78E+04	2.58E+05	3.16E+05	5.30E+04	0.2	0.81
55	4.41E+04	1.92E+05	2.36E+05	5.32E+04	0.2	0.89
50	3.24E+04	1.34E+05	1.66E+05	5.35E+04	0.2	0.97
45	2.28E+04	8.56E+04	1.08E+05	5.38E+04	0.2	1.08
40	1.52E+04	4.78E+04	6.31E+04	5.42E+04	0.2	1.22
35	9.86E+03	2.63E+04	3.61E+04	5.47E+04	0.3	1.39
30	6.18E+03	1.46E+04	2.08E+04	5.53E+04	0.3	1.63
25	3.73E+03	7.93E+03	1.17E+04	5.62E+04	0.4	1.95
20	2.14E+03	3.83E+03	5.97E+03	5.76E+04	0.5	2.44
15	1.13E+03	1.45E+03	2.57E+03	6.00E+04	0.7	3.27
10	4.88E+02	3.79E+02	8.67E+02	6.51E+04	1.0	5.01
5	1.19E+02	1.61E+02	2.80E+02	8.67E+04	2.4	11.98

Appendix D - Plate Thermal Issues

D.1. Peak Heat Flux and Refrigeration Load Estimates

D.1.1 Summary

Heat transfer estimates for high Ra, which are obtained by using the classical theory prediction to extend Wu’s results, represent the upper bound for the design. The maximum refrigeration required is for a cell with an aspect ratio of 1, and is within the capacity of the helium refrigerators at the SSC N15 site.

D.1.2 Estimate of heat transfer

From Wu’s experiments: $Nu = A Ra^n$

Aspect Ratio	A	n	Highest Ra achieved
0.5	0.17	0.29	1E15
1.0	0.22	0.285	1E12
6.7	0.146	0.286	1E11

Given the Rayleigh number, we can obtain:

- a) Convective heat transfer coefficient: $h = Nu \cdot k / L$
- b) Power input required: $q'' = h \Delta T$

D.1.3 Base case

Assume $Ra = 10^{19}$ with $D = 5\text{ m}$, $L = 10\text{ m}$, $\Delta T = 0.5\text{ K}$, and a nominal $T_{av} = (T_h + T_c) / 2 = 6\text{ K}$. ($k_{He} = 0.02\text{ W/m}\cdot\text{K}$ at 6 K, 4 bar)

D.1.4 Extrapolating Wu’s results to high Ra

If the thermodynamic conditions and ΔT are unchanged, and only L is varied, we obtain:

L (m)	Aspect Ratio	Ra	Nu	h (W/m ² -K)	q'' (W/m ²)	Q _{total} (kW)	Relative Power
10	0.5	1.00E+19	55011	110	55	1.08	1.00
5	1	1.25E+18	31626	127	63	1.24	1.15
0.75	6.7	4.22E+15	4297	115	57	1.13	1.04

Based on Wu’s correlations, a cell with an aspect ratio of 1 will require 15 % more power compared to the cell at 0.5 aspect ratio (1.24 kW vs. 1.08 kW)

D.1.5 Heat Transfer Estimates based on Classical theory

If $Nu \sim Ra^{1/3}$ as predicted by classical theory at high Ra , we expect to have higher heat transfer rates, and therefore increased refrigeration requirements. Two cases are considered:

1) Assume that the $1/3$ dependence sets in for $Ra > 10^{15}$, independent of the aspect ratio. (10^{15} is the highest Ra achieved by Wu for $D/L = 0.5$.) Hence

$$Nu = A (10^{15})^n (Ra/10^{15})^{1/3} = B Ra^{1/3} \quad \text{for } Ra > 10^{15}$$

Aspect Ratio	B
0.5	0.0381
1.0	0.0414
6.7	0.0285

We thus obtain the following power estimates:

L (m)	Aspect Ratio	Ra	Nu	h (W/m ² -K)	q'' (W/m ²)	Q _{total} (kW)	Relative Power
10	0.5	1.00E+19	81994	164	82	1.61	1.00
5	1	1.25E+18	44640	179	89	1.75	1.09
0.75	6.7	4.22E+15	4600	123	61	1.20	0.75

The power requirements obtained under this assumption are within the available refrigeration capacity (4 kW at 4.5 K).

2) If we allow that the $1/3$ dependence may set in at different Ra for different aspect ratios, specifically at the maximum Ra attained by Wu for each aspect ratio, we get larger power requirements at the higher aspect ratios, but which are still within the refrigeration capacity.

$$Nu = C Ra^{1/3}$$

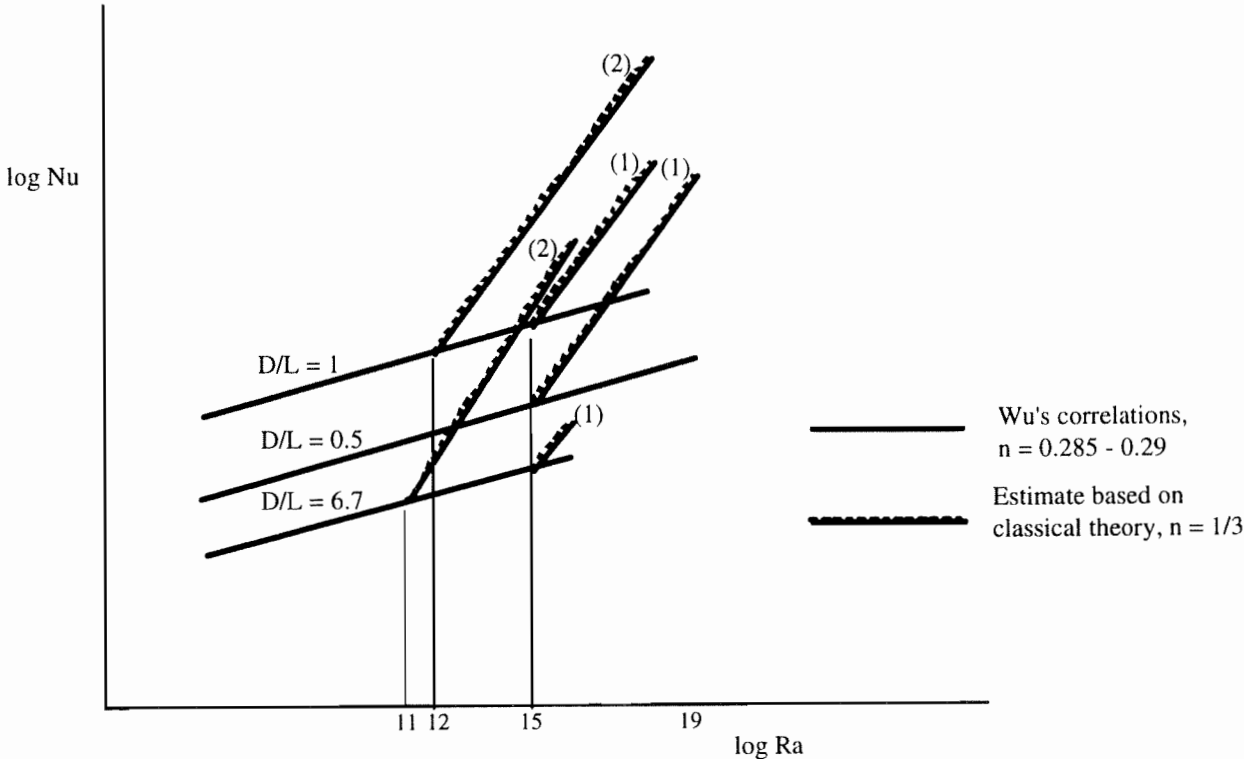
with

Aspect Ratio	C	assumed to be valid for
0.5	0.0381	$Ra > 1E15$
1.0	0.0579	$Ra > 1E12$
6.7	0.0440	$Ra > 1E11$

and

L (m)	Aspect Ratio	Ra	Nu	h (W/m ² -K)	q'' (W/m ²)	Q _{total} (kW)	Relative Power
10	0.5	1.00E+19	81994	164	82	1.61	1.00
5	1	1.25E+18	62334	249	125	2.45	1.52
0.75	6.7	4.22E+15	7114	190	95	1.86	1.16

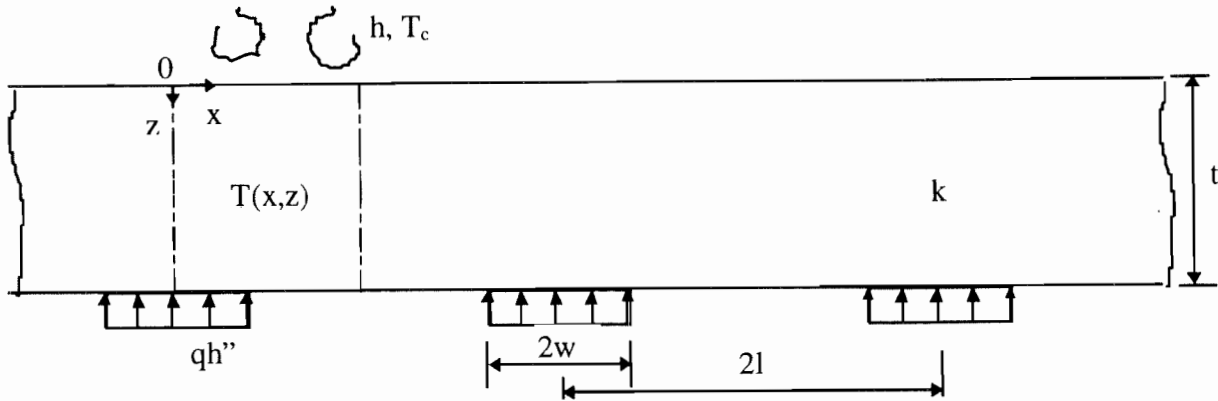
Heat Transfer Estimates based on Classical theory predictions at high Ra
(Qualitative behavior - exaggerated)



D.2. Bottom Plate Heater Arrangement

D.2.1 Temperature Distribution

Consider the temperature distribution in a slab subject to discrete surface heating on one boundary and uniform convective heat transfer on the other.



Let $\Delta T = T_h - T_c$,

where T_h and T_c are the nominal uniform surface temperatures under uniform surface heating q'' . For discrete periodic heating, the required heater power density is

$$q_h'' = q''/f,$$

where $f = 2w/2l$ is the coverage.

The resulting deviation of the plate surface temperature from the nominal value, normalized with respect to the nominal temperature difference ΔT , is given by:

$$\frac{T(0, x) - T_h}{\Delta T} = \frac{\delta T_h}{\Delta T} = \frac{2h}{f} \sum_{n=1}^{\infty} \frac{\sin(f\lambda_n l)}{\lambda_n l} \frac{\cos(\lambda_n x)}{h \cosh(\lambda_n t) + k\lambda_n \sinh(\lambda_n t)} \quad (1)$$

where $\lambda_n = n\pi/l$, $n = 1, 2, \dots$

Note: it can be shown that the above expression also represents the deviation in surface heat flux from the nominal uniform heat flux, normalized with respect to the latter.

The maximum deviation is at $x = 0$, and is directly proportional to the heat transfer coefficient h , and inversely proportional to the plate thermal conductivity k .

$$\delta T_h / \Delta T \sim h/k \quad \text{since} \quad h \cosh(\lambda_n t) \ll k\lambda_n \sinh(\lambda_n t)$$

Thermal conductivity is fixed by the choice of material, copper. Therefore, we have to be concerned with the maximum value of the heat transfer coefficient to estimate the worst case for surface temperature fluctuations. For a cell with an aspect ratio of 0.5, the peak heat transfer coefficient is estimated at $h = 164 \text{ W/m}^2\cdot\text{K}$ for $Ra = 10^{19}$ with a nominal $\Delta T = 0.5 \text{ K}$. This gives $q'' = 82 \text{ W/m}^2$ for uniform heating.

For $t = 1.5''$ (3.75 cm) thick, 72 cm wide copper plate sections ($k_{Cu} = 330 \text{ W/m}\cdot\text{K}$), we consider designs with 2, 4 and 6 uniformly spaced heater strips (36 cm, 18 cm and 12 cm apart, respectively). The resulting temperature fluctuations on the plate surface are summarized below:

	2 heater strips/section 2l = 36 cm		4 heater strips/section 2l = 18 cm		6 heater strips/section 2l = 12 cm	
Heater Strip Width 2w	Coverage f	$\delta T_h / \Delta T$	Coverage f	$\delta T_h / \Delta T$	Coverage f	$\delta T_h / \Delta T$
0.5"	0.035	10.20%	0.069	1.86%	0.104	0.57%
1"	0.069	10.04%	0.139	1.80%	0.208	0.53%
2"	0.139	9.47%	0.278	1.56%	0.417	0.40%
3"	0.208	8.67%	0.417	1.24%	0.625	0.25%
4"	0.278	7.76%	0.555	0.90%	0.833	0.10%

D.2.2 Conclusion

Heater strips, 0.5" to 1" wide, placed 12 cm apart (6 heater strips per 72 cm section) will keep the surface temperature fluctuations well within the 1% requirement relative to the cell ΔT , and will provide sufficient margin for possible nonuniformities in application, geometric irregularities near the edges of the plates or sections, discreteness along the length of the heaters (i.e. perpendicular to the plane in the above figure), etc.

Note: Extensions of Wu's correlations to higher Ra using classical theory predicts higher heat transfer rates (as much as 50% higher) for $D/L = 1$ than for $D/L = 0.5$. The recommended spacing of heaters will still keep the temperature fluctuations within 1%, but will have less margin for possible nonuniformities. Heater strips that are spaced 9 cm apart (8 per 72 cm wide section) should also be considered.

D.3. Cooling of the Top Plate

D.3.1 Helium sink

In order to provide uniform cooling over the entire plate surface, two-phase helium is circulated through the cooling channels. Heat convected across the cell (plus any additional heat supplied through the heaters discussed below) is removed through boiling heat transfer in the cooling tubes.

Two-phase flow in the cooling tubes limits the helium sink temperatures to the 4.4–4.8 K range (1.2–1.7 bar). There will be some pressure drop in the tubes, and a corresponding decrease the saturation temperature. However, $\partial T_{sat} / \partial p$ is of the order of 10^{-5} K/Pa . If the two-phase pressure drop is maintained at a few Pa, the resulting decrease in the sink temperature is not a concern.

D.3.2 Effective thermal resistance between the plate and the helium sink

If the top plate is to be operated at higher temperatures, e.g. 5.5–6.0 K, there has to be a resistance to heat flow between the plate and the helium sink in order to elevate the plate temperature. Since the copper plate has very high thermal conductivity, this 1–1.5 K temperature difference will essentially be across the resistance. The magnitude of the thermal resistance to support a 1 K temperature difference can be estimated as:

$$R_s = 1/h_s = (1 \text{ K}) / (q_u''/f_s) \quad [\text{K}/(\text{W/m}^2)]$$

where $f_s (= w_s/l)$ is the coverage for the helium sink. For a peak heat flux of 82 W/m^2 , the effective resistance R_s is therefore $34 \text{ K}/(\text{W/cm}^2)$ at 28% coverage. Considering an effective thermal resistance path of 2 cm, this requires a resistance material with a thermal conductivity of about $0.06 \text{ W/cm}\cdot\text{K}$ at 5 K. This rules out materials such as copper and high conductivity aluminum alloys, as well as stainless steels with one order of magnitude lower thermal conductivity. Candidate resistance materials are aluminum alloys or brass. Cooling channels can be extruded to the desired cross-section.

D.3.3 Heaters

The bulk resistance is sized to yield plate temperatures close to the operating temperature for the upper plate at the peak heat flux level (at the highest Ra number). When the cell is operated at lower Ra numbers, i.e. lower heat flux levels, the temperature difference across the resistance will be considerably less than 1–1.5 K, resulting in plate temperatures lower than the operating temperature. Heaters placed on the top surface will provide the additional heat flow in order to elevate the plate temperature to the desired level. Hence the helium cooling circuit will basically run at a constant load (1.5–2 kW) regardless of the Ra number, assuming the upper plate temperature is maintained at the same level for all runs.

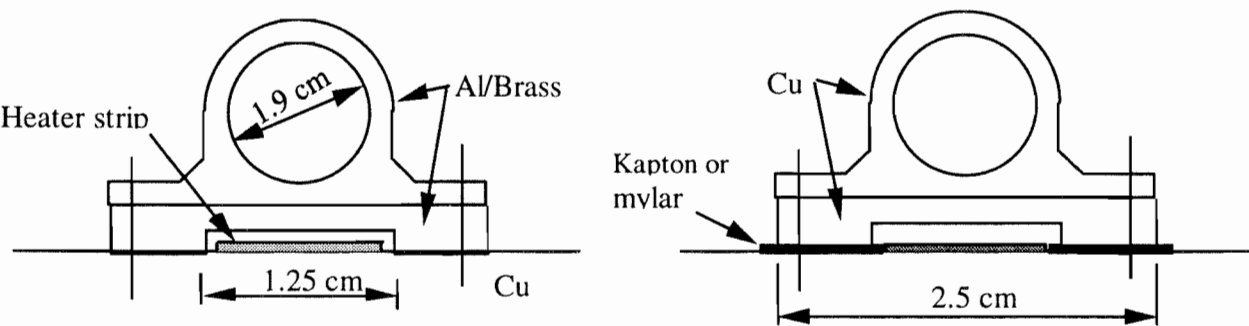
If the experiments call for different operating temperatures for the upper plate for different runs at the peak heat flux, the resistance should be sized to attain the minimum desired operating level. The heaters can then be used to raise the plate temperature above this value as needed. In this case, the refrigeration load will be higher than the peak cell heat transport estimate.

D.3.4 Contact resistance

In the above estimate for the resistance material, it is assumed that the thermal resistance is solely due the bulk material resistance. There will be additional resistances, however, due the contacts between the resistance material and the plate, and possibly between the resistance material and the cooling tube. These contact resistances should be minimized in the design of the cooling tube assembly: contact resistances vary significantly with contact pressure, and local nonuniformities in the contacts can therefore lead to large temperature variations over the surface.

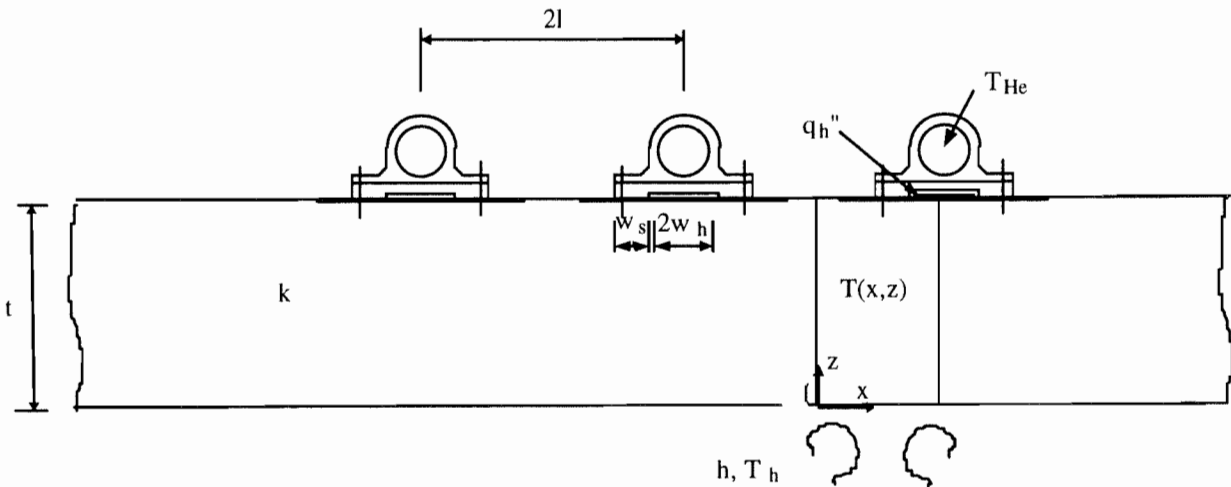
An alternative design may involve cooling assemblies made of copper. This would eliminate any potential problems associated with having cooling tube assembly and plate materials with different thermal contraction and expansion rates. The thermal resistance in this case could be provided by a thin film of kapton or mylar between the cooling tube assembly and the plate. Published data show that a 25- μm thick kapton or mylar film can provide resistances of the order discussed above at the right contact pressure. However, it will be very difficult to maintain uniform contact pressure over a 20 m^2 plate surface.

Conceptual designs for the cooling tube assemblies are shown below.



D.3.5 Minimizing temperature variations on the plate surface

Consider the temperature distribution in a slab with uniform convective heat transfer on one boundary and subject to discrete cooling and heating on the other.



The temperature distribution is governed by the steady-state Fourier heat conduction equation, with symmetry boundary conditions at the periodic x-boundaries. Heat transfer at the lower surface ($z = 0$) is given by

$$-k \frac{\partial T}{\partial z} = h \Delta T$$

where $\Delta T = T_h - T_c$; and T_h , T_c are the nominal uniform surface temperatures for the bottom and top plates respectively under uniform surface heating q_u . Boundary conditions at the upper surface ($z = t$) are

$$\begin{aligned} -k \frac{\partial T}{\partial z} &= h_s (T - T_{He}) & x \in w_s \\ -k \frac{\partial T}{\partial z} &= -q_h & x \in w_h \\ -k \frac{\partial T}{\partial z} &= 0 & x \in l - w_s - w_h \end{aligned}$$

The minimum operating temperature of the plate is taken to be 5.5 K, and the helium sink temperature is taken to be 4.5 K (@ 1.3 bar pressure). Thermal conductivity of the plate is assumed to be 3.2 W/cm·K. The plate is 3.75 cm thick.

D.3.6 Results and discussion

The heat conduction equation was solved numerically for various sink and heater coverages and spacings. Results are summarized below:

1. The helium sink and heater strips should be placed as close as possible to minimize temperature variations. Hence the center-aligned arrangement shown in the figures.
2. Helium cooling channels should be placed as close as feasible. The driving factor here is the low Ra operation in which the heaters are turned up to maintain plate temperatures 1-1.5 K above the helium sink temperature. The lowest practical spacing for the cooling channels (2l) is 9.1 cm (10 channels per 36" wide section): if the thermal resistance and the heater strips are assumed to have 1" wide contact area ($2w_s, 2w_h$), 56 % of the surface is covered by the cooling tube assemblies. Under such coverage, the surface temperature variations are kept well below the $\pm 1\%$ ΔT requirement at the high Ra numbers (high convection heat fluxes), leaving sufficient margin for potential nonuniformities. On the other hand, for operation at low Ra numbers with low cell ΔT 's (50-100 mK), this spacing cannot meet the $\pm 1\%$ (± 0.5 -1.0 mK) requirement if the heaters are turned up to raise the plate temperature. For example, with $\Delta T = 50$ mK and convective heat flux of 4.2 W/m^2 (1/20th of peak heat flux), surface temperature variations are about $\pm 1.5\%$ ΔT with no allowance for nonuniformities. The design should be improved with regard to this requirement. Further reduction in the spacing to remedy this situation is not practical. Thicker plate(s) (2" thick), and higher thermal conductivity copper for the plates should be considered. The $\pm 1\%$ ΔT requirement may also not be realistic for low ΔT 's and should be reexamined. If the $\pm 1\%$ ΔT requirement is relaxed for low Ra, low ΔT operation, 8 cooling channels per 36" section can also be used (11.4 cm apart, 42% total coverage).
3. Boiling heat flux considerations: For a 9-cm spacing between cooling channels, the peak heat flow into one channel is 0.074 W/cm ($=0.0082 \times 9$). Consider a tube diameter of $3/4"$ (1.9 cm). The average heat flux for the tube is then 0.0124 W/cm^2 , which is well below the 0.1 W/cm^2 level to enter film boiling regimes.

Appendix E - Convection Cell Operating Regimes

Two quantities have been suggested, the Busse Q (Busse 1967) and the X ratio (Wu and Libchaber 1991), which may provide measures of the non-linear behavior that will limit the interpretation of measurements made in a convection cell. The Q-Factor has particular relevance in the region of convection just above the critical Rayleigh number where it is a predictor of the cellular structure of the convection. The X - Ratio is defined as the ratio of the ΔT across the top and the bottom boundary layers on the two plates. In his paper, Wu correlates this ratio with deviations from power law behavior of the Nusselt Number observed in his measurements, and he shows that X can be predicted from the fluid properties at the conditions for the two boundary layers.

With these measures it is possible to explore the property space of helium for regions in which high Rayleigh numbers might be achieved in a satisfactory experiment. It is, of course, important to identify possibly suitable regions of operation so that the cell can be designed with the needed capabilities. The attached material represents a first attempt at such an exploration.

A cell operating point can be defined for the purposes of study by choosing a cell average temperature, average density, and a ΔT . From these values, using the NIST 1334 property correlations, all the quantities of interest can be estimated including the Q and the X measures of quality. The first of the attached plots show Rayleigh number (for a cell $L = 10 \text{ m}$) and Prandtl number at average conditions for $\Delta T = 0.5 \text{ K}$ for a number of average densities as functions of average temperature. Following are contour plots of these quantities, the X - Ratio and the Q - Factor also as functions of average density and temperature again for $\Delta T = 0.5 \text{ K}$. Two additional contour plots show the Rayleigh Number and Q-factor computed for $\Delta T = 0.1 \text{ K}$. Also among the plots is one of the mechanical equation of state of helium showing isobars as a function of temperature and density. This plot is sized to have the same scales as the contour plots. Thus a transparency of this plot can be placed over any of the contour plots to help in interpretation. Further information can be obtained by referring to table 3.1 above which lists possible operating points for the convection cell. The quantity q in the table is the heat flux in the 10 m cell predicted from the results of the measurements of Wu.

Remarks concerning the contour plots:

- 1) There are two regions in the ρ - T plane in which Q takes low values. These are in the low-density region below 20 kg/m^3 and in high density region between 60 and 80 kg/m^3 . For the present purposes I will call these Region 1 and Region 2. The region of higher Q-values that lies between these two regions is an image of the extreme conditions of the critical region translated upward in temperature along lines of constant pressure by the finite ΔT .
- 2) The behavior of Wu's X factor is qualitatively the same as the Q. That is, X takes values between 0.7 and 0.9, values for which Wu finds regular behavior in his measurements of Nusselt number, in the same general areas in which Q is below 2.

3) In Region 1 the Rayleigh number that can be achieved with a given ΔT is only a weak function of the temperature, but a nearly linear with density. In Region 2 the opposite behavior is observed; that is, the Rayleigh number varies most strongly with temperature.

4) The conclusion to be drawn from this is that operation of a convection cell in Region 2 seems to be a promising way of attaining high Rayleigh number operation, and that we should design the experiment to operate in this region. This implies a 5 bar pressure rating, a cooling system for the upper plate capable of operation at temperatures as high as 6 K, and sufficient refrigeration power for a Rayleigh number of at least 10^{19} . The Oregon cell should also be designed to operate in this region. The 1 m cell could achieve a Rayleigh number of 10^{16} , and there would seem to much interesting work to do to study the non Boussinesq effects.

Discussion of the operating point Cases listed in Table 3.1:

1) The first five cases listed in the table concern operation in Region 1. The first two are points taken from Wu's Table 3 (Wu 1991). A fact that is not immediately obvious is that the Pr found here using NIST 1334 differs from that found by Wu using NBS 631 by about 10%. The Rayleigh numbers differ by a similar amount. A quick check suggests that differences in the transport properties in the two correlations are the origin of what we see. The mechanical derivatives and heat capacities agree pretty well. It is clearly important to unravel this, and inclusion of the study of properties in our task list is justified.

2) It is apparent that the high Rayleigh number points in Wu's work have associated values of Q significantly larger than 2. It will be illuminating to calculate Q and X values for his points, and we will do this in due course.

3) Case 3 is a point at which the 10 m cell can be operated at a Rayleigh number of 10^{11} . This low density requires that the large cell be pumped down after cool-down. The very low value of q here presents a problem in achieving accurate measurements of Nusselt number at this point.

4) Case 4 in the table is the trial case presented some month ago, and Case 5 is a point slightly adjusted from that to reduce the Q and increase the Ra. If we take the Q measure seriously and choose, say, the criterion of $Q < 2$, it is going to be difficult to achieve a Rayleigh number significantly greater than 10^{17} operating the 10 m cell at points in Region 1.

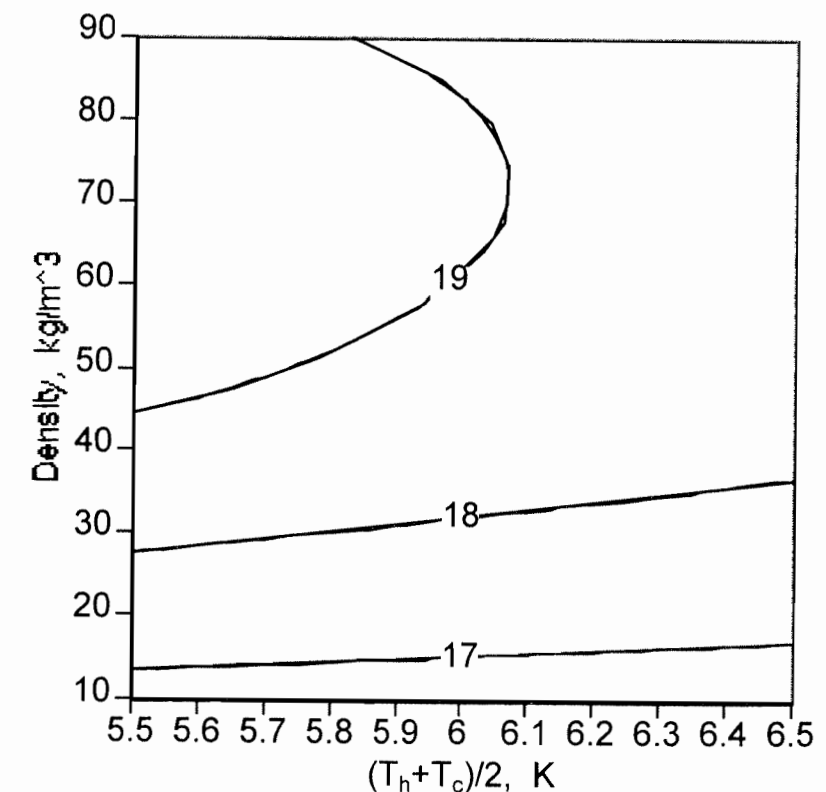
5) Cases 6 and 7 of the table are representative of operation in Region 2. Here the Rayleigh number can reach 10^{19} with $Q < 2$. The Prandtl number in Region 2 is, however, generally higher than in Region 1. The implications of this must be discussed.

6) The kinetic viscosity of helium at the conditions of average temperature and density is listed in line 7 of the table. For the highest Reynolds number operation of the towed grid

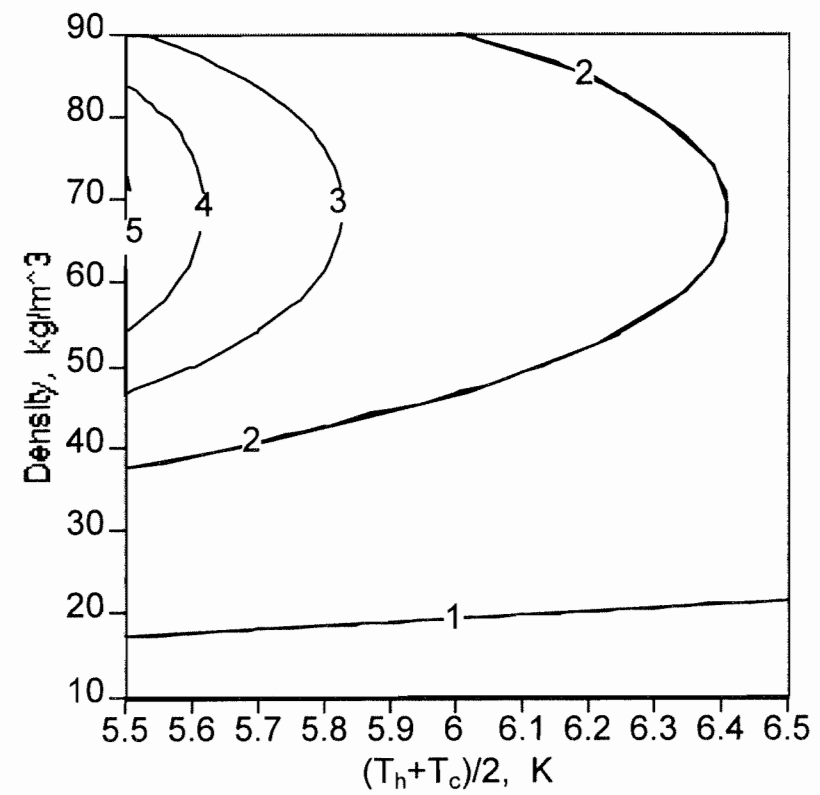
experiment, this quantity should be as low as possible. The lowest value available is with liquid helium for which $\nu = 2.6 \times 10^{-8} \text{ m}^2/\text{s}$. Operation at the high density end of Region 1 can approach within a factor of two of this value. Operation in Region 2 can reach within a factor of 1.25. The current schedule and cost estimate includes only one operating period in Region 2 and this is for the convection experiment. Operation of the towed grid in Region 2 will have to be proposed as part of a follow-on program.

6) The last case in the table gives the numbers for room temperature cell operation.

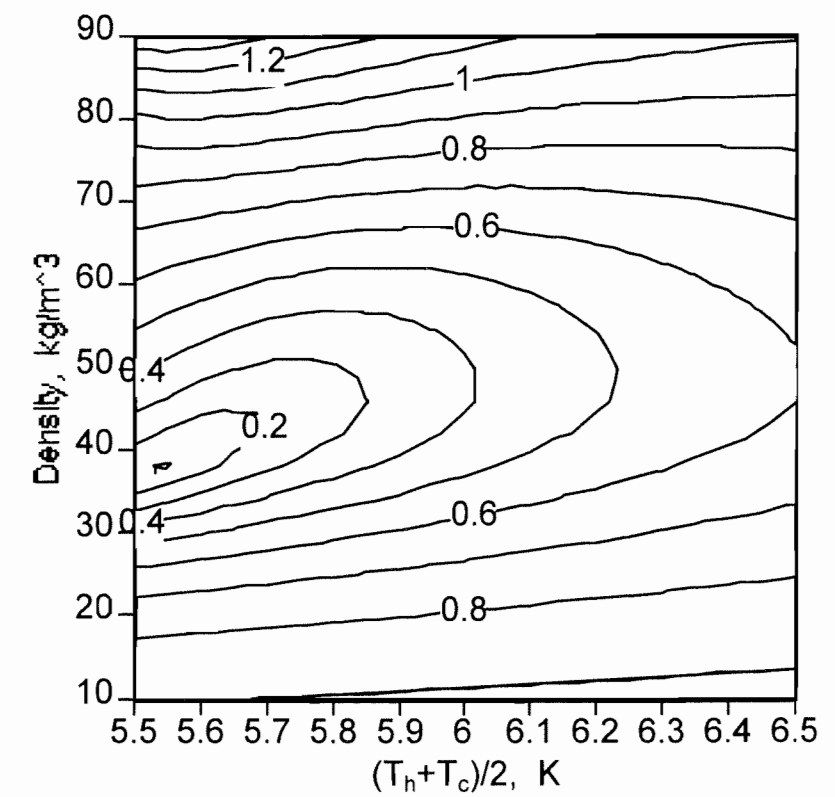
Contour Plot of log Rayleigh Number as a Function of Average Temperature and Density for a ΔT of 0.5 K



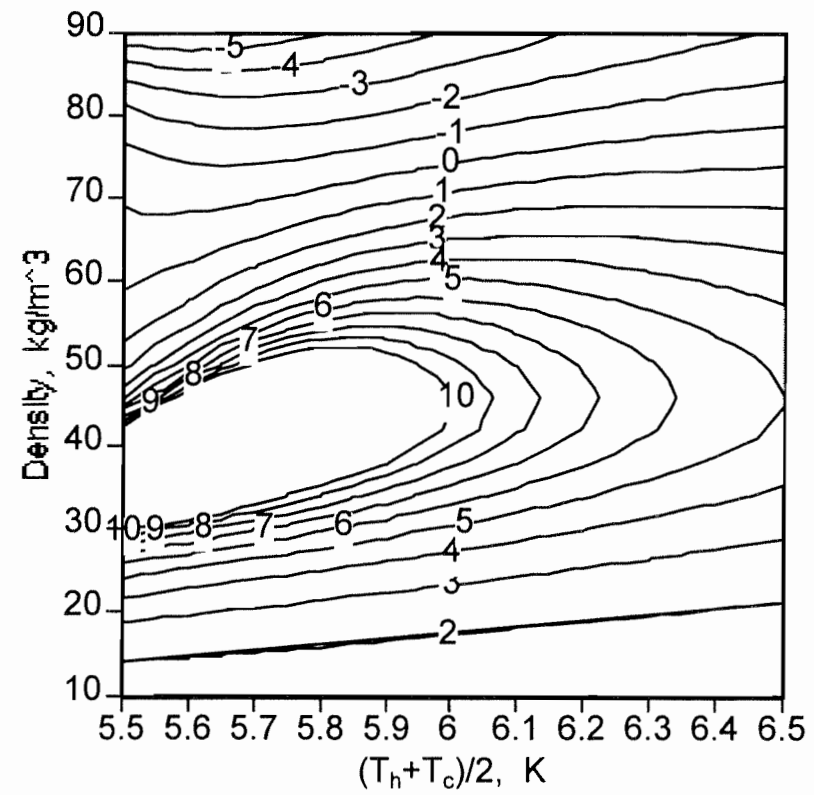
Contour Plot of Prandtl Number as a
Function of Average Temperature and Density for a ΔT of 0.5 K



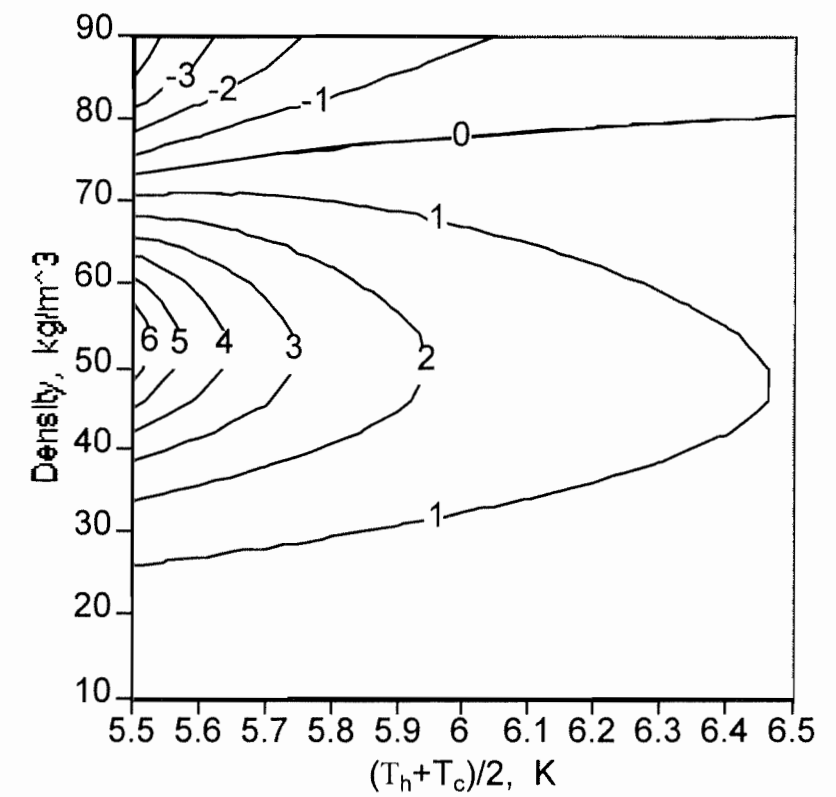
Contour Plot of X- Ratio as a
Function of Average Temperature and Density for a ΔT of 0.5 K



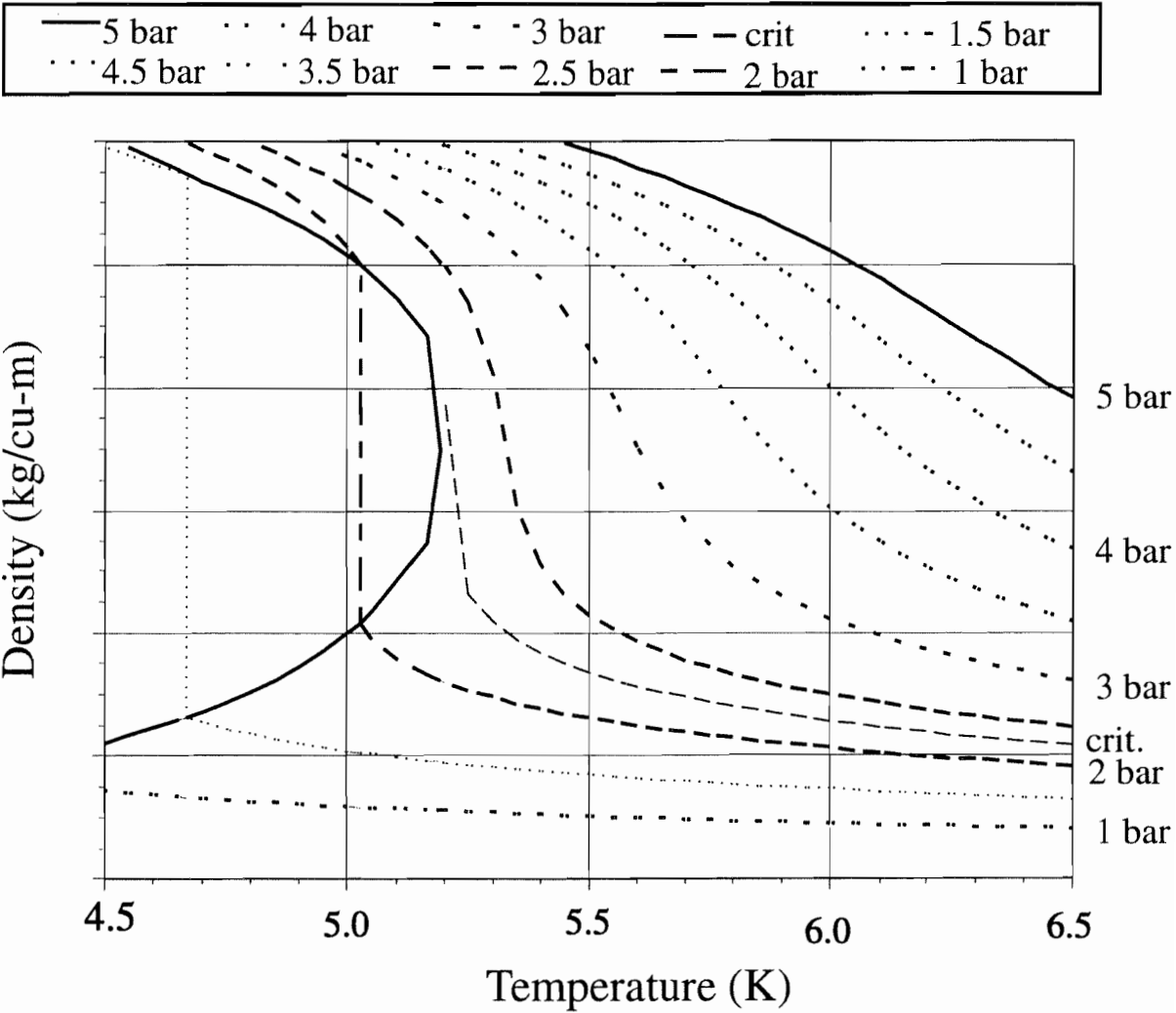
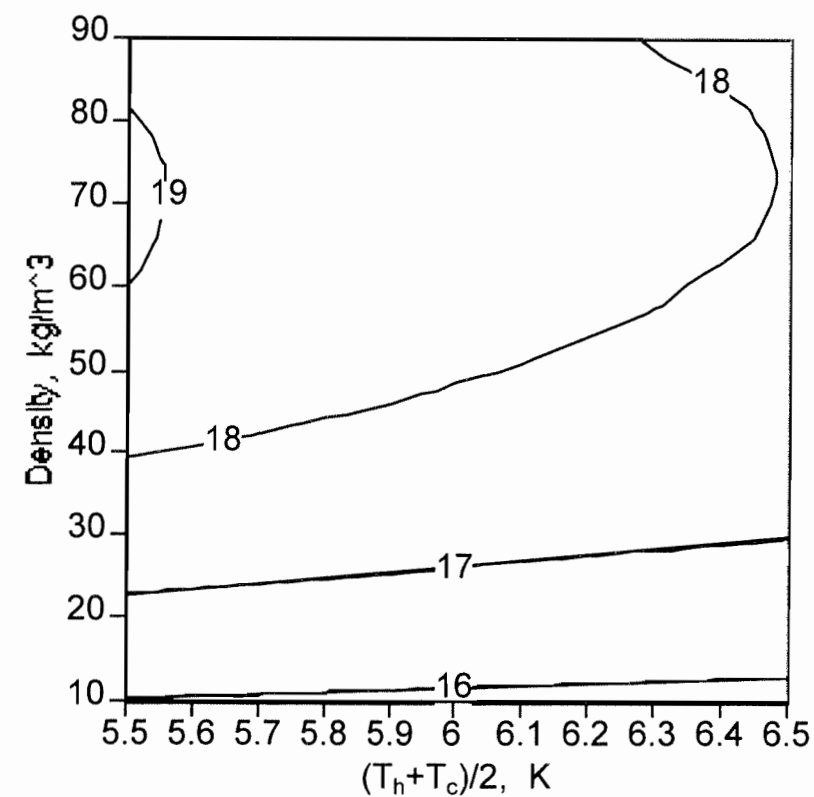
Contour Plot of Q - Factor as a
Function of Average Temperature and Density for a ΔT of 0.5 K

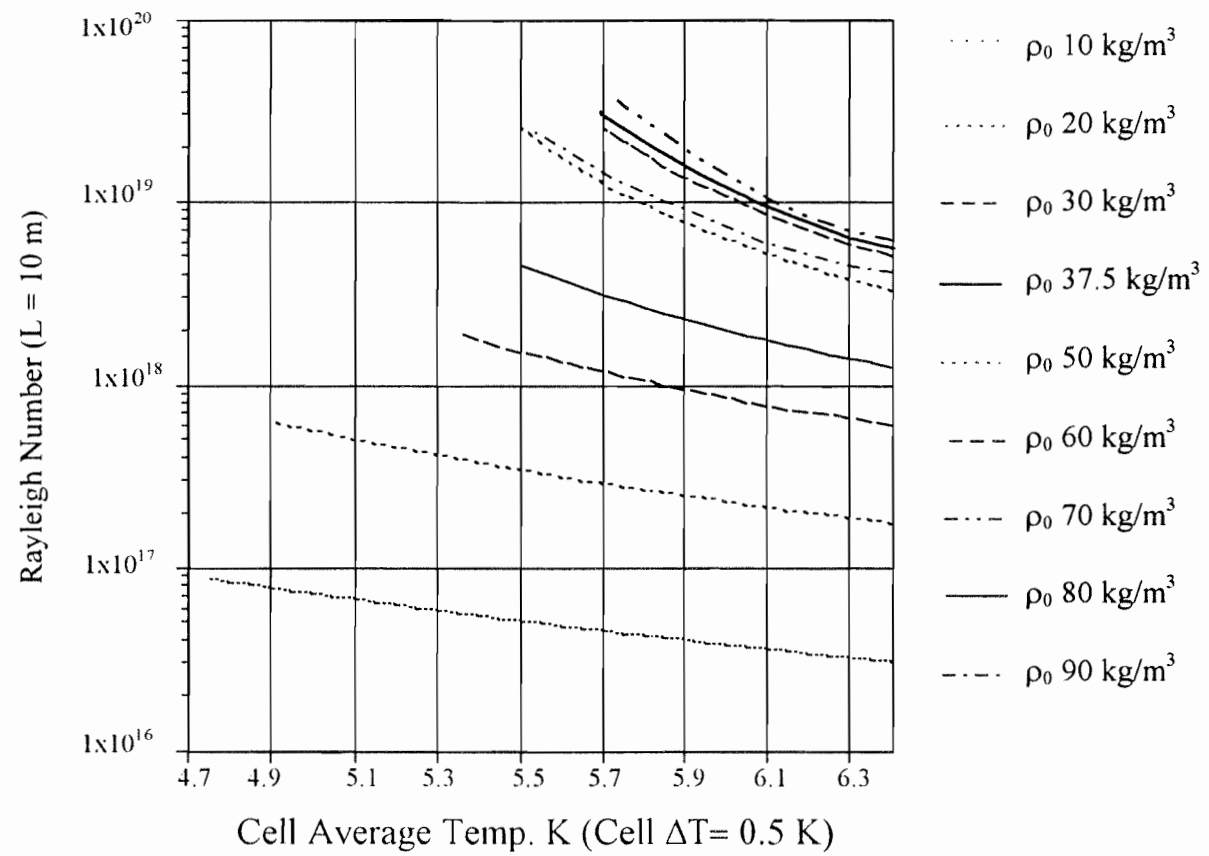


Contour Plot of Q - Factor as a
Function of Average Temperature and Density for a ΔT of 0.1 K



Contour Plot of log Rayleigh Number as a
Function of Average Temperature and Density for a ΔT of 0.1 K





Possible Convection Cell Operating Points

Case	1	2	3	4	5	6	7
Ave Density kg/m^3	20.00	37.50	10.00	16.00	70.00	70.00	0.16
Ave Temp. K	5.172	5.504	5.000	6.275	6.065	5.550	300.00
Pressure, bar	1.54	2.39	0.88	1.71	3.85	2.90	1.02
ΔT , K	0.56	0.56	0.50	0.50	0.50	0.10	50.00
NPr (at ave T)	1.14	1.99	0.88	0.91	2.44	4.56	0.66
NRa	4.87×10^{17}	4.57×10^{18}	6.86×10^{16}	1.00×10^{17}	1.01×10^{19}	1.05×10^{19}	7.34×10^{10}
Q-Factor	-5.26	-20.01	-2.22	-1.92	-1.69	-1.32	-1.85
X-Factor	0.638	0.165	0.842	0.848	0.645	0.774	0.879
$\gamma_0 = \Delta p / \rho$	0.265	1.600	0.152	0.131	0.473	0.238	0.168
$\gamma_1 = (\Delta \alpha / \alpha + \Delta \rho / \rho) / 2$	0.436	1.829	0.190	0.169	0.294	0.170	0.168
$\gamma_2 = \Delta v / v$	-0.308	-0.621	-0.226	-0.179	-0.276	-0.125	-0.283
$\gamma_3 = \Delta \lambda / \lambda$	-0.045	0.453	-0.080	-0.047	0.164	0.085	-0.115
$\gamma_4 = \Delta C_p / C_p$	0.318	1.827	0.073	0.073	0.100	0.115	0.000

Appendix F - Work Breakdown Structure Dictionary

F.1 University support programs

Includes definition of experiments to be performed. Also includes development of instrumentation and measurement techniques, measurement of helium properties, and preliminary towed grid experiments.

F.1.1 Oregon experiment

Includes constructing and operating a smaller convection cell of 1 meter height, for development of instrumentation and measurement techniques.

F.1.1.1 Design review and specify

F.1.1.2 Procure

F.1.1.3 Develop instrumentation

F.1.2 Duke university projects

Includes measurement of helium properties relevant to program of proposed experiments, and definition of operating regimes and parameters for the Oregon experiment and the 10 meter cell.

F.1.3 Yale university projects

Includes performing preliminary towed grid experiments in water. Also includes support for the Oregon experiment and 10 meter cell experiments.

F.2 Mechanical systems

F.2.1 Vessel system

The main vessel including: the vacuum jacket, the nitrogen and helium shields, the inner vessel, the top flange, the cryogenic system with all its valves, the top deck, a crane, and access stairway. A complete list is contained in Appendix A.

F.2.1.1 Design, review, and specify

Includes the engineering, drafting and management hours required to specify the system for fabrication.

F.2.1.2 Procure

Includes the engineering and management hours required to solicit, review and arrange approval of bids and contracts. Also includes the engineering and management hours required to coordinate and supervise contract for:

F.2.1.2.1 Design and review

Includes the services of a professional engineer in developing a design and procuring a manufacturing contract.

F.2.1.2.2 Fabrication, delivery and erection
Includes the main vessel with vacuum jacket, as described in detail in Appendix A.

F.2.1.3 Develop commissioning procedures

Includes engineering and management time required to develop acceptance tests and commissioning procedures.

F.2.1.4 Develop safety procedures

Includes engineering and management time required to develop safety procedures and obtain required operating permits from the host facility.

F.2.1.5 Commission

Includes: leak test insulating vacuum, neck feedthroughs, and top flange; checkout control valves; cooldown; measure heat leaks; checkout supporting systems.

F.2.2 Plate Systems

Appendix A contains a list of the materials included with the plate system.

F.2.2.1 Design, review, and specify

Includes the engineering, drafting and management hours required to specify the system for fabrication.

F.2.2.2 Procure

Includes the engineering and management hours required to solicit, review and arrange approval of bids and contracts. Also Includes the engineering and management hours required to coordinate and supervise contract for:

F.2.2.2.1 Fabrication and delivery of Plates

F.2.2.2.1.1 Design

F.2.2.2.1.2 Raw materials and parts

F.2.2.2.1.3 Machining

F.2.2.2.2 Installation equipment

Includes a trial assembly fixture with a geometry similar to the tank: a cylinder of the same diameter as the tank but only three feet deep. A single rolled angle, circumferentially welded in the middle of the cylinder will provide support for both top and bottom plates. The cylinder is to be supported on approximately 8 legs, with the bottom of the support angle six feet off the ground in order to simulate the space under to bottom plate and allow sufficient space for assembling and hanging the top plate. Also includes as yet undefined special rigging equipment that may be required for installation.

F.2.2.3 Perform trial assembly

Includes engineering and technician time required to refine plate installation procedures, by mounting both top and bottom plates on a trial assembly structure.

F.2.2.4 Install

F.2.2.4.1 Install instrumentation

Includes technician time necessary to install thermometers, and heaters.

F.2.2.4.2 Install heaters and cooling tubes

Includes technician time to bolt heater strips onto top and bottom plates, and bolt cooling tubes to top plate

F.2.2.4.3 Install in vessel

Includes technician time to install top and bottom plates in vessel, and level. Leveling equipment is assumed to be available at the host facility. (See Appendix G)

F.2.3 Cryogenic Supply System

The Cryogenic Supply System provides refrigeration to the vessel cryogenic system, including: the liquid nitrogen shield, the liquid helium shield, the top plate cooling loop and the vessel fill system. Each of the shields, the top plate, and the vessel fill system, together with the associated piping and control valves, are costed as part of the vessel. The Cryogenic Supply System includes four lines between the vessel and the refrigerator. The valves necessary for isolation at the refrigerator, already exist.

F.2.3.1 Design, review, and specify

Includes the engineering, drafting and management hours required to specify the system for fabrication.

F.2.3.2 Purchase piping

Includes the engineering and management hours required to solicit, review and arrange approval of bids and contracts. Also includes the engineering and management hours required to coordinate and supervise contract for:

F.2.3.2.1 Fabrication and delivery

Includes all items to be manufactured and delivered by vendor. It is assumed that the vacuum-jacketed pipe will be purchased in predetermined sections, with field joints that can readily be made up by technicians available at the host facility. It is further assumed that these same technicians will install all piping, and test for leaks.

F.2.3.2.1.1 Vacuum-jacketed line

Consists of three cold lines contained in a single vacuum jacket: helium supply (1.5"), helium return (2.5"), and liquid nitrogen supply (1"). All piping is stainless steel. Includes the cost of a relief valve on each line.

F.2.3.2.1.2 Warm Helium Return Line

A 4 inch stainless steel line that returns warm boil-off gas from the helium shield system to compressor suction. Includes the cost of a relief valve.

F.2.3.3 Install

Includes technician time required to install the entire system.

F.2.3.4 Test

Includes technician time required to leak test installed piping.

F.2.4 Vacuum System

The Vacuum System serves to evacuate the vacuum shell of the main vessel to a pressure of 1.3×10^{-4} Pa. It also serves to evacuate the inner vessel during pump and purge operations, and to reduce the density of cold helium gas during operation of the convection experiment. The system consists of three pumps. A 250 cu-m/hr roughing pump is used to rough both the vacuum shell and inner vessel, as well as, to adjust helium inventory after cooldown. A turbomolecular pump with a small fore pump is used to pump the vacuum shell down to its final pressure, before cooldown begins. It is assumed that technicians employed by the host facility will install all piping, pumps and valves that are external to the main vessel.

F.2.4.1 Design, review, and specify

Includes the engineering, drafting and management hours required to specify the complete system.

F.2.4.2 Purchase equipment

Includes the engineering and management hours required to solicit, review and arrange approval of bids. Also includes the management hours required to coordinate and supervise purchase of:

F.2.4.2.1 Inventory control pump

Used to rough out the vacuum jacket, the inner vessel and to reduce inventory when low operating densities are desired.

F.2.4.2.2 Gate valves

Includes the cost of two 4 inch gate valves needed to facilitate switching the inventory control pump in and out of the warm return line.

F.2.4.2.3 Exhaust valves

Includes the cost of two 1 inch ball valves on the exhaust of the pump, which allow the exhausted gas to be vented to atmosphere, or returned to compressor suction.

F.2.4.2.4 Coalescer

Filters the oil from pump exhaust before return to compressor suction. Costed as a complete system.

F.2.4.2.5 Turbo-Pump

Required to pump out vacuum jacket to acceptable vacuum.

F.2.4.2.6 Fore pump

Backing pump for turbo-pump.

F.2.4.3 Install

Includes technician time required to install the entire system.

F.2.4.4 Test

Includes technician time required to verify performance of equipment on delivery and leak test installed system.

F.2.5 Towed Grid System

The towed grid system is a collection of 1.5 inch aluminum tubing spaced 6 inches apart, center to center. The tubing that makes up the grid is non-planar. The grid is suspended by four cables which are routed over sets of pulleys connected to the inside surface of the top head and into the neck of the vessel.

F.2.5.1 Design, review, and specify

Includes the engineering, drafting and management hours required to specify the system.

F.2.5.2 Purchase system

Includes the engineering and management hours required to solicit, review and arrange approval of bids and contracts. Also includes the management hours required to coordinate and supervise contract for:

F.2.5.2.1 Engineering

F.2.5.2.2 Raw materials and parts

F.2.5.2.3 Fabrication

F.2.5.3 Install

Includes cost of technician time to install grid and heat exchanger in tank, and drive mechanism on top.

F.2.5.4 Test

Includes technical time to checkout system after installation is complete.

F.2.6 Utilities

These include compressed air, compressed nitrogen, compressed helium, cooling water, air conditioning and ventilation equipment, communication equipment, and electric utility power, all to be available at the top of the vessel.

F.2.6.1 Design, review, and specify

Includes the engineering, drafting and management hours required to specify each of the systems.

F.2.6.2 Procure

Includes the engineering and management hours required to solicit, review and arrange approval of bids and contracts. Also includes the management hours required to coordinate and supervise contracts for:

F.2.6.2.1 Utility Piping

The utility piping consists of compressed air, compressed nitrogen gas, compressed helium gas and cooling water supply and return lines. The compressed air system is used for the actuation of valves located on the cryogenic valve head of the helium cell tank as well as for powering small hand tools during construction and modification of the experimental systems. The compressed nitrogen gas and compressed helium gas lines are provided for purging and general utility use. The cooling water supply and return lines are provided for cooling auxiliary equipment such as vacuum pumps and lasers. It is assumed that each of these utilities is drawn from an existing system at the host facility and that the volume requirements will be an insignificant portion of that installed capacity. It is also assumed that the installed capacities for each of these utilities is sufficiently dry and clean for the proposed service without the addition of drying or filtering equipment. All materials are to be provided and installed by the contractor. The cost is estimated by the linear length of line being run.

F.2.6.2.1.1 Compressed air

F.2.6.2.1.2 Compressed nitrogen gas

F.2.6.2.1.3 Compressed helium gas

F.2.6.2.1.4 Cooling water supply and return

F.2.6.2.1.5 propane supply

Intended for operation of space heaters in a doghouse on top of the vessel.

F.2.6.2.2 Communications system

F.2.6.2.3 HVAC equipment

It is assumed that 220V 40 A power is available from the host facility for the operation of these units. The ventilation and air conditioning system is assumed to be purchased as a packaged system. Installation, which includes mounting and electrical hookup, is assumed to be accomplished by technicians at the host facility.

F.2.6.2.3.1 Cooling and ventilation Unit

The capacity required is estimated to be 3 tons with an air flow rate of 1500 cfm.

F.2.6.2.3.2 Ducting

Ducting is assumed to be flexible, 0.3 m diameter and 20 m in length.

F.2.6.2.4 AC power

AC utility power is required at all times immediately following the erection of the vessel at the site. Peak demand occurs during installation and modification or maintenance of the experimental systems inside the vessel. Uses include operating hand tools and welding machinery, ventilation and air conditioning systems and lighting inside the vessel. During operation of the cell utility power requirements are reduced but not eliminated. Uses include, operation of towed objects inside the experimental volume, fans, lasers and vacuum pumps. Three 220 V circuits are estimated to be required one 60 A, two 40 A. Three 110 V circuits are estimated to be required each 20 A. The distance from point of

use to point of supply is approximately 75 m. Four of the circuits will be required at the platform level of the tank and two at the base.

F.2.6.3 Install ventilation system

Includes technician time required to install HVAC system.

F.2.7 Site Work (Foundation)

The foundation is required to support the vessel and is assumed to be composed of four piers drilled to competent material. It is further assumed that the existing concrete slab will have to be cored or saw cut and demolished to allow for the drilling of the piers. Design of the piers is based on a total vessel weight of 136,000 kg, diameter of 7 m, and height of 20 m. The vessel is assumed to be placed adjacent (within 3 m) to the refrigeration building on the west side and is not anchored to the building in any manner.

F.2.7.1 Design, review, and specify

Includes the engineering, drafting and management hours required to specify the foundation.

F.2.7.2 Procure

Includes the engineering and management hours required to solicit, review and arrange approval of bids and contracts. Also includes the management hours required to coordinate and supervise contract for:

F.2.7.2.1 Installation of piers by Vendor

The complete job of installing the piers, including materials to be supplied, is assumed to be accomplished by a contractor. The system is costed by pier. The vendors costs for design, review, materials, etc. are assumed to be included in the unit price of each item.

F.2.7.2.1.1 Piers

Four piers are assumed and are estimated to be 0.5 m diameter with a 1 m x 1 m slab patch where the piers are placed through the existing slab. Each Pier is assumed to be drilled to a depth of 5 m (depth of competent material for this site) and reinforced with approximately 60 kg of reinforcing steel.

F.3 Electrical systems

F.3.1 AC power

F.3.1.1 Design, review, and specify

Engineering time required to design and review the data acquisition system. This includes specifying the number of channels, the necessary electronics, the amount of cable, and computing requirements.

F.3.1.2 Procure and take delivery

Includes the engineering and management hours required to solicit, review and select vendors and contractors for:

F.3.1.2.1 Power conditioning equipment

Two, 7.5 kVA power conditioners to supply the data acquisition and control systems.

F.3.1.2.2 Cable

F.3.1.2.3 Cable trays

One for AC power and one for signal cabling.

F.3.1.2.4 Installation contract

F.3.1.2.5 Miscellaneous materials and supplies

F.3.1.3 Checkout

F.3.2 Cryogenic supply controls

F.3.2.1 Design, review, and specify

Engineering time required to design and review a control scheme for the cryogenic supply system valves. The refrigerator control system for the N15 refrigerators is easily expanded to accommodate the convection cell, so that minimal equipment is required.

F.3.2.2 Purchase

Includes the engineering and management hours required to solicit, review and select vendors for:

F.3.2.2.1 Programmable logic controller (PLC)

This includes a crate with power supply and room for 16 Input/Output (I/O) cards.

F.3.2.2.2 Network card

Communicates with the existing Tistar control system.

F.3.2.2.3 Analog I/O cards

Combined input/output cards for control of continuously variable PID valves.

F.3.2.2.4 Digital input cards

Thirty-two channel input card for controlling remote on/off valves.

F.3.2.2.5 Digital output cards

Sixteen channel output card for controlling remote on/off valves.

F.3.2.2.6 Cabling

Multi-wire cables with twisted, shielded, pairs of #18 copper wire for cabling runs from valves to the PLC and from the PLC to the control room. (Six wires per valve)

F.3.2.3 Install

Includes the management and engineering time required to install the system.

F.3.2.4 Program

Includes engineering time to program PLC and write a page for the refrigerator controls.

F.3.2.5 Checkout and debug

Includes technician time to checkout all instrumentation and each control channel.

F.3.3 Data Acquisition System

F.3.3.1 Design, review, and specify

Engineering time required to design and review the data acquisition system. This includes specifying the number of channels, the necessary electronics, the amount of cable, and computing requirements.

F.3.3.2 Purchase

Includes the engineering and management hours required to solicit, review and select vendors for:

F.3.3.2.1 Instrumentation rack

F.3.3.2.2 Data acquisition channels

Includes VMS crate with power supply, and four 16 channel scanners with 16 bit resolution and built in current sources.

F.3.3.2.3 Computer

For data acquisition and analysis. Includes necessary interfaces and data acquisition cards, together with 1 Gbite hard drive, printer, and software.

F.3.3.2.4 Cables and hermetic connectors

Includes two twisted pairs of #36 phosphor bronze wire per sensor, for in-vessel cabling, and multi-wire cables with twisted, shielded, pairs of #18 copper wire for cabling runs to the control room. Also includes hermetic connectors, the time required to terminate all cables, install cables in trays, and install cables in the vessel.

F.3.3.2.5 Sensors

development of velocity sensors is part of the proposed program. The sensors themselves are expected to be a small part of the total data acquisition cost, and are to be provided by the universities.

F.3.3.3 Install

Includes engineering and technical time required to install the system.

F.3.3.4 Program

It is expected that much of the software development for data acquisition will be done at the University of Oregon in the 1 meter cell. Thus 1/2 man-year of time is included here for purposes of modifying the Oregon software to meet the needs of the 10 meter cell.

F.3.3.5 Checkout and debug

Includes technician time to checkout all instrumentation and each data acquisition channel.

F.3.4 Plate controls and heaters

Experimental requirements include controlling the temperature of the top plate to $\pm 1\%$ of the temperature difference between top and bottom plates. The bottom plate requires constant heat flux to within $\pm 1\%$. To achieve these requirements, each plate is divided thermally into approximately 30 sectors. Each sector contains two germanium thermometers and a heater. The top plate also contains cooling tubes to improve thermal control (see Appendix D).

F.3.4.1 Design, review, and specify

Engineering time required to design and review control schemes for the both plates.

F.3.4.2 Purchase

Includes the engineering and management hours required to solicit, review and select vendors for:

F.3.4.2.1 Germanium thermometers

Includes the cost of calibration and technical time to install in the plates.

F.3.4.2.2 Heaters

Includes cost of heaters and technical time for installation.

F.3.4.2.3 Power supplies

Includes the cost of power supplies and technical time for installation.

F.3.4.2.4 Cabling and hermetic connectors

Includes the cost of 4-wire twisted pairs for in-vessel cabling to thermometers, two wire pairs of copper wire to the heaters, multi-wire shielded, twisted-pair, cable for runs to the control room and all necessary hermetic connectors. Also included is the technical time necessary to terminate and install all cables.

F.3.4.2.5 Control channels

Includes 16 eight-channel, control cards with crate, power supply, and PLC. Also includes technical time to install.

F.3.4.2.6 Computer interface

Network card and bus necessary to interface control crate with data acquisition computer, or refrigeration controls.

F.3.4.3 Install

Includes engineering and technical time required to install the system.

F.3.4.4 Program

Includes engineering time to program controls.

F.3.4.5 Checkout and debug

Includes technician time to checkout all instrumentation and each control channel.

F.4 Operations

F.4.1 Operate towed grid

This includes a set of experiments to be performed over a six month period in the 10 meter cell, in which an aluminum grid is accelerated to a constant velocity of 2.4 m/s, after which the decay of turbulence is observed.

F.4.1.1 Prepare operating procedure

Includes time spent by scientists, research associates and engineers, preparing a detailed procedure for carrying out the proposed experiments.

F.4.1.2 Perform experiments

Includes time to perform experiments, collect and analyze data, and adjust operating procedures appropriately.

F.4.2 Operate convection cell

Includes the set of convection experiments to be performed in the 10 meter cell during the fifth year of the program.

F.4.2.1 Prepare operating procedure

Includes time spent by scientists, research associates and engineers, preparing a detailed procedure for carrying out the proposed experiments.

F.4.2.2 Commission plates

Includes the time required to test and debug the upper plate control system and become familiar with the operation of the plate system as a whole.

F.4.2.3 Perform experiments

Includes time to perform experiments, collect and analyze data, and adjust operating procedures appropriately.

Appendix G - Government Furnished Equipment

In response a request from the Department of Energy, Department of the SSC, the attached list of SSCL personal property needed for the Helium Convection Experiment was submitted on September 19, 1994. The equipment on this list falls into several categories which are discussed below:

- 1) Vacuum pumping and leak detection systems needed in order to install, commission and operate the convection cell and its associated vacuum insulated equipment.
- 2) Gas purity measuring equipment forming a system for the monitoring and control of the purity of the helium contents of the convection cell.
- 3) Handling equipment for the trial assembly, the installation, and the final alignment of the copper plates that form the top and bottom of the convection cell. Adjustments of these plates to flatness and level requirements within the tank of the cell is a difficult task requiring the use of laser metrology equipment.
- 4) Items for a variety of purposes in the installation and operation of the cell. These include LN Dewars for trap filling, machines for the threading and welding of pipe, and a system for the marking of process lines and equipment according to OSHA requirements.

The things listed here fill necessary functions in carrying out the Convection Experiment, and equipment to fill these functions have not been included in the capital equipment estimate for the program. If the items requested here are not available, equipment of equivalent functionality will have to be added to the budget estimate.

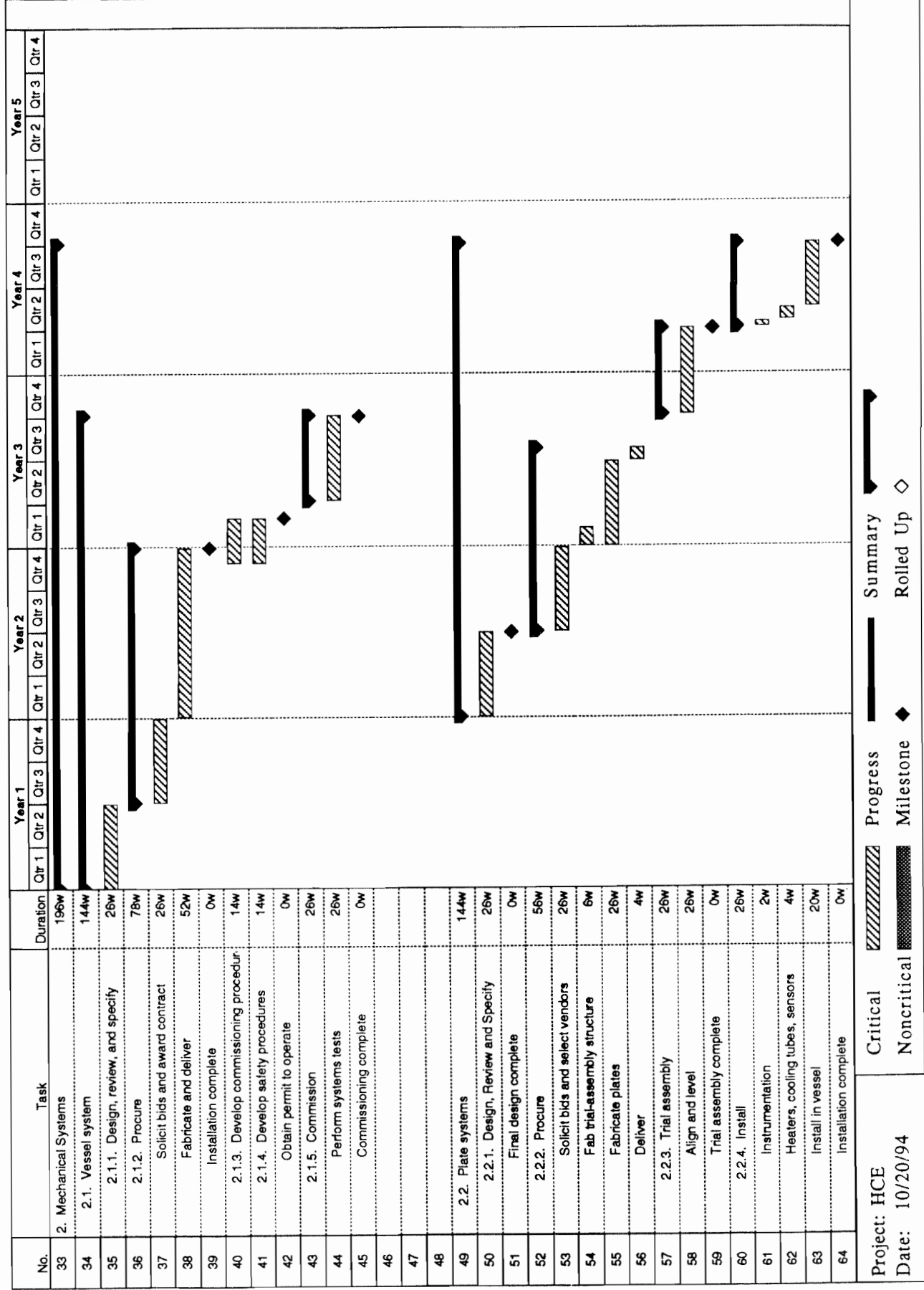
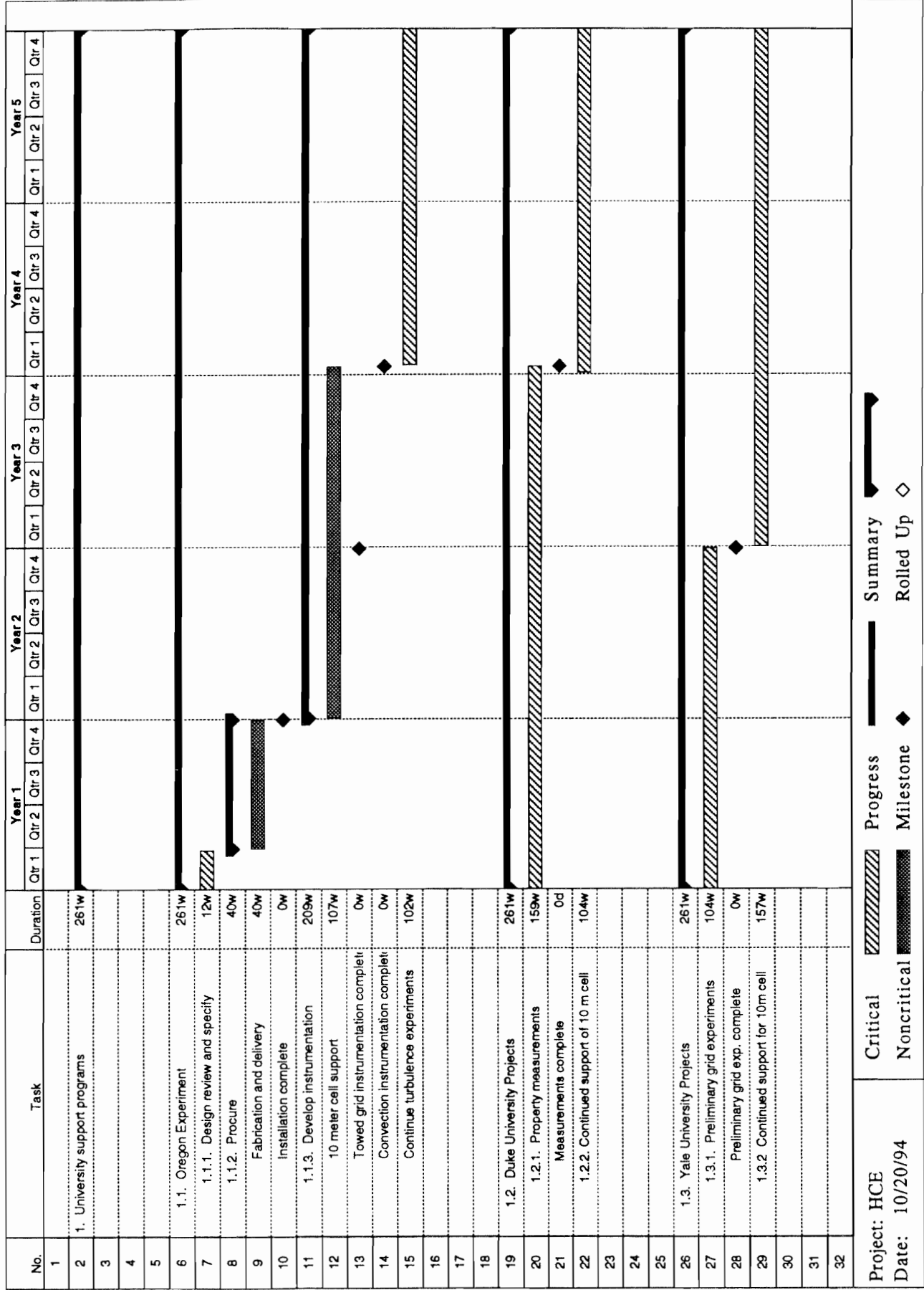
List of SSCL Personal Property Needed for the Helium Convection Experiment

September 16, 1994

Manufacturer name	Common name	Property number
Lincoln	Tig arc welder	0032507
Leybold	Rotary valve pump	0101593
Leybold	Rotary valve pump	0101616
Leybold	Rotary valve pump	0101654
Leybold	Mechanical root pump	0103016
Leybold	Mechanical root pump	0103030
Turbo Torr	Turbo molecular pump	0122345
Granville	Vacuum gage controller	0110533
Meeco	Moisture analyzer	0119390
Veeco Inst.	Leak detector	0124530
Veeco Inst.	Leak detector	0137905
Alcatel	Portable leak detector	0541580
Spectra	Gas analyzer	0137103
Hyster	Forklift	0185784
JLG	Sizzor lift	0188907
Varian	Leak detector(1 of 2)	0175679
	Pump trailer in tank farm	0160682
Veeco	LD (in trailer)	0106833
	Blower pump (in trailer)	0160620
	Gas analyzer (in trailer)	0188815
Sycrowave	Model 250 Welding Machine	0056558
Ridgid	Pipe thread machine	0163157
Brady	Labelizer	0182943
Spectra	Multi-Quad RGA	0137103
Spectra	VacScan Plus (Leda-Mass)	0129887
	Bottom pumping unit for Leda-Mass	0111714
	180 Liter Nitrogen Dewars	0160477
		0160484
		0160507
	220 Liter Nitrogen Dewars	0162082
		0162099
Renishaw	ML 10 Laser Head	0103139
Renishaw	PHC 10 Controller Probe Head	0127265
Renishaw	A 80003 0665 Squareness Optic	0152625
Renishaw	A 80003 0444 Straightness Optic Long	0152632
Renishaw	A 80003 0445 Straightness Optic Acc Kit	0152649
Renishaw	A 80003 0443 Straightness Optic Short	0152656
Renishaw	PH9A Head Probe	0522459

Appendix H - Detailed Schedule

The following schedule is representative of the timing required to complete the Cryogenic Helium Gas Convection Research in five years. It is consistent with the manpower estimates contained in the budget, as well as, those contained in the detailed cost sheets presented in Appendix I. Numbered tasks agree with the WBS, and are defined in the WBS dictionary, Appendix F. The university support programs are included with milestones indicating the timing for completion of sensor development, property measurement, and preliminary experimental work. While every attempt has been made to present a reasonably complete list of tasks and schedule them in a sensible way, no optimization has been performed.

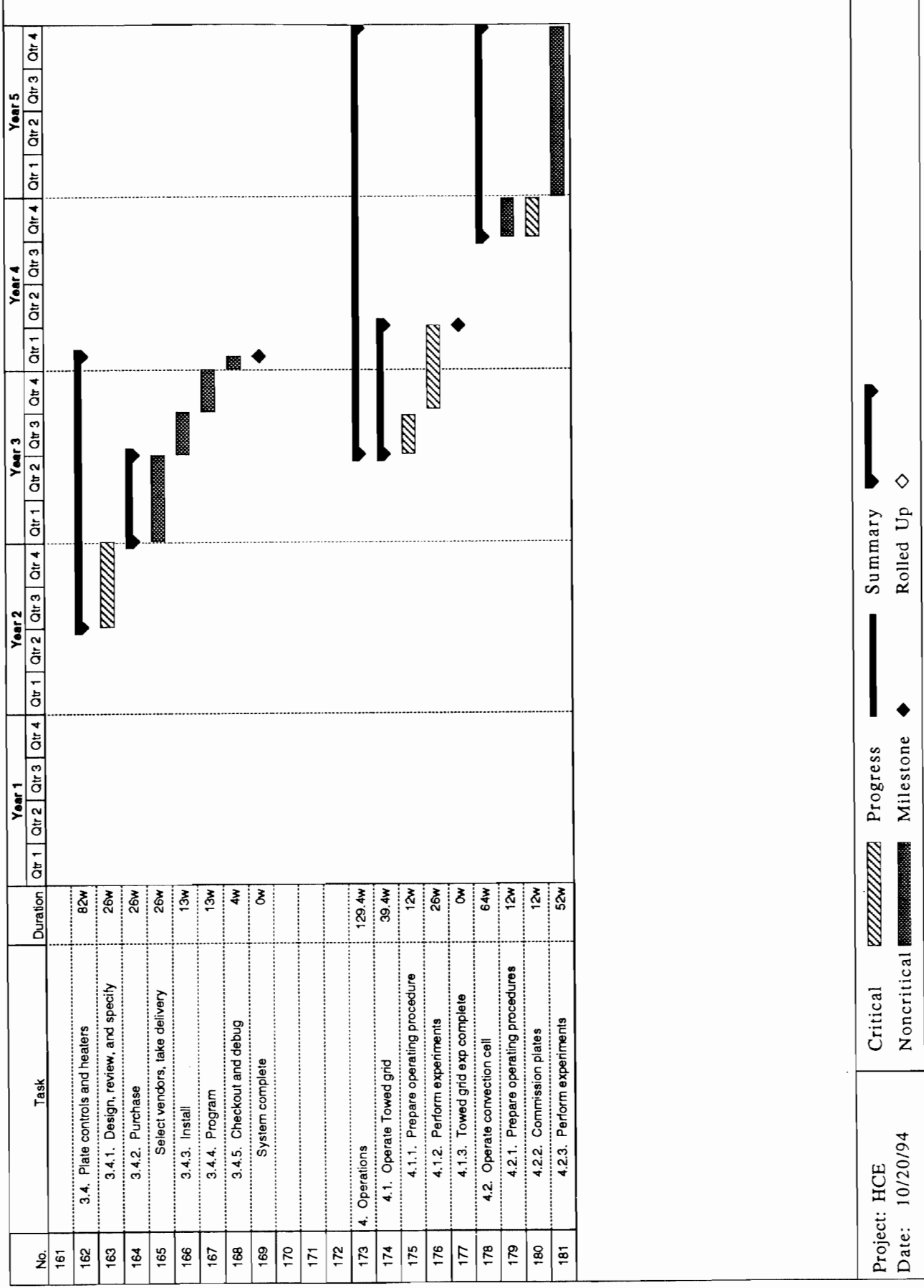
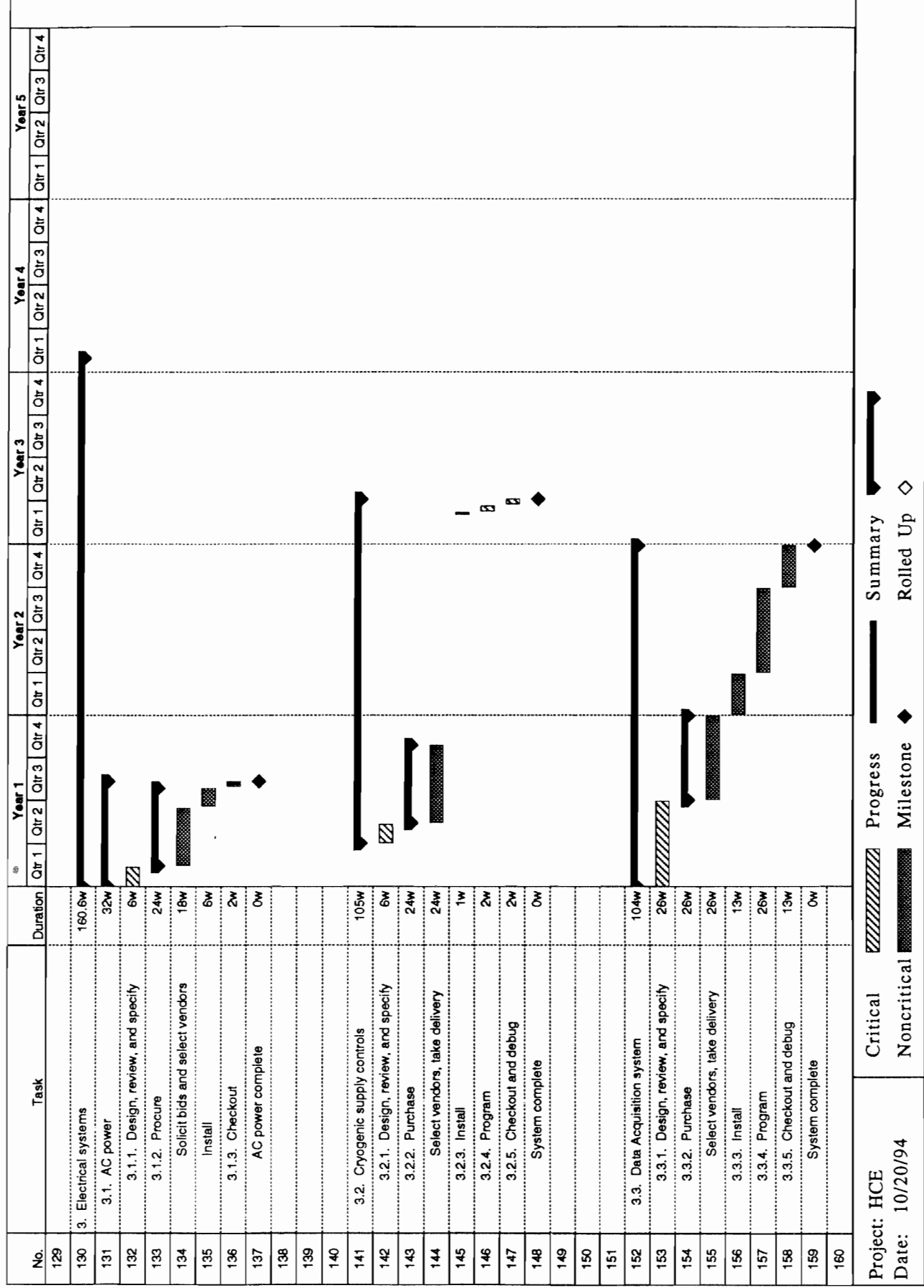


No.	Task	Duration	Year 1				Year 2				Year 3				Year 4				Year 5			
			Qtr 1	Qtr 2	Qtr 3	Qtr 4	Qtr 1	Qtr 2	Qtr 3	Qtr 4	Qtr 1	Qtr 2	Qtr 3	Qtr 4	Qtr 1	Qtr 2	Qtr 3	Qtr 4	Qtr 1	Qtr 2	Qtr 3	Qtr 4
65																						
66																						
67																						
68	2.3 Cryogenic supply system	100w																				
69	2.3.1. Design, review, and specify	6w																				
70	Final design complete	0w																				
71	2.3.2. Purchase piping	34w																				
72	Solicit bids and select vendor	18w																				
73	Fabricate	12w																				
74	Deliver	4w																				
75	2.3.3. Install	9w																				
76	Field assembly	9w																				
77	2.3.4. Test	2w																				
78	Installation and test complete	0w																				
79																						
80																						
81																						
82																						
83																						
84	2.4. Vacuum systems	97w																				
85	2.4.1. Design, review, and specify	6w																				
86	Final design complete	0w																				
87	2.4.2. Purchase equipment	18w																				
88	Select vendors, take delivery	18w																				
89	2.4.3. Install	9w																				
90	Complete installation	9w																				
91	2.4.4. Test	2w																				
92	Installation and test complete	0w																				
93																						
94																						
95																						
96																						
Project: HCE			Critical				Progress				Summary											
Date: 10/20/94			Noncritical				Milestone				Rolled Up											

H-4

No.	Task	Duration	Year 1				Year 2				Year 3				Year 4				Year 5			
			Qtr 1	Qtr 2	Qtr 3	Qtr 4	Qtr 1	Qtr 2	Qtr 3	Qtr 4	Qtr 1	Qtr 2	Qtr 3	Qtr 4	Qtr 1	Qtr 2	Qtr 3	Qtr 4	Qtr 1	Qtr 2	Qtr 3	Qtr 4
97	2.5 Auxiliary systems (Grid)	100w																				
98	2.5.1. Design, review, and specify	6w																				
99	Final design complete	0w																				
100	2.5.2. Purchase equipment	28w																				
101	Select vendors, take delivery	24w																				
102	Fabricate grid	12w																				
103	Deliver grid	4w																				
104	2.5.3. Install	7w																				
105	Field assembly	7w																				
106	Installation complete	0w																				
107	2.5.4. Test	2w																				
108	Installation and test complete	0w																				
109																						
110																						
111	2.6. Utilities	46.8w																				
112	2.6.1. Design, review, and specify	6w																				
113	2.6.2. Procure	39.8w																				
114	Solicit bids, award contracts	18w																				
115	Install utility piping	4w																				
116	Install communication equip.	1w																				
117	Install HVAC equip.	3w																				
118	Install ac power	4w																				
119	2.6.3. Installation complete	0w																				
120																						
121																						
122	2.7. Site work	36.4w																				
123	2.7.1. Design, review, and specify	4w																				
124	Final design complete	0w																				
125	2.7.2. Procure	32.4w																				
126	Solicit bids and select vendors	12w																				
127	foundation installation	4w																				
128	Installation complete	0w																				
Project: HCE			Critical				Progress				Summary											
Date: 10/20/94			Noncritical				Milestone				Rolled Up											

H-5



Appendix I - Detailed Cost Sheets

In the following appendix, each task in the WBS is shown as a line item in spreadsheet format, for purposes of estimating capital equipment costs and labor costs. Labor requirements for each task, and quantity and unit price for equipment are provided for each line item. All items from WBS elements (2) and (3) are included. In addition, operating costs and labor requirements associated with WBS (4) are included. Materials and supplies, travel expenses, contingency, and overhead are not included, but are estimated at a higher level and accounted for in the budget. University costs, however, as reported in Section 4, are not included here.

WBS No.	Item or activity Description	Unit	Qty	Cost ea. (k\$)	Eng (MW)	Sci (MW)	Post doc (MW)	Tec/Dft (MW)	Admin (MW)	Basis of estimate
2	Mechanical systems									
2.1.	Vessel system									
2.1.1.	Design review and specify				64	12	16	8	8	
2.1.2.	Procure				32	12	8		8	
2.1.2.1.	Design and review		1	100						Professional consultant
2.1.2.2.	Fabricate, and deliver		1	1150	2	12			7	Professional consultant
2.1.3.	Develop Commission procedure				5	2	3		3	
2.1.4.	Develop safety procedure				5	3			3	
2.1.5.	Commission				26	15	28		9	
2.2.	Plate Systems									
2.2.1.	Design review and specify				24	5	8	13	2	
2.2.2.	Procure				13	4	7	4	7	
2.2.2.1.	Fabrication and delivery of Plates									
2.2.2.1.1	Design		1	19						Professional consultant
2.2.2.1.2	Raw material and parts		1	200						Professional consultant
2.2.2.1.4	Machining		1	120						Professional consultant
2.2.2.1.3	Installation equip.		1	75						
2.2.3.	Perform trial assembly				8	4	16	78		
2.2.4.	Install				13	7	13	78		
2.3.	Cryogenic Supply System									
2.3.1.	Design review and specify				6	2	2	1	1	
2.3.2.	Purchase piping				3	1	1		1	
2.3.2.1.	Vacuum-jacketed line	sys	1	85						Quote
2.3.2.2.	Warm Helium Return Line		1	0.5						Engineering judgment
2.3.3.	Install		1	25	3					Engineering judgment
2.3.4.	Test									
2.4.	Vacuum System									
2.4.1.	Design review and specify				3	1	1	1		
2.4.2.	Purchase equipment				2				1	
2.4.2.1.	Inventory control pump	ea	1	13						Vendor catalog
2.4.2.2.	Gate valves	ea	2	1.5						Vendor catalog

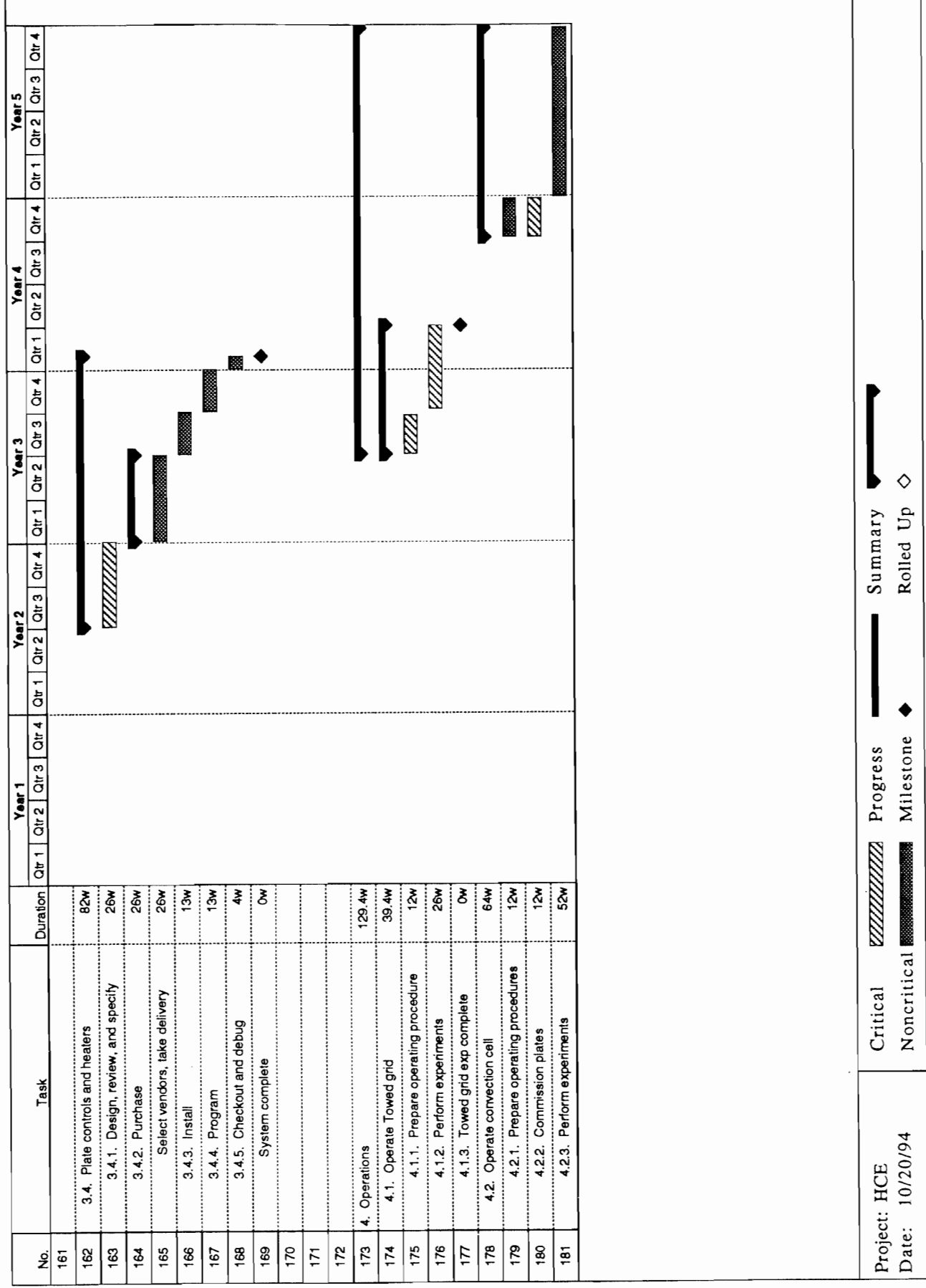
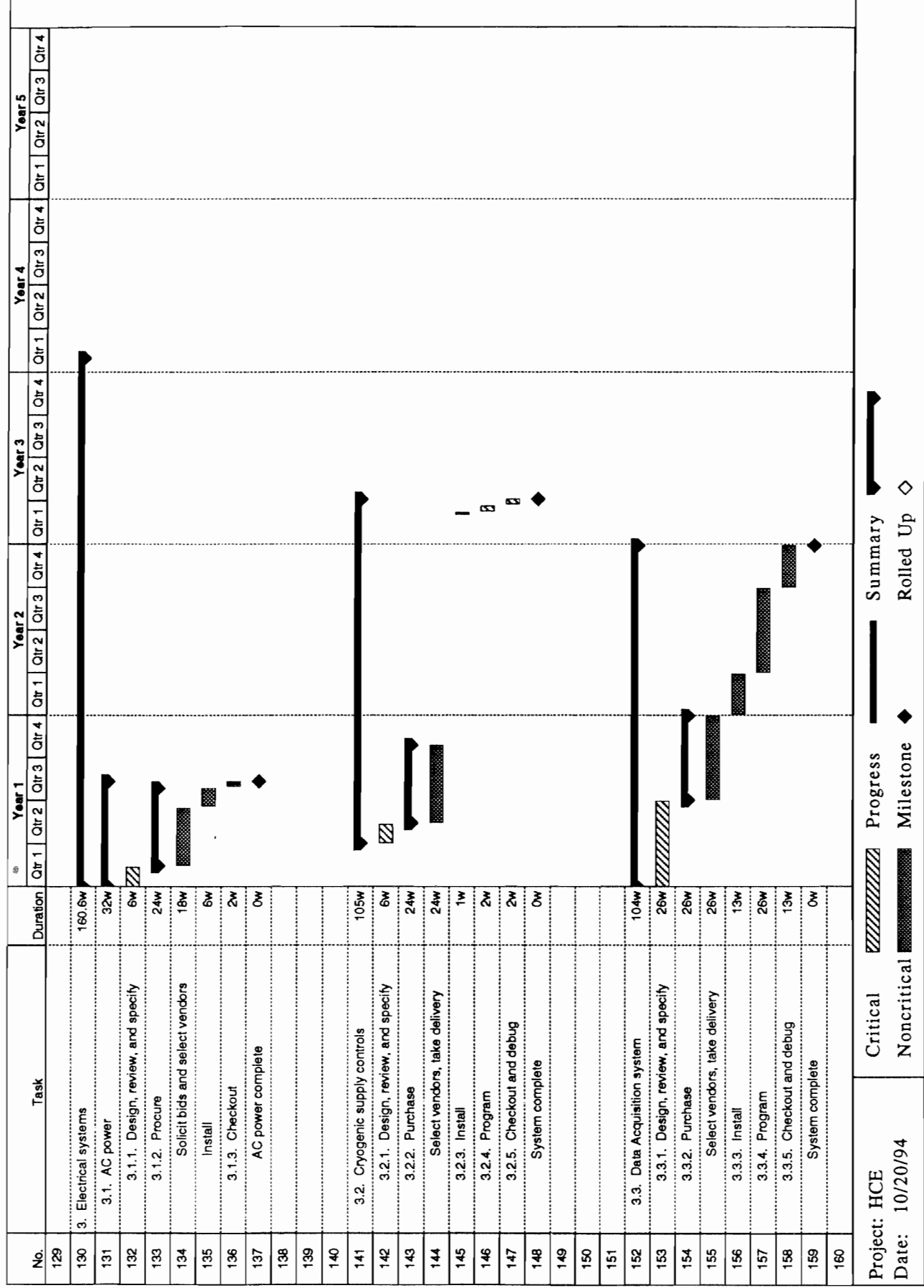
WBS No.	Item or activity Description	Unit	Qty	Cost ea. (k\$)	Eng (MW)	Sci (MW)	Post doc (MW)	Tec/Dft (MW)	Admin (MW)	Basis of estimate
2.4.2.3.	Exhaust valves	ea	2	0.2						Vendor catalog
2.4.2.4.	Coalescer	ea	1	2.5						Vendor catalog
2.4.2.5.	Turbo-Pump	ea	1	15						Vendor catalog
2.4.2.6.	Fore pump	ea	1	6						Vendor catalog
2.4.3.	Install					2	4	12		
2.4.4.	Test						2	2		
2.5.	Towed Grid System									
2.5.1.	Design review and specify				6	2	2	1	1	
2.5.2.	Purchase equipment				3	1	1		1	
2.5.2.1	Engineering		1	11.2						
2.5.2.2	Raw materials and parts		1	11.8						
2.5.2.3	Fabrication		1	45						
2.5.3.	Install					2	4	14		
2.5.4.	Test						2	2		
2.6.	Utility Systems									
2.6.1.	Design, review, and specify				1	1		2		
2.6.2.	Procure				1	1			1	
2.6.2.1.	Utility Piping	sys	1	20						Estimate
2.6.2.2.	Communications system	sys	1	2						Estimate
2.6.2.3.	HVAC equipment	sys	1	7						Cat. & Eng. judgment
2.6.2.4.	AC power	sys	1	16						Means Electrical Cost Da
2.6.3.	Install ventilation system				1	3		5		
2.7.	Site Work (Foundation)									
2.7.1.	Design review and specify				1	2		1		
2.7.2.	Procure				1	0.5				
2.7.2.1.	Installation of plers by Vendor	pler	4	2.5	1	0.2				Professional consultant
	Totals			1937.4	224	94.7	118	222	53	

WBS No.	Item or activity Description	Unit	Qty	Cost ea. k\$	Eng (MW)	Sci (MW)	Post doc (MW)	Tec/Dft (MW)	Admin (MW)	Basis of estimate
3	Electrical systems									
3.1	AC power									
3.1.1	Design, review, and specify				3	1		1	1	
3.1.2	Procure and take delivery				2	0.2			1	
3.1.2.1	Power conditioning equipment	ea	2	3.6						Sola PN23-28-275-6
3.1.2.2	Cable		1	0.2						Quote
3.1.2.3	Cable trays		1	3						Graybar quote
3.1.2.4	Installation contract		1	3						Engineering judgment
3.1.3	Checkout				1			1		
3.2	Cryogenic supply controls									
3.2.1	Design, review, and specify				3	1	1	1	1	
3.2.2	Purchase				2	1	2		1	
3.2.2.1	PLC	ea	1	2						Engineering judgment
3.2.2.2	Network card	ea	1	1						Catalog
3.2.2.3	Analog I/O cards	ea	3	1.5						Engineering judgment
3.2.2.4	Digital input cards	ea	1	1						Engineering judgment
3.2.2.5	Digital output cards	ea	1	1.2						Engineering judgment
3.2.2.6	Cabling and misc.		1	1						Engineering judgment
3.2.3	Install				1	1	3	8		
3.2.4	Program				2		2			
3.2.5	Checkout and debug				1		1	2		
3.3	Data Acquisition System									
3.3.1	Design, review, and specify				48	12	12	6	6	
3.3.2	Purchase				24	12	6	3	3	
3.3.2.1	Instrumentation rack	ea	2	0.3						Engineering judgment
3.3.2.2	Data acquisition channels	ea	64	0.5						Engineering judgment
3.3.2.3	Computer & peripherals		1	15						Engineering judgment

WBS No.	Item or activity Description	Unit	Qty	Cost ea. k\$	Eng (MW)	Sci (MW)	Post doc (MW)	Tec/Dft (MW)	Admin (MW)	Basis of estimate
3.3.2.4	Cables and hermetic connectors		1	10						Lakeshore quote
3.3.2.5	LDV system	ea	1	300						
3.3.2.7.	UPS (3kVA)	ea	1	1.5						Engineering judgment
3.3.2.6.	Laboratory equip		1	75						
3.3.3	Install				12	1	6	24		
3.3.4	Program				12	2	12		3	
3.3.5	Checkout and debug				12	1	12	24		
3.4	Plate controls and heaters									
3.4.1	Design, review, and specify				24	5	8	4	3	
3.4.2	Purchase				12	10			9	
3.4.2.1	Germanium thermometers	ea	125	0.42						Lakeshore quote
3.4.2.2	Heaters		1	6.25						Minco quote
3.4.2.3	Power supplies	ea	60	2						Catalog (Hewlett Pac)
3.4.2.4	Cabling and hermetic connectors		1	18						Lakeshore quote
3.4.2.5	Control channels	ea	120	0.5						Engineering judgment
3.4.2.6	Computer interface	ea	1	1						Engineering judgment
3.4.3	Install				2		4	12		
3.4.4	Program				6		8			
3.4.5	Checkout and debug				4		4	4		
	Totals			716	171	47.2	81	90	28	

WBS No.	Item or activity Description	Unit	Qty	Cost ea. k\$	Eng (MW)	Sci (MW)	Post doc (MW)	Tec/Dft (MW)	Admin (MW)	Basis of estimate
4	Operations									
4.1	Operate towed grid									
4.1.1.	Prepare operating procedure				2	4	10			
4.1.2.	Perform experiments			325	19	19	39	26	10	Engineering judgment
4.2	Operate convection cell									
4.2.1.	Prepare operating procedure				6	4	13			
4.2.2.	Commission plates				7	4	13			
4.2.3.	Perform experiments				13	50	200	50	25	Engineering judgment
				750						
	Totals			1075	47	81	275	76	35	

Appendix J Capabilities Fact Sheet



Appendix I - Detailed Cost Sheets

In the following appendix, each task in the WBS is shown as a line item in spreadsheet format, for purposes of estimating capital equipment costs and labor costs. Labor requirements for each task, and quantity and unit price for equipment are provided for each line item. All items from WBS elements (2) and (3) are included. In addition, operating costs and labor requirements associated with WBS (4) are included. Materials and supplies, travel expenses, contingency, and overhead are not included, but are estimated at a higher level and accounted for in the budget. University costs, however, as reported in Section 4, are not included here.

WBS No.	Item or activity Description	Unit	Qty	Cost ea. (k\$)	Eng (MW)	Sci (MW)	Post doc (MW)	Tec/Dft (MW)	Admin (MW)	Basis of estimate
2	Mechanical systems									
2.1.	Vessel system									
2.1.1.	Design review and specify				64	12	16	8	8	
2.1.2.	Procure				32	12	8		8	
2.1.2.1.	Design and review		1	100						Professional consultant
2.1.2.2.	Fabricate, and deliver		1	1150	2	12			7	Professional consultant
2.1.3.	Develop Commission procedure				5	2	3		3	
2.1.4.	Develop safety procedure				5	3			3	
2.1.5.	Commission				26	15	28		9	
2.2.	Plate Systems									
2.2.1.	Design review and specify				24	5	8	13	2	
2.2.2.	Procure				13	4	7	4	7	
2.2.2.1.	Fabrication and delivery of Plates									
2.2.2.1.1	Design		1	19						Professional consultant
2.2.2.1.2	Raw material and parts		1	200						Professional consultant
2.2.2.1.4	Machining		1	120						Professional consultant
2.2.2.1.3	Installation equip.		1	75						
2.2.3.	Perform trial assembly				8	4	16	78		
2.2.4.	Install				13	7	13	78		
2.3.	Cryogenic Supply System									
2.3.1.	Design review and specify				6	2	2	1	1	
2.3.2.	Purchase piping				3	1	1		1	
2.3.2.1.	Vacuum-jacketed line	sys	1	85						Quote
2.3.2.2.	Warm Helium Return Line		1	0.5						Engineering judgment
2.3.3.	Install		1	25	3					Engineering judgment
2.3.4.	Test									
2.4.	Vacuum System									
2.4.1.	Design review and specify				3	1	1	1		
2.4.2.	Purchase equipment				2				1	
2.4.2.1.	Inventory control pump	ea	1	13						Vendor catalog
2.4.2.2.	Gate valves	ea	2	1.5						Vendor catalog

WBS No.	Item or activity Description	Unit	Qty	Cost ea. (k\$)	Eng (MW)	Sci (MW)	Post doc (MW)	Tec/Dft (MW)	Admin (MW)	Basis of estimate
2.4.2.3.	Exhaust valves	ea	2	0.2						Vendor catalog
2.4.2.4.	Coalescer	ea	1	2.5						Vendor catalog
2.4.2.5.	Turbo-Pump	ea	1	15						Vendor catalog
2.4.2.6.	Fore pump	ea	1	6						Vendor catalog
2.4.3.	Install					2	4	12		
2.4.4.	Test						2	2		
2.5.	Towed Grid System									
2.5.1.	Design review and specify				6	2	2	1	1	
2.5.2.	Purchase equipment				3	1	1		1	
2.5.2.1	Engineering		1	11.2						
2.5.2.2	Raw materials and parts		1	11.8						
2.5.2.3	Fabrication		1	45						
2.5.3.	Install					2	4	14		
2.5.4.	Test						2	2		
2.6.	Utility Systems									
2.6.1.	Design, review, and specify				1	1		2		
2.6.2.	Procure				1	1			1	
2.6.2.1.	Utility Piping	sys	1	20						Estimate
2.6.2.2.	Communications system	sys	1	2						Estimate
2.6.2.3.	HVAC equipment	sys	1	7						Cat. & Eng. judgment
2.6.2.4.	AC power	sys	1	16						Means Electrical Cost Da
2.6.3.	Install ventilation system				1	3		5		
2.7.	Site Work (Foundation)									
2.7.1.	Design review and specify				1	2		1		
2.7.2.	Procure				1	0.5				
2.7.2.1.	Installation of plers by Vendor	pler	4	2.5	1	0.2				Professional consultant
	Totals			1937.4	224	94.7	118	222	53	

WBS No.	Item or activity Description	Unit	Qty	Cost ea. k\$	Eng (MW)	Sci (MW)	Post doc (MW)	Tec/Dft (MW)	Admin (MW)	Basis of estimate
3	Electrical systems									
3.1	AC power									
3.1.1	Design, review, and specify				3	1		1	1	
3.1.2	Procure and take delivery				2	0.2			1	
3.1.2.1	Power conditioning equipment	ea	2	3.6						Sola PN23-28-275-6
3.1.2.2	Cable		1	0.2						Quote
3.1.2.3	Cable trays		1	3						Graybar quote
3.1.2.4	Installation contract		1	3						Engineering judgment
3.1.3	Checkout				1			1		
3.2	Cryogenic supply controls									
3.2.1	Design, review, and specify				3	1	1	1	1	
3.2.2	Purchase				2	1	2		1	
3.2.2.1	PLC	ea	1	2						Engineering judgment
3.2.2.2	Network card	ea	1	1						Catalog
3.2.2.3	Analog I/O cards	ea	3	1.5						Engineering judgment
3.2.2.4	Digital input cards	ea	1	1						Engineering judgment
3.2.2.5	Digital output cards	ea	1	1.2						Engineering judgment
3.2.2.6	Cabling and misc.		1	1						Engineering judgment
3.2.3	Install				1	1	3	8		
3.2.4	Program				2		2			
3.2.5	Checkout and debug				1		1	2		
3.3	Data Acquisition System									
3.3.1	Design, review, and specify				48	12	12	6	6	
3.3.2	Purchase				24	12	6	3	3	
3.3.2.1	Instrumentation rack	ea	2	0.3						Engineering judgment
3.3.2.2	Data acquisition channels	ea	64	0.5						Engineering judgment
3.3.2.3	Computer & peripherals		1	15						Engineering judgment

WBS No.	Item or activity Description	Unit	Qty	Cost ea. k\$	Eng (MW)	Sci (MW)	Post doc (MW)	Tec/Dft (MW)	Admin (MW)	Basis of estimate
3.3.2.4	Cables and hermetic connectors		1	10						Lakeshore quote
3.3.2.5	LDV system	ea	1	300						
3.3.2.7.	UPS (3kVA)	ea	1	1.5						Engineering judgment
3.3.2.6.	Laboratory equip		1	75						
3.3.3	Install				12	1	6	24		
3.3.4	Program				12	2	12		3	
3.3.5	Checkout and debug				12	1	12	24		
3.4	Plate controls and heaters									
3.4.1	Design, review, and specify				24	5	8	4	3	
3.4.2	Purchase				12	10			9	
3.4.2.1	Germanium thermometers	ea	125	0.42						Lakeshore quote
3.4.2.2	Heaters		1	6.25						Minco quote
3.4.2.3	Power supplies	ea	60	2						Catalog (Hewlett Pac)
3.4.2.4	Cabling and hermetic connectors		1	18						Lakeshore quote
3.4.2.5	Control channels	ea	120	0.5						Engineering judgment
3.4.2.6	Computer interface	ea	1	1						Engineering judgment
3.4.3	Install				2		4	12		
3.4.4	Program				6		8			
3.4.5	Checkout and debug				4		4	4		
	Totals			716	171	47.2	81	90	28	

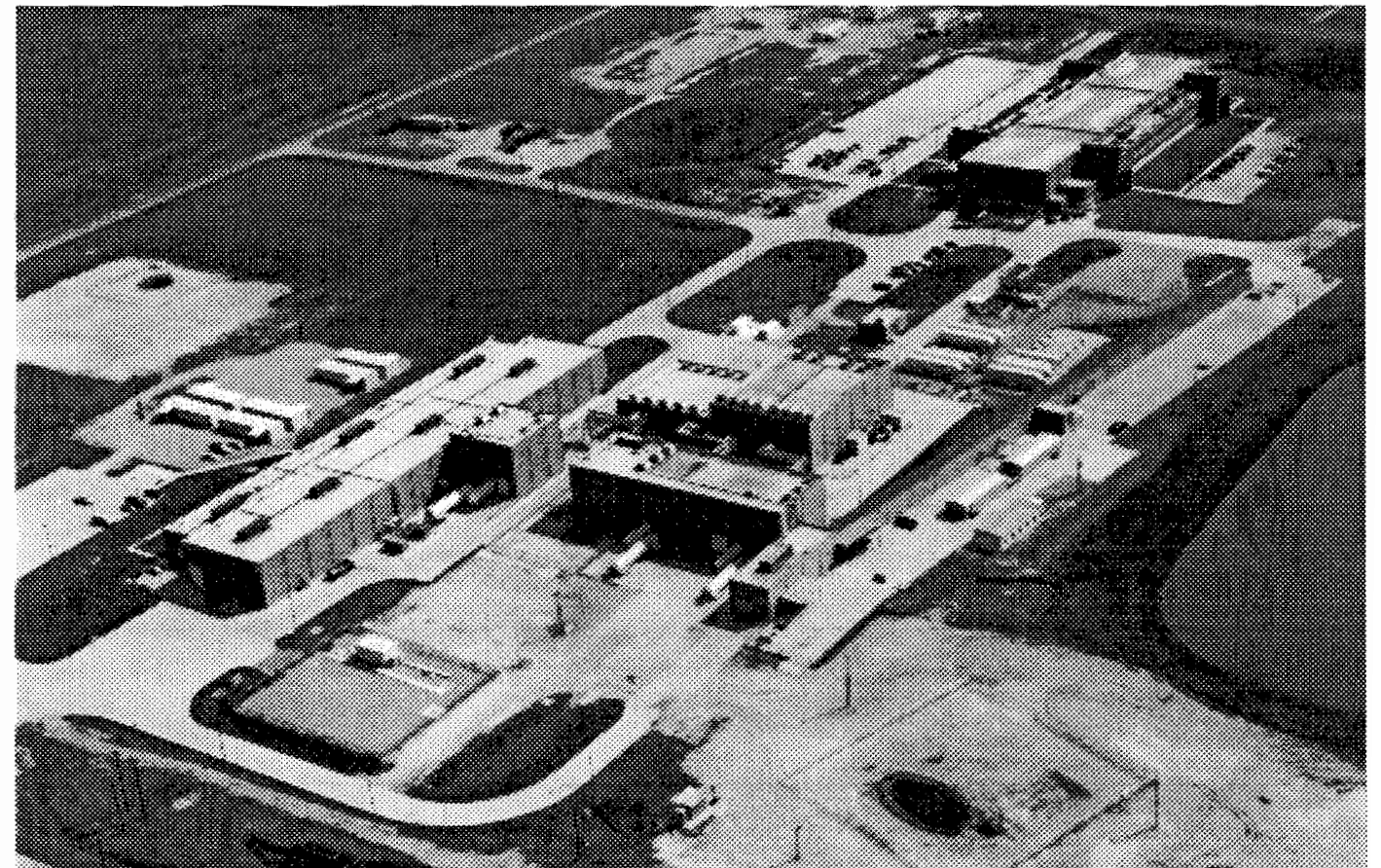
WBS No.	Item or activity Description	Unit	Qty	Cost ea. k\$	Eng (MW)	Sci (MW)	Post doc (MW)	Tec/Dft (MW)	Admin (MW)	Basis of estimate
4	Operations									
4.1	Operate towed grid									
4.1.1.	Prepare operating procedure				2	4	10			
4.1.2.	Perform experiments			325	19	19	39	26	10	Engineering judgment
4.2	Operate convection cell									
4.2.1.	Prepare operating procedure				6	4	13			
4.2.2.	Commission plates				7	4	13			
4.2.3.	Perform experiments				13	50	200	50	25	Engineering judgment
				750						
	Totals			1075	47	81	275	76	35	

Appendix J Capabilities Fact Sheet

Proposed Center for Applied Superconductivity and Cryogenics Technology

.....
Capabilities Fact Sheet

Waxahachie, Texas



Prepared for the Texas National Research Laboratory Commission

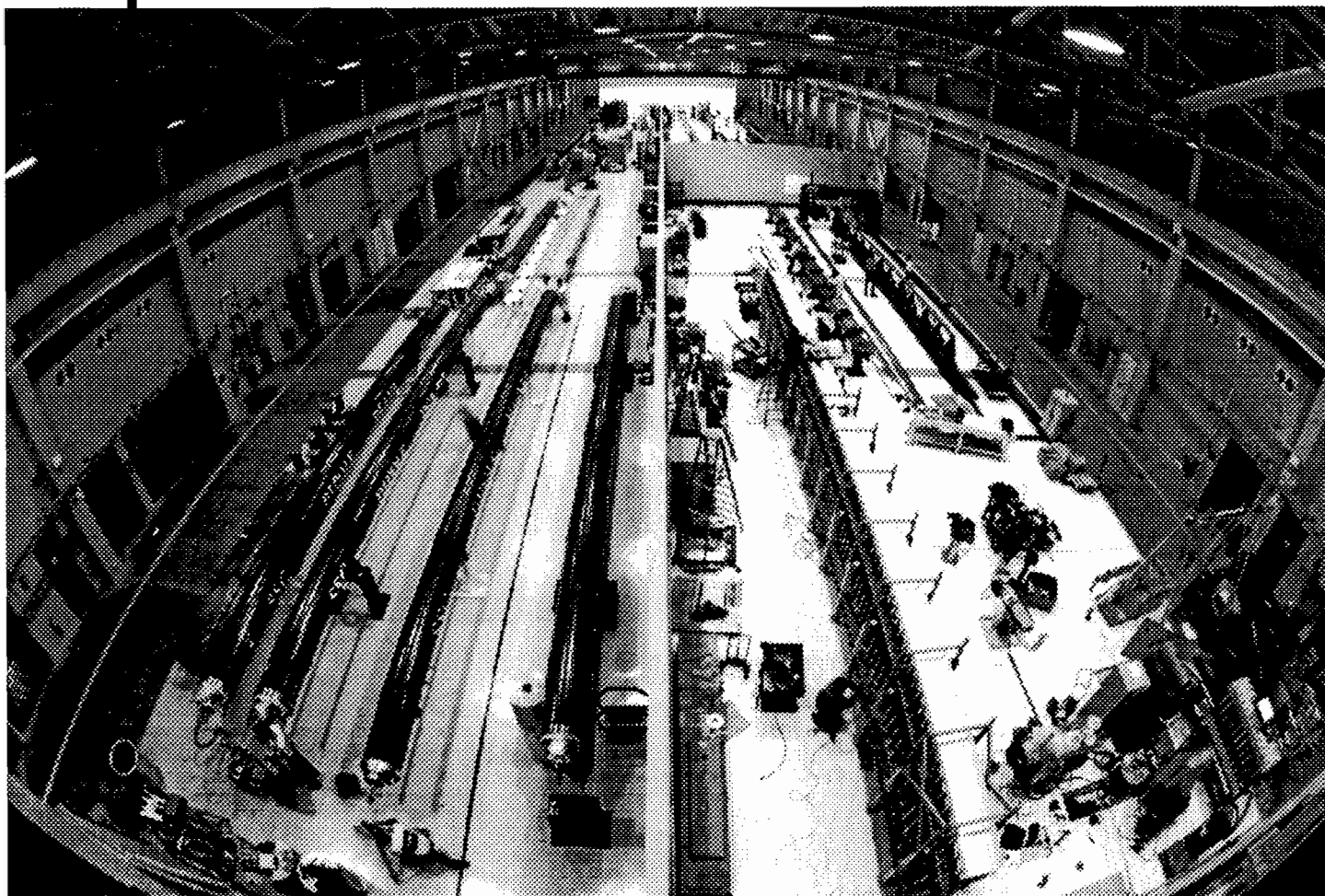
Summary

Since 1986, the United States has spent in excess of \$500M supporting research and development activities in large superconducting magnets and related cryogenics for the Superconducting Super Collider (SSC) project. Over \$300M of this investment has been made in the equipment, facilities, and infrastructure at the SSC Laboratory (SSCL) N15 site. This 100-acre site features a complex of closely-grouped, fully-integrated fabrication, test, and support buildings and three large state-of-the-art cryogenic systems. Major facilities include the Magnet Development Laboratory (MDL), the Magnet Test Laboratory (MTL), and the Accelerator Systems String Test (ASST) buildings.

A team of outstanding technical and scientific personnel remain engaged in superconducting magnet prototype development and testing programs in support of SSC shut-down activities. Technicians and trained operators, including many of the personnel who commissioned and operated the fabrication and test facilities and cryogenic systems, also remain available.

The physical and human assets assembled at the SSCL N15 site represent a national resource that can provide a means for U.S. industry to maintain and extend its international competitiveness in the areas of superconductivity and cryogenics. Many programs based on large-scale applications of these critical technologies have previously been unfeasible due to the large investments required for facilities, infrastructure, and personnel training. Industry, universities, and laboratories now have a unique opportunity to capitalize on the significant investment made in the SSC project. An Applied Superconductivity and Cryogenics Technology Center (the "Center"), established on the SSCL N15 site, could support and collaborate with participants to conduct research, prototype development, component and system testing and basic or applied science experiments in the fields of superconductivity and cryogenics.

For further information, please contact Dr. Donald W. Capone II, Texas National Research Laboratory Commission, Central Facility, 2575 Highway 77 North, Waxahachie, TX 75165, (214) 708-3137



Applied Superconductivity and Cryogenics Technology Center

The goals of the proposed Applied Superconductivity and Cryogenics Technology Center are to:

1. Enhance the competitive position of U.S. industry in the critical fields of applied superconductivity and cryogenics technology by advancing the technology in these areas, and by providing users direct access to the world-class resources available at the SSCL N15 site.
2. Establish a vigorous program to support U.S. High Energy Physics (HEP) research programs by applying the former SSCL magnet development and testing capability to U.S. and international accelerator projects.
3. Enhance educational opportunities in the fields of superconductivity and cryogenics technology.

To meet these goals, the proposed Center must remain a technology leader. This will be accomplished by pursuing a well-focused development program in relevant technical areas. An advisory board, composed of representatives from user and other participating organizations, will recommend the priorities for this Technical Base Program to ensure that it provides maximum benefit to the participants.

The following seven technical service areas will initially constitute the Technical Base Program:

1. Large-scale superconducting and cryogenic component development
2. Testing of superconducting and cryogenic components and systems
3. Enabling technology for applied and basic science experiments
4. Precision manufacturing techniques
5. Enabling cryogenic technology
6. Cabling technology for HEP, fusion, and power utility programs
7. Analysis and information transfer.

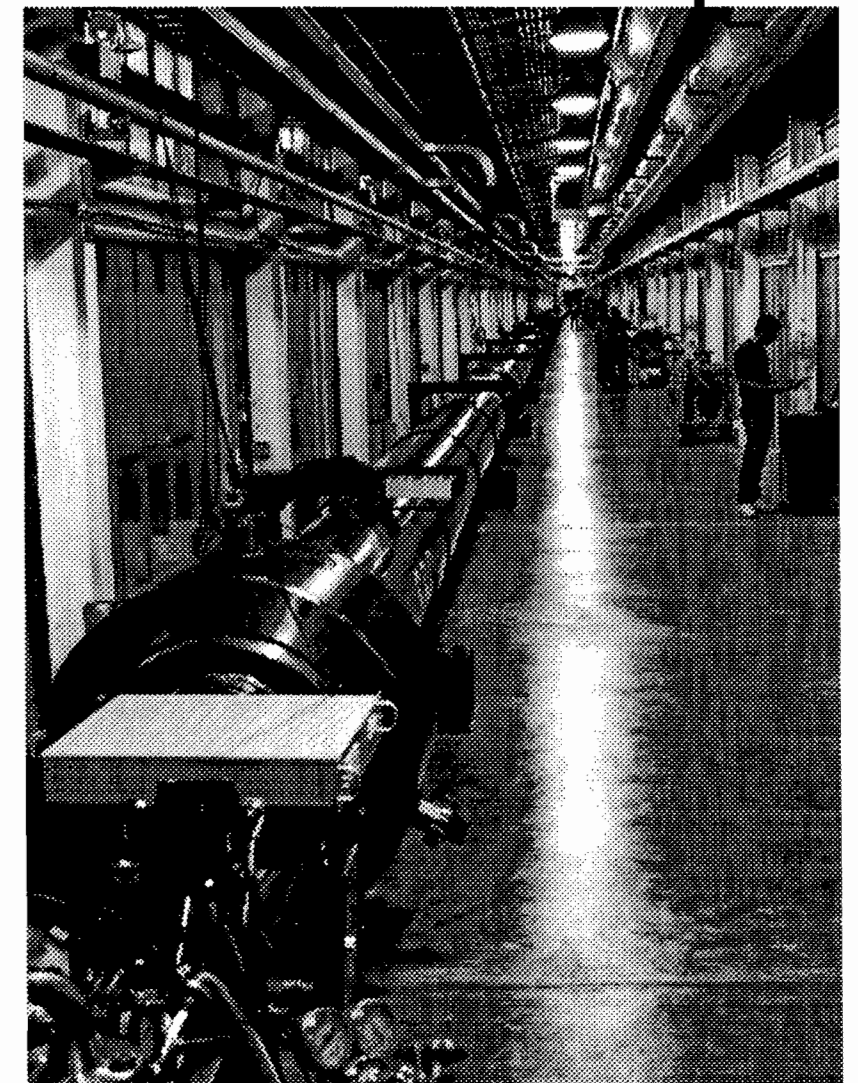
Development programs with one or multiple participants are also envisaged. These will be defined through agreements with specific companies, universities, or laboratories and will provide necessary controls on intellectual property and proprietary data.

As a user facility available to the superconductivity and cryogenics communities, the proposed Center will also provide design, analysis, prototyping, and testing services.

Left: The MDL. Shown is a fish-eye view of the central high bay with several 15-m long magnets in various stages of fabrication. This 103,000 ft² facility can support a wide range of fabrication activities for superconducting and cryogenic components.

Right: The ASST facility. Shown is a 600-ft long string of superconducting accelerator magnets. This string is connected to the ASST refrigerator and is fully instrumented and functional.

Cover: Aerial view of the 100-acre SSCL N15 site.



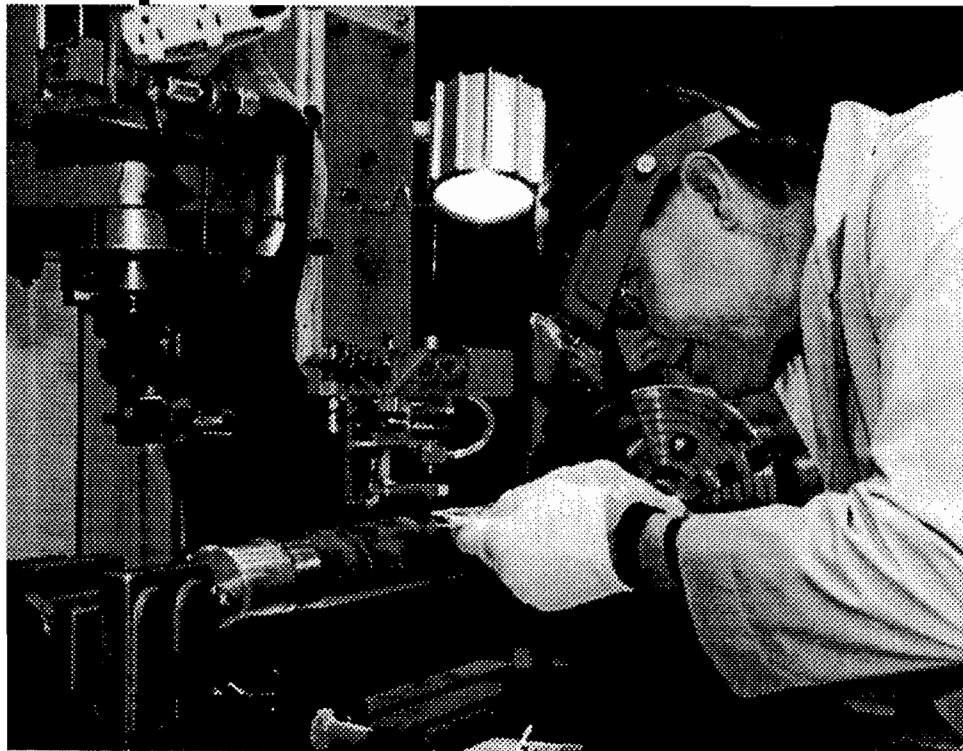
Superconductivity Capabilities

Significant technical capabilities in the areas of superconducting magnet development, fabrication, and testing were developed in support of the SSC project.

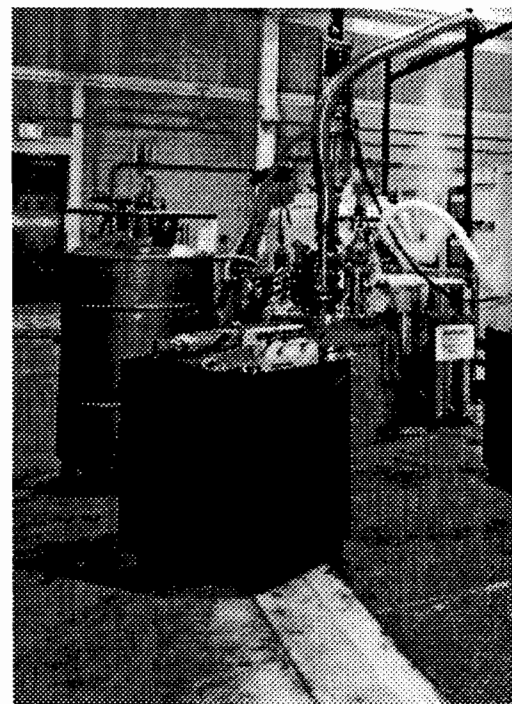
Advanced commercial and in-house computational tools contributed to the development, design, and fabrication of SSC components and subsystems. These software codes and the analysis, design, and manufacturing data associated with them are accessible through extensively networked computer systems.

Advanced superconducting-cable fabrication technology, developed in support of the SSC magnet program, includes fully-automated cable winding and insulating machines with on-line quality inspection capabilities. Coil winding, coil curing, magnet collaring, and magnet shell welding machines are available to fabricate a variety of high-field dipole and quadrupole superconducting magnets. Patented Computer Numerical Control (CNC) technology, developed to fabricate superconducting corrector magnets, accurately bonds individual wires in-place with a high packing density. This capability enables the construction of a large range of high-precision electromagnetic devices, conventional or superconducting. Conventional and CNC machining and measuring capabilities are also available to support fabrication and characterization of a full range of precision components and subassemblies.

State-of-the-art testing and analysis capabilities developed for evaluating magnets, conductors, and integrated systems are also available. A vertical test facility constructed for short magnet and cable testing is capable of supporting current testing up to 50 kA with a high speed, multi-channel data acquisition system. Horizontal test facilities can support cold testing of magnets up to 17 meters in length. Both the vertical and horizontal test facilities utilize advanced instrumentation to conduct field quality and quench performance measurements. Testing of fully-integrated systems up to 600 feet in length is supported by the ASST facility.



Left: The "direct wind" coil fabrication technology features a wiring head mounted on a 5-axis CNC machine tool to precisely assemble multi-layer coils of single-strand wire in almost any size and configuration.



Right: The short magnet and superconducting cable test facility is currently configured for testing to 20 kA. Minor reconfiguration will enable testing to 50 kA.

Cryogenics Capabilities

The SSCL N15 site features one of a class of only five helium refrigerator/liquefier facilities worldwide capable of meeting the requirements of multiple large- or small-scale simultaneous cryogenic uses. This facility, currently uncommitted and available, is of the latest design, optimizing system efficiency, load flexibility, and performance tracking.

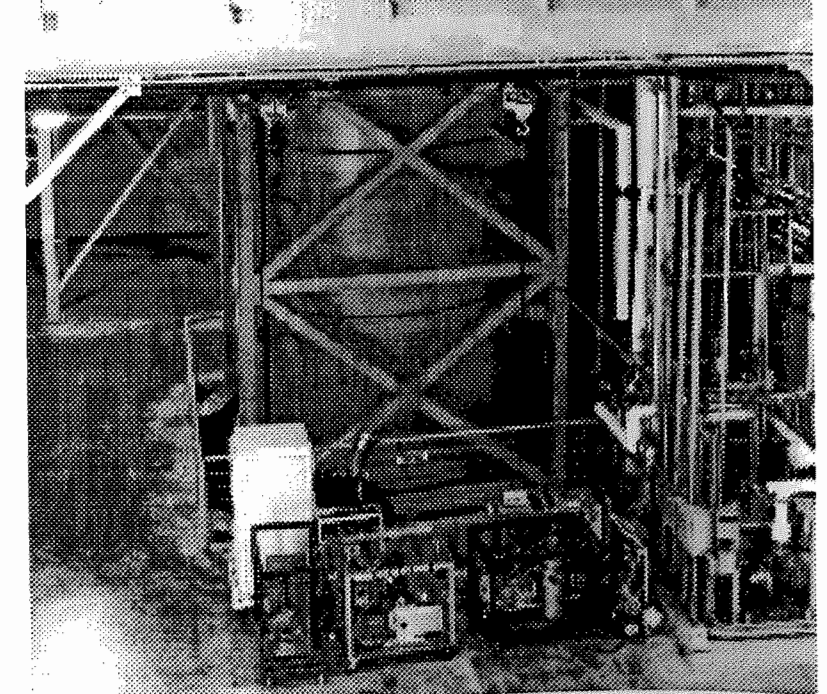
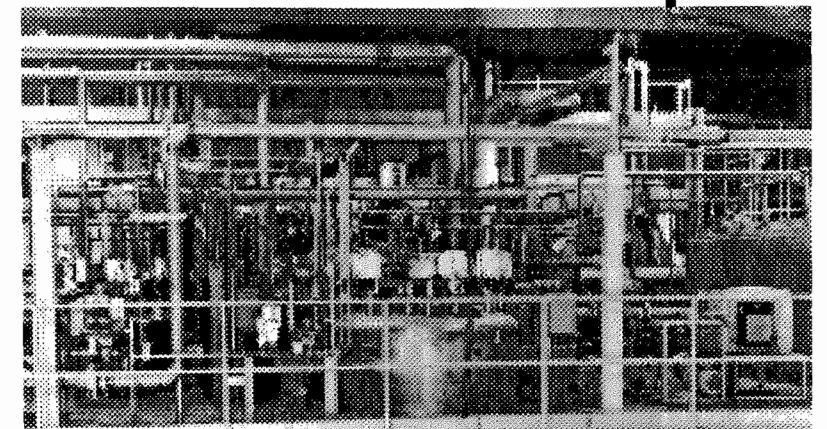
Three large-capacity refrigerators with supporting cryogenic equipment are available to support research and to perform component and system testing over a wide range of cryogenic conditions. The three refrigerators can be operated independently or in transfer-line combinations supplying up to 12 kW at 4.5K. One of the refrigerators is currently capable of operating at temperatures down to 2.5K. Some of these existing cryogenic systems could also be modified at a modest cost to provide a 1.8K (superfluid) capability. In addition, a skid-mounted refrigerator, capable of delivering 550 W at 4.5K or 240 W at 3.5K, is available to support smaller, closed-cycle experiments or component tests.

Each of the three large-capacity helium refrigerators (N15B, MTL and ASST) is optimized to deliver 2.2 kW of refrigeration and 22 g/s liquefaction at 4.5K. Each system can, however, deliver up to 4 kW of refrigeration or 37 g/s liquefaction at 4.5K. The MTL system pump box can provide supercritical flows up to 600 g/s at 4.6K, or subatmospheric temperatures at any one of five test stands using warm vacuum pumps and refrigeration recovery; e.g. 50 g/s at 2.5K to each of two test stands (to 102 W), or 100 g/s at 3.6K to each of three test stands

(to 153 W). The ASST system can provide up to 180 g/s flow at 4.5K, or 100 g/s at 3.5K (to 500 W) with the use of two cold compressors.

The operation of each refrigerator/liquefier system is supported by dedicated cryogenic equipment consisting of four main compressors, a compressor oil removal system, a cold box with dual adsorbers and four turbo-expanders, a 40,000 liter LHe dewar with integral subcooling and sparging lines, and warm gas storage capacity. Each of these systems is also supported by its own Clean-up, Cool-down, Warm-up, and Purification (CCWP) system and an 80,000 liter LN₂ dewar with gas purging & distribution.

Below: The N15B Cold Box two-story-high valve platform resides above the Cold Box vacuum shell. The opening of the vacuum shell removal floor pit can be seen below the shell.



Flexibility

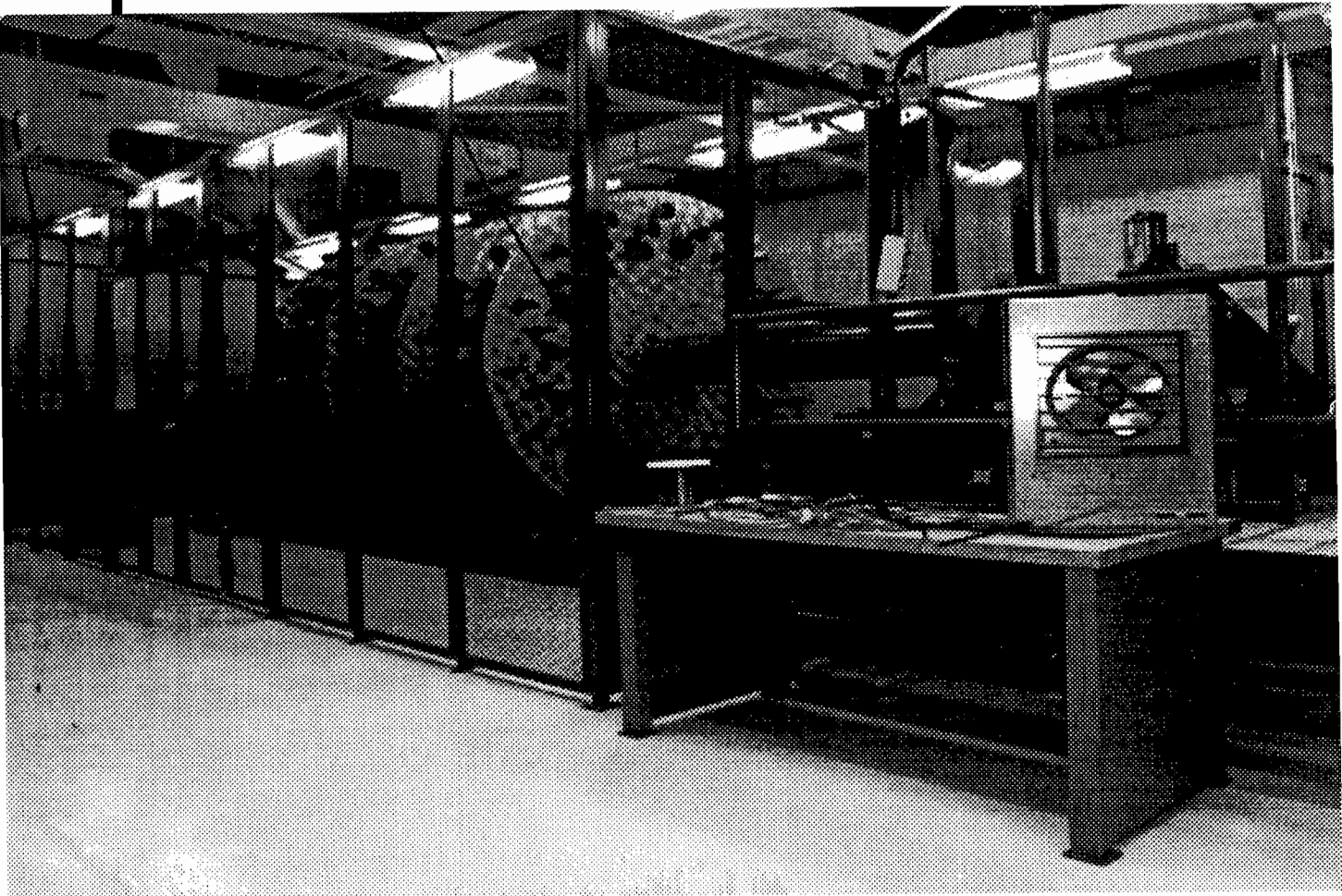
Cryogenics

- Each refrigerator/liquefier system can be operated in Energy Saver mode (1/3 input power): Refrigeration – 1kW or Liquefaction – 10 g/s
- The refrigerator capacity management system automatically controls the operating parameters of the refrigerator to maximize system efficiency between 30% and 100% capacity
- The refrigeration-dewar system design intrinsically handles sudden, major load upsets

Superconductivity

- The MDL high bay is reconfigurable to accommodate tooling for a wide range of superconducting or cryogenic components
- The MDL contains 22 individual low bay shops each with secure access to the central high bay
- The MTL has 21,000 ft² of contiguous high bay floor space unoccupied and available

Below: A cabling machine, designed to fabricate Rutherford cable with up to 48 strands, is fully automated and provides for on-line inspection.



Additional Features

Cryogenics

- Fully-instrumented process flows, pressures, and temperatures
- Integrated digital control system with historical and real time trending
- Precise load flow measurement and control
- Supercritical He pressures to 10 bar
- Monitored and alarmed for oxygen deficiency hazards

Superconductivity

- Fully-equipped weld shop with MIG and TIG welding systems and orbital welding capability
- Fully-equipped electronics shops
- Complete materials testing/analysis capability with optical, scanning-electron and transmission-electron microscopes
- Fully-equipped vacuum shop with pump carts, leak detectors, and residual gas analyzers
- Full range of advanced analysis and CAD/CAM software and hardware

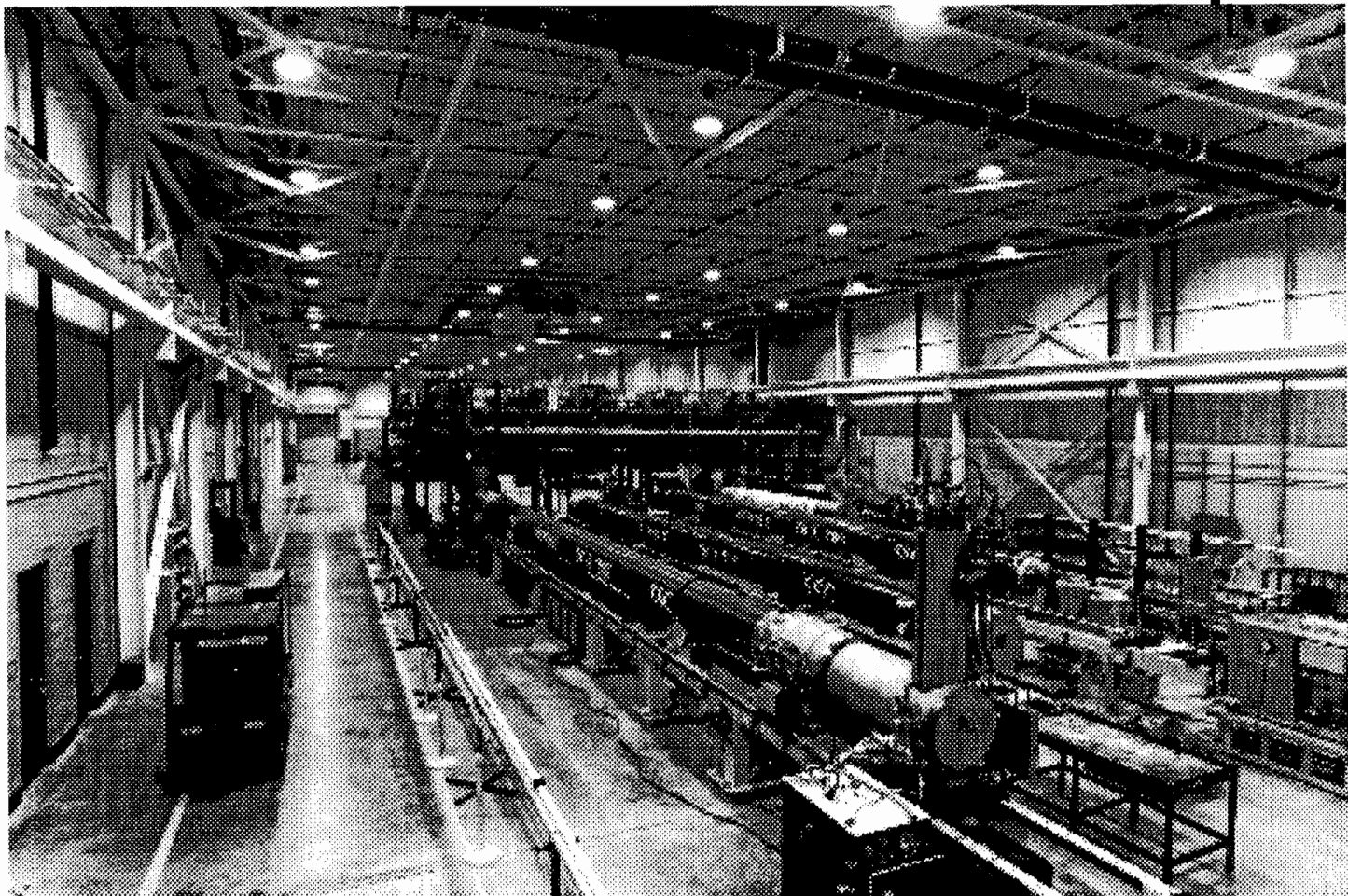
Supporting Equipment, Buildings

1. Fully integrated and operational component and system test capability (MTL, ASST)
2. Fully-equipped incoming inspection laboratories
3. Fully-equipped strain-gauge calibration laboratory
4. Distributed vacuum system
5. Distributed gaseous helium and nitrogen systems
6. Overhead, full-span 25-ton cranes in high bays
7. 3,500 ft², 14-ft ceiling height basement under distribution boxes at center of MTL high bay
8. Large, adjacent concrete hard stands
9. Office/parking space for up to 220 personnel

Building Area	Floor Space (ft ²)
MTL High Bay	41,000
MTL Low Bay (labs and shops)	13,200
MTL Compressor Room	8,700
MTL Service (cold box) Building	4,100
MDL High Bay	47,000
MDL Low Bay (22 separate shops)	28,000
MDL Office area	28,000
ASST/N15B Compressor Room	13,000
ASST/N15B Service (cold box) Building	9,500
ASST String Enclosure	9,600
ASST Shop	3,000
TOTAL	205,100

The buildings are shown in the front cover aerial view.

The high bay of the MTL building. Shown are five independent helium distribution boxes and three 15-m long magnets in various stages of installation. This equipment occupies less than half of the MTL high bay floor space. The remaining high bay floor space (background) is unoccupied and available.



Expansion Capabilities

Superconductivity

While the Magnet Development Laboratory and the Magnet Test Laboratory were constructed with the intent of fabricating and testing large superconducting accelerator magnets, the generic tooling in the MDL and the cryogenic distribution network in the MTL can be effectively utilized in the development of other small- and large-scale superconducting and “normal” conducting magnets and components.

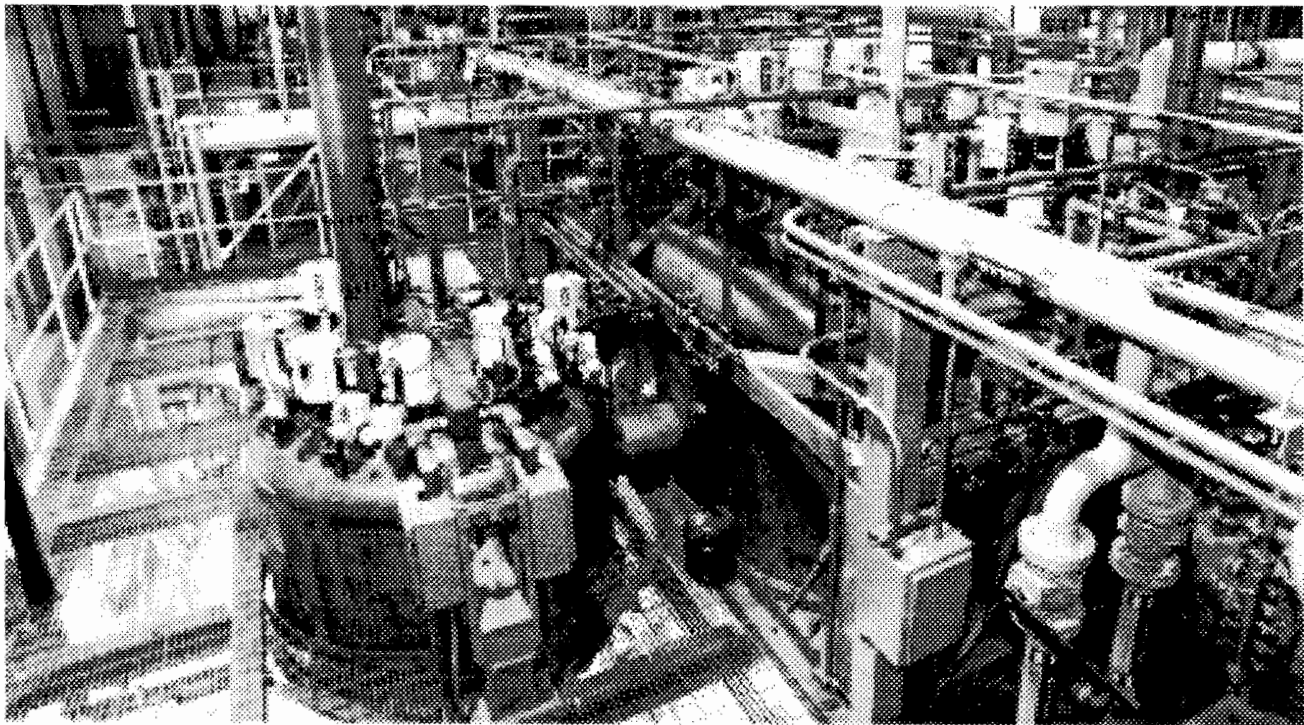
Cryogenics

The refrigerator/liquefier systems at the SSCL N15 site provide the potential to create a world-class 1.8K (superfluid) facility. Each of the three large systems could be readily and inexpensively modified to provide a 1.8K capacity to 500 W without a cold return, i.e. as a liquefaction load. This 1.8K capacity could be doubled to 1,000 W by adding refrigeration recovery equipment. The existing service and compressor buildings include extensive concrete aprons and an unused vacuum shell removal floor pit (16 feet square x 25 feet deep). Originally sized to accommodate a fourth 4 kW refrigerator, these facilities can instead accommodate a large experiment or prototype test setup.

N15 Site

Thirty acres of improved land are available for future expansion. Site improvements include a sewage treatment plant, 80,000-lb load access roads, a 24.9 kV substation (@20MW), natural gas service, cryogen storage, a central cooling tower, an evaporation pond, and reserve fire protection water. Spacious subterranean excavations also exist beneath the N15 site. These fully concrete-lined chambers can be used as a test area for experimental magnet coils or other apparatus requiring containment for safe operation.

The Turbine Pod (left) and ASST Refrigerator Cold Box (right) are in the foreground.



Appendix K Conformance Matrix

Those items specified by DOE for inclusion in this technical report are summarized below. Where the topic is of a general nature, the section number or Appendix in which that topic is addressed is given. Where the topic is more specific, the paragraph number is given. In many instances, topics are discussed in more than one place. This arises partly because of the nature of the program under study, and partly because of the nature of some topics. Every effort has been made to ensure that each specified topic is discussed at some point in the text. The authors are confident that all relevant information has been included.

DOE Report Requirement

Section in Text

1	Discussion of study findings	1
	Clear statement of goals	1
	Questions to be answered and their importance	2.2
	Relevant theoretical studies	2.2
	Review of current, pertinent knowledge	2, 7
	Discussion of other related planned or existing experiments	2.6
	Estimate of how well scientific questions are likely to be answered	2.2.11
2	Detailed description of facilities being studied, operational goals, feasibility of uses	5
3	Discussion of benefits (scientific, technical, educational and/or economic)	1
3	Comparison with similar facilities	2.6
3	Reasons why suggested facility is best utilization of SSC assets	2.1, 2.3, 2.4, 3.6
	Complete plan for carrying out experiment or facility including:	
	a) manpower required	5.5.2
	b) R&D tasks	4.3
	c) apparatus and equipment	5.1
	d) fabrication of new equipment	App. A
	e) optimal schedule for completion	5.4 & App.H
	f) estimated total cost of assembly:	
	capital costs	5.5.1
	labor costs	5.5.2
	g) university program costs	6
	h) estimated operating costs	5.5.3
	i) optimal schedule of funding	6
3	Detailed explanation of the basis for estimated costs and yearly budgets	4.8, 5.5. 6, App.I
4	Discussion of:	
	a) required construction, capital improvement, or equipment in addition to SSC assets.	5.1
	b) Documentation of infrastructure and other support assumed	5.3, App.G
5	Preliminary cost estimates	
	Annual operating costs	6
	Discussion of any potential for private investment or other cost sharing.	N.A.
	Funding sources and alternatives	5.7
6	a) Funding and/or business plan to meet operating and capital expenses	N.A.
	b) Identification of specific funding sources expected	5.7
7	Description of federal, state, and local permits required	5.6

Appendix L - Other Possible Sites for the Program of Cryogenic Helium Gas Convection Research

The technology of large-scale helium cryogenics that supports the Research program presented in this report was developed primarily in the national high energy physics laboratories of the world. In these institutions the development, first of bubble chamber technology and later of the large-scale application of superconductivity, lead to the development of a strong cryogenic engineering capability that is resident in these institutions today. The SSCL N-15 refrigeration plants were designed to support the research and development phases of the Supercollider, and as very modern equipment built with the flexibility required for research, these plants are very appropriate to the needs of the Convection Program. There are other places in the U. S and in Europe where the Program could be located, however, and where it could find adequate facilities and good technical support.

In the following paragraphs, three Department of Energy Laboratories are discussed with regard to the support that they could offer to a program of convection research. In addition, laboratories in Europe and in Japan have the technical capability required. These include the DESY Laboratory in Hamburg, CERN in Geneva, and KEK near Tokyo.

Fermi National Accelerator Laboratory: Fermilab's high energy physics program is based on the Tevatron, a superconducting electron-positron collider. The extensive cryogenic system of the Tevatron has an aggregate refrigeration capacity of in excess of 25 kW at 4.5 K, and among the facilities there is a large helium liquefier, the CHL, with a capacity of 6000 l/hr. The CHL facility obviously has the refrigeration and inventory-handling capacity needed for the convection experiment, and the laboratory can supply the cryogenic expertise and engineering and the technical help to build and operate the cell cryostat.

Brookhaven National Laboratory: Brookhaven is engaged in a construction project to build a superconducting heavy-ion collider, called RHIC. The refrigeration plant that is to be used for RHIC was built in the 1980s for the ISA Collider. This is a very large installation of about 25 kW capacity. It has good computer control, but almost no helium storage. At Brookhaven as at Fermilab there is a good cryogenic engineering department with the needed expertise.

CEBAF: This laboratory, the Continuous Electron Beam Accelerator Facility, is in the process of commissioning their superconducting recirculating linear accelerator. At CEBAF is a first of its kind superfluid helium refrigerator delivering 5 kW at 2 K. At 4.3 K the capacity of this machine is 10 kW. This is a relatively new machine with very good controls. CEBAF has a very good cryogenics department that is fresh from their construction program, but like Fermilab, their operating schedule is very full.

An important additional feature at CEBAF is the large-scale superfluid helium capability. The use of superfluid helium in high Reynolds number research and

development has unique advantages and represents a considerable opportunity for advancement of the field.

In the table below an naive attempt is made to rate the factors affecting the placement of a convection research program at these institutions. Because refrigeration capacity is a qualifying factor in choosing possible places, this factor is not specifically included on the table. Instead, the availability of refrigeration capacity in the needed amount of 2-3 kW is rated. Because the facilities at the places considered have large cryogenic plant installations, operation of the cell cryostat could only be economically reasonable if it were connected in such a way that the plant output could be shared with another user at least part of the time. Under the designation availability is placed, therefore, some judgment concerning the feasibility of working out an effective operating arrangement.

In addition to this non-technical factor, three technical factors can be identified. First among these is the adaptability of the laboratory cryogenic system to the operations of the convection experiment. In this factor is included the adaptability of the refrigeration cycle and the equipment to the convection experiment requirements and the suitability of the plant control system to perform the needed combined operation. The second factor is the inventory management capability of the plant facilities including both the storage capacity available and the ability of the plant to move the helium around. The third factor is the capability that the particular laboratory has as an institution to support the convection experiment as a user. Under this category is judged the expertise, both in cryogenics and in other branches of engineering, and the technical support that can be drawn on by the guest program.

In the table the four laboratories are rated in these four factor categories on a scale from 1 for poor to five for excellent. It is difficult to know what algorithm to apply to get a combined rating, so this has not been done. It can be argued, however, that availability should have the greatest weight, perhaps a weight of 2, and the technical factors a weight of 1 in forming a sum.

	Availability	Adaptability	Inventory	Support
SSCL N- 15	5	5	3	1
FNAL	1	2	3	4
BNL	2	4	1	3
CEBAF	1	4	4	4